

**Face It:
Cell-based therapy
for the reconstruction of cartilage defects
in the head and neck area**

Mieke Marianne Pleumeekers

Printing of this thesis was financially supported by:

- Nederlandse Vereniging voor Plastische Chirurgie
- Junior Vereniging voor Plastische Chirurgie
- Anna Fonds te Leiden
- BlooMEDical
- Chipsoft

ISBN: 978-94-6299-967-1

Cover design by: James Jardine, designyourthesis.com

Layout and printed by: Ridderprint BV, Ridderkerk, the Netherlands

© 201 M.M. Pleumeekers, Rotterdam, the Netherlands.

All rights reserved. No part of this thesis may be reproduced, stored in a retrieval system, or transmitted in any form or by any means without prior permission of the copyright holder.



De digitale versie van dit proefschrift is te vinden via <http://www.publicatie-online.nl/uploaded/flipbook/m-pleumeekers> of middels het scannen van bijgevoegde QR-code.

**Face It:
Cell-based therapy
for the reconstruction of cartilage defects
in the head and neck area**

*Celtherapie voor de behandeling en reconstructie
van kraakbeendefecten in het hoofd- halsgebied*

Proefschrift

ter verkrijging van de graad van doctor aan de
Erasmus Universiteit Rotterdam
op gezag van de
rector magnificus

Prof. dr. H.A.P. Pols

en volgens besluit van het College voor Promoties.
De openbare verdediging zal plaatsvinden op

vrijdag 29 juni 2018 om 13:30 uur

door

Mieke Marianne Pleumeekers
geboren te Rotterdam.

Promotiecommissie

Promotor	Prof. dr. G.J.V.M. van Osch
Overige leden	Prof. dr. I.M.J. Mathijssen Prof. dr. P.P.M. van Zuijlen Prof. dr. ir. J. Malda
Copromotor	Dr. ir. K.S. Stok

Contents

List of abbreviations	6
<i>Introduction</i>	9
Chapter one	General introduction 11
	Thesis aim and outline 21
<i>Cartilage properties</i>	25
Chapter two	Mechanical and biochemical mapping of human auricular cartilage for reliable assessment of tissue-engineered constructs 27
Chapter three	Structural and mechanical comparison of human ear, alar and septal cartilage 43
<i>Cell sources</i>	57
Chapter four	The <i>in vitro</i> and <i>in vivo</i> capacity of culture-expanded human cells from several sources encapsulated in alginate to form cartilage 59
Chapter five	The trophic effect of adipose-tissue-derived and bone-marrow-derived mesenchymal stem cells on chondrocytes in co-culture 83
Chapter six	Cartilage regeneration in the head and neck area: Combination of ear or nasal chondrocytes and mesenchymal stem cells improves cartilage production 107
<i>Scaffolds</i>	127
Chapter seven	Preparation and characterization of a decellularized cartilage scaffold for ear cartilage reconstruction 129
Chapter eight	Novel bilayer bacterial nanocellulose scaffold supports neocartilage formation <i>in vitro</i> and <i>in vivo</i> 147
<i>Discussion and summary</i>	173
Chapter nine	Discussion and future perspectives for clinical application. 175
Chapter ten	Summary 191
Chapter eleven	Nederlandse samenvatting 197
<i>References</i>	203
<i>Appendices</i>	221
PhD portfolio	222
Publications	225
Dankwoord	227
Curriculum vitae	231

List of abbreviations

AC	Articular cartilage/chondrocytes
ACAN	Aggrecan
AFM	Atomic force microscopy
ALP	Alkaline phosphatase
AMSC	Adipose-tissue-derived mesenchymal stem cell
ATMP	Advanced therapy medicinal product
ATR-FTIR	Attenuated total reflectance fourier transform infrared
B2M	Beta-2-microglobulin
BMP	Bone morphogenetic protein
BMSC	Bone-marrow-derived mesenchymal stem cell
BNC	Bacterial nanocellulose
BSA	Bovine serum albumin
COL1A1	Collagen type I
COL2A1	Collagen type II
COL10	Collagen type X
DC	Decellularization
DMMB	Dimethylmethylene blue
E*	Young's modulus
EDTA	Ethylene diamintetraacetate
Ein	Instantaneous modulus
Eeq	Equilibrium modulus
EC	Ear cartilage/chondrocytes
ECM	Extracellular matrix
EMA	European medicines agency
EMIMAc	1-Ethyl-3-methylimidazolium acetate
FCS	Fetal calf serum
FDA	Food and drug administration
sGAG	sulfated-Glycosaminoglycan
GAPDH	Glyceraldehyde 3-phosphate dehydrogenase
GMP	Good manufacturing practices
H	Thickness
HCT/P	Human cells and tissues and cellular- and tissue-based product
H&E	Haematoxylin and eosin
HG-DMEM	High glucose Dulbecco's modified Eagle's medium
HPRT1	Hypoxanthine phosphoribosyltransferase 1
ITS+	Supplemented insulin transferrine selenium
LG-DMEM	Low glucose Dulbecco's modified Eagle's medium
MicroCT	Micro-computed tomography
MMP13	Matrix metalloproteinase-13
MNC	Mononuclear cells
MSC	Mesenchymal stem cell

MTT	Methylthiazolyldiphenyltetrazolium bromide
NC	Nasal cartilage/chondrocytes
PA	Pharyngeal arc
PBS	Phosphate buffered saline
PD	Population doublings
PG	Proteoglycan
SHG	Second harmonic
$t_{1/2}$	Relaxation half-lifetime
TEP	Tissue-engineered product
TGF β	Transforming growth factor β
qRT-PCR	Quantitative real-time polymerase chain reaction
RC	Recellularisation
RF	Resorcin Fuchsin
SEM	Scanning electron microscopy
VCAN	Versican
W	Weight
σ_{\max}	Maximum stress
2PF	Two-photon fluorescence
2PLSM	Two-photon laser-scanning microscope
<i>B</i>	Bovine
<i>H</i>	Human

Introduction

Chapter 1

General introduction

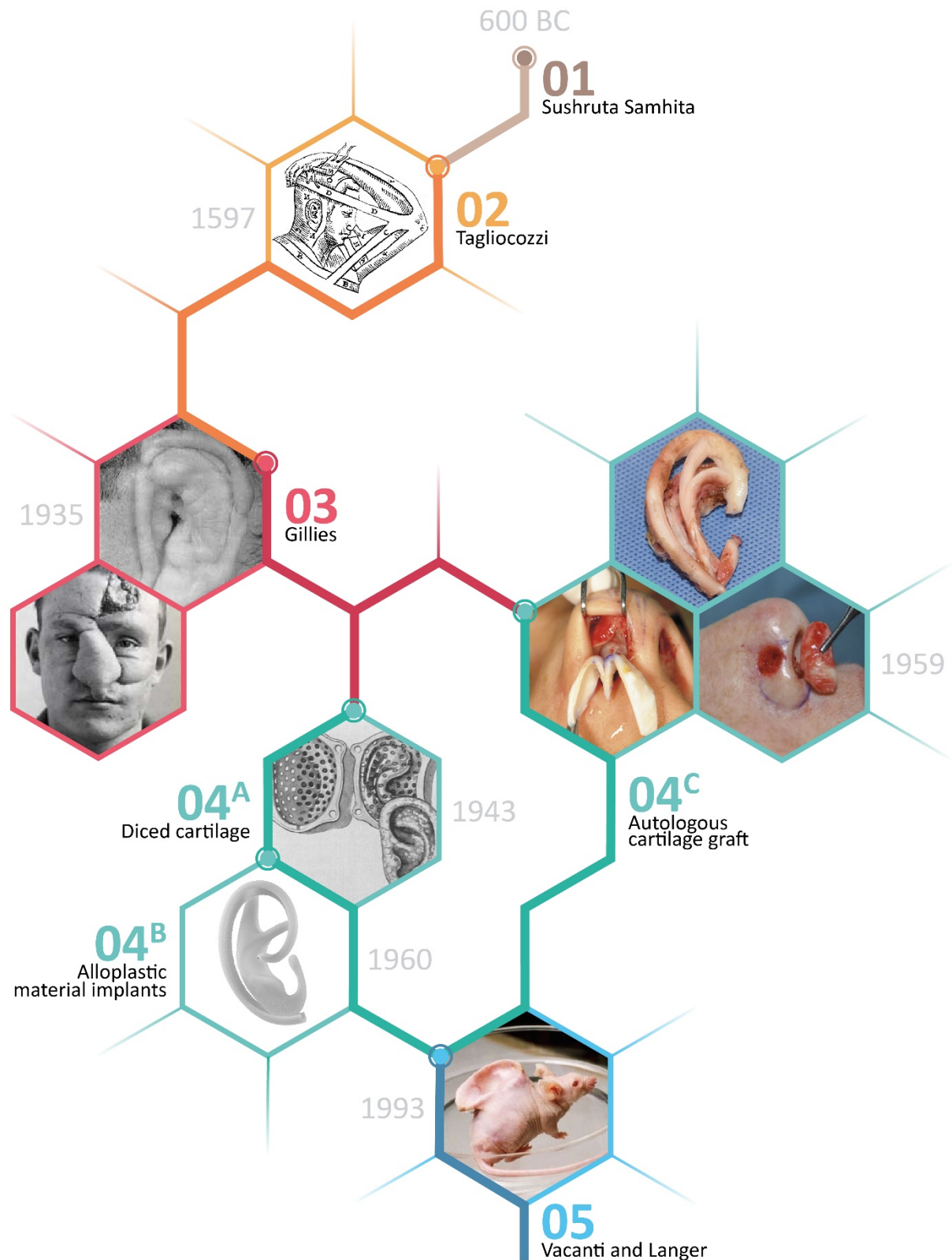


Figure 1. The history of facial cartilage reconstruction.

Deformities of the head and neck area have incredible impact on facial appearance and function. They are the result of congenital disease, trauma (including burns) or tumor destruction, subsequent ablative surgery and/or radiotherapy. Reconstruction of such deformities is extremely demanding and requires considerable skill and finesse. The main goal is to create a three-dimensional (3D) tissue with optimal functional and aesthetic outcomes. To achieve that, the reconstructive surgeon must consider both soft-tissue *coverage* as well as the underlying cartilaginous *support*.

Soft tissue coverage and supporting structures are both missing in major defects in the head and neck area. Traditionally, facial reconstruction was particularly concerned about soft tissue repair (i.e. skin coverage) instead of the reestablishment of the underlying structural support. The earliest example of such reconstruction could be found in the Hindu Book of Revelation - Sushruta Samhita - a medical text book from ancient India 600 BC. Sushruta described various local skin flap techniques for reconstruction of the nose and earlobe. [1] The method described by Sushruta continued to be practiced without substantial variation for centuries and variation on his Indian forehead flap rhinoplasty is still used for soft-tissue coverage of the nose today. Besides local skin flaps, the introduction of the pedicled distant flap by Tagliacozzi (16th century) [2, 3] and the introduction of free microvascular tissue transfer during the late 1950s [4], have extended possibilities for soft tissue reconstruction in the head and neck area.

Successful surgical reconstruction of head and neck defects are however, not only dependent on adequate soft tissue coverage. Importantly, these defects require structural support for contour as well as resistance forces of scar contraction. In the early 20th century, it was Gillies who understood that facial reconstruction required structural support in addition to healthy soft-tissue coverage. He was the first to use allogenic (maternal) costal cartilage for ear reconstruction [5] and composite chondrocutaneous grafts for nasal reconstruction [6]. Currently, application of an autologous cartilage graft remains the standard of facial reconstructive surgery. The foundation of current autologous cartilage reconstruction techniques in the head and neck area are largely based on the methods described by Tanzer [7], Brent [8], and Nagata [9] for ear reconstruction as well as the methods described by Burget and Menick [10-12] for nasal reconstruction. They recommend a multi-stage repair strategy using an autologous cartilaginous framework for underlying support as well as to give desirable face contour. In short, autologous cartilage is harvested from the ear, nasal septum or ribs, and sculpted into a solid framework. The cartilaginous framework is then implanted subcutaneously or - in case of soft-tissue shortage - covered by local flap, pedicled distant flap or free flap. [13] Although autologous cartilage grafting has been used successfully in cartilage reconstructive surgery, the procedure requires a high degree of surgical expertise, is associated with limited availability of autologous cartilage and can cause severe donor site morbidity.

For many years there has been considerable interest to simplify current approaches and thereby improve surgical outcome. In order to eliminate the variability of the surgeon's creative ability to make a realistic framework from autologous cartilage, the idea of a *prefabricated framework* was introduced. The first presentation of such framework was initiated back in the 1940s by Peer [14] after the introduction of viable diced cartilage grafting

[15]. By using a prefabricated mould, diced autologous cartilage was formed into the shape of an ear [16] and later nasoseptum [17, 18] and fused into a living prefabricated cartilaginous framework. However, due to its heterogeneous outcome, disappointing long-term survival and severe donor site morbidity, diced cartilage grafting has never achieved widespread use. In addition, its clinical use was soon forgotten after introduction of prefabricated alloplastic material implants. Nowadays, its use is only destined for specific nasal reconstruction therapies, such as dorsal nasal augmentation and nasal tip reconstruction. From the 60's until now, numerous alloplastic material implants have been used in reconstructive surgery (e.g. silicones and silicon-based elastomers, polymers such as Medpor[®], Proplast[®] Mersilene[®], and Gore-Tex[®]). [19] Their use in the head and neck area is however questioned, since these implants poorly integrate and are prone to induce a foreign body reaction and frequently lead to implant extrusion in this area (3.1-8.9%). [20, 21]

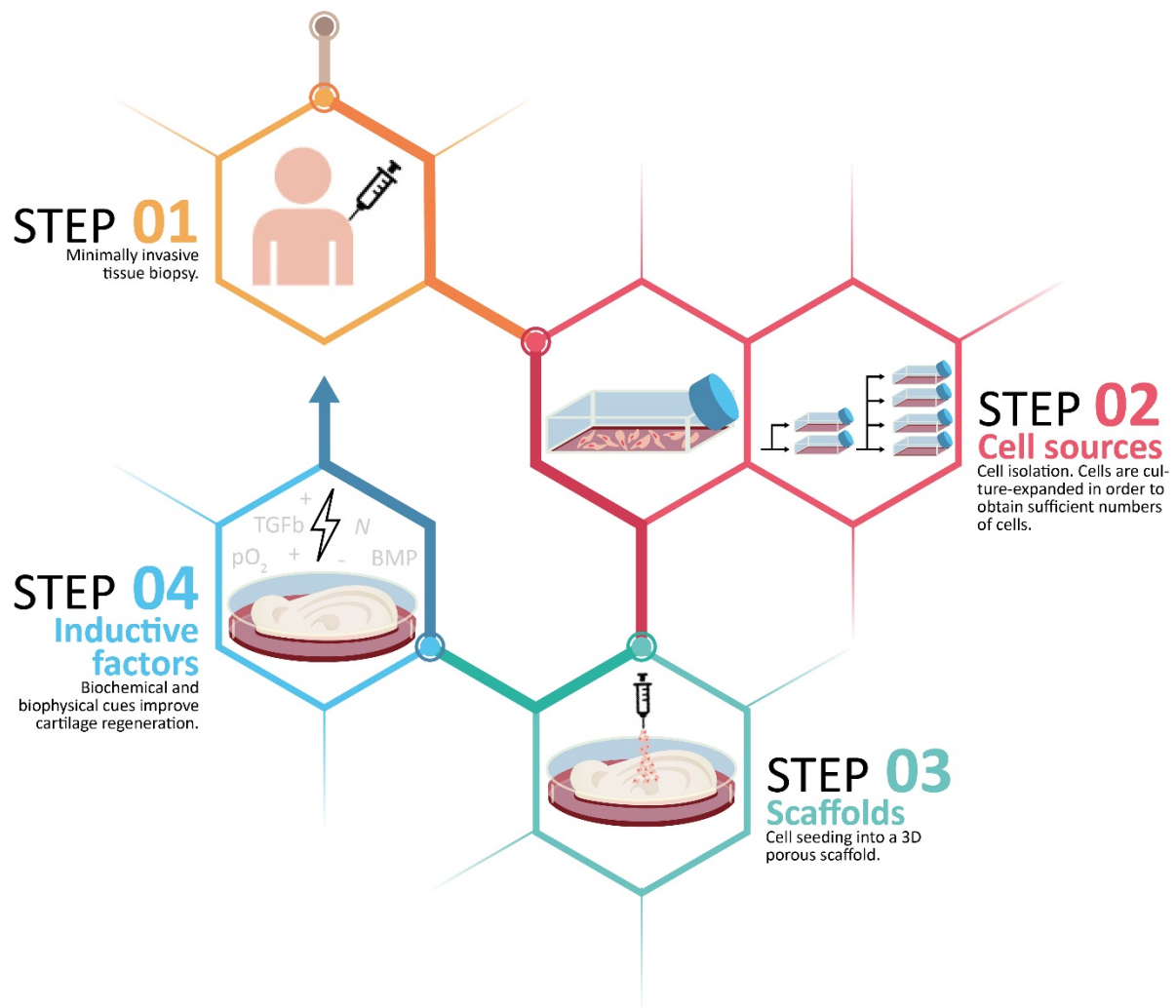


Figure 2. Cartilage tissue engineering.

The idea of a prefabricated framework was further elaborated via novel biological engineering techniques first introduced by Vacanti and Langer [22] named *tissue engineering*. Tissue engineering has the potential to overcome limitations of current treatments, reestablishing unique biological and functional properties of the tissue. It endeavors to develop functional living cartilage by using cells, inductive signals and a prefabricated scaffold or framework. In short, cartilage tissue engineering starts with a small tissue biopsy, from which the residing cells are isolated. Thereafter, cells are proliferated *in vitro* under controlled conditions, seeded into a prefabricated scaffold and implanted subcutaneously. (Figure 2) Tissue engineering is a promising solution for restoring missing or damaged cartilage in the head and neck area, as it translates complex biological science into a living prefabricated cartilaginous framework. Future surgical techniques are thereby simplified, improving surgical outcomes. Besides, tissue engineering aims to circumvent the resulting donor-site morbidity by engineering rather than harvesting cartilage tissue. Therefore, in this work, I aim to develop a cell-based cartilaginous framework for the surgical repair of cartilage defects in the head and neck area by using a tissue engineering strategy.

Cartilage form and function

Cartilage plays an important role in the form and function of the face as it provides flexibility and mechanical support to soft tissues. However, mechanical properties of facial cartilage are sparsely investigated, and limited data are available on human ear [23, 24] and nasal cartilages [25-30].

Cartilage rigidity and elasticity are due primarily to the properties of its complex extracellular matrix (ECM). It constitutes by a complex network of various macromolecules. The most abundant ECM macromolecule is collagen, making up 60-80% of the dry weight of cartilage, followed by approximately 20-30% of proteoglycans (PGs). Collagen, mostly collagen type 2, form a highly organized fiber network defining form and tensile strength. [31] Within this collagen network, PGs are intertwined, of which aggrecan is most common. Their negatively charged glycosaminoglycan (GAG) side chains are responsible for compressive strength by attracting large amounts of water to the cartilage ECM. Basically, 60-80% of the wet weight of cartilage is water. [32] Finally, elastin, the main component of elastic fibers, is variably found in the cartilage ECM and provides elastic recoil and resilience to the tissue. [31] Other matrix constituents, only form a small fraction of the total dry weight of cartilage and are not further discussed.

Depending on the exact composition and organization of the ECM, three major cartilage subtypes can be distinguished with variable flexibility and mechanobiology: hyaline, elastic and fibrous cartilage. (Figure 3) The most prevalent cartilage subtype is hyaline cartilage. It is characterized by a homogeneous ECM that mainly consists of collagen type 2 fibers, PGs and water. In the head and neck area, hyaline cartilage is located in the nasal septum, trachea and larynx. Outside this area, hyaline cartilage is mainly found at the articular surfaces of joints and on the ventral ends of ribs. Besides, it is also transitorily involved in skeletal development through the process of endochondral ossification. Elastic cartilage also consists of a refined network of collagen type 2 fibers, PGs and water. It additionally contains insoluble elastin fibers. Elastic cartilage is found in the pinna of the ear, Eustachian tube and

epiglottis. Fibrous cartilage is mostly found in regions of the body that are subjected to tensile stresses such as the menisci, pubic symphysis and annulus fibrosus of intervertebral discs. The ECM is characterised by a dense network of collagen type 1 and, to a lesser extent, type 2 fibers, thereby increasing the rigidity of the tissue. [33]

All mature cartilage subtypes consist of only a relatively small amount of specialized cells (1-5%), termed chondrocytes. [34] They are essential for producing, maintaining and remodelling the ECM. Nutritional and oxygen supply of chondrocytes is mainly achieved by the perichondrium, a dense connective tissue that covers most cartilages in the head and neck area. This process is achieved through diffusion. In cartilage types lacking a perichondrium, such as hyaline articular and fibrous cartilage, diffusion of nutrients and oxygen is provided by synovial fluid [35], vertebral endplates [36], and - in case of the meniscus and pubic symphysis - effectuated by limited blood supply [37, 38].

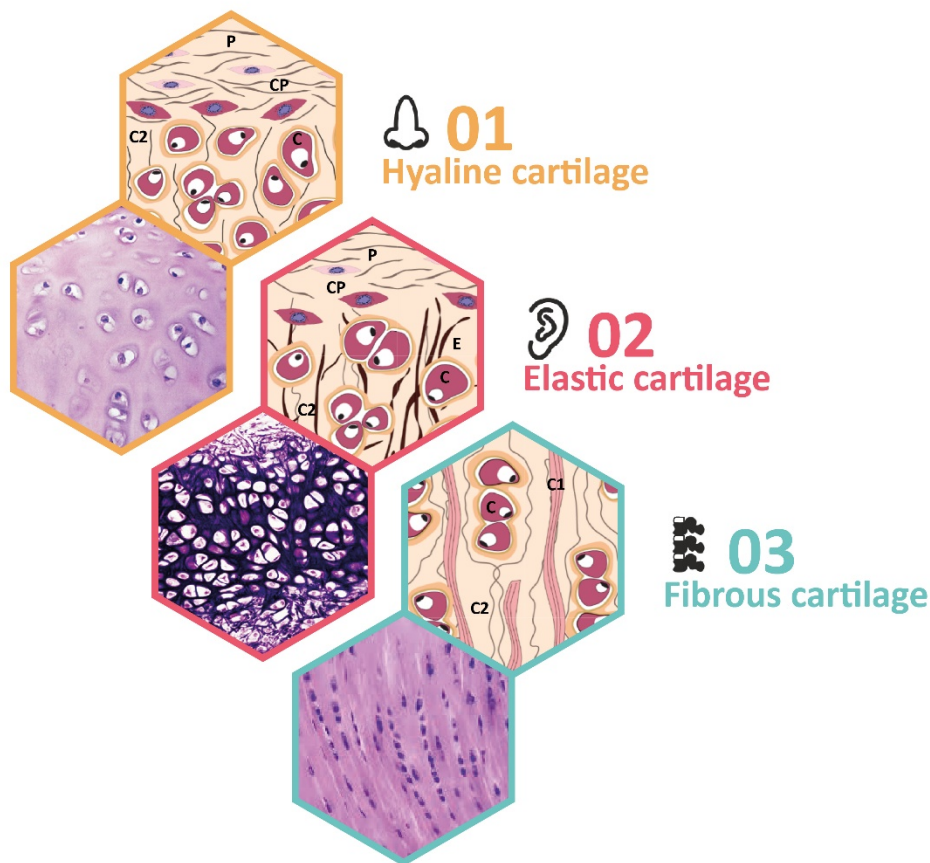


Figure 3. Cartilage subtypes.

Depending on the exact composition and organization of the ECM, three major cartilage subtypes can be distinguished: hyaline, elastic and fibrous cartilage. P = Perichondrium ; C = Chondrocyte ; CP = Chondroprogenitor ; C1 = Collagen type 1 ; C2 = Collagen type 2 ; E = Elastin.

Cartilage tissue engineering

Tissue engineering is described as “the interdisciplinary field that applies the principles of engineering and life sciences toward the development of biological substitutes that restore, maintain, or improve tissue function”. [22] Tissue engineering attempts to mimic functional tissue that has features similar to native tissue. The development of such an engineered tissue requires a careful selection of three major components, also known as the “tissue engineering triad”: (1) cells; (2) a supporting structure or scaffold; and (3) inductive factors that trigger tissue regeneration cascades. (Figure 2) These components are discussed more extensively below.

Cell sources

Defining an appropriate cell source for cartilage tissue engineering is a major challenge. The ideal cell source is one that is abundantly available, can be easily isolated or expanded, and forms cartilage tissue that is similar to that of native tissue. The most obvious choice are chondrocytes themselves. Therefore, chondrocytes from several anatomical locations (e.g. joint, rib, nose, ear, meniscus) have been investigated for their applicability. [39-60] Typically, autologous chondrocytes are isolated by enzymatic digestion from small cartilage biopsies, to minimize donor site morbidity. However, large numbers of chondrocytes are required to generate a construct of reasonable size. Therefore, after cell-isolation, cells are expanded *in vitro* until a sufficient cell number is obtained. Unfortunately, culture-expansion results in chondrocyte dedifferentiation: they change phenotypically to a fibroblast-like morphology and lose their chondrogenic gene-expression capacity, which usually results in fibrous and mechanically inferior cartilage. [61] In recent years, considerable progress has been made to remedy current limitations. Multiple biological and biophysical cues have been introduced to inhibit the process of chondrocyte-dedifferentiation and improve chondrocyte redifferentiation, as discussed below.

Next to chondrocytes, mesenchymal stem cells (MSCs) have been introduced and demonstrated to be an attractive cell source for cell-based cartilage repair. [62] These cells are easily available from several tissues, including bone marrow, adipose tissue, synovium, peripheral blood, dental pulp, placenta, umbilical cord, and skeletal muscle. [63] Of these MSCs, adipose-tissue-derived MSCs (AMSCs) and bone-marrow-derived MSCs (BMSCs) are best characterized. They can undergo multiple population doublings without losing their chondrogenic potential and have the capacity to differentiate into cartilage tissue under appropriate culture conditions. [64-68] A potential limitation to their application in cell-based cartilage repair is that differentiated MSCs become hypertrophic, a process called terminal differentiation. Hypertrophic MSCs produce cartilage tissue that is unstable and predisposed for tissue mineralisation and ossification *in vivo*. [69-72] Taken together, the individual use of chondrocytes or MSCs is at present not yet ideal for cell-based cartilage repair in the head and neck area.

As an alternative to the individual use of cells, the concept of co-culture was introduced. [73] It became clear that combination of chondrocytes and MSCs extenuate many disadvantages of individually studied cell types. In particular, co-cultures of chondrocytes and MSCs demonstrated improved chondrogenesis [74] as well as reduced hypertrophy and tissue

mineralization [73, 75]. Moreover, by decreasing the amount of chondrocytes required ($\leq 20\%$ of the total cell mixture), culture-expansion was no longer necessary, which allowed the use of freshly isolated primary chondrocytes leading to improved cartilage formation. [76] Unfortunately, co-culture research has mainly focused on articular cartilage repair. The effect of non-articular chondrocytes in co-culture, such as ear [77-79] or nasal chondrocytes (NCs) [80], are sadly underexposed, although they seem essential for cell-based cartilage repair in the head and neck area.

In depth understanding of the cellular interaction pathways between MSCs and chondrocytes is still under debate in literature: It is thought that the co-culture effect is either credited to (1) chondrocyte-driven MSC-differentiation or ascribed to (2) chondrocytes, whose cartilage-forming capacity and proliferation activity are enhanced in the presence of MSCs. [81] In recent years, the trophic and paracrine functions of MSCs appeared most critical in this process, rather than the simple chondrogenic differentiation of MSCs alone. However, little is known as to whether their trophic function is a general characteristic of MSCs or dependent on the origin of the MSC source.

Scaffolds

For successful cartilage regeneration, the properties of the 3D matrix are of equivalent importance: (1) it must provide temporary or permanent cell-support while maintaining size and shape when subjected to the forces of the implanted environment; and (2) it needs to mimic the natural microenvironment to provide specific structural, mechanical and biological cues to cells, which guide tissue remodelling. [82] Currently, several 3D-scaffolds have been developed and investigated for their use in cartilage tissue engineering. [83] They can be roughly classified into synthetic and natural scaffolds. Synthetic scaffolds that are most intensely studied in the field of cartilage tissue engineering are the biodegradable polymers, such as polylactic acid (PLA), polyglycolic acid (PGA), and their co-polymers. [84] Their main benefit is that they can be fabricated in large quantities under controlled conditions and have predictable and reproducible physical properties. Although these materials are advantageous to work with, they are prone to induce a foreign body reaction which can inhibit cartilage regeneration and lead to tissue extrusion. [83] Next to synthetic materials, natural scaffolds have been introduced, such as hydrogels (e.g. alginate, chitosan, collagen, gelatine, hyaluronic acid, fibrin), bacterial nanocellulose, and decellularized ECM. [85] Unlike synthetic scaffolds, natural polymers are distinguished by low risk of toxicity and a reduced foreign body reaction. [85] On the contrary, their properties are less reproducible and more heterogeneous. Also, purification issues relevant to clinical use, represent a major challenge. Unfortunately, to date, no ideal scaffold has emerged as a promising scaffold for future clinical application for cell-based cartilage repair in the head and neck area. This thesis focuses on natural scaffolds. In particular, this thesis focusses on the quality and suitability of alginate, bacterial nanocellulose and decellularized ECM for tissue-engineering purposes in the head and neck area.

Alginate is a hydrogel and formed from polysaccharides derived from brown algae. It consists of a mixture of β -D-mannuronic acid (M) and α -L-guluronic acid (G) residues. [86] Both cell adhesion and hydrogel stiffness can be influenced by M to G ratio. [87] Alginate mechanical stiffness is however low and range from 1 to 1000 kPa. [88] Although alginate itself

is too weak to withstand scar contraction forces after direct subcutaneous implantation, it enables a homogeneous cell distribution and prevents cells from floating out while permitting nutrient diffusion and oxygen transfer to the cells in order to create an environment to form new cartilage matrix with sufficient properties. [89] Therefore, alginate is an excellent cell-carrying gel for cell-based cartilage repair in the head and neck area.

Bacterial nanocellulose is the extracellular product of the *Gluconacetobacter xylinus* bacterium. These gram-negative aerobic bacteria produce pure nanocellulose fibrils in the presence of sugar and oxygen. [90] More recently, medical devices made from bacterial nanocellulose were introduced into the clinic as wound and burns dressings (e.g. Dermafill[®], Bioprocess[®], XCell[®] and Biofill[®]), surgical meshes (e.g. Xylos[®], Macro-Porous Surgical Mesh[®] and Securian[®]) and dura mater substitutes (Synthecel Dura Repair[®]). Bacterial nanocellulose is extremely hydrophilic and can hold as much as 100 times its dry weight of water. [91] This property, combined with the distinct physical and mechanical properties of bacterial nanocellulose, including its insolubility, rapid biodegradability, tensile strength, elasticity, durability, nontoxic and non-allergenic features, make bacterial nanocellulose a candidate biomaterial for cartilage TE in the head and neck area. [92]

Recently, natural acellular ECM scaffolds have become increasingly popular. These acellular ECM scaffolds are acquired by a process called decellularization: a method that requires chemical, physical and/or enzymatic treatments. [93] Decellularized ECM scaffolds provide a 3D ECM structure with immediate functional support without evoking an adaptive immune response upon implantation due to the absence of donor cellular antigens. [94] To date, various cartilaginous structures have already been decellularized including tracheal cartilage [94-99], articular cartilage [100-103], intervertebral discs [104, 105] and meniscal cartilage [106-109]. So far, little research has been executed on decellularized ECM in the head and neck area such as nasal cartilage [106, 110] or ear cartilage.

Inductive factors

Cartilage development and homeostasis is influenced by several inductive factors that induce, improve or accelerate cartilage regeneration. They include both biochemical and biophysical factors. (Reviewed by Wescoe *et al.* [111]) Growth factors, especially those from the Transforming Growth Factor beta family, Insulin-like Growth Factors and Fibroblast Growth Factors, are signalling factors most extensively investigated in cartilage tissue engineering. [112-114] These factors regulate cellular migration, adhesion, proliferation, differentiation, and cell survival, and ultimately improve cartilage formation and stability. [115] The easiest and most common way to deliver growth factors to the culture environment is through direct supplementation to culture media. However, the quantity and fast release of such inductive factors may impede cartilage regeneration. In order to more closely replicate the *in vivo* situation, inductive factors have been more gradually delivered using drug-eluting scaffolds or gene therapy. Still, further research needs to study efficacy and spatiotemporal kinetics of future delivery systems as well as safety and reliability of gene therapy. Recently, the endogenous delivery of inductive factors through co-culture was introduced. Mixed-cell-cultures provide cell populations that secrete trophic factors to regulate local cellular activity for cartilage regeneration more similar to normal cartilage development. [116]

Application of cartilage tissue engineering in clinical practice

In past decades, application of tissue-engineering technology on facial reconstructive surgery have markedly increased. However, cartilage regenerative medicine plays a relatively small role in current clinical practice (mainly in tracheal reconstruction [117] or articular joint resurfacing [118]) and have not yet been described for facial cartilage reconstruction. So far, only one study has reported proof-of-principle for human nasal reconstruction using tissue-engineered cartilage in five patients. [119] Assumedly, this opened the way to future clinical research of tissue-engineered facial cartilage and its utility in facial reconstructive surgery.

For translation toward clinical application of cell-based cartilage repair, it is important to provide an one-step surgical procedure rather than multistage surgery. Such a procedure aims to generate a tissue-engineered construct intraoperatively, prohibiting the need for *in-vitro* culture expansion. One-step surgery would not only improve patient safety and cost-effectiveness but also reduce the risk of regulatory and ethical issues related to *in-vitro* culture expansion.

THESIS AIM AND OUTLINE

Cartilage tissue engineering can offer promising solutions for restoring cartilage defects in the head and neck area and has potential to overcome limitations of current treatments. The primary objective of this thesis is to ultimately improve cartilage regeneration and develop an one-step surgical therapy for the repair of facial cartilage defects. Therefore, I focus on the generation of a cell-based cartilaginous framework and evaluate the suitability of *cells* or combination of cells on natural *scaffolds*.

Based on my objectives, the following research questions were formulated:

- Q1** What are the biomechanical and biochemical characteristics of native facial cartilages (i.e. ear and nasal cartilages)?
- Q2** Which cells or combination of cells are most suitable for cell-based cartilage repair in the head and neck area?
- Q3** Which natural scaffolds (i.e. alginate, bacterial nanocellulose, decellularized ECM) are a suitable candidate for future cell-based cartilage repair in the head and neck area?

Ideally, tissue-engineered cartilage should possess similar biomechanical and biochemical properties to the native tissue. **Chapter two and three** establish a precise biomechanical and biochemical characterization of native human ear and nasal cartilages (i.e. nasoseptal and alar cartilages) in order to set a benchmark against which to evaluate cartilage tissue engineering attempts.

For successful cell-based cartilage repair in the head and neck area, selection of an appropriate cell source is crucial. In **chapter four**, the performance of culture-expanded chondrocytes and MSCs from several anatomical locations (i.e. chondrocytes derived from ear, nose and joint, and MSCs derived from adipose tissue and bone marrow) is evaluated. Culture-expansion has however certain disadvantages: (1) it results in chondrocyte dedifferentiation, which usually results in fibrous and mechanically inferior cartilaginous tissue; (2) it requires a two-step surgical procedure. As the basic principle for the development of a one-step surgical repair procedure, co-cultures of primary chondrocytes and MSCs is further elucidated in **chapter five and six**. **Chapter five** describes the trophic effect of AMSCs or BMSCs on chondrocytes and whether their effect is origin-dependent or a general MSC-characteristic. **Chapter six** evaluates the use of ECs and NCs in combination with BMSC for their use in future one-step cell-based cartilage repair in the head and neck area.

For successful cartilage regeneration, the properties of the 3D scaffold are of equivalent importance. Scaffold design should herein substitute for the cell natural environment providing instantaneous cell support and guiding tissue development and remodelling. Intuitively, native ECM has the potential to be the most ideal scaffold for tissue engineering and regenerative therapies. Preservation of native ECM is best retained through the process of decellularization. **Chapter seven** displays the preparation of decellularized cartilage scaffolds and extensively characterize their biochemical and biomechanical properties, as well as investigate their cytocompatibility.

Another way to - at least partially - mimic structural and functional characteristics of native tissue microenvironment is the generation of ECM-inspired scaffolds. Alginate, typically used as a cell-laden hydrogel, is used for all of our cell-culture studies since it supports cartilage tissue regeneration and homeostasis. However, it appears to have inferior mechanical properties compared to native cartilage. Therefore a novel bilayer bacterial-nanocellulose scaffold is introduced in ***chapter eight***. These bacterial-nanocellulose scaffolds are seeded with an alginate-cell suspension and evaluated for their use in one-step cell-based cartilage repair.

Finally, the last chapter of the thesis will provide an overview of the main results and discuss the requirements for cell-based cartilage repair for future treatment of cartilage defects in the head and neck area. In particular, recent advances and remaining questions will be debated.

Cartilage properties

Chapter 2

Mechanical and biochemical mapping of human auricular cartilage for reliable assessment of tissue-engineered constructs

L. Nimeskern, M.M. Pleumeekers, D.J. Pawson, J.L.M. Koevoet, I. Lehtoviita, M.B. Soyka, C. Rösli, D. Holzmann, G.J.V.M. van Osch, R. Müller, K.S. Stok

Journal of Biomechanics, 2015. 48(10): p. 1721-9.

ABSTRACT

It is key for successful ear cartilage tissue-engineering to ensure that the engineered cartilage mimics the mechanics of the native tissue. This study provides a spatial map of the mechanical and biochemical properties of human auricular cartilage, thus establishing a benchmark for the evaluation of functional competency in ear cartilage tissue engineering. Stress-relaxation indentation (instantaneous modulus, E_{in} ; maximum stress, σ_{max} ; equilibrium modulus, E_{eq} ; relaxation half-life time, $t_{1/2}$; thickness, h) and biochemical parameters (content of DNA; sulfated-glycosaminoglycan, sGAG; hydroxyproline; elastin) of fresh human ear cartilage were evaluated. Samples were categorized into age groups and according to their harvesting region in the human auricle (for ear cartilage only).

Ear cartilage displayed significantly lower E_{in} , σ_{max} , E_{eq} , sGAG content; and significantly higher $t_{1/2}$, and DNA content than nasal cartilage. Large amounts of elastin were measured in ear cartilage (>15% elastin content per sample wet mass). No effect of gender was observed for either ear or nasoseptal samples. For auricular samples, significant differences between age groups for h , sGAG and hydroxyproline, and significant regional variations for E_{in} , σ_{max} , E_{eq} , $t_{1/2}$, h , DNA and sGAG were measured. However, only low correlations between mechanical and biochemical parameters were seen ($R < 0.44$).

In conclusion, this study established the first comprehensive mechanical and biochemical map of human ear cartilage. Regional variations in mechanical and biochemical properties were demonstrated in the auricle. This finding highlights the importance of focusing future research on efforts to produce cartilage grafts with spatially tunable mechanics.

INTRODUCTION

Surgical reconstruction with autologous cartilage or alloplastic implants is the only existing treatment for auricular defects. The current gold-standard technique - autologous ear reconstruction [120] - is a multi-staged time-consuming procedure [9, 121], that ranks among the most complicated of reconstructive surgeries [122]. In short, autologous cartilage is harvested from the ribs, shaped appropriately and implanted subcutaneously. Ear cartilage tissue-engineering (TE) is a potential alternative that endeavors to circumvent the resulting donor-site morbidity by engineering rather than harvesting cartilage. [58, 123-137]

Ideally tissue-engineered ear cartilage should possess similar mechanical properties to the native tissue in order to withstand daily load (e.g. wearing spectacles, helmets, ear phones, etc.) and without causing discomfort. [138] Selecting autologous material for ear cartilage surgical reconstruction is difficult, where donations come from the nasal septum, auricle and rib. Whether the graft qualifies mechanically for surgical implantation is usually made from simple palpation. Mechanical properties of hyaline (e.g. nasoseptal, costal, articular cartilage) and fibrocartilage (e.g. intervertebral disk) have been extensively documented. [139-141] The structure-function relationship linking composition and architecture to mechanical competency has been established for these cartilage subtypes. [140, 142] The mechanical properties of ear cartilage are, however, sparsely investigated [143], and limited data are available for human cartilage. [24, 138] Unlike hyaline and fibrocartilage, ear cartilage contains large amounts of elastin fibers. Those fibers play a mechanical role in tissues such as arteries and skin [144, 145], therefore the mechanical properties of ear cartilage are expected to vary from other cartilage types [138].

Mechanical evaluation has often been overlooked in ear cartilage TE attempts. Many authors [58, 123, 125-137] report a qualitative mechanical assessment, while a few publications report quantitative data but without comparison to human ear cartilage [146-150]. Indentation has been shown previously to be a good and sensitive first approximation for direct comparison between native and tissue-engineered constructs. [151]

In light of this, the aim of this work is to establish a mechanical characterization of native human ear cartilage in order to set a benchmark against which to evaluate TE constructs. Mechanical and biochemical properties of fresh ear cartilage are determined and compared to hyaline nasoseptal cartilage. Additionally spatial variation in mechanical properties, the influence of patient gender and age, and correlations between mechanical properties and biochemical composition are investigated.

MATERIALS AND METHODS

Chemicals were obtained from Sigma-Aldrich, USA unless stated otherwise.

Sample harvesting and preparation

Cadaveric auricles were harvested by Science Care (Phoenix, Arizona, USA, $n=4$) and Erasmus Medical Center (Rotterdam, the Netherlands, $n=11$) according to ethical guidelines of the respective institution. Additionally ear (EC) and nasoseptal (NC) cartilage was obtained from patients ($n=30$, EC; $n=69$, NC) undergoing middle ear or cholesteatoma surgery (EC) and functional septo- or septorhinoplasties (NC) at University Hospital Zurich (Zurich, Switzerland), and Ulm University Medical Center (Ulm, Germany) according to the ethics regulations of the respective institution. EC samples were harvested from 15 male and 12 female donors, NC samples were harvested from 40 male and 12 female donors. Samples were pooled according to anthropomorphic age (child, <20 years; young adult, 20–34; middle adult, 35–49; and old adult, ≥ 50). [152] All samples were shipped at 4°C in phosphate buffered saline (PBS) supplemented with antibiotic/antimycotic (Gibco, Invitrogen Corporation, California, USA) to ETH Zurich (Zurich, Switzerland). The perichondrium was removed from EC samples, and cylindrical plugs (5 mm, 1–2 mm thick) were cut perpendicular to the surface. Six harvesting regions were defined (anti-helix, AH; anti-tragus, AT; concha, CO; helix, HE; scapha, SC; tragus, TR). (Figure 1A) NC plugs were similarly prepared, where samples originated from the center of the nasal septum. (Figure 1B) Differences in sample number for biomechanical and biochemical assays is due to sample loss during processing, unusual sample shape preventing mechanical analysis or limitations of biochemical assays.

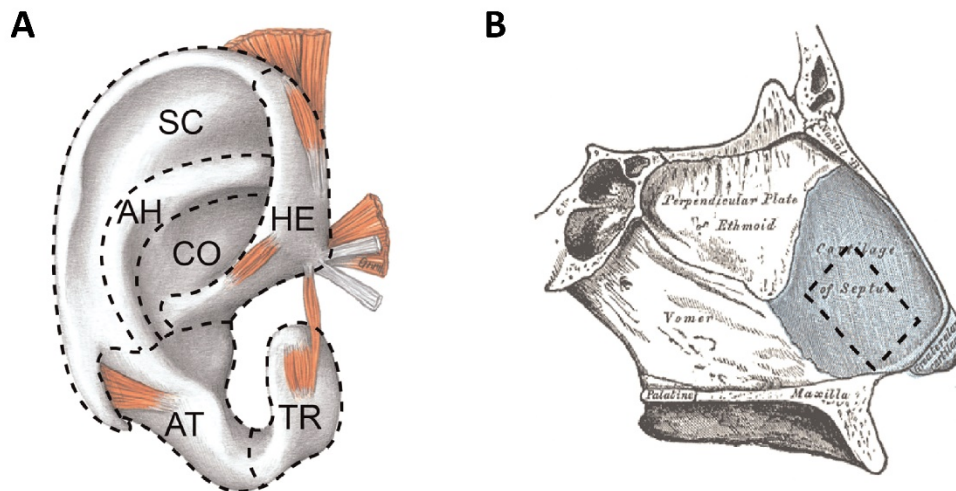


Figure 1. Anatomy of human ear and nasal septum.

(A) Map of the human auricle. Six harvesting regions are identified based on the ear morphology: anti-helix, AH, anti-tragus, AT, concha, CO, helix, HE, scapha, SC and tragus TR. Adapted from *Atlas der Anatomie des Menschen*, B.N. Tillmann, Springer-Lehrbuch. [153] **(B)** Harvesting site for nasoseptal cartilage. Adapted from *Gray's Anatomy of the Human Body*, Henry Gray. [154]

Mechanical evaluation

Cartilage samples (EC: $n=183$; NC: $n=103$) were placed in close-fitting stainless steel cylindrical wells, and tested with a materials testing machine (Zwick Z005, Ulm, Germany) equipped with a 10 N load cell, built-in displacement control, and a cylindrical, plane-ended, stainless steel indenter (0.35 mm). During testing samples were immersed in PBS supplemented with antibiotic/antimycotic, and stress relaxation indentation tests were performed at room temperature, as described previously. [155, 156] Briefly, a preload of 3 mN was applied to locate the sample surface and measure sample thickness, h , and held for 5 min. Five successive strain steps (5% of h per step) were applied, and specimens were left to relax for 20 min at each step. An in-house Matlab® script converted force and displacement data to stress and strain, and instantaneous modulus (E_{in}), maximum stress (σ_{max}), equilibrium modulus (E_{eq}), relaxation half life time ($t_{1/2}$) were determined. To estimate viscoelastic relaxation, $t_{1/2}$ is computed after the first strain application. It is defined as the time needed for stress to decrease from its maximum value halfway to its equilibrium value. [155]

Biochemical evaluation

Following mechanical testing, each sample was cut into two and frozen at -80°C until processing. Samples were defrosted, and wet weight of each half was measured. One half was digested overnight at 60°C with papain buffer (0.2 M NaH_2PO_4 , 0.01 M EDTA, pH 6.0 and freshly added 250 $\mu\text{g}/\text{mL}$ papain, and 5 mM L-cystein), and analyzed for DNA, sGAG, and hydroxyproline content. The second half was analyzed for elastin content.

DNA content

Amount of DNA (EC: $n=223$; NC: $n=153$) was determined by ethidium bromide (GibcoBR1), using calf thymus DNA as a standard. Samples were analyzed with a spectrofluorometer (Wallac 1420 Victor 2; Perkin-Elmer, Wellesley, USA), using an extinction (340 nm) and an emission (590 nm) filter. DNA content was normalized to sample wet mass.

Glycosaminoglycan content

Sulfated-glycosaminoglycan content (sGAG) (EC: $n=223$; NC: $n=154$) was quantified using the 1,9-Dimethylmethylene blue (DMMB) dye-binding assay, where metachromatic reaction was monitored using a spectrophotometer. Absorption ratios of 540 nm and 595 nm were used to determine sGAG content with chondroitin sulfate C (shark) as a standard. sGAG values were normalized to sample wet mass.

Hydroxyproline content

Hydroxyproline content was measured to estimate collagen quantity (EC: $n=189$; NC: $n=140$) using the Total Collagen Assay (QuickZyme Biosciences, Leiden, the Netherlands) according to the manufacturer's instructions. Briefly, papain digests were hydrolyzed with equal volumes of 12 M HCL at 95°C for 18–20 hours. Hydroxyproline content was measured using a modification of the Prockop and Udenfriend method [157], and normalized to sample wet mass.

Elastin content

Elastin content (EC: $n=48$) was measured using the Fastin Elastin Assay (Biocolor, Carrickfergus, UK) according to the manufacturer's instructions. Briefly, the sample was converted to water soluble α -elastin by three 12 hour heat extraction cycles at 100°C in 0.25 M oxalic acid before adding the kit's dye. Absorbance was measured at 513 nm on an Infinite F200 PRO (Tecan, Giessen, the Netherlands) plate reader. α -elastin from bovine neck ligament (from the manufacturer) was used as a standard. Elastin values were normalized to sample wet mass. Since NC samples contain no elastin [143], elastin was only quantified for EC samples.

Histology

EC samples from all ear regions and young and old adult age groups were embedded in OCT (Tissue-Teks O.C.T™ Compound, Sakura). Samples were cryosectioned at a 5 mm slice thickness and stained with Sirius red, Resorcin-Fuchsin and Safranin-O to visualize the collagen network, elastic fibers and sGAG, respectively.

Statistical analysis

A linear mixed-effect model, where donor was a random effect, and cartilage subtype, gender, age group and harvesting location were fixed effects, was used to analyze statistical differences between mechanical (E_{in} , σ_{max} , E_{eq} , $t_{1/2}$) and biochemical (DNA, sGAG, hydroxyproline) results. Additionally bivariate, correlation analyses between mechanical and biochemical parameters were performed for EC and NC samples. All calculations were performed with SPSS (version 22.0, IBM Corp., New York, USA). All data are displayed as mean \pm standard deviation, where * indicates significance ($p<0.05$).

RESULTS

Results show that subtype (EC or NC) is significantly different for all measured values (Ein, σ_{\max} , Eeq, $t_{1/2}$, DNA, sGAG), except hydroxyproline. (Figure 2) Measured values of Ein, σ_{\max} , Eeq, $t_{1/2}$, DNA, sGAG and hydroxyproline showed no significant differences between male and female sex for both EC and NC. All male and female data points were pooled for further analysis.

Due to the limited number of EC samples available in child and middle adult groups, only young adult and old adult groups were used to investigate age differences. Results indicate age dependent differences in h, sGAG and hydroxyproline (Figure 3E,G,H), where older adults had thicker EC and lower sGAG and hydroxyproline content. Age groups were pooled for all parameters showing nonsignificant effects of age, i.e. Ein, σ_{\max} , Eeq, $t_{1/2}$, DNA and elastin.

	Ein	σ_{\max}	Eeq	$t_{1/2}$	h	DNA	sGAG	HYP	ELN
Harvesting location	•	•	•	•	•	•	•		
Age					•		•	•	

Table 1.

Significant effects observed for ear cartilage samples. Corresponding values for each region and age group are displayed in Figure 3.

• Indicates significant differences, where $p < 0.05$.

All values except hydroxyproline and elastin showed significant differences with harvesting location. (Table 1) Regional variation patterns across the auricle were observed for Ein, σ_{\max} and Eeq (Figure 3A,B,C), where the helix (HE) values were lowest, and the anti-tragus (AT) highest. This was significantly different from all regions except the tragus (TR). A different pattern was observed for $t_{1/2}$ with slower relaxation measured in the AH and HE. (Figure 3D) AT was thickest, with little variation seen in other regions. (Figure 3E) Likewise biochemical properties (DNA and sGAG content) presented regional variations. (Figure 3F,G). DNA content was highest in the scapha (SC) and lowest in the AT and TR. The highest sGAG content was measured in the AT and TR. No regional variations were observed for hydroxyproline and elastin content. (Figure 3H,I)

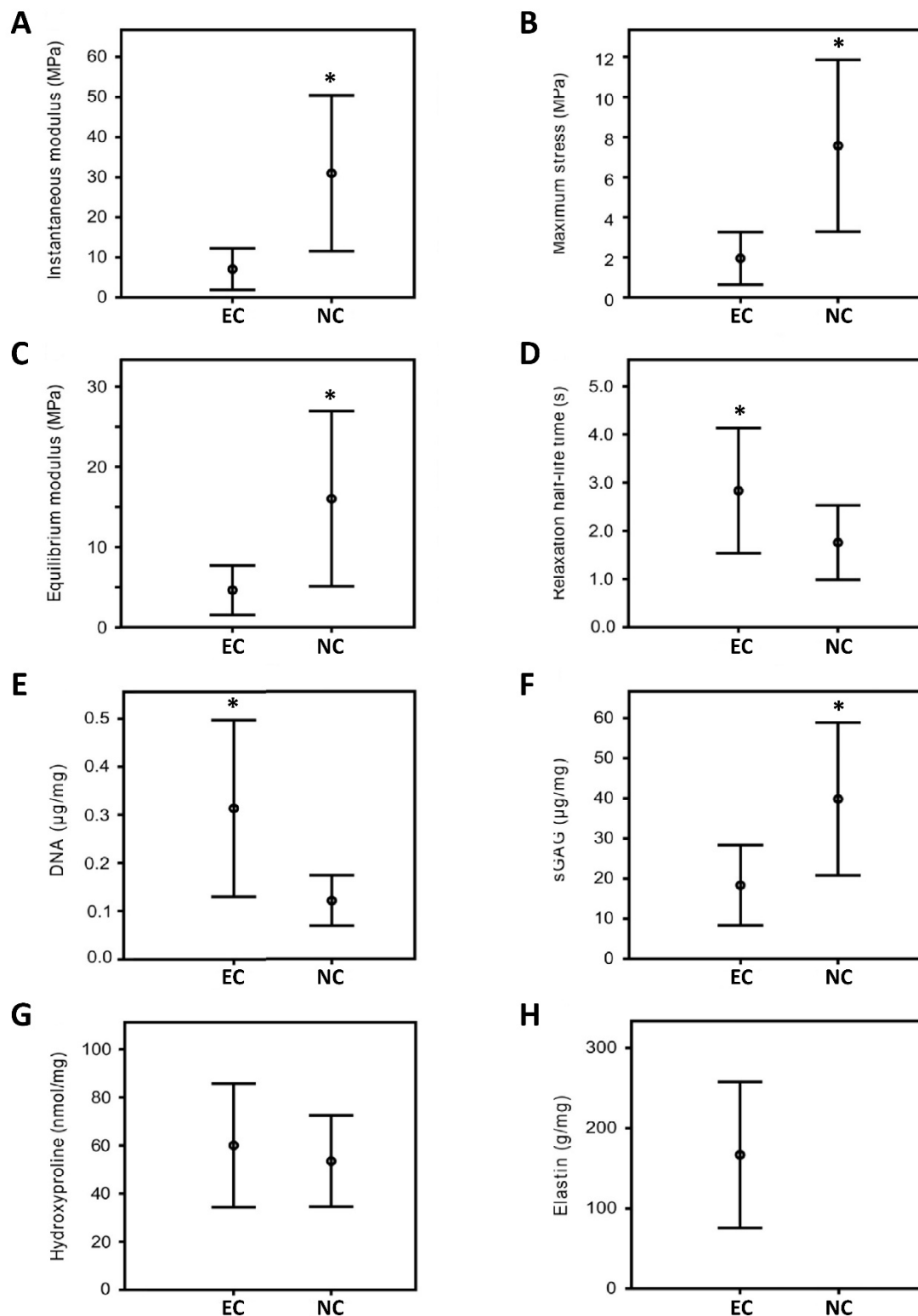


Figure 2. Mechanical and biochemical properties of ear and nasal cartilage.

(A–D) Summary of mechanical (E_{in} , σ_{max} , E_{eq} , $t_{1/2}$) and (E–H) biochemical parameters (DNA, sGAG, HYP and ELN) measured for ear and nasoseptal cartilage. Cartilage subtype is significantly different for all measured variables, except hydroxyproline ($p < 0.05$). As nasoseptal cartilage is known to contain no elastin [143], elastin is quantified for ear samples only.

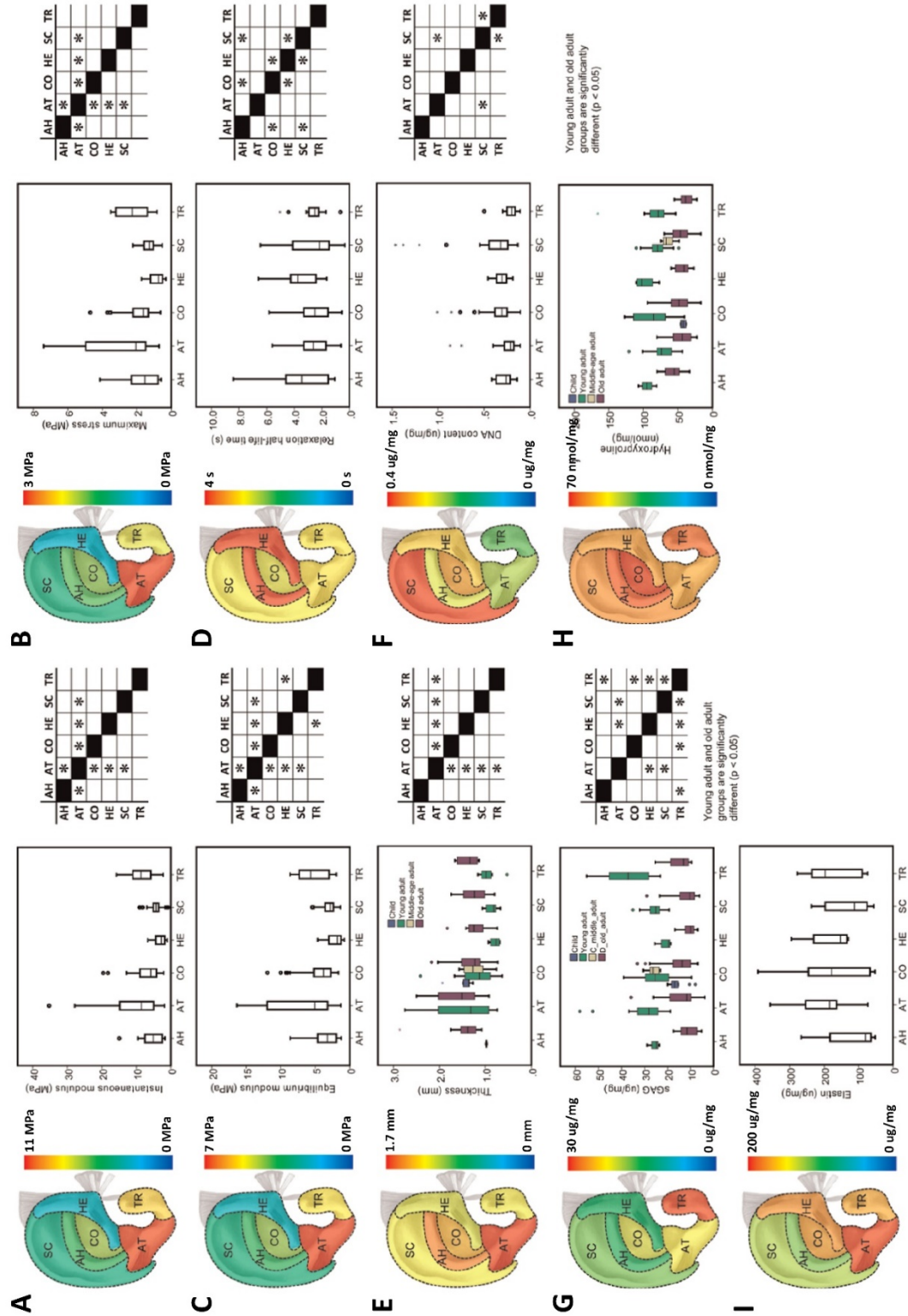


Figure 3.

(A–E) Summary of mechanical (E_{in} , σ_{max} , E_{eq} , $t_{1/2}$) and (F–I) biochemical parameters (DNA, sGAG, HYP and ELN) measured for ear cartilage. Harvesting location is significantly different for E_{in} , σ_{max} , E_{eq} , $t_{1/2}$, h , DNA and sGAG, as indicated by the tables adjacent to the graphs (* indicates $p < 0.05$). The color coded maps display the average values measured in each ear region. Age groups are significantly different for h , sGAG and hydroxyproline ($p < 0.05$), see (E, G and H). Samples for the child and middle-age adults age groups could only be obtained from the CO and the SC regions.

Similarly, NC samples showed no significant differences with age or gender for all measured parameters. Correlation coefficients between mechanical and biochemical parameters (Table 2) show that for EC, DNA, sGAG and elastin correlated significantly with Ein, σ_{\max} , Eeq, and DNA correlated significantly with $t_{1/2}$, and hydroxyproline with Ein. For NC, DNA correlated significantly with Ein, σ_{\max} , and Eeq, and sGAG correlated significantly with $t_{1/2}$. All correlations between mechanical and biochemical measures yielded low correlation coefficients; specifically, for Eeq and sGAG content, $R=0.32$, $p<0.05$, $n=171$, and for Eeq and elastin content, $R=0.44$, $p<0.05$, $n=41$.

<i>R</i>		h	DNA	sGAG	HYP	ELN
EC	Ein	0.55 [•]	-0.23 [•]	0.31 [•]	0.16 [•]	0.39 [•]
	σ_{\max}	0.61 [•]	-0.25 [•]	0.26 [•]	-0.10	0.44 [•]
	Eeq	0.54 [•]	-0.27 [•]	0.32 [•]	-0.10	0.44 [•]
	$t_{1/2}$	0.10	-0.24 [•]	-0.11	-0.02	-0.17
NC	Ein	0.48 [•]	-0.31 [•]	0.05	-0.03	-
	σ_{\max}	0.63 [•]	-0.33 [•]	0.07	-0.12	-
	Eeq	0.44 [•]	-0.25 [•]	0.04	-0.09	-
	$t_{1/2}$	-0.01	-0.18	-0.32 [•]	-0.10	-

Table 2.

Pearson coefficients (*R*) observed between the measured mechanical (Ein, σ_{\max} , Eeq and $t_{1/2}$) and biochemical parameters (DNA, sGAG, hydroxyproline and elastin) for EC and NC samples.

• Indicates significant differences, where $p<0.05$.

Sirius red, Resorcin-Fuchsin and Safranin-O staining of histological sections of native human EC for all ear regions and for young and old adult groups show high cell density in EC samples. (Figure 4) Lighter Safranin-O staining for old adult reflects lower sGAG content measured by the DMMB assay. (Figure 3)

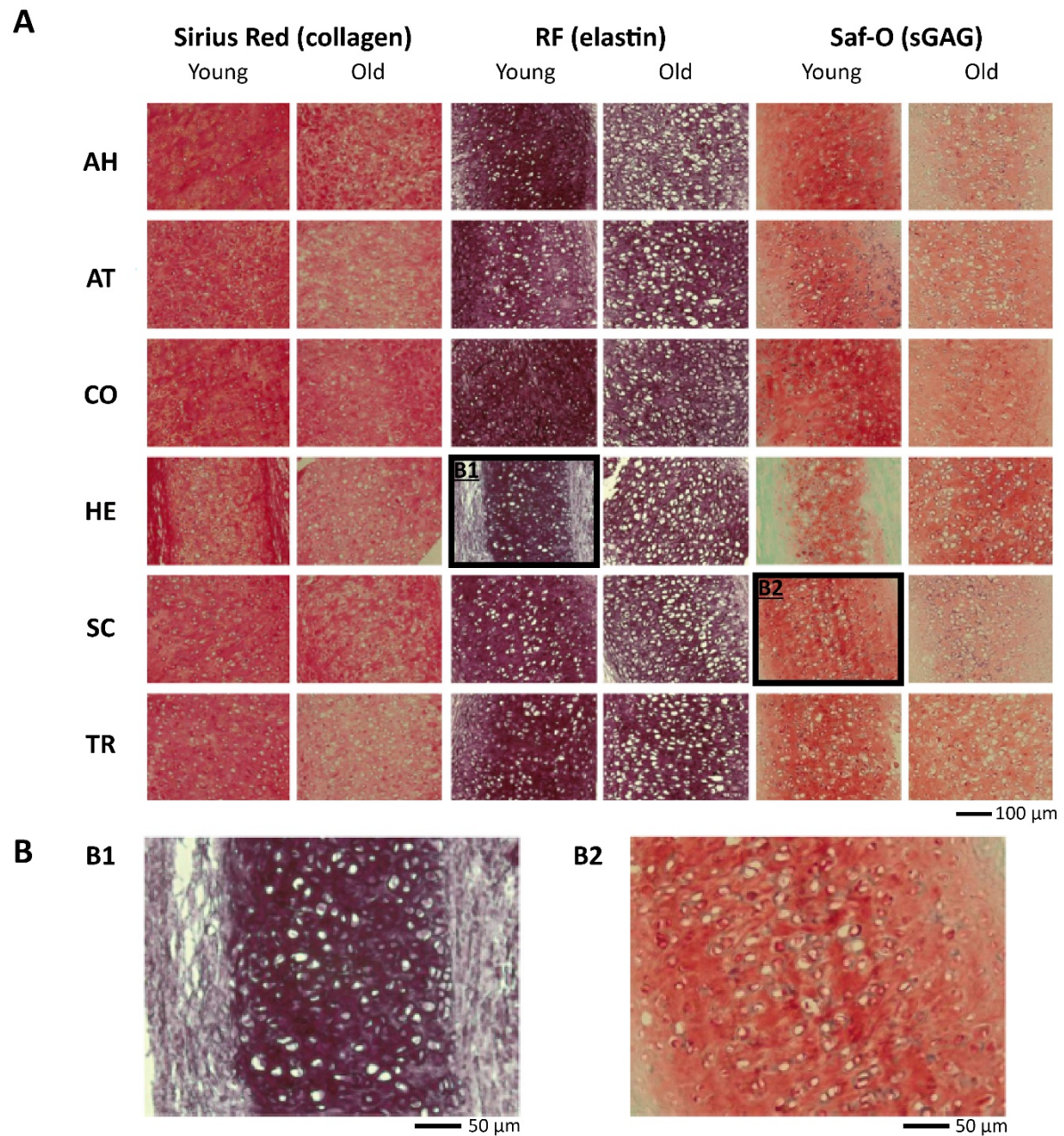


Figure 4. Histological staining of ear cartilage.

(A) Sirius red, Resorcin-Fuchsin and Safranin-O staining of histological sections of native human ear cartilage for all ear regions and for young and old adult age groups. The high cell density of ear cartilage can be observed **(B)**. The lighter sirius red and Safranin-O staining in the old adult samples reflect the lower collagen and sGAG content measured by DMMB assay (see Figure 3). The Resorcin-Fuchsin staining demonstrates the high elastin content of the cartilage and the surrounding perichondrium.

DISCUSSION

There has been a long and ongoing wish to cultivate human cartilage in a shape or manner that can be used in reconstructive and plastic surgery. Autologous material is preferred for grafting, and cartilage donations come from the nasal septum, auricle and rib. Surgically, clinicians or surgeons are looking for a material where the decision whether the graft qualifies for implant is usually made by palpation; i.e. compressive stiffness. Bending and tensile properties would be more reflective of functional material properties, but also require large sample dimensions. With growing interest in TE materials, the primary interest was to obtain a benchmark of mechanical performance against which to evaluate TE strategies, and therefore, a stress-relaxation indentation and biochemical map of human native ear cartilage is presented.

Ear cartilage has significantly lower strength, stiffness and sGAG content; and significantly higher relaxation time and DNA content compared to nasoseptal cartilage. Ear cartilage also contains >15% elastin content per sample wet mass; and significant differences between age groups were observed for thickness and matrix components (sGAG and hydroxyproline), and significant regional variations were observed for all mechanical parameters, DNA and sGAG content. Relatively large E_{eq} values (10–15 MPa) were measured for nasoseptal cartilage compared to typical values reported in literature for articular cartilage (1–2 MPa). [158] Although articular and nasoseptal cartilage are classified as hyaline, they present different architectures (no Benninghoff arcade in nasoseptal cartilage) and functions (articular provides joint lubrication and stress distribution, while nasoseptal cartilage provides mechanical support), which could explain the different moduli.

Stress-relaxation indentation is able to capture both instantaneous (E_{in}) and equilibrium behavior (E_{eq}) of cartilage. [159] In literature, reports of quantitative mechanics for TE constructs are given for confined compression [148, 160], unconfined compression [150] and tension [149, 161]. While no comparison can be made with tension, the indentation results in this study E_{eq} compare well with compressive equilibrium or apparent modulus in literature. TE constructs are inferior to native tissue, where all values are less than 1 MPa [146, 148, 150, 160] compared to 2.2 ± 1.2 MPa in the softest region (HE) up to 7.2 ± 4.7 MPa in the stiffest region (AT) in this work.

Chondrocytes from ear and nasoseptal cartilage have different proliferations rates and gene expression profiles. [40, 56] In this work, higher DNA and lower sGAG contents were observed in ear cartilage. Higher DNA content is likely a direct consequence of high cellularity [143], confirmed by histology. Hydroxyproline content, an indicator for collagen content, was not significantly different between ear (60.0 ± 25.7 nmol/mg) and nasoseptal cartilage (53.5 ± 19.0 nmol/mg), but nasoseptal cartilage displayed an almost two times higher sGAG content. The effect of this was observed mechanically; i.e. significantly higher E_{in} , σ_{max} , and E_{eq} in NC. Indeed sGAG side-chains are negatively charged, which generates an osmotic swelling pressure that attracts interstitial fluid. Under compression, load applied on hyaline cartilage is carried simultaneously by the solid matrix (collagen network with its fixed charge density) and resistance to fluid flow induced by compression. [162] Higher sGAG content observed in nasoseptal cartilage was consistent with higher mechanical properties. Ear cartilage, on the

other hand, presents a significantly higher $t_{1/2}$, again indicating that different mechanisms are at play in these cartilage subtypes; ear cartilage has a more elastic behavior, i.e. lower viscous dissipation of strain energy, and differences in architecture and composition. [143] The presence of elastin is most likely responsible for these differences.

Differences in post-maturity growth rate of the auricle between male and female donors have been reported in literature [163], however this was not reflected in the parameters measured here, where no significant differences were observed. For the purpose of establishing a benchmark for TE ear cartilage, a distinction between male and female is considered unnecessary.

Within ear cartilage samples, significant age-related differences were identified. Increasing h with age was observed while sGAG and hydroxyproline contents decreased. Age-related augmentation of tissue thickness is consistent with previous reports of continued growth of the auricle during adult life. [163-165] This is likely due to altered quality of the fiber network, specifically elastic fibers become increasingly fragmented and heterogeneous with age. [164] Additionally, cleavage of collagen fibers has been linked in articular cartilage to increased thickness [166], and a similar mechanism could exist in ear cartilage. Age-related decreases in sGAG and hydroxyproline content were not reflected in mechanical properties. While sGAG and collagen fiber network are known to govern mechanical behavior in articular cartilage [162], it is hypothesized that in ear cartilage the contribution of sGAG and collagen to mechanical properties is reduced due to the elastin network. A large contribution would likely come from this extensive network, since it is mechanically critical in other tissues. [144, 145] Elastin is responsible for elasticity in human skin [144], elastic recoil of lung tissue [167], and reversible extensibility in large elastic arteries [168].

Measured parameters were observed to vary significantly between different regions of the ear; where AT was stiffest and HE was softest. DNA and sGAG content displayed similar variations, with correlative trends to mechanical parameters. No regional variations were observed for hydroxyproline and elastin content. This suggests that unlike hyaline cartilage, an altered mechanical–chemical–architectural relationship exists in elastic cartilage, and tissue composition alone cannot fully explain local mechanics. Literature on hyaline cartilage [158, 159, 162, 169-175] supports the idea that ear cartilage mechanics are linked to architecture and composition. Functionally, specific local mechanical properties are necessary for three dimensional structure. The human auricle has large vestigial musculature anchoring the head (extrinsic) and connecting regions of the auricle (intrinsic). [122] Local variation highlights the need for TE strategies aimed at producing scaffolds and grafts with spatially tunable mechanics. [155] However since these differences are quite small it may also be worth investigating whether thickness variation is sufficient to provide the necessary mechanical integrity in TE constructs.

Significant correlations, despite weak Pearson coefficients, were observed between biochemical and mechanical parameters. sGAG content has been linked to mechanical behavior in articular cartilage [162], while DNA content does not. Nonetheless, higher cell density implies that extracellular matrix occupies a lower volume fraction, and assuming that chondrocytes present lower mechanical properties than the matrix [176], increased cell density would result in lower mechanics and explain the negative correlations.

Limitation of this work includes the lack of control of sample thickness during preparation, since perfectly cylindrical samples cannot be obtained. Indentation testing [158] requires a well-defined surface only around the indenter; and since maximizing sample number was key, the sample height was kept to that with only the perichondrium removed. Although significant correlations were observed between thickness and mechanical properties (R between 0.4 and 0.7, $p < 0.05$, Table 2), sample and indenter geometries were used which limit their bias on measured properties. [177] The test setup could additionally be modeled using an appropriate finite element approach. Since ear cartilage displays a different tissue composition and architecture to articular cartilage, it cannot be assumed that models used for articular cartilage would yield relevant results for ear cartilage. Only very recently, a first model has been proposed for ear cartilage. [24]

Furthermore, tests were performed at room (20°C) rather than physiological (37°C) temperature. Literature indicates no change in mechanical properties for articular cartilage between 20°C and 37°C [178], and room temperature is routinely used [179].

Although numerous attempts to develop tissue-engineered ear cartilage have been reported, nearly no data is available on the native mechanical properties. One reason is likely the difficulty accessing fresh tissue. Although samples obtained for this work were collected over four years, it was not possible to obtain equal sample numbers for all groups. Additionally, hydroxyproline content as an indicator of collagen content is not ideal since both collagen and elastin contain hydroxyproline (12.5% and 2% of protein mass respectively [180], therefore a fraction of hydroxyproline measured in ear cartilage is due to elastin.

In conclusion, this study establishes the first mechanical and biochemical map of human ear cartilage, enabling reliable assessment of engineered ear cartilage sufficient to sustain daily loading, while also ensuring cartilage grafts are not stiffer than necessary. The extensive elastic fiber network of ear cartilage is a key functional component. Regional variations are demonstrated, and biochemical composition alone does not fully account for observed mechanical variation indicating a probable contribution from local architecture. It would be of interest, in future, to have numerical models for ear cartilage and an understanding of the role of elastin. (Table 3)

Acknowledgements

The authors would like to thank the donors and their families who enabled this research, and Prof. dr. G.J. Kleinrensink, Y. van Steinvoort and B.J. Korstanje (Department of Anatomy and Neuroscience, Erasmus MC, University Medical Center, Rotterdam, the Netherlands) and dr. N. Rotter (Department of Otorhinolaryngology, Ulm University Medical Center, Ulm, Germany) for their assistance in obtaining human donor tissue. This study was supported by the Swiss National Science Foundation (NRP63) and ERA-NET/EuroNanoMed (EAREG-406340-131009/1).

	Ein (MPa)	σ_{\max} (MPa)	Eeq (MPa)	$t_{1/2}$ (s)	Thickness (mm)	
					Young adult	Old adult
AH	5.57 ± 3.77	1.65 ± 1.01	3.57 ± 2.05	3.62 ± 2.28	0.98 ± 0.02	1.48 ± 0.48
AT	11.02 ± 8.39	3.11 ± 2.06	7.23 ± 4.70	2.73 ± 1.21	1.47 ± 0.68	1.62 ± 0.46
CO	6.98 ± 3.74	1.87 ± 0.85	4.48 ± 2.23	2.55 ± 1.19	1.20 ± 0.42	1.32 ± 0.35
HE	3.27 ± 1.84	0.87 ± 0.47	2.22 ± 1.21	3.62 ± 1.61	0.79 ± 0.12	1.24 ± 0.33
SC	4.59 ± 1.85	1.33 ± 0.41	3.07 ± 0.98	2.63 ± 1.66	0.86 ± 0.13	1.24 ± 0.26
TR	8.61 ± 3.72	2.21 ± 0.97	5.40 ± 2.42	2.68 ± 1.07	0.95 ± 0.20	1.38 ± 0.22

	DNA ($\mu\text{g}/\text{mg}$)		sGAG ($\mu\text{g}/\text{mg}$)	Hydroxyproline (nmol/mg)		Elastin ($\mu\text{g}/\text{mg}$)
		Young adult	Old adult	Young adult	Old adult	
AH	0.28 ± 0.08	25.72 ± 2.79	10.78 ± 4.01	94.17 ± 13.23	63.10 ± 19.73	121.41 ± 87.42
AT	0.25 ± 0.14	30.94 ± 11.08	14.39 ± 7.07	73.33 ± 19.88	55.24 ± 21.46	207.89 ± 86.84
CO	0.34 ± 0.15	25.03 ± 7.59	15.05 ± 6.83	88.62 ± 27.23	65.13 ± 29.67	176.96 ± 107.79
HE	0.31 ± 0.08	20.84 ± 3.19	10.66 ± 2.84	97.83 ± 15.31	55.78 ± 26.77	182.21 ± 76.33
SC	0.40 ± 0.28	25.77 ± 4.18	11.98 ± 5.03	79.75 ± 17.52	57.54 ± 21.54	132.59 ± 69.66
TR	0.21 ± 0.09	37.07 ± 10.63	15.08 ± 5.57	88.14 ± 36.98	61.42 ± 36.23	174.69 ± 89.75

Table 3.

Mean ± standard deviation measured for mechanical (Ein, σ_{\max} , Eeq and $t_{1/2}$) and biochemical parameters (DNA, sGAG, hydroxyproline and elastin) for ear samples.

Chapter 3

Structural and mechanical comparison of human ear, alar and septal cartilage

E.J. Bos, M.M. Pleumeekers, M. Helder, N. Kuzmin, K. van der Laan, M.L. Groot, G.J.V.M. van Osch, P.P.M. van Zuijlen

Plastic and Reconstructive Surgery Global Open, 2018. 6(1): p. 1-9.

ABSTRACT

In the human ear and nose cartilage plays a key role in establishing its form and function. Interestingly, there is a noticeable paucity on biochemical, structural and mechanical studies focussed on facial cartilages. Such studies are needed to provide elementary knowledge that is useful for tissue engineering of cartilage. Therefore, in this study a comparison is made of the biochemical, structural and mechanical differences between ear, ala nasi and septum on the extracellular matrix level.

Cartilage samples were harvested from cadaveric donors ($n=10$). Each sample was indented 10 times with a nano-indentor to determine the effective Young's modulus. Structural information of the cartilage was obtained by Multiple-photon laser scanning microscopy capable of revealing matrix components at subcellular resolution. Biochemistry was performed to measure sulphated-glycosaminoglycan (sGAG), DNA, elastin and collagen content.

Significant differences were seen in stiffness between ear and septal cartilage ($p=0.011$), and ala nasi and septal cartilage ($p=0.005$). Elastin content was significantly higher in ear cartilage. Per cartilage subtype, effective Young's modulus was not significantly correlated with cell density, sGAG or collagen content. However, in septal cartilage, low elastin content was associated with higher stiffness. Laser microscopy showed a distinct difference between ear cartilage and cartilage of nasal origin.

Proposed methods to investigate cartilage on the extracellular level provided good results. Significant differences were seen not only between ear and nasal cartilage but also between the ala nasi and septal cartilage. Albeit its structural similarity to septal cartilage, the ala nasi has a matrix stiffness comparable to ear cartilage.

INTRODUCTION

Cartilage plays a key role with respect to form and function of facial features. When cartilage of the nose or ear is damaged by injury it does not have the capacity to regenerate. This means that an ear or nose remains mutilated once its cartilage structure is disrupted. A reconstructive procedure is then necessary to create a new framework with a good three-dimensional (3D) structure capable of withstanding normal mechanical forces. Practically, the reconstruction of the ala nasi or minor ear defects is most often performed using auricular or septal cartilage grafts. [181, 182] In more extensive cases costal cartilage can be used, offering more material for harvest and providing a more rigid support. Ear, septal or costal cartilage can be used for reconstruction but the availability of material for transplantation is generally limited and donor site morbidity remains a risk. This is especially the case in burn patients who often suffer from extensive damage to the nose and ears due to their protruded position and thin skin coverage. [181, 183, 184] As such, regenerative medicine offers exciting possibilities to overcome these problems. New developments in the field of tissue engineering have already found their way to the clinic. Yanaga and colleagues for example performed several clinical experiments in which newly developed cartilage from autologous chondrocytes isolated from the ear was used for ear framework reconstruction. [182, 185] With increased attention for tissue engineered alternatives we need structural information on the tissues we are seeking to replicate. However, there is little data in literature on the mechanical characteristics and differences in composition and structure between the various facial cartilage types, in particular the ear, alar and septal cartilage.

Although they share a common embryonic origin, facial cartilage soon differentiates into distinct cartilage subtypes according to their specific structural function. In the early stage of developing vertebrates, the embryonic region that is to become the head and neck is transiently divided into segments known as the pharyngeal arcs (PA's). The ear has a combined origin and is derived from PA1 and PA2 that form the hillocks of His at six weeks development. Eventually these six hillocks fuse together to form the outer ear. [186, 187] PA1 grows further outwards to form the lower mandibular process and upper maxillary process. The latter later forms the frontal prominence and the medial and lateral nasal processes which will form into the alar nasi and after final fusion into the septum. [188]

Mature ear cartilage consists of an intricate network of elastin fibers and collagen bundles surrounded by a layer of perichondrium. This high elastin content makes it unique among the various cartilage subtypes in the facial region. The anatomy of the human nose on the other hand consists of several separate structural elements. A major part is the septum providing support for the bridge of the nose and on either side the septolateral and lobular cartilages to support the ala nasi. The lateral area further comprises of several sesamoid cartilages and accessory cartilages. In contrast with ear cartilage, the nasal structures are all made of hyaline cartilage. Hyaline cartilage consists mainly of collagen, in particular type II and is divided into several zones. [189]

The extracellular matrix (ECM) structure and its biochemical composition are essential to the mechanical function of cartilage. Standard biochemistry assays can be used to determine the concentration of the main tissue components. In order to visualise the 3D

structure of the ECM, multiple-photon laser scanning microscopy has been used for other tissues such as articular cartilage. [190] This method is capable of revealing essential matrix components i.e. chondrocytes, collagen and elastin fibers, label-free, with sub-cellular resolution and deep penetration. [191]

The reported stiffness of facial cartilage types varies considerably. Because different techniques are used to measure the cartilage it is difficult to give a general value. Besides tensile or indentation measurements having different limitations and advantages [192], it is also important to discern the different magnitudes or scale of mechanical testing. For the assessment of gross mechanical traits, important for maintaining of large shapes especially in surgical reconstruction, various techniques have been described. [26, 29, 147, 160] The same applies for atomic force microscopy (AFM), where extensive research has been conducted on surface micro mechanics of cartilage. [193-195] However, the mechanical conditions of the scaffold's cellular environment, between AFM and gross mechanical testing have important influence on the behaviour of cells [196] and as such are fundamental to adequate regeneration of cartilage [158]. Therefore, insight in the local mechanical properties and structure on the ECM level is required to provide the right environment for cell differentiation. The device used in this study allows indentation on the micrometre scale at higher depth ranges providing essential mechanical information on the different cartilage subtypes.

Understanding the fundamentals of tissue structures is essential for adequate tissue engineering. From practice, surgeons are familiarized with the gross mechanical traits of cartilage in reconstructive surgery. Mechanical behaviour however is essentially determined on the microscopic scale through an intricate symbiosis of cells and their surrounding structures. In this paper, we aim to provide fundamental information on the differences between the facial cartilage types on a structural and mechanical level with the use of novel technology to evaluate these parameters on the ECM level. Although without direct practical implications, it may also offer surgeons new insights and inspiration in optimizing their reconstructive efforts by providing better understanding on the nature of the tissues they work with. With the advancement of regenerative medicine, surgeons will come to a point where this knowledge will prove invaluable.

MATERIALS AND METHODS

Chemicals were obtained from Sigma-Aldrich, USA unless stated otherwise.

Samples

Cartilage samples were harvested from fresh frozen cadaveric donors ($n=8$ male; $n=2$ female), average age 66.5 ± 6 years at UMCU (University Medical Center of Utrecht, the Netherlands) according to the ethical guidelines of the institution. From each donor 2 adjacent samples from the ear concha, medial nasoseptal cartilage and lateral alar cartilage were removed with a 4 mm biopsy puncher. The samples were shipped at -20°C to either the VUmc (Vrije Universiteit Medical Center, Amsterdam, the Netherlands) for biomechanical and microscopic evaluation or EMC (Erasmus Medical Center, Rotterdam, the Netherlands) for biochemical evaluation. Samples were thawed prior to experiments and remaining tissue and perichondrium were surgically removed.

Indentation

To determine mechanical properties indentation measurements were performed using a novel commercial nano-indenter (Piuma, Optics11, the Netherlands). The device utilizes a ferrule-top cantilever probe [197] to apply load and simultaneously measure indentation depth using a fiber optic based readout. (Figure 1A and C) In this set up a $78\text{ }\mu\text{m}$ diameter spherical probe was used capable of applying forces ranging from $0.1\text{ }\mu\text{N}$ to 7.5 mN at indentation depths ranging 1 to $17\text{ }\mu\text{m}$. Cantilever bending calibrations were performed prior to each series of experiments by indenting a rigid surface and equating cantilever bending to probe displacement. Each sample was indented 10 times on the same anatomical location in a grid pattern with $100\text{ }\mu\text{m}$ distance between measurements. The resulting stress strain curves (Figure 1B) were analysed using the mathematic model derived by Oliver and Pharr for a spherical indenter to determine the effective Young's modulus (E^*). [198] The indentation protocol was carefully optimized to minimize viscoelastic effects from influencing the measurements. (Data not shown)

Biochemical evaluation

Prior to biochemical analysis, wet weight was determined of all cartilage samples which were then digested overnight at 60°C in a papain solution ($0.2\text{ M Na}_2\text{H}_2\text{PO}_4$, $0.01\text{ M EDTA}\cdot 2\text{H}_2\text{O}$, $250\text{ }\mu\text{g/mL}$ papain, 5 mM L-cystein , $\text{pH } 6.0$). The amount of DNA measured in each papain-digested cartilage sample was determined by Ethidium bromide (GibcoBR1), using calf thymus DNA as a standard. Samples were analysed with a spectrofluorometer (Wallac 1420 Victor 2; Perkin-Elmer, Wellesley, USA), using an extinction filter (340 nm) and an emission filter (590 nm).

A 1,9-Dimethylmethylene Blue (DMMB; $\text{pH } 3.0$) assay was performed to measure the sulphated-glycosaminoglycan (sGAG) content in each papain-digested cartilage sample. The metachromatic reaction of DMMB was monitored using a VersaMax spectrophotometer at 530 and 590 nm . Shark chondroitin sulphate C was used as a standard.

Hydroxyproline content was measured to estimate collagen quantity using the Total Collagen Assay (QuickZyme Biosciences, Leiden, the Netherlands) according to the manufacturer's instructions. Briefly, papain digests were hydrolysed with equal volumes of 12 M HCL at 95°C for 18–20 hours. Hydroxyproline content was measured using a modification of the Prockop and Udenfriend method [157], and normalized to sample wet mass.

Elastin content of the cartilage samples was measured using the FastinTM Elastin Assay (Biocolor, Carrickfergus, UK) according to manufacturer's instructions. Briefly, cartilage samples were converted to water-soluble α -elastin by 3 overnight heat extraction cycles at 100°C in 0.25M oxalic acid before adding the kit's dye. Absorption was measured at 513 nm on a VeraMax plate reader. α -elastin from bovine neck ligament (provided by manufacturer) was used as a standard.

Multiphoton Microscopy

Structural information of the cartilage was obtained by Multiple-photon laser scanning microscopy using intrinsic optical signals from unprocessed cartilage. The imaging setup consisted of a commercial two-photon laser-scanning microscope (2PLSM, TrimScope I, Lavision BioTec GmbH) and a femtosecond laser source. (Figure 1D) The laser source was a femtosecond Ti-sapphire laser (Coherent Chameleon Ultra II) generating ~200 femtosecond pulses at 800 nm with linear polarization and repetition rate of 80 MHz. The laser beam was focused on the cartilage sample by a 25 \times /1.10 large N.A. water-dipping objective (Nikon APO LWD), providing transverse resolution ~0.5 μ m and axial resolution of ~2 μ m. The laser power on the sample was adjusted in the range 5–50 mW to attain sufficient signal-to-noise ratio and avoid tissue photodamage. The laser beam was transversely scanned over the sample by a pair of galvo mirrors. Depth scanning was accomplished by moving the objective with a stepper motor.

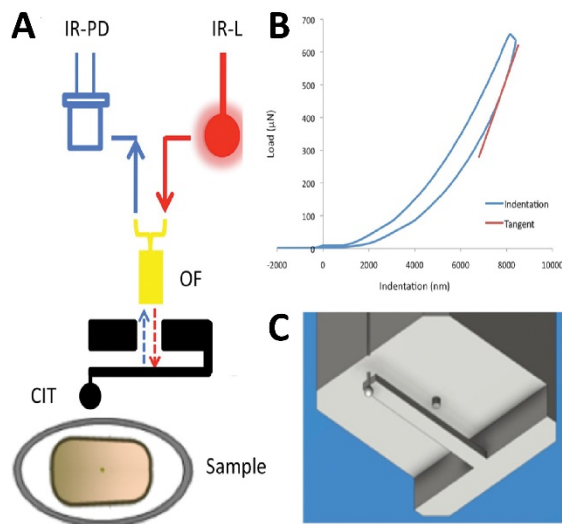
The second harmonic (SHG) and two-photon fluorescence (2PF) photons were generated by collagen (SHG, 2PF) and elastin (2PF) fibers as well as by intracellular auto-fluorescent proteins and were collected in the epi-detection geometry. The SHG and 2PF photons were filtered from the 800 nm excitation photons by a dichroic mirror (Chroma T695lpxrt), then split into SHG and 2PF channels by a dichroic mirror (Chroma 425lp), passed through interference filters for SHG (Chroma Z400/10X) and 2PF (Chroma HQ500/140M-2P) and detected by high-sensitivity GaAsP photomultiplier tubes (Hamamatsu H7422-40). (Figure 1 E,F)

Data acquisition was performed with the TriMScope I software ("Inspector Pro"), images stacks were stored in 16-bit tiff-format and further processed and analysed with "ImageJ" software (MacBioPhotonics).

Statistical analysis

Biochemical differences were analysed using Mixed Models with Bonferroni correction. Differences in effective Young's modulus between groups were determined through Generalized Estimating Equations. To measure the correlation between stiffness and biochemical content a Bivariate Correlations Model was used. All analyses were performed using PASW Statistics 22.0 (SPSS inc. Chicago, USA). A *p*-value of less than 0.05 was considered significant.

Indentation



Microscopy

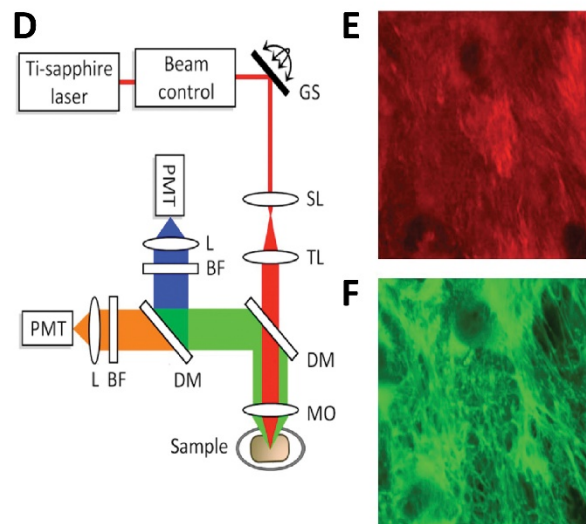


Figure 1. Overview of indentation and multi-photon laser microscopy technology.

(A) Set-up of cantilever indentation device. (B) Example of indentation curve of a cartilage measurement. Red tangent represents the slope of the unloading curve to determine the effective Young's modulus. (C) Graphic detail of the indenter tip. The ball forms the tip of the indenter (\varnothing 78 μ m). (D) Optical set-up of multi-photon laser-scanning microscope TriMScope I. (E) SHG channel showing collagen bundles. (F) 2PF channel showing elastin fibers. IR-PD = Infrared laser diode ; IR-L = Infrared laser ; OF = Optical Fiber ; CIT = Cantilever Indentation Tip. Ti = Titanium ; GS = X-Y Galvo Scanner mirrors ; SL = Scan Lens ; TL = Tube Lens ; DM = Dichroic Mirror ; MO = Microscope Objective ; BP = Band-Pass filters ; L = Lenses in front of the PMTs ; PMT = PhotoMultiplier Tubes.

RESULTS

Indentation

Indentation revealed significant differences ($p=0.011$) in stiffness between ear cartilage (1.14 ± 0.71 MPa) and septal cartilage (2.65 ± 1.78 MPa), and ala nasi cartilage (1.26 ± 0.51 MPa), and septal cartilage ($p=0.005$). (Figure 2) Comparison of ala nasi with ear cartilage showed no significant differences however. The stiffness per cartilage type varied considerably between donors. (Data not shown)

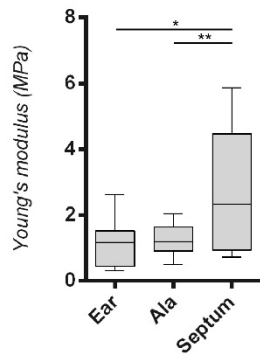


Figure 2. Biomechanical properties of ear, alar and septal cartilages.

Indentation revealed significant differences in stiffness between ear cartilage and septal cartilage ($*p=0.011$), and ala nasi cartilage and septal cartilage ($**p=0.005$). No significant differences between ala nasi and ear cartilage were seen.

Biochemistry

Cell density based on DNA content was significantly higher in ala nasi cartilage (2.35 ± 1.20 $\mu\text{g}/\text{mg}$ dry weight) than in cartilage from the ear (1.13 ± 0.23 $\mu\text{g}/\text{mg}$ dry weight) or septum (0.94 ± 0.52 $\mu\text{g}/\text{mg}$ dry weight) ($p=0.005$ and $p=0.001$ respectively). (Figure 3A) Auricular cartilage (141.40 ± 27.2 $\mu\text{g}/\text{mg}$ dry weight) had a significantly higher elastin content than ala nasi (60.12 ± 18.35 $\mu\text{g}/\text{mg}$ dry weight) and septum (17.38 ± 16.71 $\mu\text{g}/\text{mg}$ dry weight). (Figure 3B) Water and collagen content were not significantly different between the cartilage types. (Figure 3C) In the nose, septum (96.00 ± 23.21 $\mu\text{g}/\text{mg}$ dry weight) appeared to have slightly higher sGAG content (than ala nasi (64.61 ± 30.42 $\mu\text{g}/\text{mg}$ dry weight)). (Figure 3D)

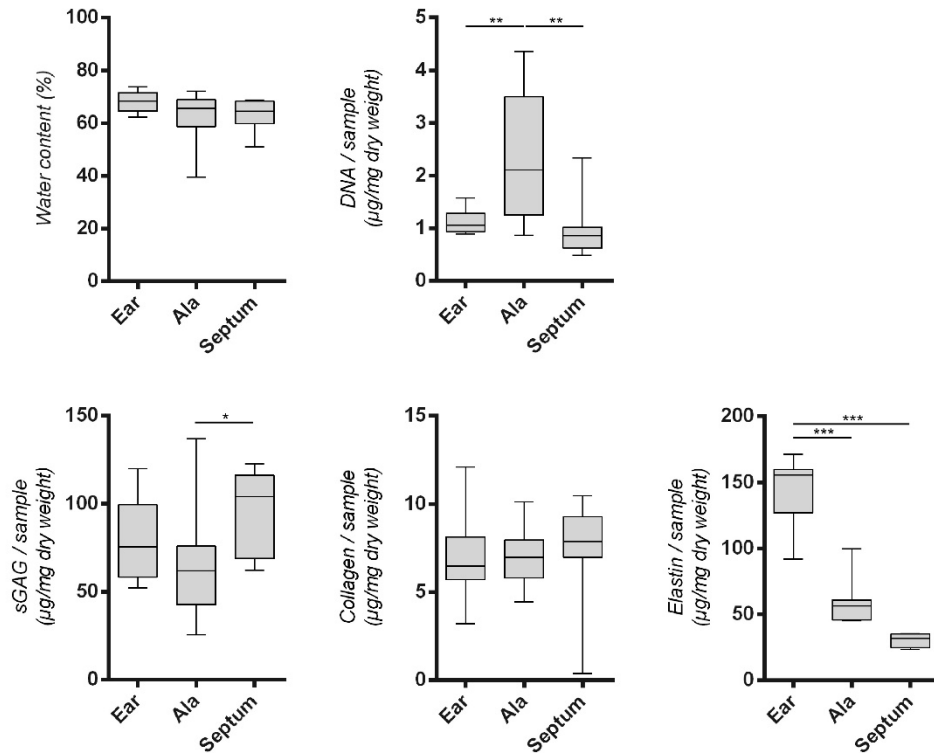


Figure 3. Biochemical analysis shows distinct differences in composition between cartilage types.

Although ala nasi cartilage and septum bear strong similarities in tissue architecture they significantly differ in DNA and sGAG content ($p=0.001$ and $p=0.024$ respectively). The nasal cartilages contain very limited elastin. This might be partially attributable to connective tissue remnants though caution was taken to remove these as much as possible. *, ** or *** indicates p-value smaller than 0.05, 0.01 or 0.001 respectively compared to the other cartilage types.

Per cartilage subtype, the effective Young's modulus was not significantly correlated with cell density, sGAG or collagen content. However, in septal cartilage, low elastin content was associated with higher stiffness. (Table 1)

Multiphoton Microscopy

The cartilage samples of two donors were imaged in the mid segment in the sagittal plane. The second harmonic (SHG) and two-photon fluorescence (2PF) microscopy generated showed a distinct difference between ear cartilage and the cartilage of nasal origin. (Figure 4) Not only the absence of elastin fibers (green) was evident, also the general structure of nasal cartilages was different from the ear. Cartilage from the nasal area gives a much more diffuse image compared to the dense fibrous network of the ear cartilage. Chondrons, agglomerates of chondrocytes within their pericellular matrix, appeared larger in the ala nasi than in the septum in both donors.

<i>Young's modulus</i>		DNA	sGAG	COL	ELN
Ear	<i>R</i>	0.040	-0.302	0.080	0.096
	<i>p</i>	0.913	0.396	0.826	0.838
	<i>n</i>	10	10	10	7
Ala nasi	<i>R</i>	-0.427	0.327	-0.549	-0.217
	<i>p</i>	0.219	0.357	0.100	0.641
	<i>n</i>	10	10	10	7
Septum	<i>R</i>	0.405	0.105	0.408	-0.951 [•]
	<i>p</i>	0.246	0.774	0.242	0.049
	<i>n</i>	10	10	10	7

Table 1.

Pearson coefficients (*R*) observed between the measured Young's modulus and biochemical parameters (DNA, sGAG, COL and ELN) for ear, ala nasi and nasoseptal cartilage samples.

• Indicates correlation is significant at a 0.05 level (2-tailed).

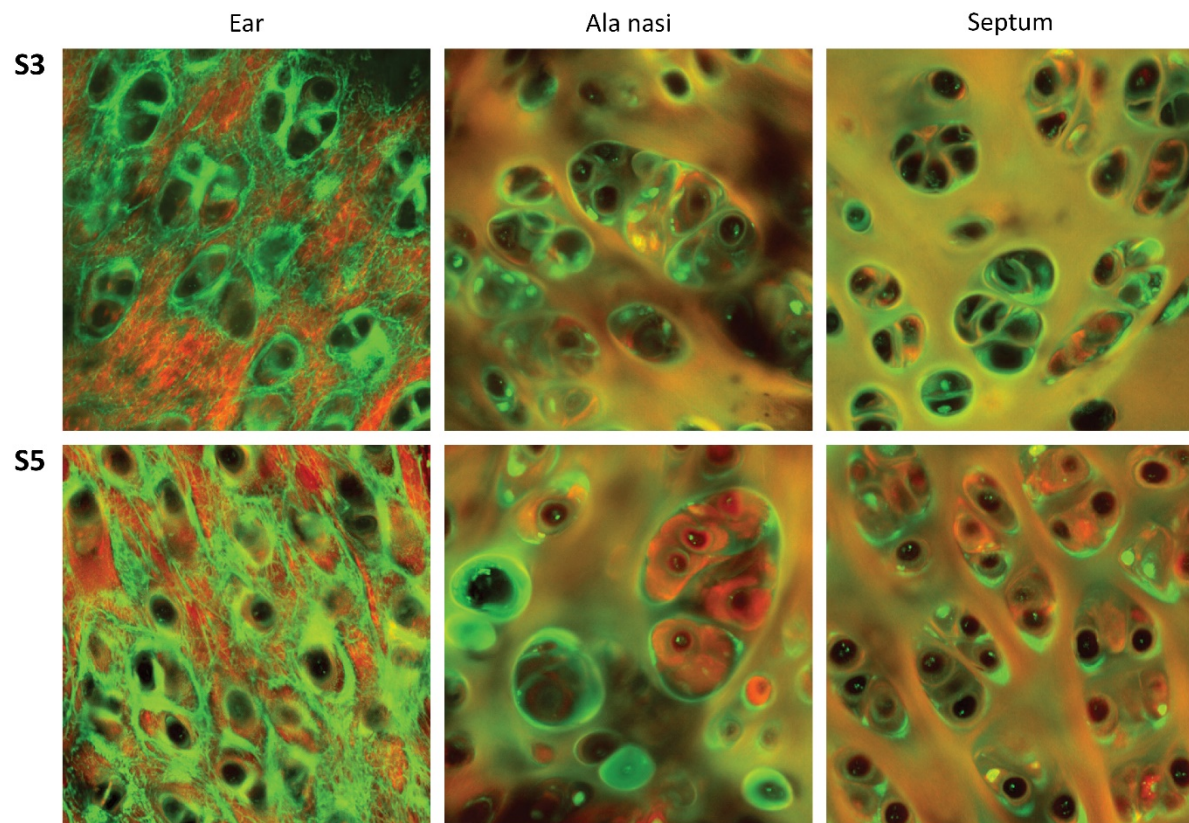


Figure 4. Multi-photon laser scanning microscopy.

Experiments were performed with cartilage donor samples 3 and 5 (S3 and S5). Green = Elastin ; Red = Collagen. The fibrous structures in the ear cartilage are clearly discernible compared to the diffuse green background signal in the nasal cartilage samples.

DISCUSSION

To our knowledge this is the first study that compares the biochemical, 3D structural and mechanical differences between all three facial cartilage types in human donors. By measuring differences in cartilage composition, structure, and stiffness on the ECM level we aimed to identify significant aspects of facial cartilage architecture necessary for adequate tissue engineering.

This is relevant for tissue engineering of cartilage, which has received massive attention the last decade. A variety of different cell types and scaffolds have been proposed for auricular or nasal cartilage engineering. [52, 56, 58, 199-201] Although promising results have been obtained, most regenerated tissues generally are only a very marginal substitution of the original tissue. This study reveals that there are significant differences between cartilage types on the ECM scale, even if they are similar in mechanical properties.

The composition of ear cartilage is known to be different compared to septal cartilage in that it contains elastic fibers. [201] We could measure small amounts of elastin in nasal cartilage with biochemical analyses. This is in line with a study in white New Zealand rabbit's where, using immunohistochemical staining, high elastin content was found specifically in the ear cartilage matrix compared to only moderate elastin content in the nasal septal pericellular regions. [143] The fact that the matrix comprises for a substantial part of elastin suggests that this may offer an important attribution to the mechanical qualities of ear cartilage. [138]

The effective Young's modulus was significantly lower in auricular and ala nasi cartilage than in nasal septum cartilage. However, stiffness between ear and ala nasi cartilage was not statistically different, although there was a clear difference in elastin content. These findings match the observations of Griffin and colleagues who found similar differences in stiffness between ala nasi and septal cartilage. [28]

In a recent paper Nimeskern and colleagues [202] explored how elastin influences the mechanical behaviour of cartilage. They found different viscoelastic behaviours of bovine hyaline articular cartilage and ear cartilage, with ear cartilage being more elastic whereas articular cartilage demonstrated a higher resistance to instantaneous loading. Upon enzymatic treatment to remove elastin and/or sGAG, they demonstrated that the compressive mechanical properties of ear cartilage appeared to be mainly due to the elastin fiber network whereas these properties were provided by collagen in articular cartilage. Moreover, the influence of sGAG on mechanical behaviour appeared different between the cartilage types: in ear cartilage sGAG had no major influence on mechanics whereas in articular cartilage sGAG had a clear influence. Although a different tissue, this apparent discrepancy between the expected role of elastin and the actual mechanical properties was also noted in dermal scar tissue. [203] This demonstrates the complex role of tissue composition in mechanical function of the tissue.

The differences in mechanical behaviour between the cartilage types could be determined not only by their biochemical compositions but also by tissue architecture. Using Multiple-photon laser scanning microscopy, the 3D structure of the different cartilage types could be depicted in high detail. Interestingly, the ala nasi, although very similar in appearance

to the septal cartilage and low in elastin content, demonstrated mechanical behaviour that is more comparable to ear cartilage.

While similar in general appearance, we observed that chondron size seemed to be different between ala nasi and septum cartilage. Sample size was small however and no statistical evidence was gathered to support this side finding.

Donor variability is large and general comparison of our data with literature is difficult as no research has previously been performed comparing these three cartilage types both mechanically, structurally and biochemically. Our data match the observations of Nimeskern and colleagues [201] that septal cartilage is stiffer and contains higher sGAG than auricular cartilage but lower DNA, indicative for lower cell concentration. Our findings also match the results of a study performed by Griffin and colleagues [28] who measured lower stiffness of the ala nasi cartilage compared to the septum. For tissue engineering purposes the scale at which the indentation experiments were performed gives a good reference for the appropriate scaffold stiffness on the cellular level. SHG proved a good tool to non-invasively depict the collagen and elastin bundle architecture in 3D.

This information could be translated to serve as a structural template for 3D printing of scaffolds and together with the data on mechanics and biochemical content provide a new step towards scaffold optimisation for facial cartilage reconstruction.

We used cartilage samples from donors at higher age (average 66.5 ± 6 years). Mechanical behaviour and histology might differ in younger patients due to calcifications and structural changes during aging. Ears for example continue to expand in volume throughout a lifetime which is attributed to alterations in the elastic fibers during aging. [164] For the septum however Richmon and colleagues [26] found no significant differences in mechanical properties between age or gender. Although samples were taken from the same anatomical location in all donors, minor variation might have occurred. This is a limitation, as several studies indicate that within the separate cartilage types there are regional differences in content. [28] Despite their localisation and comparable role as soft tissue support suggesting similar characteristics, the facial cartilages are in fact quite different from another. The specific function of cartilage tissue, for example compression for articular cartilage and flexibility for ear cartilage, may demand different mechanical testing regimes. We chose micro-indentation to explore the stiffness of the ECM, in regard of our findings perhaps a combination of mechanical tests is necessary to be able to elicit the different structural roles of the various cartilage components. In the future it might be interesting to also include macroscopic mechanical testing, as gross mechanical traits are also influenced by other factors such as the perichondrium and anatomical form. [29, 204]

From a surgical perspective, it is interesting to note that tissue composition and mechanical behaviour are not always related as expected. We did not find an explanation for the lower stiffness of ala nasi cartilage. It does support the concept that tissue transplants from different origins can serve as structural surrogate in reconstructive surgery. The use of concha tissue for ala nasi reconstruction is an excellent example thereof. Other fields that are not covered in this paper but are important to consider are cellular interaction including proteomics and metabolism, as cell survival and behaviour are key to tissue engineering and long-term successful transplantation. The finding that the facial cartilage types not only structurally

differ but also vary in cell content may hold implications for surgical reconstruction, as tissues with higher cells concentrations potentially demand a more nutrient rich environment when transplanted. The merging of knowledge from practical experience and fundamental research in our opinion will prove essential in a world where tissue engineering is rapidly becoming reality, a development that should not be overlooked by surgeons.

In conclusion, understanding the complete composition of tissue, both structural, mechanical and biochemical, is essential in order to regenerate an appropriate scaffolding environment for facial cartilage regeneration. This is particularly reflected by the finding that albeit it's 3D structural similarity to septal cartilage, the ala nasi has a matrix stiffness that is more comparable to ear cartilage. In that light, the role of elastin remains to be further elicited, and perhaps we should question whether its name is not misleading in regard of its contribution to tissue mechanics.

Acknowledgements

We wish to thank Prof. dr. Bleys MD from the Department of Anatomy UMCU and the staff of the Dr. Tulp Foundation for providing the tissue samples. The research by MMP was financially supported by SenterNovem in the framework of EuroNanoMed (EAREG-406340-131009/1). The research was supported by the Dutch Burns Foundation. We further wish to thank Wendy Koevoet, Department of Otorhinolaryngology Erasmus MC for technical support with biochemical assays and Birgit Witte from the Department of Biostatistics of the VUMC for statistical support.

Cell sources

Chapter 4

The *in vitro* and *in vivo* capacity of culture-expanded human cells from several sources encapsulated in alginate to form cartilage

M.M. Pleumeekers, L. Nimeskern, J.L.M. Koevoet, N. Kops, R.M.L. Poublon, K.S. Stok, G.J.V.M. van Osch

European Cells & Materials, 2014. 27: p. 264-80.

ABSTRACT

Cartilage has limited self-regenerative capacity. Tissue engineering can offer promising solutions for reconstruction of missing or damaged cartilage. A major challenge herein is to define an appropriate cell source that is capable of generating a stable and functional matrix. This study evaluated the performance of culture-expanded human chondrocytes from ear, nose and articular joint as well as bone-marrow-derived and adipose-tissue-derived mesenchymal stem cells both *in vitro* and *in vivo*.

All cells (at least three donors per source) were culture-expanded, encapsulated in alginate and cultured for five weeks. Subsequently, constructs were implanted subcutaneously for eight additional weeks. Before and after implantation, glycosaminoglycan (sGAG) and collagen content were measured using biochemical assays. Mechanical properties were determined using stress-strain-indentation tests. Hypertrophic differentiation was evaluated with qRT-PCR and subsequent endochondral ossification with histology.

Articular chondrocytes had higher chondrogenic potential *in vitro* than the other cell sources, as assessed by gene-expression and sGAG-content ($p < 0.001$). However, after implantation, articular chondrocytes did not further increase their matrix. In contrast, ear and nasal chondrocytes continued producing matrix *in vivo* leading to higher sGAG-content ($p < 0.001$) and elastic modulus. For constructs containing nasal chondrocytes, matrix-deposition was associated with the elastic modulus ($R^2 = 0.477$, $p = 0.039$). Although all cells - except articular chondrocytes - expressed markers for hypertrophic differentiation *in vitro*, there was no bone formed *in vivo*.

Our work shows that cartilage formation and functionality depends on the cell source used. Articular chondrocytes possess the highest chondrogenic capacity *in vitro*, while ear and nasal chondrocytes are most potent *in vivo*, making them attractive cell sources for cartilage repair.

INTRODUCTION

Cartilage is a highly specialized avascular connective tissue located at a variety of anatomical locations such as the ear, nose, trachea, ribs and articular joints. In general, cartilage predominantly consists of an extracellular matrix (ECM), which is produced, maintained and remodeled by a relatively small amount of specialized cells (1-10%). [34] The exact composition of the ECM is mainly dependent on the tissue's function and thus three major subtypes can be distinguished: hyaline, fibrous and elastic cartilage. It is well known that due to its avascular origin, cartilage itself has a limited self-regenerative capacity. As a result, cartilage deficits can lead to severe pain, disability and aesthetic impairment. Currently, surgical repair of cartilage requires either autogeneic cartilage grafts or artificial material implants. However, these conventional treatments are (1) associated with a limited availability of autogeneic tissue, (2) can cause donor site morbidity, and - in case of artificial implants - (3) are prone to generate a foreign body reaction.

To overcome these problems, tissue engineering (TE) can offer a promising solution for restoring missing or damaged cartilage. TE-approaches have focused on the production of functional cartilage that has features similar to native tissue. In cartilage TE, small tissue biopsies are harvested, thus generating minimal donor site morbidity. Cells are isolated from the biopsies and stimulated to proliferate in culture providing large quantities of cells. These cells are subsequently stimulated to produce cartilage tissue which should structurally and morphologically resemble native tissue. One of the major challenges in cartilage TE is defining an appropriate cell source. The most obvious cell source is cartilage itself. Hyaline articular cartilage is most frequently used for cartilage TE, although some experiments have been published on the use of non-articular cartilages (e.g. nasal, ear and costal cartilage). [205] Next to chondrocytes, mesenchymal stem cells (MSCs) with their multi-lineage differentiation potential and easy availability from bone marrow or adipose tissue have been demonstrated as an attractive cell source for cartilage TE. [64, 66]

To date, we and others have evaluated the use of chondrocytes and MSCs of several anatomical locations for their applicability in cartilage regenerative medicine. [39, 42-44, 46-59, 206-209] However, precise comparison of the performance of culture-expanded human cells is lacking. This knowledge is important to be able to select an optimal cell source for each application of cartilage TE. The current study was designed to evaluate the performance of culture-expanded cells of several sources for generating a stable and functional ECM *in vitro* and *in vivo*. Therefore, human chondrocytes from ear, nose and articular joint and MSCs derived from bone marrow and adipose tissue were compared. Cartilage matrix production was evaluated using qRT-PCR and biochemical assays during *in vitro* culture. Biochemical assays, histology and mechanical tests were used to determine tissue stability and functionality of cartilage constructs after subsequent subcutaneous implantation *in vivo*.

MATERIALS AND METHODS

Chemicals were obtained from Sigma-Aldrich, USA unless stated otherwise.

Cell sources

Ear (EC: $n=5$, median age 69, range 17-75 years) and nasal cartilage (NC: $n=8$, median age 24, range 18-46 years) were obtained from patients undergoing reconstructive subtotal septorhinoplasty. For articular cartilage (AC), both healthy ($n=2$, traumatic amputation) and diseased knee cartilage ($n=7$, osteoarthritis) were harvested. Since no clear differences in chondrogenic potential were visible between both healthy and diseased AC (data not shown), we combined them for further experiments (total $n=9$, median age 68, range 43-88 years). To obtain adipose-tissue-derived mesenchymal stem cells (AMSC), subcutaneous abdominal adipose tissue was used from patients undergoing reconstructive breast surgery ($n=7$, median age 51, range 34-71 years). All these tissue samples were obtained as waste material after surgery with approval of the local Medical Ethics Committee (MEC-2011-371). Finally, bone-marrow-derived mesenchymal stem cells (BMSC) were harvested from femoral-shaft biopsies during total hip-replacement surgery, after informed consent had been acquired and with approval of the local Medical Ethics Committee (MEC-2004-142) ($n=11$, median age 63, range 39-72 years).

Cell isolation and culture

Expansion

To isolate chondrocytes, macroscopically intact cartilage pieces were washed after careful resection of the perichondrium (in the case of nasal and ear cartilage). Cartilage pieces were diced into small fragments and incubated for one hour with protease (2 mg/mL), followed by overnight incubation with collagenase B (Roche Diagnostics, Mannheim, Germany) in high glucose (4.5 g/L) Dulbecco's modified Eagle's medium (HG-DMEM; Gibco, Carlsbad, USA) with 10% fetal calf serum (FCS; Gibco), 50 $\mu\text{g/mL}$ gentamycin (Gibco), and 0.5 $\mu\text{g/mL}$ amphotericin B (Fungizone; Life Technologies, Breda, the Netherlands). To remove small parts of undigested cartilage, the cell suspension was filtered through a nylon 100- μm mesh. Prior to cell seeding, cell viability was tested using the trypan blue exclusion test, and cell number was calculated with a hemocytometer. Chondrocytes were finally seeded at an initial density of 7500 cells/ cm^2 in 'standard chondrocyte expansion medium' containing HG-DMEM supplemented with 10% FCS, 50 $\mu\text{g/mL}$ gentamycin, and 0.5 $\mu\text{g/mL}$ Fungizone.

Bone-marrow-derived heparinized aspirates were seeded at a density of $2\text{-}5 \times 10^5$ nucleated cells/ cm^2 and cultured overnight in 'standard MSC expansion medium' containing low glucose (1.5 g/L) Dulbecco's modified Eagle's medium (LG-DMEM), supplemented with 10% FCS; 50 $\mu\text{g/mL}$ gentamycin; 0.5 $\mu\text{g/mL}$ Fungizone; 10^{-4} M L-ascorbic acid 2-phosphate; and 1 ng/mL basic Fibroblast Growth Factor 2 (bFGF2; AbD Serotec, Kidlington, UK). After 24 hours, non-adherent cells and cell debris were washed out and adherent BMSC were further expanded using 'standard MSC expansion medium'.

To extract AMSCs, excised human adipose tissue was washed with LG-DMEM, minced, and suspended in 0.1% collagenase type I solution (Invitrogen, Carlsbad, CA, USA) in the

presence of 1% Bovine Serum Albumin (BSA; PAA Laboratories GmbH, Cölbe, Germany) in LG-DMEM. After 60 minutes of enzymatic digestion in an orbital shaker, floating adipocytes were separated from the precipitating MSC fraction by centrifugation (10 minutes, 1500 RPM), washed with 'standard MSC expansion medium', and filtered through a 100- μ m nylon mesh. Before cell seeding, the amount of nucleated cells was calculated using methylene blue, and cell number was calculated with a hemocytometer. The cell suspension was seeded at an initial density of 40,000 cells/cm² in 'standard MSC expansion medium'.

All cells were cultured at 37°C in air containing 5% carbon dioxide. Medium was changed twice a week. When cell cultures reached 80% confluence, chondrocytes and MSCs were trypsinized using 0.05% trypsin–EDTA. Chondrocytes were seeded at a 7500 cells/cm² and MSCs at a 2300 cells/cm² cell density for further expansion to increase cell number. All third-passage (P3) cells which were approaching subconfluence were detached and cultured in a three-dimensional alginate system (as described below) to promote chondrogenesis.

In order to determine the proliferation rate of cultured ECs, NCs, ACs, BMSCs and AMSCs, growth kinetics of three donors from each cell source were evaluated in monolayer expansion using the number of population doublings (PD) until subconfluency and the time to reach passage four. Therefore we have calculated the PD/D (Population Doublings per Day) by using the formula: $PD/D = (\ln(N_2/N_1) / \ln(2))/D$; where N1 was the number of cells at the beginning of each passage, N2 the number of cells at subconfluency and D the amount of days to reach passage four.

Chondrogenic differentiation

For three-dimensional alginate culture, isolated cells from four donors of each cartilage source and six donors from each of the MSC-sources were suspended at a density of 4×10^6 cells/mL in clinical grade 1.1% low viscosity alginate solution dissolved in 0.9% NaCl (Batch MG-004, CellMed, Alzenau, Germany). Afterwards, the cell-alginate mixture was transferred into a 10-mL sterile syringe from which the suspension was slowly passed through a 23-gauge needle to produce drops, which fell into a 102 mM CaCl₂. Following instantaneous gelation, the beads were allowed to further gelate for a period of 10 minutes in the CaCl₂ solution. After being washed once with 0.9% NaCl and HG-DMEM, the beads were transferred to 24-well plates. Controls were cultured in 150 μ L/bead 'control differentiation medium' containing serum-free HG-DMEM supplemented with 50 μ g/mL gentamycin; 0.5 μ g/mL Fungizone; 1 mM sodium pyruvate (Gibco); 40 μ g/mL L-proline (Sigma-Aldrich); supplemented Insulin Transferrine Selenium (ITS+ ; B&D Bioscience, Bedford, USA); 10^{-7} M dexamethason; and 25 μ g/mL L-ascorbic acid 2-phosphate. In the experimental condition ('chondrogenic differentiation medium') 10 ng/mL Transforming Growth Factor β 1 (TGF β 1; R&D Systems, Minneapolis, USA) was added to induce chondrogenesis. Medium was changed twice a week. After two and five weeks, alginate beads were processed for biochemical or gene-expression analysis as described below. For all *in-vitro* experiments four donors for the chondrocyte sources and six donors for the MSC sources were used, with at least duplicate samples per analyses for each individual donor.

To study *in-vivo* functionality and stability of cartilage TE constructs after *in-vitro* cell-culture, larger flat constructs were created from cells of three donors of each cell source as

previously described. [210] In short, alginate suspensions containing 4×10^6 cells/ml were injected into a custom-designed slab mold consisting of two calcium-permeable membranes (Durapore® 5.0 μ m membrane filters, Millipore) rigidly supported by stainless-steel meshes and separated by a stainless-steel casting frame. Part of these constructs were harvested after five weeks of cell-culture for analyses and a part was implanted subcutaneously on the dorsal side of athymic mice. For the *in-vivo* experiments a total of six constructs per cell source were used, with duplicate samples for three different donors.

Subcutaneous implantation in vivo

In total, seventeen nine-week old, female NMRI nu/nu mice (Charles River Laboratories, the Netherlands) were used to evaluate the performance of constructs cultured with or without TGF β 1. Mice were placed under general anesthesia using 2.5% isoflurane. Two separate subcutaneous incisions of approximately 1.0 cm were made along the central line of the spine (one at the shoulders and one at the hips), after which four separate subcutaneous pockets were prepared by blunt dissection of the subcutaneous tissue. For implantation the alginate constructs were randomly assigned to these four pockets. Eight weeks after subcutaneous implantation, animals were sacrificed and samples were explanted for histological, biomechanical and biochemical analyses. Animal experiments were carried out with approval of the local Animal Experiments Committee of the Erasmus MC and were approved as outlined in the national Animals Act (EMC 2429).

Gene expression analyses

For total RNA isolation, alginate was dissolved in ice-cold 55 mM sodium citrate (150 μ L/bead) and 20 mM Ethylene Diaminetetraacetate (EDTA) in 150 mM NaCl and centrifuged at 2.5 G for 8 minutes. Each pellet was subsequently suspended in 1 mL RNA-Bee™ (TEL-TEST, Fiendswood, USA). RNA was extracted with chloroform and purified from the supernatant using the RNeasy Micro Kit (Qiagen, Hilden, Germany) according to the manufacturer's guidelines by on-column DNA-digestion. Extracted total RNA was quantified using NanoDrop® ND-1000 Spectrophotometer (NanoDrop Technologies, Wilmington, USA) at 260/280 nm. Total RNA of each sample was reverse transcribed into cDNA using RevertAid™ First Strand cDNA Synthesis Kit (MBI Fermentas, Germany).

For quantitative real-time Polymerase Chain Reaction (qRT-PCR) analysis, forward and reverse primers were designed using PrimerExpress 2.0 software (Applied Biosystems, Foster City, CA) to meet TaqMan or SYBR Green requirements. They were designed to bind separate exons to avoid co-amplification of genomic DNA. Gene specificity of all primers was guaranteed by Basic Local Alignment Search Tool (BLASTN), as listed in table 1. The following genes were analyzed: Aggrecan (*ACAN*), Collagen type IIA1 (*COL2A1*), Collagen type X (*COL10*), Alkaline Phosphatase (*ALP*), and Matrix MetalloProteinase-13 (*MMP13*). GlycerAldehyde 3-Phosphate DeHydrogenase (*GAPDH*), and Hypoxanthine PhosphoRibosylTransferase 1 (*HPRT1*) were used as housekeeping genes. The expression of *GAPDH* and *HPRT1* did not differ between cell sources and both were used to calculate the best housekeeper index. [211] Using repeated pair-wise correlation analysis, data were normalized by calculating the 'best housekeeper index'. (Data not shown) Polymerase Chain Reactions were performed using

TaqMan® Universal PCR Mastermix (Applied Biosystems) or qPCR Mastermix Plus for SYBR Green (Eurogentec, Nederland BV, Maastricht, the Netherlands) according to the manufacturers' guidelines and using an ABIPRISM® 7000 with SDS software version 1.7 (Applied Biosystems, Nieuwerkerk a/d IJssel, the Netherlands). Amplification efficiencies for all assays were between 90-110%. Relative gene expressions of triplicate samples of each donor were calculated by means of the $2^{-\Delta CT}$ formula.

Primers and probes	
GAPDH	Fw: ATGGGGAAGGTGAAGGTCG Rev: TAAAAGCAGCCCTGGTGACC Fam-CGCCAATACGACCAAATCCGTTGAC
HPRT1	Fw: TATGGACAGGACTGAACGTCTTG Rev: CACACAGAGGGCTACAATGTG Fam-CGCCAATACGACCAAATCCGTTGAC
ACAN	Fw: TCGAGGACAGCGAGGCC Rev: TCGAGGGTGTAGCGTGTAGAGA Fam-ATGGAACACGATGCCTTTCACCACGA
COL2A1	Fw: GGCAATAGCAGGTTCACGTACA Rev: CGATAACAGTCTTGCCCCACTT Fam-CCGGTATGTTTCGTGCAGCCATCCT
COL10	Fw: CAAGGCACCATCTCCAGGAA Rev: AAAGGGTATTTGTGGCAGCATATT Fam-TCCAGCACGCAGAATCCATCTGA
ALP	Fw: GACCCTTGACCCCCACAAT Rev: GCTCGACTGCATGTCCCT Fam-TGGACTACCTATTGGGTCTCTTCGAGCCA
MMP13	Fw: AAGGAGCATGGCGACTTCT Rev: TGGCCCAGGAGGAAAAGC Fam-CCCTCTGGCCTGCGGCTCA

Table 1. Sequences of primers and probes for qRT-PCR.

Biochemical evaluation of the extracellular matrix

Sample preparation

At room temperature, alginate beads and discs were dissolved in 55 mM sodium citrate and 20 mM EDTA in 150 mM NaCl. All samples were then digested overnight at 60°C with papain buffer to a final concentration of 250 µg/mL papain (0.2 M NaH₂PO₄, 0.01 M EDTA, pH 6.0 and freshly added 250 µg/mL papain, and 5 mM L-cystein), and later subjected to biochemical analyses to determine the DNA, glycosaminoglycan, and hydroxyproline contents.

DNA content

The amount of DNA measured in each papain-digested sample was determined by Ethidium bromide (GibcoBR1), using calf thymus DNA as a standard. Samples were analyzed with a

spectrofluorometer (Wallac 1420 Victor 2; Perkin-Elmer, Wellesley, USA), using an extinction filter (340 nm) and an emission filter (590 nm).

Glycosaminoglycan content

Sulfated glycosaminoglycans (sGAGs) were quantified using the 1,9-Dimethylmethylene blue (DMMB) dye-binding assay. To be suitable for cell cultures containing alginate, the DMMB-pH-level was decreased to pH 1.75, as described previously. [212] The metachromatic reaction of DMMB was monitored using a spectrophotometer. Absorption ratios of 540 and 595 nm were used to determine the sGAG content with chondroitin sulphate C (shark) as a standard. For each sample, the amount of sGAG was corrected for the amount of DNA.

Hydroxyproline content

The hydroxyproline content was quantified using a method described previously. [213] Briefly, the papain digests were hydrolyzed with equal volumes of 12 M HCL at 108°C for 18–20 hours. Samples were then dried and redissolved in 150 µL water. Hydroxyproline contents were measured using a colorimetric method (extinction, 570 nm), with chloramine-T and dimethylaminobenzaldehyde as reagents and hydroxyproline (Merck, Darmstadt, Germany) as a standard.

Histological evaluation of the extracellular matrix

After eight weeks of subcutaneous implantation, alginate discs were harvested, set in 2% agarose, fixed in 4% formalin in PBS and embedded in paraffin. Paraffin-embedded sections (6 µm) were deparaffinized and rehydrated.

Immunohistochemistry for collagen type II, elastin and human vimentin

To allow the use of monoclonal mouse antibodies on constructs which have been implanted in athymic mice, we used a method to couple the first and second antibody before applying them on the sections to prevent unwanted binding of the anti-mouse antibodies to mouse-immunoglobulins. [214] In short, primary antibodies were pre-coupled overnight with goat anti-mouse biotin at 4°C (Jackson Laboratories, Bar Harbor, USA), followed by a two-hour incubation in 0.1% normal mouse serum (CLB, Amsterdam, the Netherlands) in order to capture the unbound second antibody.

Antigen retrieval for the collagen type II (Developmental Studies Hybridoma Bank, Iowa, USA) antibody was performed through incubation with 0.1% pronase in PBS for 30 minutes at 37°C, continued with a 30 minutes incubation with 1% hyaluronidase in PBS for at 37°C. Antigen retrieval for elastin (BA4) required incubation with 0.25% trypsin in PBS for 20 minutes at 37°C. Non-specific binding sites were blocked with 10% goat serum in PBS and sections were stained with the pre-treated primary antibodies against collagen type II (1:100) or elastin (1:1000) for 60 minutes. Sections were then incubated with enzyme-streptavidin conjugate (Label, 1:100, Biogenex, HK-321-UK, California, USA) in PBS/1% BSA, followed by incubation with Neu Fuchsin substrate (Chroma, Köngen, Germany). Positive staining for collagen II and elastin was confirmed with the use of native ear cartilage. A mouse monoclonal negative control antibody (mlgG1: X0931, Dako) was used as an isotype control.

To study whether cells in the alginate constructs harvested after *in-vivo* implantation were originated from human origin, a monoclonal mouse anti-human vimentin antibody was used (AMF-17b, Developmental Studies Hybridoma Bank, Iowa, USA), as described previously. [56] In short, slides were incubated in 3% aqueous hydrogen peroxidase solution, in order to inhibit endogenous peroxidase and allow for peroxidase-antiperoxidase staining. Antigen retrieval required incubation in Rodent Decloaker® for 60 minutes at 95°C. Non-specific binding sites were blocked with Rodent Block M® followed by a 30 minute staining with vimentin (1:40, V6630). Thereafter, the MM-polymer-HRP® secondary antibody was used, succeeded by incubation with 3'diaminobenzidine chromogen solution. Tissue specificity was confirmed by the absence of staining on sections of mouse liver tissue. A mouse monoclonal negative control antibody was used as an isotype control.

Von Kossa/Thionin/Resorcin-Fuchsin staining

To evaluate tissue calcification, a Von Kossa staining was performed. Slides were immersed in 5% silver nitrate solution for 10 minutes, rinsed in MiliQ and exposed to light for another 10 minutes. Sections were counterstained with Nuclear fast red (Merck).

sGAGs were visualized using 0.4% Thionin in 0.01 M aqueous sodium acetate (pH 4.5) for 5 minutes at room temperature. To check whether we stained sGAGs rather than the remaining alginate, sections were pre-treated with 20 mM EDTA. As EDTA treatment did not change the intensity and/or localization of Thionin on our slides, we confirmed that alginate did not interfere with our sGAG-staining protocol. The presence, as well as the arrangement of the elastic fibers, were visualized using Weigert's Resorcin-Fuchsin staining (Klinipath, Duiven, the Netherlands).

We used a semi-quantitative scoring system - The Bern Score [215] - to evaluate the chondrogenic capacity of alginate-encapsulated cells after subcutaneous implantation. (Table 2) In short, the scoring system evaluates cartilage formation based on three elements: (1) the uniformity and/or intensity of the Thionin and collagen type II staining; (2) the distance between cells and the extent of matrix produced; and (3) the cellular morphology. Each category has scores ranging from 0 to 3, resulting in a possible minimum collective score of 0 and a maximum of 9. Samples that were either not visible anymore after eight weeks of subcutaneous implantation or were dissolved during formalin fixation were scored 0.

Scoring categories	Score
(1) Uniformity and darkness of the stain	
No stain	0
Weak stain of poorly formed matrix	1
Moderately even stain	2
Even dark stain	3
(2) Distance between cells / amount of matrix accumulated	
High cell densities with no matrix in between (no spacing between cells)	0
High cell densities with little matrix in between (cells <1 cell-size apart)	1
Moderate cell density with matrix (cells approximately 1 cell-size apart)	2
Low cell density with moderate distance between cells (>1 cell) and an extensive matrix	3
(3) Cell morphologies represented	
Condensed/necrotic/pycnotic bodies	0
Spindle/fibrous	1
Mixed spindle/fibrous with rounded chondrogenic morphology	2
Majority rounded/chondrogenic	3
Maximum score	9

Table 2. The Bern Score: Histological evaluation of engineered cartilage constructs.

Biomechanical analysis

For mechanical characterization of engineered cartilage constructs after *in-vitro* and *in-vivo* cell culture, we used 2.5 mm thick and 5 mm diameter constructs. The samples were placed in a close-fitting Ø5 mm stainless steel cylindrical wells. Mechanical testing was performed with a materials testing machine (Zwick Z005, Ulm, Germany) equipped with a 10 N load cell, a built-in displacement control, and a cylindrical, plane ended, stainless steel indenter (Ø1.2 mm). During mechanical testing the samples were immersed in PBS. Stress-strain testing was performed: the samples were compressed to a final height of 0.5 mm at a loading rate of 5 mm per minute. An in-house Matlab® script was used to locate the sample surface and measure the sample thickness. The sample surface was identified by detecting the corresponding slope discontinuity of the force-displacement curve using its second derivative. Force-displacement curves were then converted to stress-strain curves. Compressive modulus at 40% strain (E40%), defined as the derivative of the stress-strain curve at 40% strain, was determined for every sample ($n=98$).

Statistical analysis

All data were analyzed with PASW Statistics 20.0 (SPSS inc. Chicago, USA). The mean and standard deviations are presented. For statistical evaluation, a mixed linear model was used. Cell source, time point and treatment (TGFβ1) were defined as fixed factors in the model. Donor and sample number were treated as random factors. Values of $p<0.05$ were considered statistically significant. For histological scoring we used the Kruskal-Wallis followed by the

Mann-Whitney-U tests for their statistical analysis ($p < 0.05$). In order to determine whether mechanical properties were enhanced by the deposition of matrix components, a multiple regression analyses was performed using sGAG and collagen deposition as independent variables ($p < 0.05$).

RESULTS

Cell expansion

The cell sources showed clear differences in growth rate. NCs proliferated significantly faster than ECs, ACs and AMSCs ($p < 0.05$). NCs had gone through 8.9 ± 1.7 population doublings (PD) in four passages taking 28 ± 5 days, ECs had gone through 6.8 ± 1.3 in 38 ± 6 days and ACs through 3.9 ± 1.1 PD in 44 ± 13 days. It took 39 ± 8 days for BMSCs and 48 ± 8 days for AMSCs to complete four passages. (Table 3)

	PD/D	Statistically significantly different from
EC	0.18 ± 0.04	NC ($p=0.015$) ; AC ($p=0.008$)
NC	0.32 ± 0.07	EC ($p=0.015$) ; AC ($p<0.001$) ; AMSC ($p=0.013$)
AC	0.10 ± 0.05	EC ($p=0.008$) ; NC ($p<0.001$) ; BMSC ($p=0.001$)
BMSC	0.25 ± 0.09	AC ($p=0.001$)
AMSC	0.16 ± 0.04	NC ($p=0.013$)

Table 3. Population Doubling Time of different cell types over four passages.

NCs proliferated faster than ECs, ACs and AMSCs. The proliferation rate of BMSCs did not differ from AMSCs. Data are shown as mean \pm SD. PD/D = Population Doublings per Day ($PD/D = (\ln(N_2/N_1) / \ln(2))/D$) ; EC = Ear Chondrocytes ($n=3$ donors) ; NC = Nasal Chondrocytes ($n=3$ donors) ; AC = Articular Chondrocytes ($n=3$ donors) ; BMSC = bone-marrow-derived Mesenchymal Stem Cells ($n=3$ donors) ; AMSC = adipose-tissue-derived Mesenchymal Stem Cells ($n=3$ donors).

Chondrogenic differentiation *in vitro*

After cell-expansion, cells were encapsulated in clinical-grade alginate to promote chondrogenesis. Alginate beads cultured without TGF β 1 had maintained their DNA content after five weeks of culture. Addition of TGF β 1 significantly increased the total amount of DNA in alginate beads seeded with ECs and NCs ($p < 0.001$), which was also significantly higher compared to the other cell sources ($p < 0.05$), indicating that those cells were able to proliferate after encapsulation in alginate. The other cell conditions remained at a stable cell content. (Figure 1A)

Chondrocytes did express low levels of *COL2A1* and *ACAN* without TGF β 1. After chondrogenic induction (with TGF β 1), the *COL2A1* and *ACAN* gene expression levels increased in all cell source used. Both genes were most highly expressed by ACs ($p < 0.001$), followed by BMSCs. (Figure 1B) This was already seen after two weeks of culture (data not shown), suggesting that chondrogenesis was not only enhanced but also accelerated.

Matrix production was quantified by sGAG and collagen content of alginate beads during *in-vitro* culture. Without TGF β 1 very little sGAG was formed *in vitro*. Addition of TGF β 1 enhanced sGAG-production and after five weeks of culture ACs deposited significantly more sGAGs ($p < 0.01$). When sGAG content was adjusted to the amount of DNA, similar but more pronounced differences were observed (ACs produced most sGAGs: 60.89 ± 53.04 μ g sGAG / μ g DNA; $p < 0.001$). sGAG content per alginate bead in constructs containing BMSCs, ECs, NCs

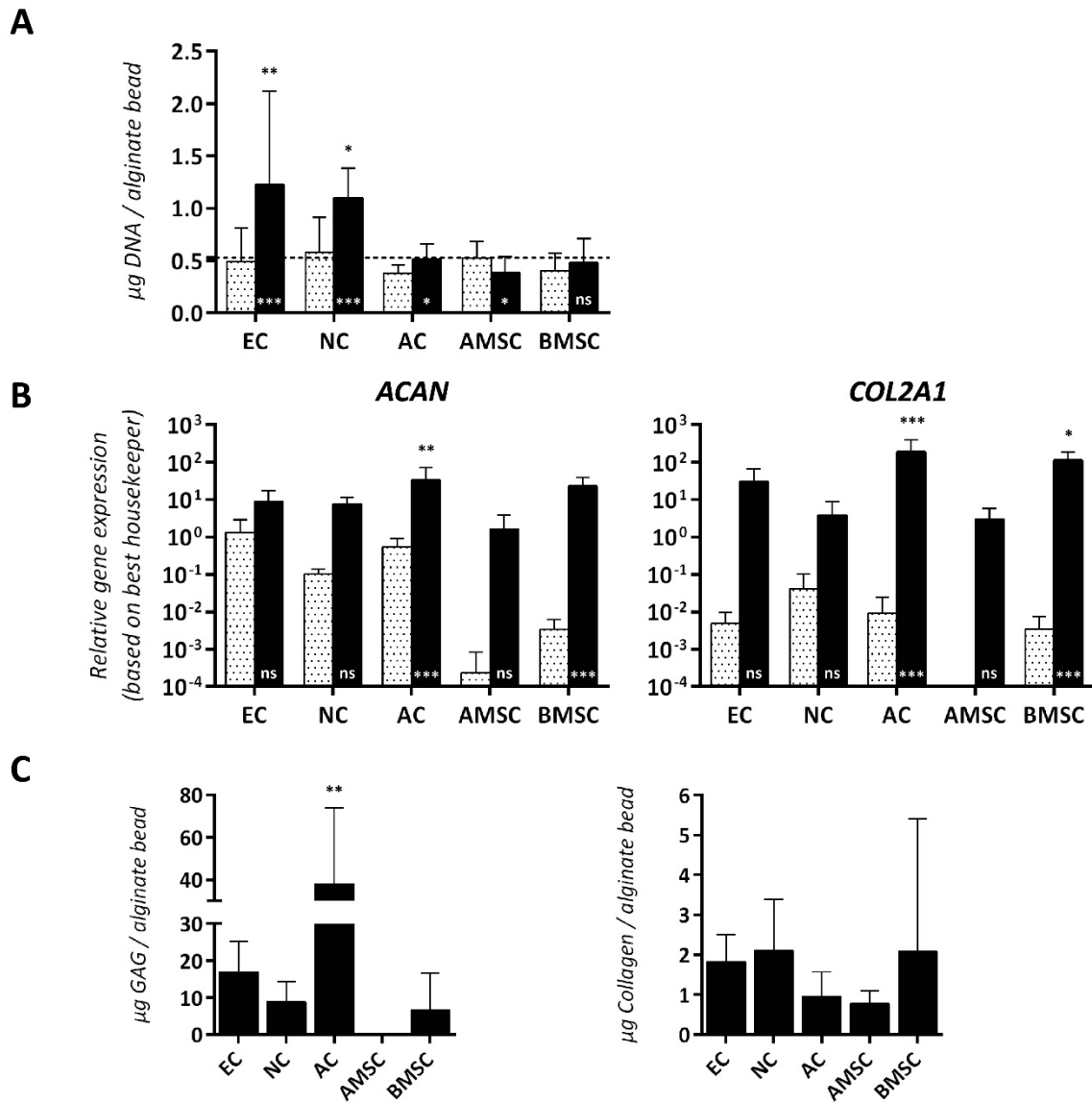


Figure 1. Cartilage matrix formation by several cell types *in vitro*.

To promote chondrogenesis, cells were encapsulated in alginate beads and cultured without (*dotted*) or with (*black*) TGFβ1 for 5 weeks. **(A)** DNA content was determined before culture (*dotted* line), being on average 0.53 ± 0.183 µg DNA per alginate bead, and after 5 weeks of culture. The amount of DNA was significantly higher in constructs containing ECs or NCs. **(B)** Relative gene expression levels of *COL2A1* and *ACAN* were corrected for the best housekeeper index. All cell sources expressed *ACAN* and *COL2A1* after chondrogenic induction. **(C)** Biochemical evaluation of sGAG and collagen content after chondrogenic induction in alginate beads. ACs deposited most sGAGs. Collagen-production was low *in vitro*. Data are shown as mean \pm SD. For statistical evaluation, a mixed model was used. *, ** or *** indicates *p*-values smaller than 0.05, 0.01 or 0.001 respectively compared to the control condition (asterisk is shown in the bar) or compared to the other cell sources (asterisk is shown above the bar). EC = Ear Chondrocytes (*n*=4 donors) ; NC = Nasal Chondrocytes (*n*=4 donors) ; AC = Articular Chondrocytes (*n*=4 donors) ; BMSC = Bone-marrow-derived Mesenchymal Stem Cells (*n*=6 donors) ; AMSC = Adipose-tissue-derived Mesenchymal Stem Cells (*n*=6 donors). Per donor, 2-3 samples were used for analyses.

and AMSCs was not significantly different, although a large donor variation was observed. Also with large variation between donors, AMSCs performed worse. The amount of collagen deposited was just above background for all cell sources after five weeks of chondrogenic differentiation, being on average $1.53 \pm 1.84 \mu\text{g}$ collagen per alginate bead. (Figure 1C)

Chondrogenic differentiation *in vivo*

To study the stability and quality of TE cartilage *in vivo*, alginate constructs were first differentiated *in vitro* for five weeks and subsequently implanted subcutaneously on the dorsal side of athymic mice for an additional eight weeks of culture. Constructs seeded with ECs or NCs, pre-cultured with TGF β 1, had a macroscopically white opaque appearance and were relatively strong on handling. Conversely, constructs pre-cultured without TGF β 1 or constructs encapsulating ACs, BMSCs or AMSCs, were fragile and also did not resemble cartilaginous tissue macroscopically. (Figure 2A and 3A)

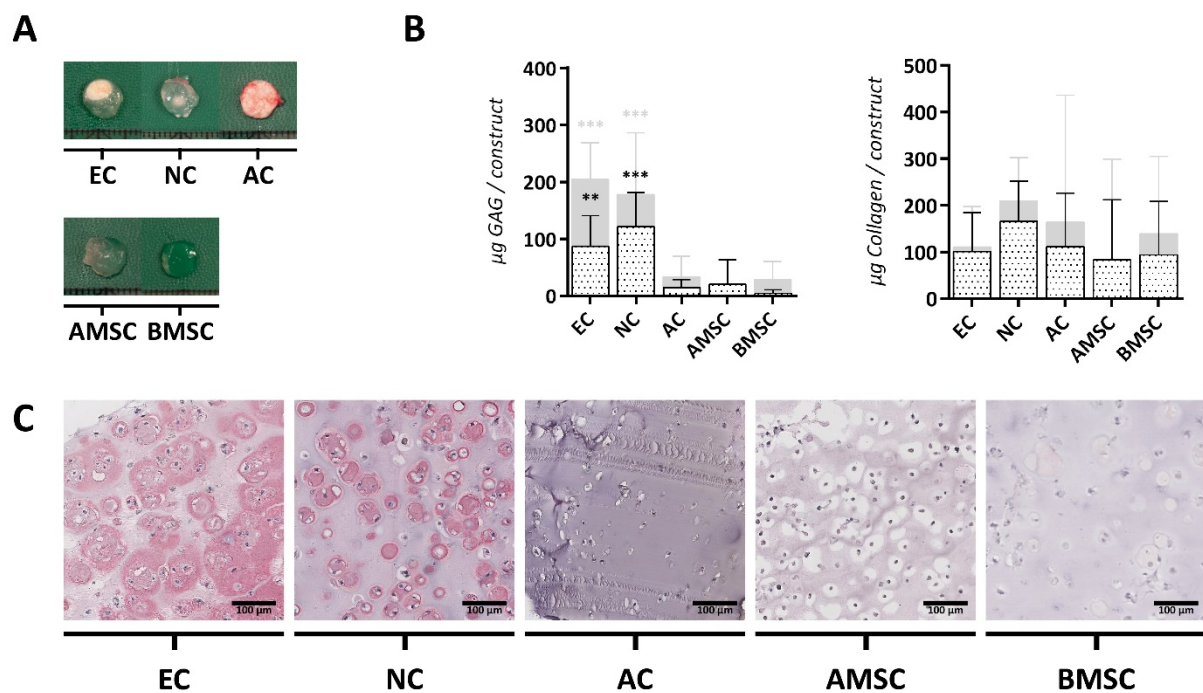


Figure 2. Cartilage matrix formation by several cell types *in vivo*.

Prior to subcutaneous implantation, constructs were cultured *in vitro* for 5 weeks in the absence of TGF β 1. **(A)** Macroscopic view of engineered cartilage constructs after 8 weeks of subcutaneous implantation. **(B)** Biochemical evaluation of the sGAG and collagen content after subcutaneous implantation. ECs and NCs deposited most sGAGs *in vivo*. Collagen-production was increased *in vivo*, but did not differ between the cell sources. The grey bars represent the *in vivo* biochemical data of constructs cultured *in vitro* for 5 weeks in the presence of TGF β 1 (Figure 3). **(C)** ECs and NCs demonstrated a collagen-type-II-rich matrix in almost all cartilage constructs. Biochemical data are shown as mean \pm SD. For statistical evaluation, a mixed model was used. *, ** or *** indicates *p*-value smaller than 0.05, 0.01 or 0.001 respectively compared to the other cell sources. EC = Ear Chondrocytes (*n*=3 donors) ; NC = Nasal Chondrocytes (*n*=3 donors) ; AC = Articular Chondrocytes (*n*=3 donors) ; BMSC = Bone-marrow-derived Mesenchymal Stem Cells (*n*=3 donors) ; AMSC = Adipose-tissue-derived Mesenchymal Stem Cells (*n*=3 donors). Per donor, 2 samples were used for analyses.

Prior to implantation, constructs pre-cultured without TGFβ1 produced very little sGAG *in vitro*, being on average $1,10 \pm 1,20 \mu\text{g}$ sGAG per construct. After *in vivo* implantation, these constructs greatly increased their production of matrix components, although they did not reach levels which equaled the matrix content found in constructs cultured with TGFβ1. (Figure 2B) After subcutaneous implantation preceded by chondrogenic culture (with TGFβ1), ACs, BMSCs and AMSCs retained their sGAG content but did not further increase it. On the contrary, ECs and NCs significantly enhanced matrix formation *in vivo* (EC 7.26-fold and NC 2.86-fold; both $p < 0.001$) leading to a superior sGAG-deposition after implantation compared to the other cell sources (both $p < 0.001$). These results were further confirmed by a Thionin-staining (data not shown). Total collagen deposition was hugely increased after implantation and no significant differences could be detected between the different cell sources. (Figure 3B)

Constructs containing ACs, BMSCs or AMSCs exhibited a very weak staining for cartilage-specific collagen type II (Figure 3C), which was in contrast to the overall production of collagens (Figure 3B), thus indicating that other collagens were also produced (e.g. collagen type I or type III). The cartilage matrix of constructs containing ECs and NCs showed a strong staining for collagen type II, although the dissimilar distribution of collagen-type-II fibers within the cartilage matrices were apparent. The semi-quantitative histological scores of constructs containing ECs or NCs were significantly better than the scores of the other cell sources. (Figure 3C)

The presence of elastin was determined to evaluate differentiation into elastic cartilage. There was no elastin detectable in any of the constructs with an elastin immunostaining after five weeks of *in-vitro* cell culture. (Data not shown) After subcutaneous implantation, elastin was only present in alginate constructs containing ECs, and predominantly found in constructs which were pre-cultured with TGFβ1. Most elastin was located around the cell. (Figure 3D)

To ensure that these cartilage constructs were from human origin, a human-specific vimentin stain was used on histological sections. It confirmed that the cartilage constructs were indeed of human origin (Figure 3E), while the surrounding fibrous tissue was not (data not shown).

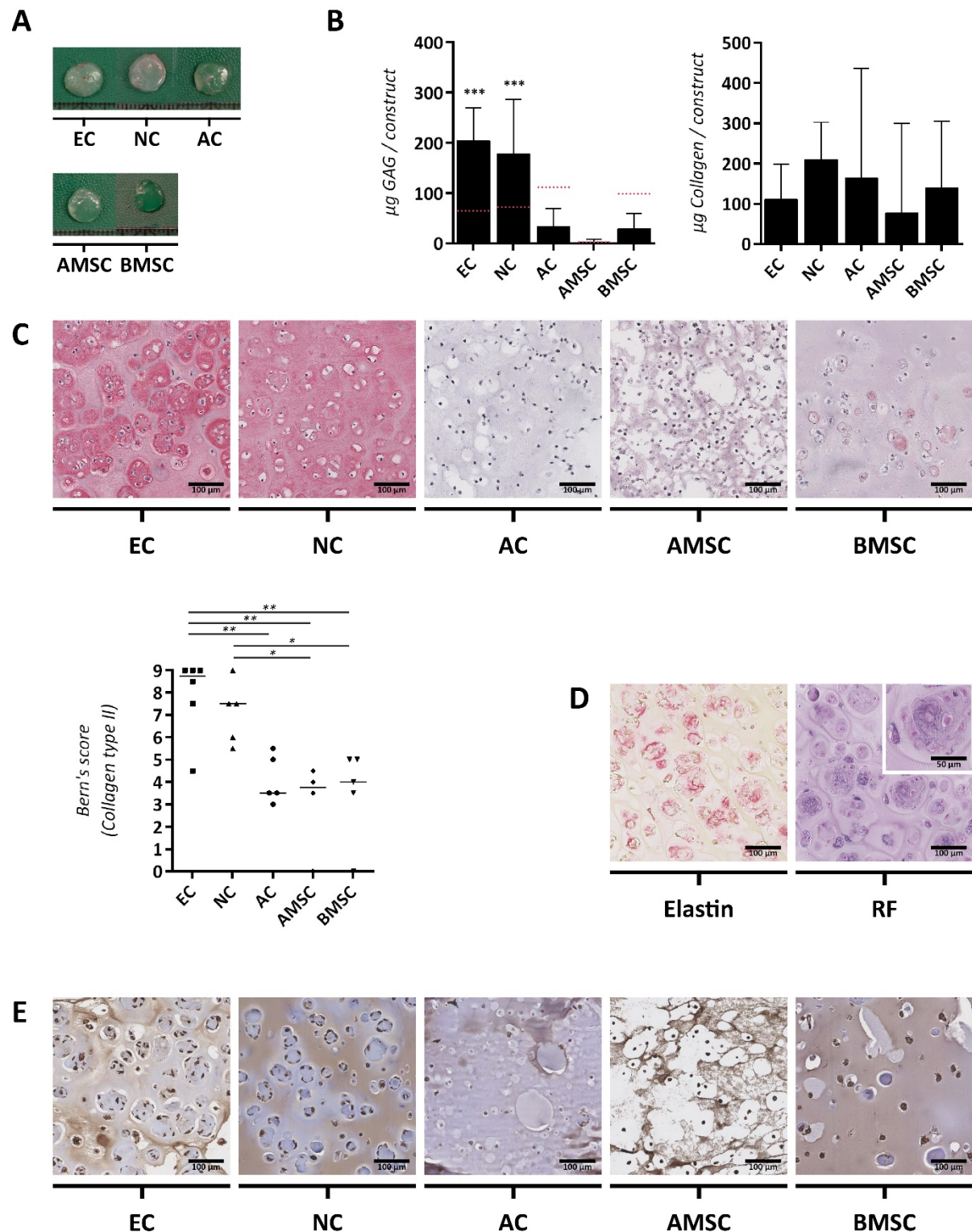


Figure 3. Cartilage matrix formation by several cell types *in vivo*.

Prior to subcutaneous implantation, constructs were cultured *in vitro* for 5 weeks in the presence of TGF β 1. **(A)** Macroscopic view of engineered cartilage constructs after 8 weeks of subcutaneous implantation. **(B)** Biochemical evaluation of the sGAG and collagen content after subcutaneous implantation. ECs and NCs deposited most sGAGs *in vivo*. Collagen-production was increased *in vivo*, but did not differ between the cell sources. **(C)** ECs and NCs demonstrated a collagen-type-II-rich matrix in almost all cartilage constructs, leading to significantly better semi-quantitative Bern's scores than the other cell sources. **(D)** Elastin was not formed *in*

vitro. After subcutaneous implantation, only constructs containing ECs were able to produce elastin. Most elastin fibres were found around the cell. Elastin = Immunohistochemical staining for elastin ; RF = Resorcin Fuchsin, chemical staining for elastin. **(E)** All cartilage constructs were of human origin. Biochemical data are shown as mean \pm SD. For statistical evaluation, a mixed model was used. Histological data are shown as the median of individual data points. For statistical evaluation, a Kruskal-Wallis test was used followed by Mann-Whitney-U comparison. *, ** or *** indicates *p*-values smaller than 0.05, 0.01 or 0.001 respectively compared to the other cell sources. EC = Ear Chondrocytes (*n*=3 donors) ; NC = Nasal Chondrocytes (*n*=3 donors) ; AC = Articular Chondrocytes (*n*=3 donors) ; BMSC = Bone-marrow-derived Mesenchymal Stem Cells (*n*=3 donors) ; AMSC = Adipose-tissue-derived Mesenchymal Stem Cells (*n*=3 donors). Per donor, 2 samples were used for analyses.

Cartilage stability

Hypertrophic differentiation is an unwanted phenomenon in cartilage regeneration, resulting in cartilage that can remodel into bone when implanted *in vivo*. To evaluate hypertrophy *in vitro*, we have studied gene expression of a panel of three hypertrophic markers during five weeks of cell culture (i.e. *COL10*, *ALP* and *MMP13*; Figure 4A). Cultured with TGF β 1 *COL10* expression was highest in NCs (*p*<0.05) and BMSCs (*p*<0.001), and was minimally expressed by ACs. *MMP13* was expressed by all cells and significantly highest in NCs. *ALP* was significantly higher in constructs with BMSCs compared to the other cell sources (*p*<0.05). In addition, constructs with BMSCs already expressed high *COL10* and *ALP* after two weeks of culture indicating early hypertrophic differentiation. (Data not shown)

Although BMSCs expressed all hypertrophic markers *in vitro*, they did not mineralize or form bone after eight weeks of subcutaneous implantation. Also, no signs of tissue calcification or bone formation were observed in construct containing AMSCs. On the contrary, 100% (3/3) of the cell-free constructs and, unexpectedly, 58.3% (7/12) of constructs encapsulating ACs did calcify *in vivo*. Also, calcification was more often seen in constructs pre-cultured in control medium (without TGF β 1) compared to constructs cultured in chondrogenic medium (with TGF β 1). (Figure 4B)

Cartilage structure and functionality

The elastic modulus of constructs was low *in vitro*, irrespective of the cell source used, being on average 7.42 ± 2.10 kPa. However, after subcutaneous implantation, mechanical properties improved in constructs containing either ECs (23.68 ± 10.20) or NCs (55.12 ± 59.25), but was not perceived in constructs containing ACs, BMSCs or AMSCs. (Figure 5) Since tissue calcification misrepresents the biomechanical properties of the cartilage matrix; we excluded calcified cartilage constructs from further analyses.

To determine whether the mechanical properties were enhanced by the deposition of matrix components, a multiple regression analyses was performed for all cell sources separately using sGAG and collagen deposition as independent variables. Only for constructs containing NCs, matrix components significantly associated with the biomechanical functionality of the constructs ($R^2=0.477$, $F=4.558$, $p=0.039$). For these constructs, only sGAG-deposition associated significantly with the biomechanical properties of the cartilage constructs independently (sGAG: $\beta=0.689$, $p=0.013$; collagen: $\beta=0.044$, $p=0.851$).

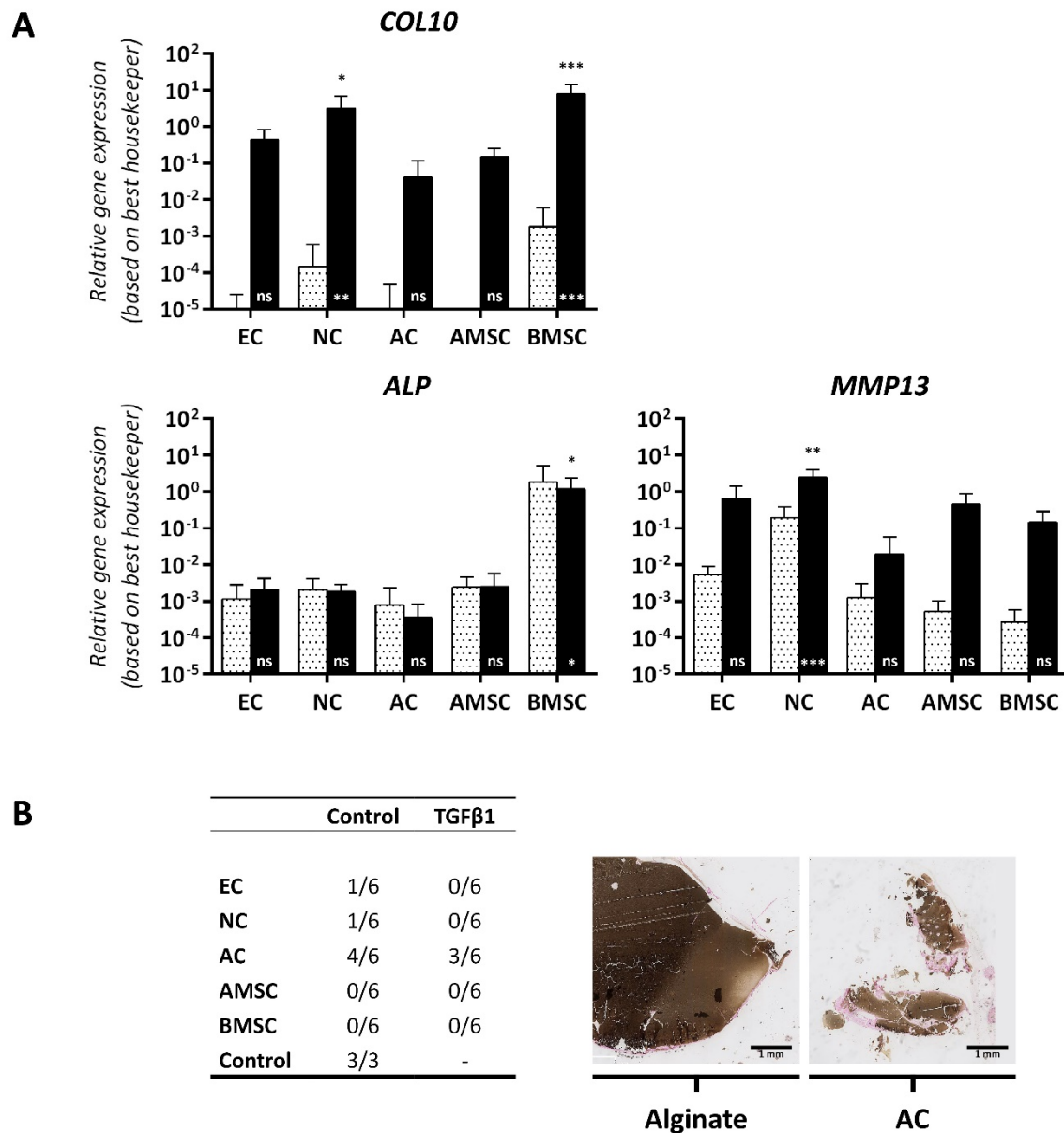


Figure 4. Stability of cartilage constructs *in vitro* and *in vivo*.

(A) Relative gene expression levels of *COL10*, *ALP* and *MMP13* were examined after 5 weeks of culture and corrected for the best housekeeper index. Hypertrophic genes were highest expressed by BMSCs and NCs. Data are shown as mean \pm SD. For statistical evaluation, a mixed model was used. *, ** or *** indicates *p*-values smaller than 0.05, 0.01 or 0.001 respectively compared to the control condition (asterisk is shown in the bar) or compared to the other cell sources (asterisk is shown above the bar). EC, NC and AC: *n*=4 donors each; BMSC, AMSC: *n*=6 donors each. **(B)** Von Kossa staining was used to evaluate construct calcification *in vivo*. MSCs did not calcify the construct *in vivo*. Non-seeded alginate and constructs encapsulating ACs did calcify. For each cell source we had a total of 6 alginate constructs: duplicate samples of 3 different donors. EC = Ear Chondrocytes ; NC = Nasal Chondrocytes; AC = Articular Chondrocytes; BMSC = Bone-marrow-derived Mesenchymal Stem Cells; AMSC = Adipose-tissue-derived Mesenchymal Stem Cells.

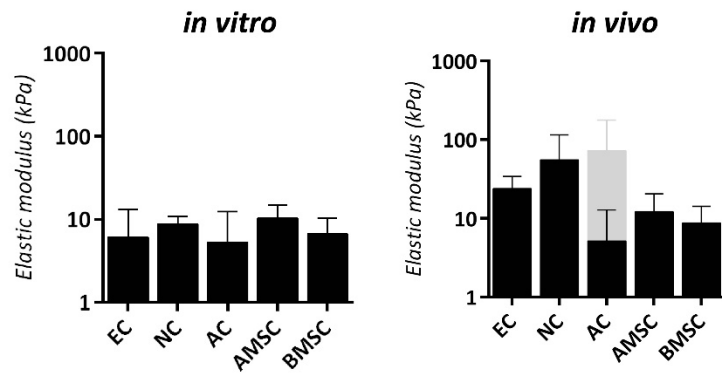


Figure 5. Biomechanical evaluation of constructs with different cell types

Biomechanical properties enhanced after *in vivo* implantation. ECs and NCs tended to exhibit superior mechanical properties *in vivo* compared to the other cell sources. Since tissue calcification misrepresents the biomechanical properties of the cartilage matrix; we excluded calcified cartilage constructs for further analyses (grey bar represents the mechanical properties of both calcified and non-calcified constructs). Biomechanical data are shown as mean \pm SD. EC = Ear Chondrocytes ($n=3$ donors) ; NC = Nasal Chondrocytes ($n=3$ donors) ; AC = Articular Chondrocytes ($n=3$ donors) ; BMSC = Bone-marrow-derived Mesenchymal Stem Cells ($n=3$ donors) ; AMSC = Adipose-tissue-derived Mesenchymal Stem Cells ($n=3$ donors). Per donor, 2 samples were used for analyses.

DISCUSSION

For successful regeneration of cartilage tissue, selection of the most appropriate cell source is crucial. This study demonstrates that cartilage matrix formation and functionality is cell source dependent; articular chondrocytes (ACs) possess the highest chondrogenic capacity *in vitro*, while ear chondrocytes (ECs) and nasal chondrocytes (NCs) are most potent for cartilage regeneration after subcutaneous implantation *in vivo*.

To date, we and others have evaluated the use of chondrocytes and mesenchymal stem cells (MSCs) of several anatomical locations for their applicability in cartilage regenerative medicine. [39, 42-44, 46-59, 206-209] However, these studies often used non-expanded cells isolated from animals. Moreover, a detailed direct comparison between various chondrocyte and MSC-sources was lacking. Therefore, this study is the first to systematically compare the quality and tissue stability of engineered cartilage constructs produced by culture-expanded ACs, NCs, ECs, BMSCs and AMSCs of human origin.

We have used culture-expanded human cells, to closely simulate the clinical situation. For clinical application, the use of autogeneic cells is favorable, since these cells do not elicit a tissue rejection response. However, it has been difficult to obtain appropriate numbers of cells, as donor tissue is limited and harvesting can cause large donor site morbidity. Consequently, monolayer cell-expansion has become an essential step in the process of cartilage TE. To fulfil this requirement, we culture-expanded all cells for four passages. It was obvious that different cells went through a different number of population doublings during these four passages; ACs had gone through the least number of population doublings confirming earlier findings of slow proliferation of ACs. [44, 48, 54, 57]

To be able to use expanded cells for the reconstruction of cartilage defects, cells should be stimulated to regain their cartilage-matrix-forming capacity. Several research groups have shown that expanded cells can regain their chondrogenic potential under specific culture conditions: (1) the use of a 3D-culture system (2) and/or the administration of chondrogenic factors, such as TGF β . [216] In order to generate a 3D-culture environment, we have encapsulated all cells in clinical grade alginate, since alginate enables a homogeneous cell distribution, prevents cells from floating out while permitting nutrient diffusion and oxygen transfer to the encapsulated cells and promotes the synthesis of cartilage-specific matrix components, such as sGAGs and collagen type II. [89] Surprisingly, we showed that alginate appears to have the tendency to calcify *in vivo*, since 20% of all constructs calcified during subcutaneous implantation. Especially, cell-free constructs and constructs encapsulating ACs suffered from this phenomenon. Also, calcification was more often seen in constructs pre-cultured in medium without TGF β 1. To our knowledge, calcium-cross-linked alginate calcifies through binding the surrounding phosphate ions to form calcium phosphate crystals. Those crystals are stable in neutral to basic environments and do not appear at pH less than 6.8. [217] We believe that the calcified constructs were possibly generated a neutral to alkaline environment prior to implantation, since these constructs were either not metabolically active (non-seeded alginate) or had a low metabolic activity due to stable cartilage formation (ACs) or due to the deficiency of TGF β 1. Obviously, in these constructs, calcification did not seem to be a consequence of instable cartilage formation, but was more likely a typical characteristic

of alginate itself. Surprisingly and in contrast to our previous work with MSCs in collagen scaffolds [71] or in pellets without scaffold [218], constructs containing MSCs (both BMSCs and AMSCs) never mineralized *in vivo*, although signs of endochondral differentiation were observed prior to implantation. The absence of endochondral ossification during *in vivo* implantation was accompanied by lack of neovascularization or vessel ingrowth within the matrix, which is known to be extremely important for endochondral ossification [219]. We believe that alginate prevented this process, by the fact that endothelial cells lack receptors to bind to alginate polymers, prohibiting neovascularization or vessel ingrowth. [220] Therefore, it seemed that alginate could be an excellent cell-carrying gel for cartilage regeneration although future work needs to clarify which approach is required to exclude alginate calcification after *in vivo* implantation.

In addition to a 3D-culture environment, specific growth and differentiation factors will help to regain and induce a chondrocyte-like phenotype. *In vitro*, culture-expanded cells of all sources studied failed to differentiate towards the chondrogenic lineage in the absence of TGF β 1, as assessed by an almost negligible deposition of sGAGs and the inferior expression of both *ACAN* and *COL2A1* in alginate constructs. The presence of TGF β 1 induced chondrogenic differentiation *in vitro*, where ACs exhibit a superior chondrogenic capacity *in vitro*, compared to the other cell sources. The beneficial effect of culturing with TGF β 1 during *in-vivo* chondrogenesis was present, although less obvious. Constructs cultured without TGF β 1 increased their production of matrix components after *in-vivo* implantation, but were not able to reach levels found in constructs cultured with TGF β 1.

Even after four passages of culture-expansion, chondrocytes demonstrated some clear subtype specific differences. Firstly, ACs possessed the highest chondrogenic capacity *in vitro*, but were not able to further increase their cartilage matrix *in vivo*. The inability of ACs to promote cartilage formation *in vivo* may be due to the lack of mechanical loading or growth factor stimulation after subcutaneous implantation which may have led to a loss of chondrogenic capacity. ACs, different from the other cell sources, are exposed to mechanical loading within native articular cartilage and unloading is known to induce sGAG-release from the cartilage matrix and to reduce cell proliferation and sGAG-synthesis within the matrix. [221] Secondly, chondrocytes from ear cartilage were able to form an elastin network after subcutaneous implantation *in vivo*. Elastin was predominantly found in constructs which were cultured with TGF β 1. *In-vitro* culture did not demonstrate elastin deposition at all, which was in accordance with our previous work. [56] The capability of culture-expanded ECs to produce elastin *in vivo* suggests that these cells retain their capability to form an elastic cartilage matrix. Both findings - the inability of ACs to promote cartilage formation *in vivo* without mechanical loading and the ability of cultured expanded ECs to produce elastin - indicate that both cell types preserved their subtype specific phenotype after culture expansion, confirming our previous study where gene expression profiles of culture expanded NCs and ECs displayed clear differences that were related to their developmental origin. [56]

Besides chondrocytes, MSCs have been demonstrated to be an attractive cell source for cartilage TE. [62, 64, 66, 222] Although bone marrow offers the most common source of MSCs, adipose tissue has been proven to be an attractive alternative in respect to the abundant and easily accessible pool of MSCs. [67, 68] We have demonstrated that both BMSCs

and AMSCs underwent chondrogenic differentiation *in vitro* and *in vivo*, although matrix production was less than in constructs containing chondrocytes (ACs, NCs or ECs). Constructs containing BMSCs had a higher chondrogenic potential than AMSCs, demonstrated by an increased *ACAN* and *COL2A1* gene-expression and an improved sGAG-deposition. With the exception of a few studies [223-226], this confirms other studies [55, 207, 227-235]. Nevertheless, the assumptions that MSCs are fundamentally less chondrogenic than chondrocytes and that BMSCs are more in favor for cartilage regeneration than AMSCs, seems unjustified. It appears that cell culture conditions for both BMSCs and AMSCs remain to be improved. For instance, it was found that another member of the TGF β -superfamily, Bone Morphogenetic Protein 6, is obligatory to improve chondrogenic differentiation in AMSCs. [236]

Finally, in order to understand how the distribution and composition of matrix components resulted in a mechanically functional cartilage matrix, the compositional biomechanical relationship of the cartilage constructs was evaluated. After *in-vivo* implantation, mechanical properties increased in constructs containing ECs and NCs. Only for constructs containing NCs, matrix components were significantly correlated to their biomechanical functionality. It is already known that sGAGs and collagens, the main components of the ECM, are both associated with the biomechanical properties of native cartilage: (1) the negatively charged sGAGs provide an osmotic pressure within the tissue ; (2) the architecture of the collagen network capture the sGAGs and prevent them from leaking out of the tissue. [237] In contrast, the elastic fiber network in constructs containing ECs might have influenced the biomechanical properties *in vivo* as well, although the exact contribution of elastin to mechanical functionality is not yet fully understood. Besides the existence of matrix components, the quality of the matrix is not only determined by the amount of matrix components deposited, but also influenced by the number of cross-links between matrix molecules (i.e. collagen cross links). [238] The distribution of matrix components in the ECM was clearly different between cell sources: ECs deposited most matrix components pericellularly, whereas NCs deposited these matrix components homogenously throughout their matrix, which was clearly visible on the immunohistochemical collagen type II staining. It is well-known that a heterogeneous distributed matrix alters the biomechanical properties of the matrix, as the physical properties are determined by the weakest point in the matrix [140].

The present study has certain limitations. Firstly, cell density plays a critical role in functional and stable cartilage formation. Others have demonstrated that cell densities greater than 20×10^6 cells per milliliter are desirable, while low cell densities resulted in decreased cartilage formation. [239] Therefore, a potential drawback of our study is that we only could use a cell-seeding density of 4×10^6 cells per milliliter of alginate, since the size of our experimental set-up did not enable higher densities. Secondly, as mentioned before, we have culture-expanded all cells until passage four to obtain a sufficient number of cells. In order to be able to compare all different cell sources, we have used standardized protocols for the culture-expansion of both chondrocytes and MSCs. Differences in expansion rates between the different cells were obvious. While culture-expansion is associated with chondrocyte dedifferentiation and replicative cell senescence, the enforcement of population

doublings instead of culture passages might have been more appropriate, since population doublings more accurately reflect cell growth and thus cell aging. However, since nasal chondrocytes had most doublings in four passages but still produced most cartilage, a direct link between doublings and cartilage formation seems unlikely. How all the parameters such as number of doublings, expansion speed, initial seeding density, growth factors present in the medium or produced by the cells themselves exactly determine dedifferentiation and possible loss of chondrogenic capacity during monolayer expansion remains to be elucidated. Finally, we have demonstrated large donor variation in constructs containing ACs or BMSCs. Nevertheless these differences were not based on a donor-age effect nor explained by the use of healthy versus diseased ACs. Moreover, donors for nasal cartilage appeared younger than other sources. Although there is a possibility that the donor-age has influenced the general outcome of our study, improved chondrogenic and proliferative capacity of nasal chondrocytes was also stated by others in literature. [39, 48, 52]

In summary, we have demonstrated that cartilage matrix formation and functionality are cell source dependent. ACs possess the highest chondrogenic capacity *in vitro*, while ECs and NCs are most potent for cartilage regeneration after subcutaneous implantation, making ECs and NCs attractive cell sources for future cell-based cartilage repair. Only for constructs containing nasal chondrocytes, sGAG and collagen content were associated with biomechanical functionality of the constructs, indicating the differences in matrix component assembly by different cell sources. The inability of ACs to increase cartilage matrix *in vivo* may be due to a loss of chondrogenic capacity in the absence of mechanical loading or growth factor stimulation. Although MSCs are considered as a promising cell sources for the reconstruction of cartilage defects, it appears that improvements in cell culture conditions for both BMSCs and AMSCs are needed.

Acknowledgment

The authors thank the Departments of Orthopaedic Surgery, Plastic and Reconstructive Surgery, and Otorhinolaryngology at Erasmus MC for their assistance in obtaining ear, nasal and articular cartilage as well as bone marrow and adipose tissue, and CellMed (Alzenau, Germany) for providing the clinical grade alginate. The study was performed within the framework of EuroNanoMed (EAREG-406340-131009/1) and funded by SenterNovem (ENM09001).

Chapter 5

Trophic effects of adipose-tissue-derived and bone-marrow-derived mesenchymal stem cells enhance cartilage generation by chondrocytes in co-culture

M.M. Pleumeekers, L. Nimeskern, J.L.M. Koevoet, M. Karperien, K.S. Stok, G.J.V.M. van Osch

PLoS One, 2018. 13(2): p. 1-23.

ABSTRACT

Combining mesenchymal stem cells (MSCs) and chondrocytes has great potential for cell-based cartilage repair. However, there is much debate regarding the mechanisms behind this concept. We aimed to clarify the mechanisms that lead to chondrogenesis (chondrocyte driven MSC-differentiation versus MSC driven chondro-induction) and whether their effect was dependent on MSC-origin. Therefore, chondrogenesis of human adipose-tissue-derived MSCs (*hAMSCs*) and bone-marrow-derived MSCs (*hBMSCs*) combined with bovine articular chondrocytes (*bACs*) was compared.

hAMSCs or *hBMSCs* were combined with *bACs* in alginate and cultured *in vitro* or implanted subcutaneously in mice. Cartilage formation was evaluated with biochemical, histological and biomechanical analyses. To further investigate the interactions between *bACs* and *hMSCs*, (1) co-culture, (2) pellet, (3) Transwell® and (4) conditioned media studies were conducted.

The presence of *hMSCs* - either *hAMSCs* or *hBMSCs* - increased chondrogenesis in culture; deposition of sGAG was most evidently enhanced in *hBMSC/bACs*. This effect was similar when *hMSCs* and *bAC* were combined in pellet culture, in alginate culture or when conditioned media of *hMSCs* were used on *bAC*. Species-specific gene-expression analyses demonstrated that *aggrecan* was expressed by *bACs* only, indicating a predominantly trophic role for *hMSCs*. *Collagen-10*-gene expression of *bACs* was not affected by *hBMSCs*, but slightly enhanced by *hAMSCs*. After *in-vivo* implantation, *hAMSC/bACs* and *hBMSC/bACs* had similar cartilage matrix production, both appeared stable and did not calcify.

This study demonstrates that replacing 80% of *bACs* by either *hAMSCs* or *hBMSCs* does not influence cartilage matrix production or stability. The remaining chondrocytes produce more matrix due to trophic factors produced by *hMSCs*.

INTRODUCTION

Cartilage has a very limited capacity for self-regeneration. Untreated lesions - caused by trauma, tumors, congenital malformation or age related degeneration - persist indefinitely and ultimately require surgical intervention. However, current treatments are unsuccessful for long-term repair; resulting in a need for novel repair strategies. Cell-based cartilage repair holds promise for restoring missing or destroyed cartilage and has the potential to overcome limitations of current treatments, while re-establishing the unique biological and functional properties of the tissue.

One of the major challenges herein is defining an appropriate cell source. Current cell-based surgical treatments for cartilage lesions are predominantly based on the use of either (1) chondrocytes or (2) mesenchymal stem cells (MSCs). These cell-based procedures are however associated with specific disadvantages. Chondrocytes from several anatomical locations (e.g. joint, rib, nose, ear, meniscus) have been investigated for their application in cartilage regeneration. [39-59] However, to generate a construct of reasonable size, large numbers of chondrocytes are required, necessitating the use of culture-expansion. In monolayer culture-expansion, chondrocytes dedifferentiate; they change phenotypically to a fibroblast-like morphology and lose their chondrogenic gene-expression capacity. Chondrocyte-dedifferentiation usually results in fibrous and mechanically inferior cartilage, making them less suitable for cell-based cartilage repair. [61] In contrast, multipotent cells, like MSCs, achieved considerable attention as alternative cells, as they can undergo multiple population doublings without losing their chondrogenic potential and have the capacity to differentiate into cartilage tissue under appropriate culture conditions. [64-68] Furthermore, MSCs are easily available from several tissues, including bone marrow and adipose tissue, which makes culture-expansion unnecessary. However, the single use of MSCs for cell-based cartilage repair is currently debated, since the cartilage tissue formed is unstable and predisposed to mineralization and ossification *in vivo*. [69-71, 240, 241]

Currently, combining both cell sources holds great promise for cell-based cartilage repair as it reduces the required number of chondrocytes and diminishes many disadvantages of both individual cell types. Moreover, by decreasing the amount of chondrocytes required ($\leq 20\%$ of the total cell mixture), culture-expansion is no longer necessary, which would allow the use of freshly isolated primary chondrocytes leading to improved cartilage formation. [76] Unfortunately, in depth understanding of the cellular interaction pathways between MSCs and chondrocytes is under debate in literature: It is thought that the co-culture effect is either credited by (1) chondrocyte driven MSC-differentiation or ascribed to (2) chondrocytes, whose cartilage-forming capacity and proliferation activity are enhanced in the presence of MSCs. [81] In recent years, the trophic and paracrine functions of MSCs appeared most critical in this process, rather than the simple chondrogenic differentiation of MSCs alone. However, little is known as to whether their trophic function is a general characteristic of MSCs or dependent on the origin of the MSC source. MSCs from several anatomical locations have been applied in co-culture. Independent on their origin, mixed cell cultures of chondrocytes and MSCs have been demonstrated to generally improve chondrogenesis as well as to reduce hypertrophy and tissue mineralization. [75, 81, 242] In contrast, three co-culture studies using adipose-

tissue-derived MSCs (AMSCs) showed limited or decreased effects of MSCs on chondrogenesis. [243-245] Such effect was hardly seen in co-culture studies using bone-marrow-derived MSCs (BMSCs), which may propose that, compared to BMSCs, AMSCs are less efficient in co-culture. Due to methodological heterogeneity however, a direct comparable analysis between AMSCs and BMSCs in co-culture could not be easily made. So far, only three research groups have directly compared the effect of AMSCs and BMSCs on chondrocytes in co-culture. [80, 246, 247] Unfortunately, these studies demonstrate conflicting outcomes and have never translated to animal research.

Therefore, we aim to investigate whether MSCs undergo chondrogenic differentiation upon contact with chondrocytes or by trophic effects of MSCs on chondrocytes. Whether the co-culture effect is dependent on MSC-origin or a general characteristic of MSCs, is further elucidated. Therefore, chondrogenesis of human AMSCs (*hAMSCs*) and BMSCs (*hBMSCs*) combined with bovine articular chondrocytes (*bACs*) is compared. The xenogeneic set-up using *hMSCs* and *bACs* will allow conclusions about the cell type responsible for chondrogenesis. As cellular interactions can be influenced or overruled by exogenous growth factors, no growth factors are added to the culture system to study cartilage formation of the co-cultures *in vitro*. Moreover, cartilage formation will be evaluated after immediate subcutaneous implantation of the constructs in mice. To further elucidate the interactions between MSCs and ACs, different *in-vitro* culture systems will be used: (1) co-culture system of *hMSC/bACs* in alginate, (2) pellet co-culture system of *hMSC/bACs*, (3) Transwell® system of singular isolated *hMSCs* and *bACs* in alginate, and (4) conditioned media culture systems of conditioned medium of *hMSCs* on *bACs* and vice versa.

MATERIALS AND METHODS

Chemicals were obtained from Sigma-Aldrich, USA unless stated otherwise.

Cell sources

All human samples were obtained after approval by the Erasmus MC Medical Ethical Committee. Human mesenchymal stem cells (*hMSCs*) were isolated from either adipose tissue (*hAMSCs*) or bone-marrow aspirates (*hBMSCs*). *hAMSCs* were obtained from subcutaneous abdominal adipose tissue as waste material without the need for informed consent (protocol # MEC-2011-371) ($n=3$ independent donors: F 52Y ; F 51Y ; F 53Y). *hBMSCs* were isolated from bone-marrow heparinized aspirates, after written informed consent had been acquired (protocol # MEC-2004-142 and Albert Schweitzer Hospital 2011/7) ($n=3$ independent donors: M 67Y ; F 75Y ; M 22Y). Both *hAMSCs* and *hBMSCs* were seeded and cultured overnight in medium consisting of Minimum Essential Medium Alpha (MEM- α ; Gibco, USA), supplemented with 10% fetal calf serum (FCS ; Lonza, the Netherlands), 10^{-4} M L-ascorbic acid 2-phosphate, and 1 ng/mL basic Fibroblast Growth Factor 2 (bFGF2 ; AbD Serotec, UK). [248-250]

Articular chondrocytes (ACs) were selected, to study the trophic effect of *hAMSCs* or *hBMSCs* on chondrocytes. To obtain primary bovine articular chondrocytes (*bACs*), macroscopically intact cartilage was harvested from the metatarsophalangeal joints of calves ≤ 6 months old (T. Boer & Zn., Nieuwerkerk aan den IJssel, the Netherlands), and washed with saline ($n=4$ pools of 3 donors each). To isolate cells, cartilage pieces were incubated for 1 hour with 2 mg/mL protease (type XIV derived from *Streptomyces griseus*), followed by overnight incubation with 1.5 mg/mL collagenase B (Roch Diagnostics, Germany) in High Glucose - Dulbecco's Modified Eagle's Medium (HG-DMEM ; Gibco) with 10% FCS, 50 μ g/mL gentamycin (Gibco), and 0.5 μ g/mL amphotericin B (Fungizone ; Life Technologies, Breda, the Netherlands). To extract small parts of undigested cartilage, the cell suspension was filtered through a nylon 100- μ m mesh. Prior to cell culture, cell viability was tested using the trypan blue exclusion test, and cell number was calculated with a hemocytometer.

Chondrogenesis

For *in-vitro* and *in-vivo* studies, all cells were encapsulated in alginate (Batch MG-004, CellMed, Germany), a hydrogel known of its high biocompatibility [251] and chondrogenic capacity [89]. Moreover, alginate hydrogels enable homogeneous cell distribution and allow paracrine factors to access all cells equally [89], making them suitable scaffolds for following research purposes.

Second-passaged *hMSCs* and non-expanded primary *bACs* were harvested and cultured in a 3D-alginate hydrogel. Cells were suspended at a density of 4×10^6 cells/mL in clinical grade 1.1% low viscosity alginate solution dissolved in 0.9% NaCl as single-cell-type populations or as a combination of 80% *hMSCs* (either *hAMSCs* or *hBMSCs*) and 20% *bACs*. (Table 1) A 4:1 ratio was selected based on our previous experience [252] and that of others [74, 253].

Human stem cells			Bovine chondrocytes	
	Source	Cell density (x10 ⁶)	Source	Cell density (x10 ⁶)
hAMSC	hAMSCs	4 nc/mL	x	x
hBMSC	hBMSCs	4 nc/mL	x	x
bAC	x	x	bACs	4 nc/mL
hAMSC/bAC	hAMSCs	3.2 nc/mL	bACs	0.8 nc/mL
hBMSC/bAC	hBMSCs	3.2 nc/mL	bACs	0.8 nc/mL
Control bAC	x	x	bACs	0.8 nc/mL

Table 1. Construct conditions.

Cell density is displayed as the number of cells (nc) in 1 milliliter of alginate. *hAMSC* = human Adipose-tissue-derived Mesenchymal Stem Cell ; *hBMSC* = human Bone-marrow-derived Mesenchymal Stem Cell ; *bAC* = bovine Articular Chondrocyte.

Flat constructs (8 mm diameter ; 2 mm height) were processed as previously described. [40] In short, alginate suspensions were injected into a custom designed slab mold consisting of 2 calcium-permeable membranes (Durapore® 5.0 µm membrane filters, Millipore) rigidly supported by stainless-steel meshes and separated by a stainless-steel casting frame. Alginate was instantaneously gelled for 30 minutes in 102 mM CaCl₂ and thereafter washed with 0.9% NaCl and HG-DMEM. Sterile biopsy punches (Spengler, Asnières sur Seine, France) were used to create alginate constructs suitable for mechanical testing. Constructs were either cultured *in vitro* or directly implanted subcutaneously in mice. (Figure 1A)

In vitro, constructs were cultured in ‘basic medium’ containing serum-free HG-DMEM supplemented with 50 µg/mL gentamycin; 0.5 µg/mL Fungizone; 1 mM sodium pyruvate (Gibco); 40 µg/mL L-proline; supplemented Insulin Transferrine Selenium (ITS+ ; B&D Bioscience, Bedford, MA, USA); 10⁻⁷ M dexamethason; and 25 µg/mL L-ascorbic acid 2-phosphate without the addition of growth factors. For each condition referred to in table 1, 3 independent donors were used in triplicate (total *n*=54). After 3 and 5 weeks, constructs were processed for biochemical and gene-expression analysis.

In-vivo studies were completed after 8 weeks of subcutaneous implantation. In total, 10 9-week-old, female NMRI nu/nu mice (Charles River Laboratories, the Netherlands) were used. Two separate incisions were made along the central line of the spine (1 at the shoulders and 1 at the hips), after which 4 separate subcutaneous dorsal pockets were prepared by blunt dissection. For each condition referred to in table 1, 3 independent donors were used in duplicate (total *n*=36). Moreover, cell-free constructs were used as controls (*n*=4). For implantation, alginate constructs were randomly assigned to these 4 pockets. After 8 weeks, animals were sacrificed and samples were explanted for histological, biomechanical and biochemical analyses. Animal experiments were carried out to the guidelines prescribed by the Dutch National Institutes of Health, and were approved by the Dutch equivalent of the Institutional Animal Care and Use Committee, the Erasmus MC Dier Ethische Commissie (protocol # EMC 2429).

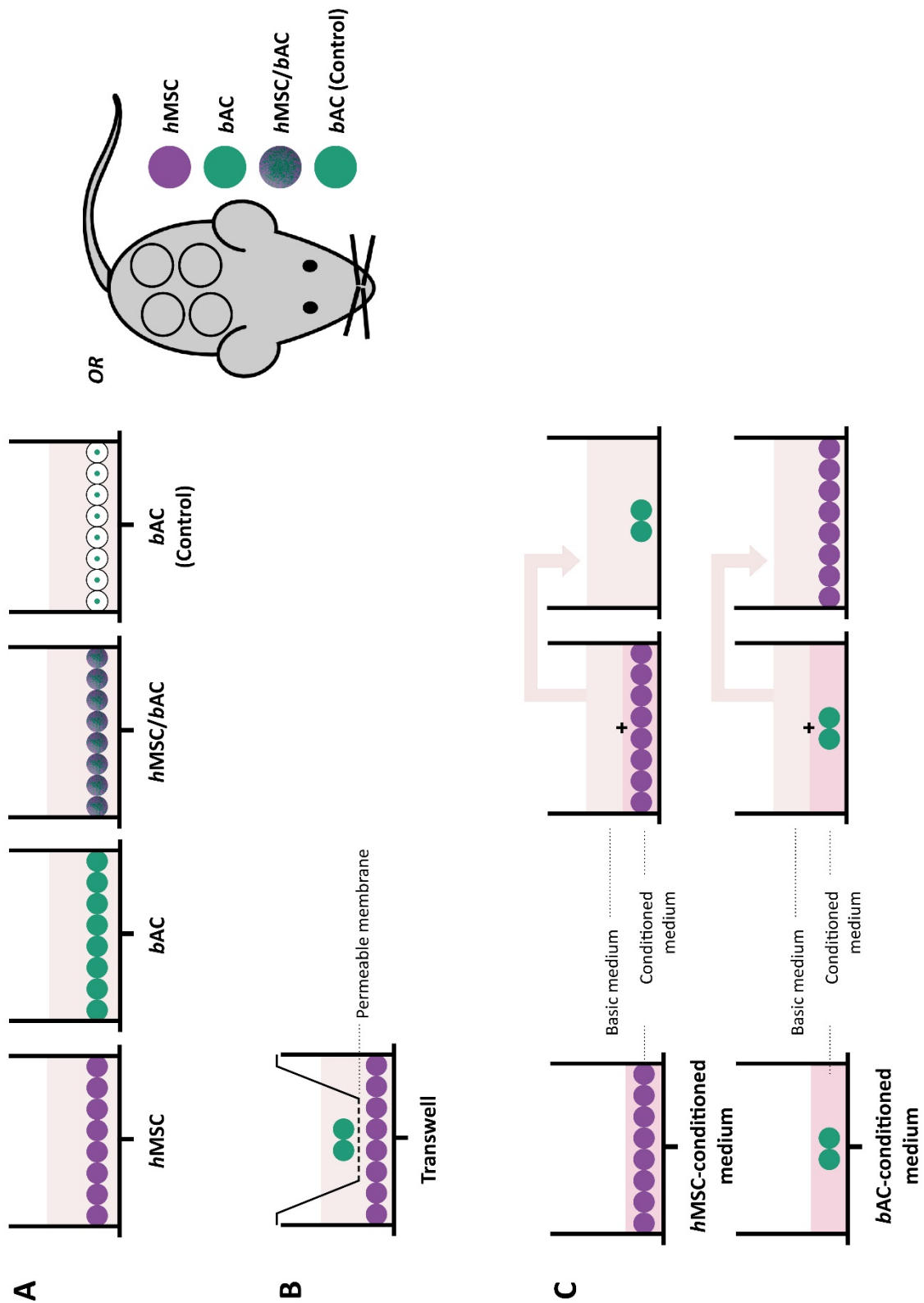


Figure 1. Cellular interaction.

Cells were encapsulated in alginate beads separately and alginate and pellet co-cultures (**A**, **control conditions**). Furthermore, hMSCs and bACs were co-cultured in (**B**) a Transwell® system as well as in (**C**) medium conditioned by the other cell type, to further understand the complex cellular communication pathways between hMSCs and bACs. In purple: hMSCs = human Mesenchymal Stem Cells ; in green: bACs = bovine Articular Chondrocytes.

Cellular interaction

To further understand the complex cellular communication pathways between MSCs and ACs, cell types (*hAMSCs* (F 53Y) ; *hBMSCs* (M 22Y) ; *bACs* pool of 3 donors) were co-cultured as follows: (1) *hMSCs* and *bACs* were combined and cultured in alginate as previously described; (2) *hMSCs* and *bACs* were cultured in pellets, allowing direct cell-cell contact. Furthermore, *hMSCs* and *bACs* were encapsulated in alginate separately and co-cultured in (3) a Transwell® system ; as well as (4) in medium conditioned by the other cell type. (Figure 1) The ratio of *hMSCs* to *bACs* in each culture system was kept 80:20 for all conditions. All constructs were cultured under standardized nutritional conditions. Medium was changed 3 times a week. After 3 weeks, alginate beads and pellets were processed for biochemical or gene-expression analysis.

(1) Co-culture

hMSCs and *bACs* were suspended at a density of 4×10^6 cells/mL in clinical grade alginate solution as a mixed-cell-type population at a 80:20 ratio as described above. (Figure 1A)

(2) Pellet culture

To study the effects of direct cell-cell contact in co-cultures, *hMSCs* and *bACs* were cultured in pellets. Therefore, a mixture of 80% *hMSCs* and 20% *bACs* was suspended in basic medium and a total number of $2,5 \times 10^5$ cells in 0.5 mL were transferred into polypropylene tubes and pellet were formed by centrifuging at 200 G for 8 minutes. To induce proper pellet formation, addition of Transforming Growth Factor $\beta 1$ (TGF $\beta 1$; R&D Systems, USA) for 24 hours was required. This exposure was not sufficient to induce chondrogenesis in *hMSCs* (data not shown). After 24 hours, pellet were exposed to the 'basis medium' without addition of any growth factors. (Figure 1A)

(3) Transwell® system

hMSCs and *bACs* were suspended at a density of 4×10^6 cells/mL in clinical grade alginate solution as single-cell-type populations and transferred into a 10-mL sterile syringe. Thereafter, the cell-suspension was slowly passed through a 23-gauge needle to produce drops, which fell into a 102 mM CaCl₂ creating alginate beads. Following instantaneous gelation, beads were allowed to further gelate for a period of 10 minutes in the CaCl₂-solution. After being washed once with 0.9% NaCl and HG-DMEM, the beads were transferred to a Transwell® system (Corning Life Science, USA). The Transwell® inserts separated *hMSCs* and *bACs* by a porous membrane of 8 μ m, allowing paracrine signaling between *hMSCs* and *bACs*. (Figure 1B)

(4) Conditioned medium

Alginate beads containing *hMSCs* or *bACs* were produced as described above and cultured in medium conditioned by the other cell types. To obtain *bACs*, *hAMSCs* and *hBMSCs* conditioned media, alginate beads were cultured in 'basic medium' for 3 days. After 3 days of culture, conditioned media were collected, enriched with 1:1 'basic medium' and immediately added

to alginate cultures of the other cell types. Again, a 80:20 ratio between *hMSCs* and *bACs* was maintained. (Figure 1C)

Biochemical evaluation of the extracellular matrix

Alginate constructs were digested overnight at 56°C in papain (250 µg/mL in 0.2 M NaH₂PO₄, 0.01 M EDTA, containing 5 mM L-cystein ; pH 6.0) ; pellets were digested overnight at 56°C in proteinase K (1 mg/mL in Tris/EDTA buffer containing 185 µg/mL iodoacetamide and 1 µg/mL pepstatin A ; pH 7.6). After digestion, samples were subjected to biochemical analyses to determine DNA, sulfated-glycosaminoglycan (sGAG), and hydroxyproline contents as described previously. [40] In short, the amount of DNA was determined by Ethidium bromide (GibcoBR1), using calf thymus DNA as a standard. sGAGs were quantified by the 1,9-Dimethylmethylene blue (DMMB) dye-binding assay, using shark chondroitin sulphate C as a standard. To be suitable for cell cultures containing alginate, the DMMB-pH-level was adjusted to pH 1.75, as described previously. [212] For the hydroxyproline content, digests were hydrolysed, dried and redissolved in 150 µL water. Hydroxyproline contents were measured using chloramine-T and dimethylaminobenzaldehyde as reagents and hydroxyproline (Merck, Germany) as a standard. Collagen content was subsequently estimated from the hydroxyproline content, assuming that one collagen triple helix molecule contains 300 hydroxyproline residues.

Histological evaluation

After 8 weeks of subcutaneous implantation, constructs were harvested, set in 2% agarose, fixed in 4% formalin in PBS and embedded in paraffin. Paraffin-embedded sections (6 µm) were deparaffinised and rehydrated.

To evaluate tissue calcification, Von Kossa staining was performed. Slides were immersed in 5% silver nitrate solution for 10 minutes, rinsed in MilliQ and exposed to light for another 10 minutes. Excess silver nitrate was removed with 5% sodium-thiosulphate and slides were rinsed in distilled water afterwards. Sections were counterstained with Nuclear fast red (Merck).

To allow the use of monoclonal mouse antibody collagen type II (II-II6B3 1:100; Developmental Studies Hybridoma Bank, USA) on constructs which had been implanted in mice, the primary antibody was pre-coupled overnight with goat anti-mouse biotin at 4°C (1:500 ; Jackson Laboratories, USA), followed by a 2-hour incubation in 0.1% normal mouse serum (CLB, the Netherlands), to prevent unwanted binding of the anti-mouse antibodies to mouse immunoglobulins. [214]

Antigen retrieval was performed through incubation with 0.1% pronase for 30 minutes at 37°C, continued with a 30 minutes incubation with 1% hyaluronidase at 37°C. Non-specific binding sites were blocked with 10% goat serum and sections were stained with the pre-treated antibodies for 60 minutes. Sections were then incubated with enzyme-streptavidin conjugate (Label, 1:100, Biogenex, HK-321-UK, USA) in PBS/1% BSA, followed by incubation with Neu Fuchsin substrate (Chroma, Germany).

Biomechanical analysis

In order to distinguish the mechanical strength of alginate itself, cell containing constructs were prepared and directly taken for mechanical testing as described previously. [40] In short, for mechanical characterization of engineered cartilage constructs after *in vivo* cell culture, constructs 2.5 mm thick and 5 mm in diameter were used. The samples were placed in close-fitting Ø 5 mm stainless steel cylindrical wells. Mechanical testing was performed with a materials testing machine (Zwick Z005, Ulm, Germany) equipped with a 10 N load cell, a built-in displacement control, and a cylindrical, plane ended, stainless steel indenter (Ø 1.2 mm). During mechanical testing the samples were immersed in PBS. Stress-strain testing was performed: the samples were compressed to a final height of 0.5 mm at a loading rate of 5 mm per minute. An in-house Matlab® script was used to locate the sample surface and measure the sample thickness. Force-displacement curves were then converted to stress-strain curves. Measurements of compressive modulus at 40% strain, E40%, were determined for every sample.

Gene-expression analyses

For total RNA isolation, alginate was dissolved in ice-cold 55 mM sodium citrate and 20 mM Ethylene Diaminetetraacetate (EDTA) in 150 mM NaCl and centrifuged. Each cell-pellet was subsequently suspended in 1 mL RNA-Bee™ (TEL-TEST, USA). For total RNA isolation from pellets, pellets were manually homogenized and suspended in 300 µL/pellet RNA-Bee™. RNA was extracted with chloroform and purified from the supernatant using the RNAeasy Micro Kit (Qiagen, Germany) according to the manufacturer's guidelines by on-column DNA-digestion. Extracted total RNA was quantified using NanoDrop® ND-1000 Spectrophotometer (NanoDrop Technologies, Wilmington, DE, USA) at 260/280 nm. Total RNA of each sample was reverse transcribed into cDNA using RevertAid™ First Strand cDNA Synthesis Kit (MBI Fermentas, Germany).

For quantitative real-time Polymerase Chain Reaction (qRT-PCR) analysis, forward and reverse primers were designed using PrimerExpress 2.0 software (Applied Biosystems, USA) to meet TaqMan or SYBR Green requirements. Gene specificity of all primers was guaranteed by Basic Local Alignment Search Tool (BLASTN). Analysed genes are listed in table 2. qRT-PCR was performed using qPCR Mastermix Plus for SYBR Green (Eurogentec, the Netherlands) according to the manufacturers' guidelines and using ABI PRISM® 7000 with SDS software version 1.7 (Applied Biosystems, The Netherlands). Relative gene expressions were calculated by means of the $2^{-\Delta CT}$ formula.

Primers and probes	
Human specific genes	
<i>hsGAPDH</i>	Fw: AGCTCACTGGCATGGCCTTC Rev: CGCCTGCTTCACCACCTTCT
<i>hsACAN</i>	Fw: CAGCCACCACCTACAAACGCAG Rev: CTGGGTGGGATGCACGTCAGC
<i>hsCOL2A1</i>	Fw: ACGAGGCCTGACAGGTCCCA Rev: GCCCAGCAAATCCCGCTGGT
Bovine specific genes	
<i>bsGAPDH</i>	Fw: GTCAACGGATTTGGTCGTATTGGG Rev: TGCCATGGGTGGAATCATATTGG
<i>bsACAN</i>	Fw: GGACACTCCTTGCAATTTGAGAA Rev: CAGGGCATTGATCTCGTATCG
<i>COL2A1</i>	Fw: GGCAATAGCAGGTTACGTACA Rev: CGATAACAGTCTTGCCCCACTT

Table 2. Sequences of primers for qRT-PCR.

GAPDH = GlycerAldehyde 3-Phosphate DeHydrogenase ; *ACAN* = AggreCAN ; *COL2A1* = Collagen type 2 ; *hs* = human-specific ; *bs* = bovine-specific.

Statistical analysis

All data were analyzed with PSAW statistics 20.0 (SPSS inc. Chicago, USA). For *in vitro* alginate co-cultures, the mean and standard deviation represents at least three independent donors per cell source performed in triplicate. For statistical evaluation, a mixed linear model was used followed by a Bonferroni's post-hoc comparisons test. Condition and time point were defined as fixed factors in the model. Donor and sample number were treated as random factors. For *in vivo* alginate co-cultures, the mean and standard deviation represents at least three independent donors per cell source performed in duplicate. For the evaluation of the cellular communication pathways between MSCs and ACs, the mean and standard deviation represents one donor per cell source performed in sextuple. For statistical evaluation, the Kruskal-Wallis followed by the Mann-Whitney-U tests was used followed by a Bonferroni's post-hoc comparisons test. For all tests, values of $p < 0.05$ were considered statistically significant.

RESULTS

Cartilage regeneration in co-cultures

In vitro outcomes

After 3 weeks, DNA content of alginate constructs containing either co-cultures of *hMSCs* and *bACs* or single-cell-type populations, did not change in relation to their initial DNA content. (Figure 2A) Because the amount of DNA had not changed significantly in any of the conditions, matrix deposition was expressed per construct and per initially seeded primary ACs. After 5 weeks, DNA content did significantly decrease in constructs containing *hBMSCs* only ($p<0.001$), but remained unchanged in the remaining culture conditions. (Supplementary figure 1)

Since constructs were cultured in the absence of chondrogenic factors, constructs containing solely *hAMSCs* or *hBMSCs* produced very little sGAG (Figure 2B) and collagen (Figure 2C). To demonstrate the additional effect of *hMSCs* in mixed-cell-type populations, a control condition - containing similar numbers of *bACs* (0.8×10^6 nc/mL) without the supplementation of *hMSCs* - was evaluated (Figure 2 dotted lines). The addition of either *hAMSCs* or *hBMSCs* to *bACs* demonstrated a significant increase in the production of sGAG over their controls (*hAMSC/bACs* $p=0.018$; *hBMSC/bACs* $p<0.001$). Compared to constructs containing single-cell-type populations, the deposition of sGAG was most evidently enhanced in co-cultures combining *hBMSCs* and *bACs* ($p<0.001$). Constructs containing *hAMSC/bACs* deposited significantly less sGAG compared to *hBMSC/bACs* ($p<0.001$) and equal amounts compared to constructs containing *bACs* only. (Figure 2B) The production of collagen was enhanced in co-cultures of both *hAMSC/bACs* and *hBMSC/bACs* compared to single-cell-type populations (*hAMSC/bACs* $p=0.002$; *hBMSC/bACs* $p<0.001$). (Figure 2C) Normalization of the total sGAG content to the initially seeded primary ACs revealed even more distinct differences between co-cultures and single-cell-type populations: *hBMSC/bACs* produced significantly more sGAG compared to *bACs* only and co-cultures of *hAMSC/bACs* (both $p<0.001$) ; collagen production was significantly enhanced in both co-cultures (*hAMSC/bACs* $p=0.013$; *hBMSC/bACs* $p<0.001$). (Figure 2B and 2C) Similar results were obtained after 5 weeks of culture. (Data not shown) These results demonstrate that co-cultures of *hMSCs* and *bACs* improve cartilage formation *in vitro*, depending on the *hMSC*-source used ($hBMSC \geq hAMSC$).

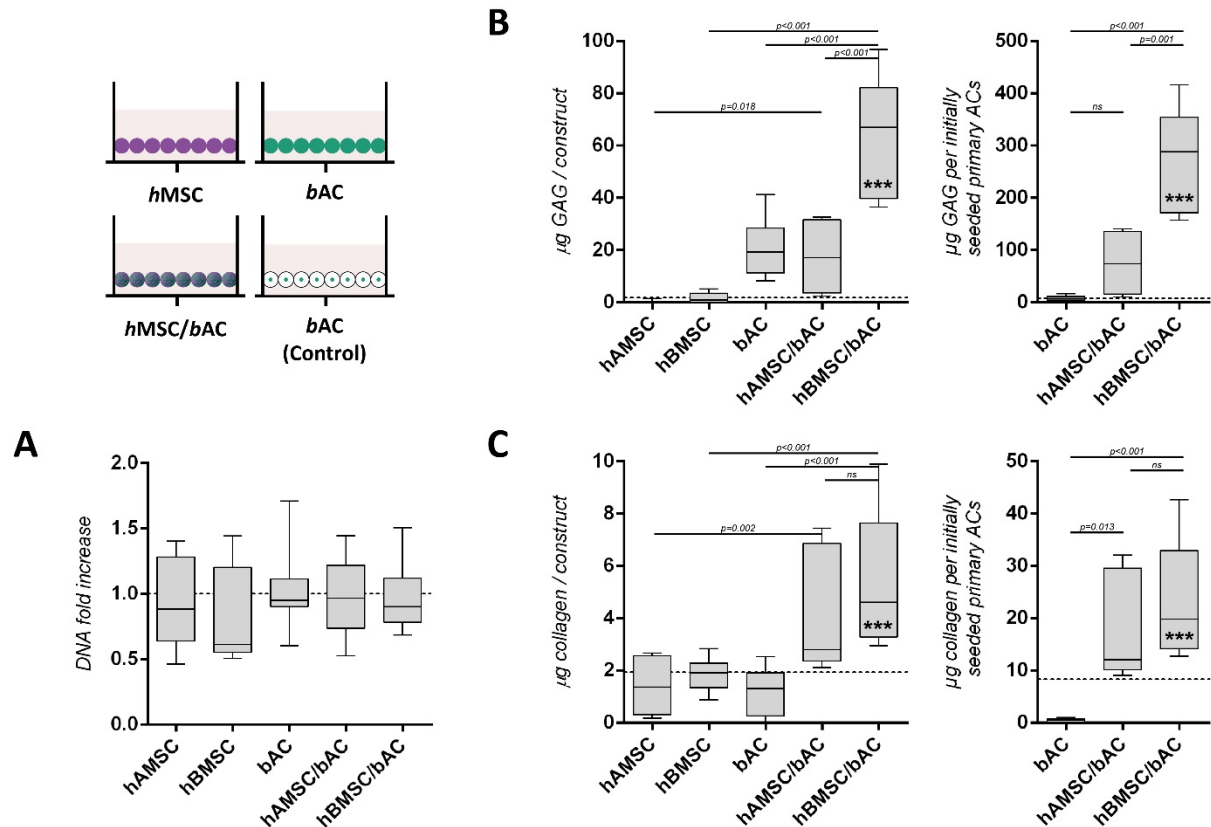


Figure 2. Cartilage matrix formation in constructs containing hMSCs and/or bACs, 3 weeks after *in-vitro* culture.

(A) The DNA content of none of the constructs had changed compared to their initial DNA content prior to cell-culture (dotted line). Biochemical evaluation of the sGAG **(B)** and collagen **(C)** content, 3 weeks after culture in alginate. The left graphs demonstrate the amount of matrix components per construct, whereas for the right graphs matrix production is normalized to the initially seeded primary ACs. A control condition - containing similar amounts of bACs (0.8×10^6 nc/ml) without supplementation of hMSCs - was evaluated to determine the additional effect of hMSCs (3.2×10^6 nc/ml) on bACs in co-cultures (dotted line). *, ** or *** indicates *p*-values smaller than 0.05, 0.01 or 0.001 respectively compared to the control condition. Data are shown as mean \pm SD. For statistical evaluation, a mixed model was used followed by a Bonferroni's post-hoc comparisons test. hAMSC = human Adipose-tissue-derived Mesenchymal Stem Cell ($n=3$ experiments with 3 independent donors) ; hBMSC = human Bone-marrow-derived Mesenchymal Stem Cell ($n=3$ experiments with 3 independent donors) ; bAC = bovine Articular Chondrocyte ($n=3$ experiments with 3 pools of donors). Per experiment, 3 samples were used for analyses.

***In vivo* outcomes**

Cell-free alginate constructs (controls ; $n=4$) and alginate constructs containing hBMSC/bACs, hAMSC/bACs or hBMSC, hAMSC or bAC only, were generated and immediately implanted subcutaneously in athymic mice. After 8 weeks, all but 5 ($n=3$ hAMSC, $n=2$ hBMSC) of the 40 constructs could be identified and harvested. Unfortunately however, the remaining hMSC-constructs (either hAMSCs or hBMSCs) and cell-free alginate constructs were lost during the embedding process. Constructs containing bACs or hBMSC/bACs resembled cartilage tissue in both color and texture, while the appearance of constructs containing hAMSC/bACs was

particularly donor-dependent. (Figure 3) None of the constructs had mineralized or ossified. Also, vascularization within the construct, was never observed. Cells were more heterogeneously distributed in constructs containing either *hAMSC/bACs* or *hBMSC/bACs* compared to *bACs* only. Collagen type II was abundantly present in constructs containing *bAC* or *hBMSC/bACs*. Again, *hAMSC/bACs* contained collagen type II in a donor-dependent manner. (Figure 3)

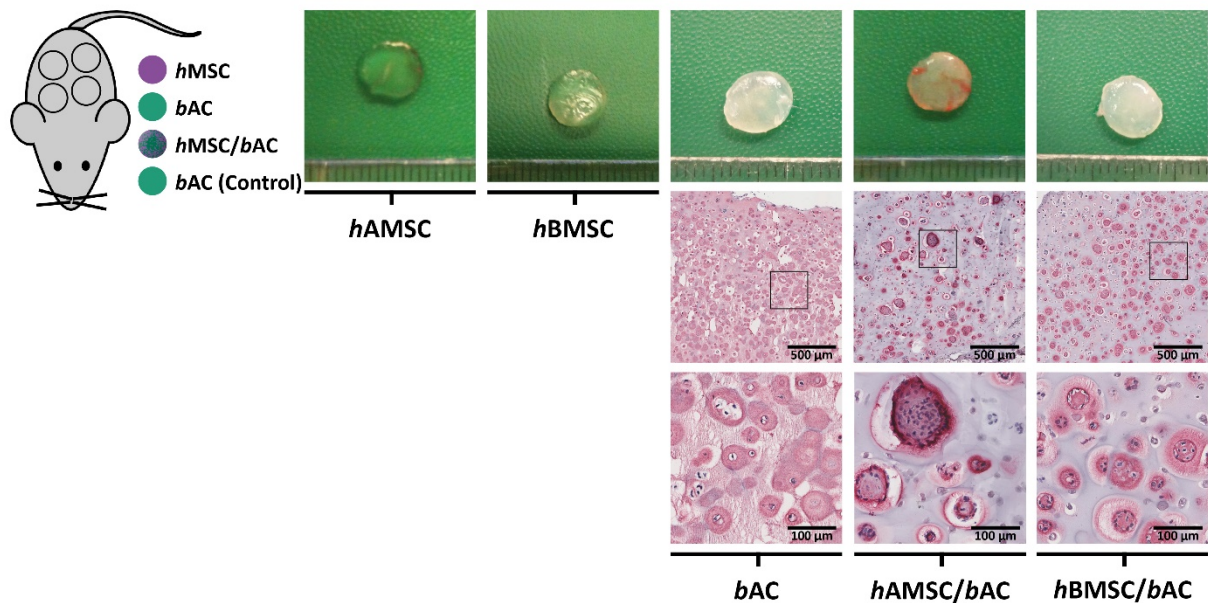


Figure 3. Macroscopic appearance and immunohistochemical analyses of constructs containing *hMSCs* and/or *bACs*, 8 weeks after subcutaneous implantation in mice.

Macroscopic appearance (top row) of cartilage constructs, as well as a collagen type II immunohistochemical staining (bottom rows), 8 weeks after subcutaneous implantation.

hAMSC = human Adipose-tissue-derived Mesenchymal Stem Cell ($n=3$ experiments with 3 independent donors) ; *hBMSC* = human Bone-marrow-derived Mesenchymal Stem Cell ($n=3$ experiments with 3 independent donors) ; *bAC* = bovine Articular Chondrocyte ($n=3$ experiments with 3 pools of donors). Per experiment, 2 samples were used for analyses.

In vivo, DNA- and sGAG-content were not detected in cell-free alginate constructs. (Data not shown) *hAMSC/bACs* and *hBMSC/bACs* contained similar quantities of cartilage matrix as constructs containing *bACs* only. Moreover sGAG formation in co-cultures was independent of the origin of the *hMSC*-source used ($p=0.916$). (Figure 4A) Collagen production demonstrated a similar trend, again without statistical significant differences between *hAMSC/bACs* and *hBMSC/bACs* ($p=1.000$). (Figure 4B) Normalization of the data to their initially seeded primary ACs revealed more distinct differences between mixed-cell-type and single-cell-type populations: *hAMSC/bACs* and *hBMSC/bACs* produced significantly more sGAG and collagen per initially seeded primary ACs compared to *bACs* (*hAMSC/bACs* $p<0.01$; *hBMSC/bACs* $p<0.05$). (Figure 4) After subcutaneous implantation, the elastic modulus was

highest in constructs containing *hAMSC/bACs* and *hBMSC/bACs*, albeit this did not reach statistical significance due to the large variation between samples. (Figure 4C) These results confirm our *in-vitro* results by showing that co-cultures of *hMSCs* and *bACs* improve cartilage formation. However, *in vivo* this phenomenon seems independent of the *hMSC*-source used, although large donor variation is observed.

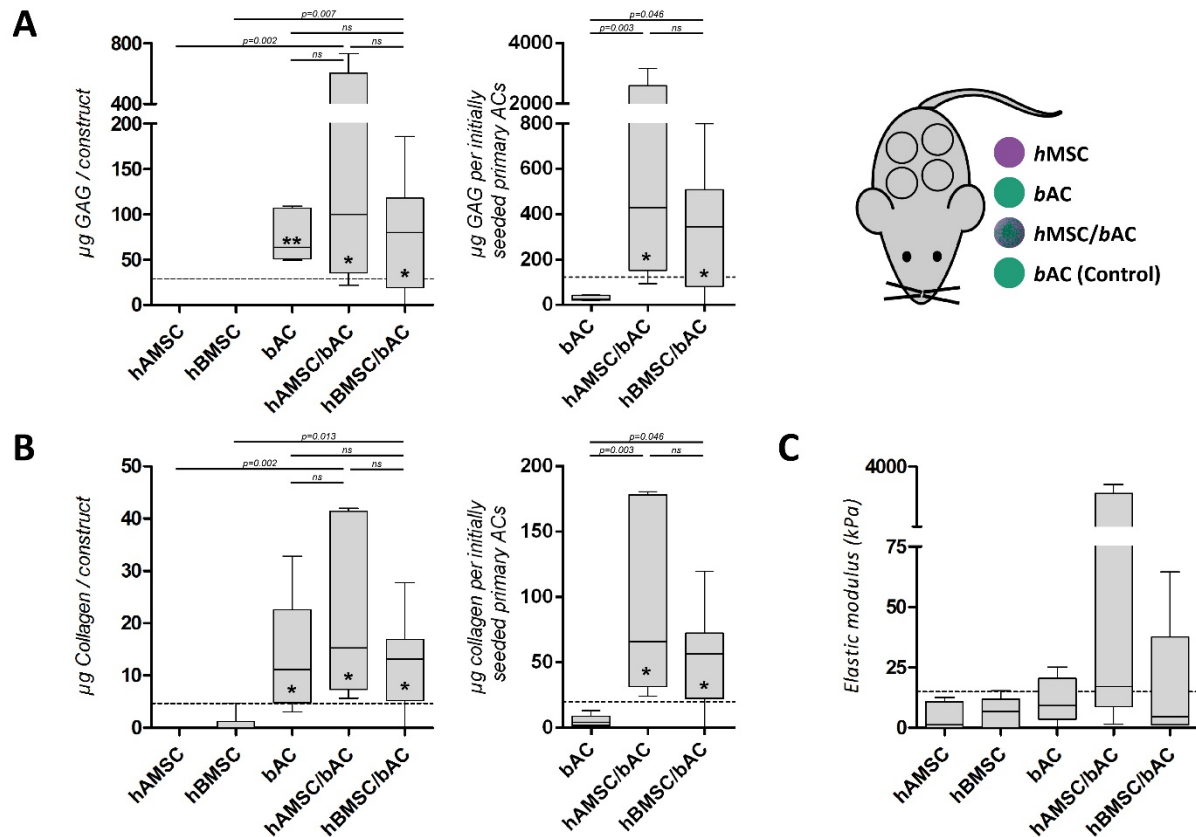


Figure 4. Cartilage matrix formation in constructs containing *hMSCs* and/or *bACs*, 8 weeks after subcutaneous implantation in mice.

Biochemical (sGAG (**A**) and collagen (**B**) content) and biomechanical evaluation (**C**), 8 weeks after subcutaneous implantation. The left graphs in A and B, demonstrate the amount of matrix components per construct, whereas for the right graphs matrix production is normalized to the initially seeded primary ACs. A control condition - containing similar amounts of *bACs* (0.8×10^6 nc /ml) without supplementation of *hMSCs* - was evaluated to determine the additional effect of *hMSCs* (3.2×10^6 nc /ml) on *bACs* in co-cultures (dotted line). *, ** or *** indicates *p*-values smaller than 0.05, 0.01 or 0.001 respectively compared to the control condition. Data are shown as box-whisker plots. For statistical evaluation, a Kruskal-Wallis followed by the Mann-Whitney-U test was used followed by a Bonferroni's post-hoc comparisons test. *hAMSC* = human Adipose-tissue-derived Mesenchymal Stem Cell ($n=3$ experiments with 3 independent donors) ; *hBMSC* = human Bone-marrow-derived Mesenchymal Stem Cell ($n=3$ experiments with 3 independent donors) ; *bAC* = bovine Articular Chondrocyte ($n=3$ experiments with 3 pools of donors). Per experiment, 2 samples were used for analyses.

Differentiation versus chondro-induction

Using a xenogeneic *in-vitro* culture system enabled us to determine the contribution of each individual cell type (i.e. *hBMSCs*, *hBMSCs* or *bACs*) to cartilage matrix production using species-specific gene-expression analyses.

First, *GAPDH*-gene expression was analyzed after 5 weeks of *in-vitro* culture. *hAMSC/bACs* and *hBMSC/bACs* contained cells from both bovine (*AC*) and human (*AMSC* or *BMSC*) origin. (Figure 5A) Then, chondrogenic gene expression was evaluated by the *ACAN* and *COL2A1* genes. In a growth-factor-free environment, *hAMSCs* and *hBMSCs* hardly expressed *hsACAN* and *hsCOL2A1*. Besides, *chondrogenic genes* were hardly expressed in *hAMSC/bACs* or *hBMSC/bACs* either. Conversely, *hAMSC/bACs* or *hBMSC/bACs* - containing solely 20% bovine articular chondrocytes - expressed as much or even higher levels of *bsACAN* compared to 100% *bACs* (*hAMSC/bACs* vs *bACs* $p>0.05$; *hBMSC/bACs* vs *bACs* $p<0.001$). *hAMSC/bACs* and *hBMSC/bACs* expressed *COL2A1*, although gene-expression of *hsCOL2A1* was negligible. This means that the *COL2A1* expressed was from bovine origin. (Figure 5B) These data indicate that the formed cartilage matrix was from *bAC*-origin, which suggests a more trophic role for *hMSCs* herein.

Cellular interactions

To further understand the complex cellular interaction between *hMSCs* and *bACs*, cells were encapsulated in separate alginate constructs and co-cultured in a Transwell® system as well as in medium conditioned by the other cell type. (Figure 6A and 7A) In addition cell combination were also cultured in pellets, allowing direct cell-cell contact.

Alginate constructs containing solely *bACs*, *hAMSCs* or *hBMSCs* cultured in 'basic medium' maintained their DNA content over the 3 weeks of culture. Exposure to paracrine factors of *bAC* via Transwell® system or *bAC*-conditioned medium, did not alter the amount of DNA in alginate constructs seeded with either *hAMSCs* or *hBMSCs*. (Figure 6B) The presence of factors secreted by *hMSC* significantly increased the total amount of DNA in constructs containing *bACs* ($p<0.01$). This effect was independent on the origin of the *hMSCs* (i.e. *hAMSCs*, *hBMSCs*) and co-culture system used (i.e. Transwell® system, *hMSC*-conditioned medium). (Figure 7B) This suggests *MSC* have paracrine effects on chondrocytes.

Alginate constructs containing *hAMSCs* or *hBMSCs*, formed very little sGAG after 3 weeks of culture. sGAG-production remained similarly low when *hMSC*-constructs were cultured in the presence of paracrine factors of *bAC* via Transwell® system or *bAC*-conditioned medium. (Figure 6B) The production of sGAG was higher in constructs containing *bACs*. Exposure to paracrine factors of *hMSC* significantly increased sGAG-production, irrespective to the *hMSC*-source used (i.e. *hAMSCs*, *hBMSCs*, $p<0.01$). Since the amount of DNA was also enhanced in these constructs, sGAG content was adjusted to the amount of DNA, still showing pronounced differences. sGAG formation was significantly increased in Transwell® system compared to constructs cultured with *bAC*-conditioned medium ($p<0.01$). (Figure 7B) Similar trends were observed at *COL2A1* gene-expression level. (Figure 7D) This provides further indications that the effect of the combination of *hMSCs* and *bACs* on chondrogenesis is due to paracrine effect of *hMSCs* on chondrocytes.

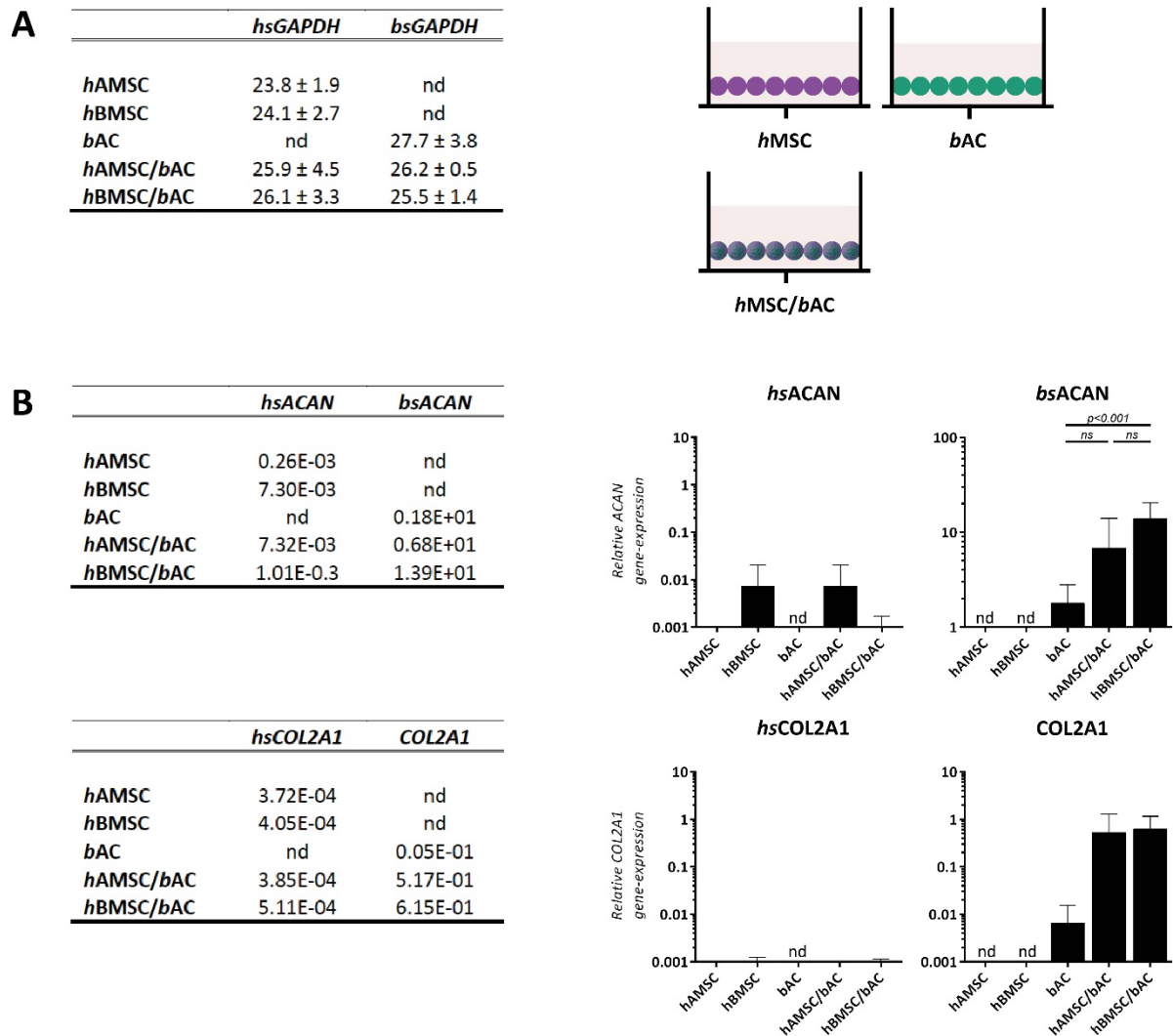


Figure 5. Gene-expression analysis, 5 weeks after *in vitro* culture.

Data are shown as mean CT-values ± SD of housekeeping genes **(A)** and average relative gene-expression of chondrogenic genes **(B)**. nd = not detected (ct-value > 35.00) ; *hsGAPDH* = human-specific *GAPDH* ; *bsGAPDH* = bovine-specific *GAPDH* ; *hsACAN* = human-specific *ACAN* ; *bsACAN* = bovine-specific *ACAN* ; *hsCOL2A1* = human-specific *COL2A1* ; *hAMSC* = human Adipose-tissue-derived Mesenchymal Stem Cell ($n=3$ experiments with 3 independent donors) ; *hBMSC* = human Bone-marrow-derived Mesenchymal Stem Cell ($n=3$ experiments with 3 independent donors) ; *bAC* = bovine Articular Chondrocyte ($n=3$ experiments with 3 pools of donors). Per experiment, 3 samples were used for analyses.

Based on previous results, we further wanted to evaluate signs of hypertrophy in these constructs, since hypertrophic differentiation is an unwanted phenomenon in cartilage regeneration. *bACs* cultured in ‘basic medium’ expressed hardly any *COL10* after 3 weeks of culture. In addition, when *bACs* were exposed to paracrine factors of *hMSC* either via Transwell® system or *hMSC*-conditioned medium, *COL10*-gene-expression was upregulated and significantly increased in constructs exposed to paracrine factors of *hAMSCs* (Transwell® system $p=0.004$; *hAMSC*-conditioned medium $p=0.028$). Although *COL10*-gene-expression was slightly upregulated in constructs exposed to paracrine factors of *hBMSC*, no significant

differences could be observed in comparison with constructs cultured in ‘basic medium’ (both Transwell® system and *h*BMSC-conditioned medium $p>0.05$). (Figure 7D)

This indicates that *h*MSCs have the ability to improve cartilage matrix formation in co-culture, by improving *b*AC-proliferation capacity as well as increasing *b*AC-sGAG-production. Moreover, when exposed to paracrine factors of *h*BMSC, hypertrophic differentiation was not significantly enhanced compared to untreated *b*ACs. In pellet co-culture, matrix production was similarly produced as in 3D-alginate constructs, meaning that direct cell-cell contact is not required for co-cultures of *h*MSCs and *b*ACs. (Figure 7C)

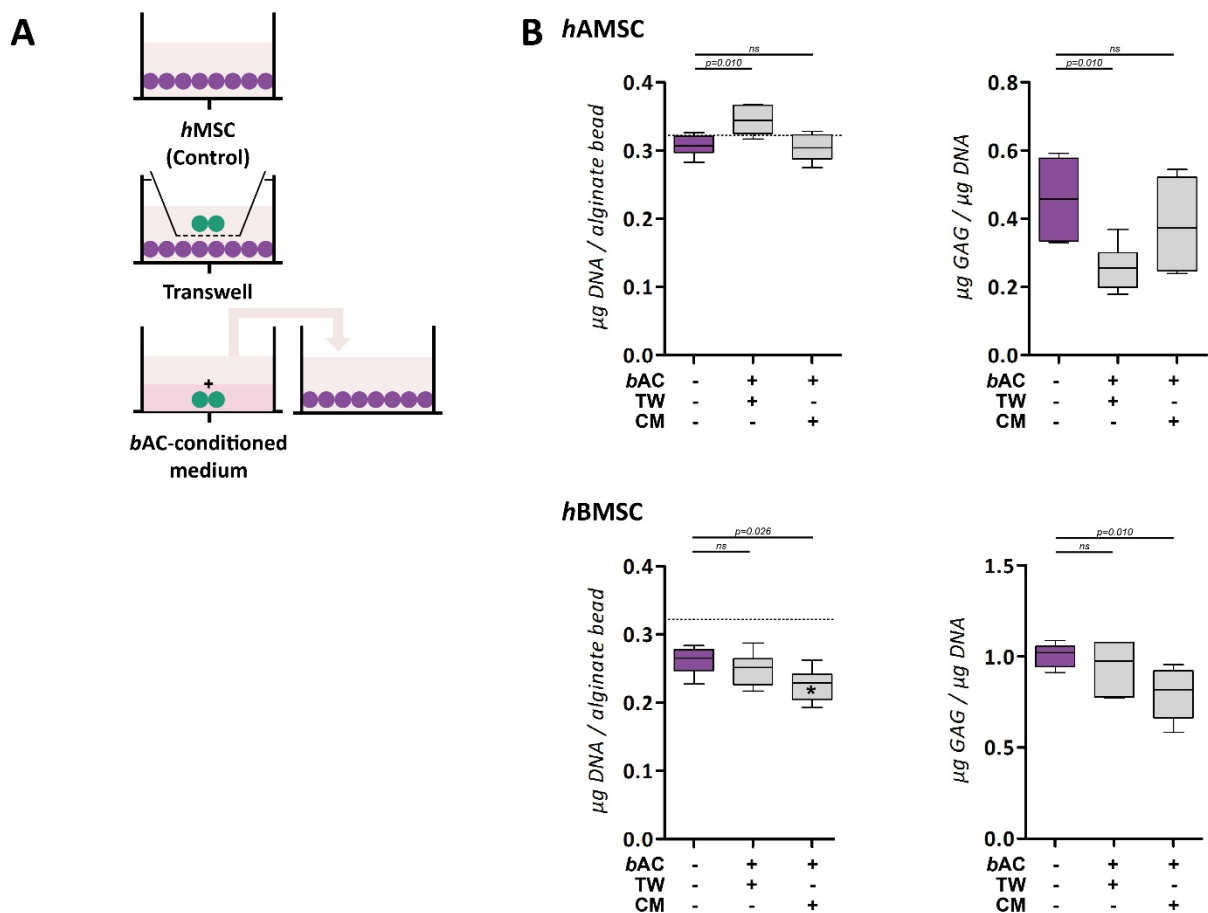


Figure 6. Paracrine effect of *b*ACs on *h*AMSCs and *h*BMSCs.

(A) Schematic overview. In purple: *h*MSCs ; in green: *b*ACs. **(B)** The DNA and sGAG content of *h*AMSCs and *h*BMSCs in the presence of paracrine factors of *b*ACs via Transwell® system or *b*AC-conditioned medium. The DNA content after 3 weeks of culture was compared to the initial DNA content prior to cell-culture (dotted line). *, ** or *** indicates p -values smaller than 0.05, 0.01 or 0.001 respectively compared to the amount of DNA prior to cell culture. Data are shown as box-whisker plots of 6 samples of one experiment. For statistical evaluation, a Kruskal-Wallis followed by the Mann-Whitney-U test was use followed by a Bonferroni's post-hoc comparisons test. TW = Transwell ; CM = Conditioned Medium ; *h*AMSC = human Adipose-tissue-derived Mesenchymal Stem Cell ; *h*BMSC = human Bone-marrow-derived Mesenchymal Stem Cell ; *b*AC = bovine Articular Chondrocyte.

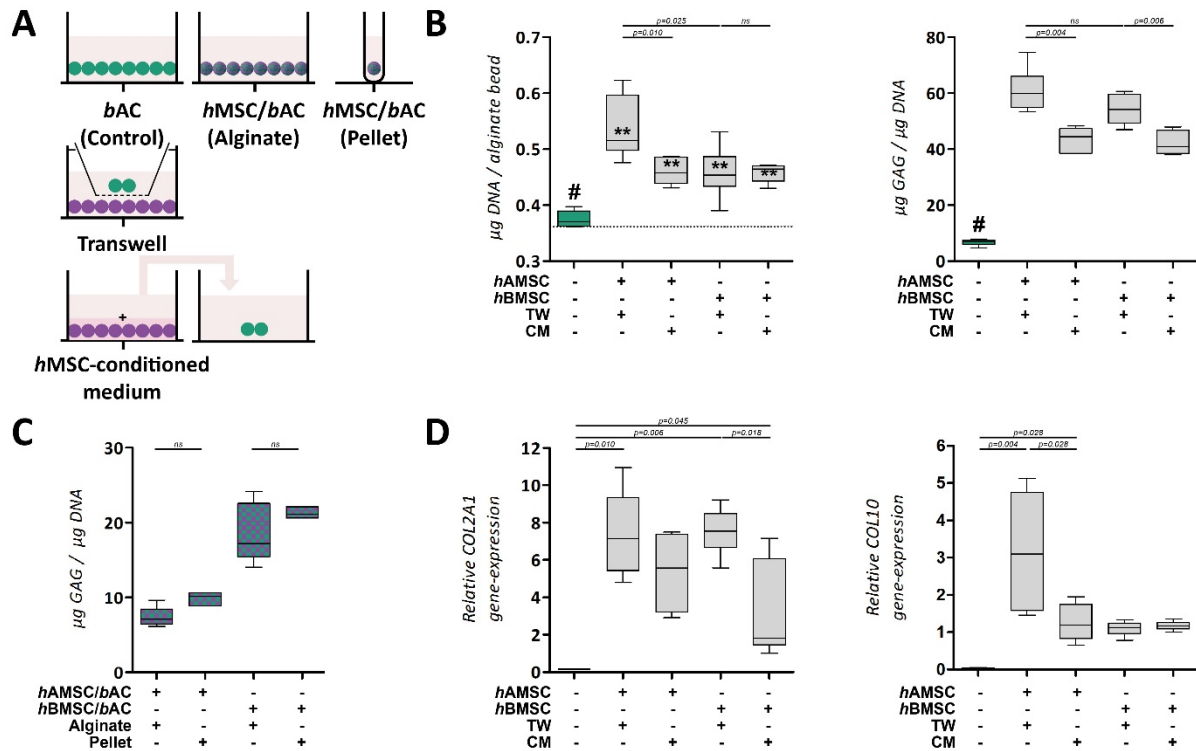


Figure 7. Paracrine effect of *hAMSC*s and *hBMSC*s on *bAC*s.

(A) Schematic overview. In purple: *hMSC*s ; in green: *bAC*s. **(B)** The DNA and sGAG content of *bAC*s in the presence of paracrine factors of *hMSC*s via Transwell® system or *hMSC*-conditioned medium. The DNA content after 3 weeks of culture was compared to the initial DNA content prior to cell-culture (dotted line). **(C)** Co-culture in alginate constructs and pellet culture, allowing direct cell-cell contact. **(D)** Relative gene-expression analysis, 3 weeks after culture in alginate. *, ** or *** indicates *p*-values smaller than 0.05, 0.01 or 0.001 respectively compared to the amount of DNA prior to cell culture. # indicates significant differences from all conditions ($p < 0.01$). Data are shown as box-whisker plots of 6 samples of one experiment. For statistical evaluation, a Kruskal-Wallis followed by the Mann-Whitney-U test was used followed by a Bonferroni's post-hoc comparisons test. TW = Transwell ; CM = Conditioned Medium ; *hAMSC* = human Adipose-tissue-derived Mesenchymal Stem Cell ; *hBMSC* = human Bone-marrow-derived Mesenchymal Stem Cell ; *bAC* = bovine Articular Chondrocyte.

DISCUSSION

Combining chondrocytes and MSCs holds great promise for cell-based cartilage repair as it reduces the required number of chondrocytes and diminishes many disadvantages of individually used cell types leading to enhanced cartilage matrix formation with low hypertrophic differentiation. In line with former research, *hAMSC/bACs* and *hBMSC/bACs* produced similar or even improved quantities of cartilage matrix components as constructs containing *bACs* only, both *in vitro* and *in vivo*. Moreover, hypertrophic gene expression (*COL10*) was not affected by *hBMSCs*, but slightly enhanced by *hAMSCs*. However, constructs containing either *hAMSC/bACs* or *hBMSC/bACs* appeared stable and did not calcify *in vivo*. This suggests that 80% of *bACs* can be replaced by either *hAMSCs* or *hBMSCs* without influencing cartilage matrix production nor stability. Therefore, mixed-cell-cultures of MSCs and chondrocytes could be very valuable for cell-based cartilage repair, as appropriate numbers of cells are more easily acquired from bone-marrow aspirates or adipose tissue than from cartilage biopsies.

The cellular mechanism responsible for enhanced cartilage production in co-culture is however still debated. Numerous cellular communication pathways have been hypothesized in order to explain the beneficial effect in co-cultures [73]. We found no evidence that cartilage formation was the consequence of chondrogenic lineage differentiation of *hMSCs*, as stated by others [80, 253-262]. In contrast, cartilage matrix clearly originated from *bACs*, which suggests a predominantly trophic role for *hMSCs* in these constructs: both *hAMSCs* and *hBMSCs* improved *bAC*-proliferation as well as *bAC*-sGAG-formation. This confirms previous studies where the co-culture effect has been ascribed to *ACs*, whose cartilage-forming capacity and proliferation activity appears to enhance in the presence of *MSCs*. [74, 246, 263-268] The trophic and paracrine function of *MSCs* herein appeared essential rather than *MSCs* actively undergoing chondrogenic differentiation. We show that this is a general feature that applies to both *AMSCs* and *BMSCs*.

To date, only three studies have compared the trophic effect of several *MSC*-sources - such as *AMSCs* and *BMSCs* - on *ACs* in co-culture. [80, 246, 247] Unfortunately, these studies demonstrate conflicting outcomes and have never translated to animal research. Therefore, to our knowledge, we are the first to systematically compare the cartilage forming capacity of either *hAMSC/bACs* and *hBMSC/bACs* *in vitro* and *in vivo*. *In vitro*, *hBMSC/bACs* contained significantly more cartilage matrix components than *hAMSC/bACs*. Cartilage formation after 8 weeks of subcutaneous implantation was, however, not different in constructs containing *hAMSC/bACs* and *hBMSC/bACs*, although large donor variations were observed, in particular in *hAMSC/bACs*. Our results support a general trophic or immunomodulatory role for *hAMSCs* and *hBMSCs* on *bACs* in co-culture, as stated by Wu [246] and Maumus *et al* [247]. Although both cell sources share comparable immunomodulatory modalities, they do not necessarily behave the same. In monocultures there are clear differences observed between *hAMSCs* and *hBMSCs*. For instance, they possess distinctive proliferation capacities and a dissimilar potential to chondrogenically differentiate. [40] Moreover, both cell sources secrete different subsets of paracrine factors: compared to *hBMSCs*, *hAMSCs* secrete significantly more VEGF-D [269], IGF-1 [269, 270], IL-8 [269] and IL-6 [269, 271], and significantly less SDF-1 [272] and

TFG β 1 [272]. In co-cultures, differences between *hMSC*-cell sources appear less clear. Acharya *et al.* demonstrated enhanced chondrocyte proliferation capacity and improved sGAG formation in pellets containing *hBMSC/bACs* compared to *hAMSC/bACs*. [80] Besides, 3 independent co-culture studies using *AMSCs* only showed limited or decreased effects of *MSCs* on chondrogenesis. [243-245] Such effect was hardly seen in co-culture studies using *BMSCs* only, which may propose that, compared to *BMSCs*, *AMSCs* seem less efficient in co-culture. Although we could not find a general beneficial effect of *hBMSCs* in co-cultures compared to *hAMSCs in vitro* and *in vivo*, we did show that *in vitro*, *hBMSC/bACs* outperformed *hAMSC/bACs* and hypertrophic gene expression was lower in *hBMSC/bACs*. True dissimilarities between *hAMSCs* and *hBMSCs* in co-culture are unfortunately hard to expose, as *hMSC*-cultures are highly heterogeneous and distinct population subsets will probably interfere with the reciprocal communication pathways in co-culture. Therefore, the purification of distinct subsets of *hMSCs* might enhance the particular capability of *hAMSCs* and *hBMSCs* in co-culture by eliminating interfering cells with limited potential, or even cells with inhibitory activity. Future research still needs to clarify whether the trophic role of *MSCs* in co-culture is truly a general *MSC*-characteristic produced by a distinct subset of the *MSC*-population or dependent on the original origin of the *MSCs*.

Our data and that of others emphasize the importance of paracrine signaling pathways in co-culture comparatively to juxtacrine or gap-junctional signaling. Although the importance of direct cell-cell contact is still unclear in literature [263], such signaling pathways remained less important in our study, since alginate hydrogel impedes direct cell-cell contact and in pellet culture no beneficial effect of direct cell-cell contact was observed. On the contrary, *bACs* produced less cartilage matrix in Transwell® system with *hMSCs* and the amount of cartilage matrix was further reduced in *hMSC*-conditioned medium. Although direct cell-cell contact seems less significant than paracrine signaling, it seems correspondingly important to secure a certain cell-cell distance for optimal cell communication.

Furthermore, for optimal cell communication and subsequent cartilage regeneration, an optimal cell density and ratio of *MSCs* to *ACs* is imperative. Additionally, for cell-based cartilage repair, it would be ideal to only use low numbers of primary chondrocytes. Although Puelacher *et al* already recommended cell densities greater than 20×10^6 cells per milliliter [239], we could not increase the cell seeding density over 4×10^6 cells per milliliter, as the size of our experimental set-up did not enable higher densities. Additionally, we have replaced 80% of the *bACs* by *hMSCs* (at a 4:1 ratio), as described previously. [74, 246] However, no consensus on optimal co-culture ratios is yet available. Future research needs to clarify if we could increase cell density while further reduce the number of primary chondrocytes (increase the *MSC*-chondrocyte-ratio) without inhibiting cartilage matrix production and stability.

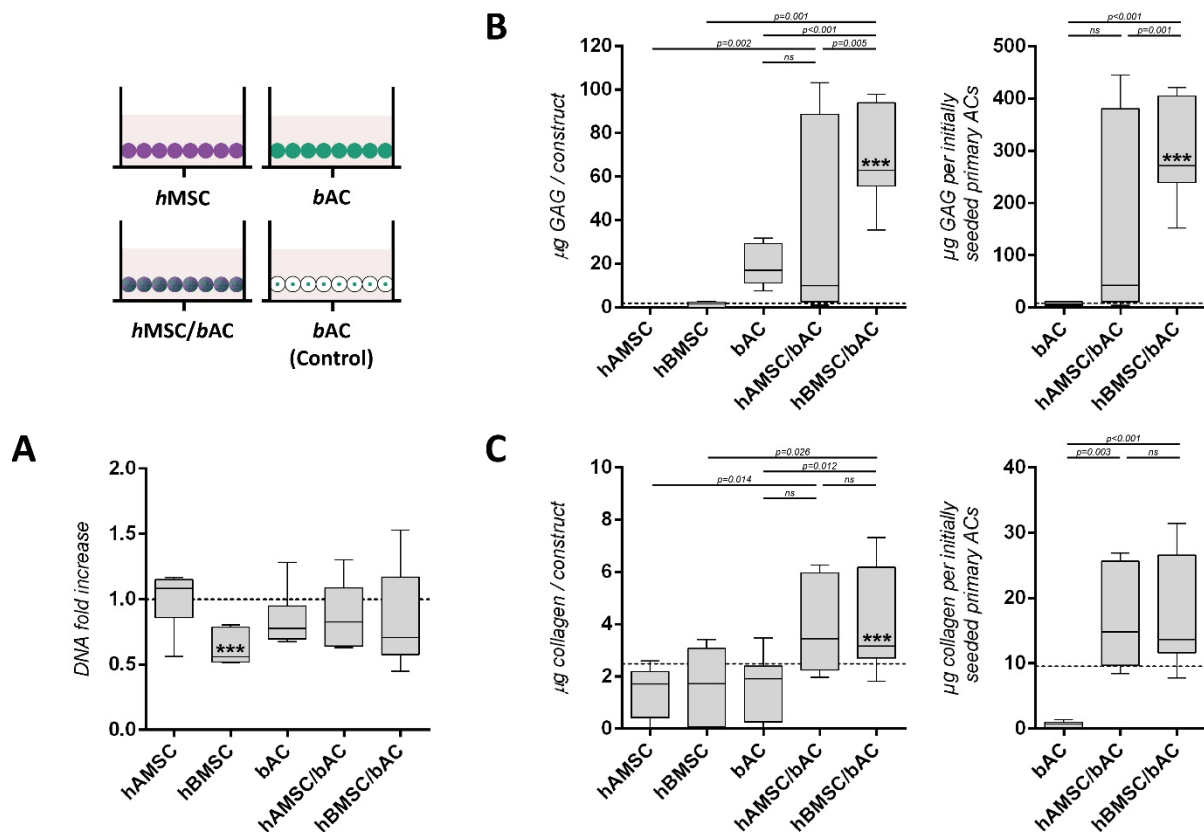
The species mismatch limited the translation of presented basic research to clinical application. However, the species mismatch was chosen to be able to discriminate between the role of the different cell types. We do not expect huge differences in fully human co-culture models, as both xenogeneic and autologous co-culture models have resulted in comparable outcomes, indicating that in both models comparable mechanisms are likely operational. [74] Our results confirmed previously published results of *hMSCs* combined with

xenogeneic chondrocytes. [74, 273-275] Therefore, it appears to be an excellent model to study cell-specific contributions to tissue formation.

In conclusion, this study demonstrates that 80% of chondrocytes can be replaced by either *hAMSCs* or *hBMSCs* without influencing cartilage matrix production nor stability. Besides, our results support a general trophic role for *hAMSCs* and *hBMSCs* on chondrocytes in co-culture that does not need direct cell-cell contact. These data provide information that can be used to further optimize cell-based cartilage repair.

Acknowledgements

The authors would like to thank dr. Jeanine Hendriks (CellcoTec, Bilthoven, the Netherlands) for her valuable ideas during preparation of this manuscript. We also acknowledge the Department of Orthopaedic Surgery (Erasmus MC, University Medical Center, Rotterdam, the Netherlands) for their assistance in obtaining bone marrow aspirates. The study was performed within the framework of EuroNanoMed (EAREG-406340-131009/1) and funded by SenterNovem.



Supplementary figure 1. Cartilage matrix formation in constructs containing hMSCs and/or bACs, 5 weeks after *in-vitro* culture.

(A) After 5 weeks, the DNA content of constructs containing hBMSCs significantly decreased compared to their initial DNA content prior to cell-culture (dotted line). Biochemical evaluation of the sGAG **(B)** and collagen **(C)** content, 5 weeks after culture in alginate. The left graphs demonstrate the amount of matrix components per construct, whereas for the right graphs matrix production is normalized to the initially seeded primary ACs. A control condition - containing similar amounts of bACs (0.8×10^6 nc/ml) without supplementation of hMSCs - was evaluated to determine the additional effect of hMSCs (3.2×10^6 nc/ml) on bACs in co-cultures (dotted line). *, ** or *** indicates *p*-values smaller than 0.05, 0.01 or 0.001 respectively compared to the control condition. Data are shown as mean \pm SD. For statistical evaluation, a mixed model was used followed by a Bonferroni's post-hoc comparisons test. hAMSC = human Adipose-tissue-derived Mesenchymal Stem Cell ($n=3$ experiments with 3 independent donors) ; hBMSC = human Bone-marrow-derived Mesenchymal Stem Cell ($n=3$ experiments with 3 independent donors) ; bAC = bovine Articular Chondrocyte ($n=3$ experiments with 3 pools of donors). Per experiment, 3 samples were used for analyses.

Chapter 6

Cartilage regeneration in the head and neck area: Combination of ear or nasal chondrocytes and mesenchymal stem cells improves cartilage production

M.M. Pleumeekers, L. Nimeskern, J.L.M. Koevoet, M. Karperien, K.S. Stok, G.J.V.M. van Osch

Plastic and Reconstructive Surgery, 2015. 136(6): p. 762e-74e.

ABSTRACT

Cartilage tissue engineering can offer promising solutions for restoring defected cartilage in the head and neck area and has the potential to overcome limitations of current treatments. However, to generate a construct of reasonable size, large numbers of chondrocytes are required, which limits its current applicability. Therefore, we evaluate the suitability of a combination of cells for cartilage regeneration: bone-marrow-derived mesenchymal stem cells and ear or nasal chondrocytes.

Human bone-marrow-derived mesenchymal stem cells were encapsulated in alginate hydrogel as single-cell-type populations or in combination with bovine ear or nasal chondrocytes at a 80:20 ratio. Constructs were either cultured *in vitro* or directly implanted subcutaneously in mice. Cartilage formation was evaluated with biochemical and biomechanical analyses. The use of a xenogeneic co-culture system enabled the analyses of the contribution of the individual cell types using species-specific gene-expression analyses.

In vivo, constructs containing a combination of human bone-marrow-derived mesenchymal stem cells with bovine ear or nasal chondrocytes contained similar amounts of cartilage components to that of constructs containing chondrocytes only (i.e. bovine ear and nasal chondrocytes). *In vitro*, species-specific gene-expression analyses demonstrated that chondrogenic gene *ACAN* was expressed by the chondrocytes only, which suggests a more trophic role for human bone-marrow-derived mesenchymal stem cells. Furthermore, the additional effect of human bone-marrow-derived mesenchymal stem cells was more pronounced in combination with bovine nasal chondrocytes.

By supplementing low numbers of bovine ear or nasal chondrocytes with human bone-marrow-derived mesenchymal stem cells, we were able to engineer cartilage constructs with similar properties to that of constructs containing chondrocytes only. This makes the procedure more feasible for future applicability in the reconstruction of cartilage defect in the head and neck area since less chondrocytes are required.

INTRODUCTION

Cartilage defects in the head and neck area are a commonly encountered problem in reconstructive surgery. Currently, these defects are reconstructed with autologous cartilage grafts or artificial implants. Although autologous cartilage grafting has been used successfully, the procedure requires a high degree of surgical expertise, is associated with limited availability of autologous cartilage and can cause severe donor site morbidity. Besides, the use of artificial implants as an alternative is questioned in the head and neck area, since implants in this area are prone to induce a foreign body reaction and frequently lead to extrusion. [276] Cartilage tissue engineering (TE) can offer a promising solution for restoring missing or destructed cartilage and has the potential to overcome limitations of current treatments, re-establishing unique biological and functional properties of the tissue.

To generate a construct of reasonable size, large numbers of cells are required. Currently, cartilage TE is predominantly based on the use of two distinct cell types: chondrocytes or mesenchymal stem cells (MSCs). Each cell type is however associated with specific disadvantages. Chondrocytes of several anatomical location have been investigated for their applicability. [39, 40, 42, 44, 46-53, 55-60] Yet, to obtain sufficient numbers of autologous cells, culture-expansion seems an inevitable step in chondrocyte-based cartilage repair, resulting in generally more fibrous and mechanically inferior cartilage. [61] MSCs on the contrary, are easily available from several tissues, can undergo multiple population doublings without losing their chondrogenic potential and have the capacity to differentiate into cartilage tissue under appropriate culture conditions. [64-68] However, their use is currently debated, as the formed cartilage tissue is unstable and predisposed for tissue mineralisation and ossification *in vivo*. [69-72] Taken together, the individual use of chondrocytes or MSCs is at present not ideal for cell-based cartilage repair in the head and neck area.

At present, the combination of both cell sources holds great promise for cartilage TE as it reduces the required number of chondrocytes and extenuates most disadvantages of both individual cell types. Contiguous thereto, mixed-cell cultures of chondrocytes and MSCs have been demonstrated to improve chondrogenesis [74] as well as to reduce hypertrophy and tissue mineralization [73, 75]. Moreover, by decreasing the amount of chondrocytes ($\leq 20\%$ of the total cell mixture), culture-expansion is no longer necessary, which allows the use of freshly isolated primary chondrocytes leading to improved cartilage formation. [76] Moreover, by using primary cells, the procedure is more translatable towards a one-step clinical application.

To date, most research on mixed-cell-based cartilage repair has been performed with chondrocytes obtained from articular cartilage. So far, little research was executed on mixed-cell cultures of MSCs and non-articular chondrocytes, such as ear (ECs) [77-79] or nasal chondrocytes (NCs) [80]. Nonetheless, the translation of such basic research into a one-step clinical application is yet unfeasible. Primarily as these studies made use of non-optimal culture conditions, such as the use of culture-expanded chondrocytes [77, 78, 80], or the paradoxical use of additional growth factors [77, 80]. Moreover, only few studies have yet evaluated the cartilage-forming capacity of MSC/ECs [77, 79] and MSC/NCs (none) *in vivo*. In an attempt to translate experimental research towards a one-stage cell-based cartilage repair

procedure for cartilage defects in the head and neck area, the *in-vitro* and *in-vivo* capacity of bone-marrow-derived MSCs mixed with primary ECs or NCs were studied. The formation of functional and stable non-mineralised cartilage was evaluated, along with the relative contribution of each individual cell population (i.e. chondrocytes, MSCs) to mixed-cell-based cartilage repair.

MATERIALS AND METHODS

Chemicals were obtained from Sigma-Aldrich, USA unless stated otherwise.

Cell sources

To obtain primary bovine chondrocytes from ear (*bECs*) and the cartilaginous part of the nasoseptal (*bNCs*) origin, macroscopically intact cartilage was harvested from calves ≤ 6 months old, and washed with saline after careful resection of the perichondrium ($n=3$ pools of 3 donors). To isolate cells, cartilage pieces were incubated for 1 hour with 2 mg/mL protease, followed by overnight incubation with 1.5 mg/mL collagenase B (Roch Diagnostics, Germany) in Dulbecco's Modified Eagle's Medium (DMEM; Gibco, USA). Non-expanded primary chondrocytes were harvested and directly cultured in 3D-alginate hydrogel.

Human bone-marrow-derived mesenchymal stem cells (*hBMSCs*) were isolated from bone-marrow heparinized aspirates, after informed consent had been acquired and with approval of the local Medical Ethics Committee (MEC-2004-142 and Albert Schweitzer Hospital 2011/7) ($n=3$: M 67Y; F 75Y; M 22Y) and seeded and cultured overnight in medium consisting of Minimum Essential Medium Alpha (MEM- α ; Gibco), supplemented with fetal calf serum, L-ascorbic acid 2-phosphate, and 1 ng/mL basic Fibroblast Growth Factor 2 (bFGF2; AbD Serotec, UK). Second-passaged cells were harvested and cultured in 3D-alginate hydrogel.

Chondrogenesis

For 3D-alginate culture, cells were suspended at a density of 4×10^6 cells/mL in clinical grade 1.1% low viscosity alginate solution dissolved in 0.9% NaCl (Batch MG-004, CellMed, Germany) as single-cell-type populations or as combination of 80% *hBMSCs* and 20% *bECs* or *bNCs*. (Table 1)

Human stem cells			Bovine chondrocytes	
	Source	Cell density ($\times 10^6$)	Source	Cell density ($\times 10^6$)
<i>hBMSC</i>	<i>hBMSCs</i>	4 nc/mL	x	x
<i>bEC</i>	x	x	<i>bECs</i>	4 nc/mL
<i>bNC</i>	x	x	<i>bNCs</i>	4 nc/mL
<i>hBMSC/bEC</i>	<i>hBMSCs</i>	3.2 nc/mL	<i>bECs</i>	0.8 nc/mL
<i>hBMSC/bNC</i>	<i>hBMSCs</i>	3.2 nc/mL	<i>bNCs</i>	0.8 nc/mL
Control <i>bEC</i>	x	x	<i>bECs</i>	0.8 nc/mL
Control <i>bNC</i>	x	x	<i>bNCs</i>	0.8 nc/mL

Table 1. Construct conditions.

Cell density is displayed as the number of cells (nc) in 1 milliliter of alginate. *hBMSCs* = human Bone-marrow-derived Mesenchymal Stem Cells ; *bECs* = bovine Ear Chondrocytes ; *bNCs* = bovine Nasal Chondrocytes.

Flat constructs (8 mm diameter; 2 mm height) were processed as previously described. [40] Constructs were either cultured *in vitro* or directly implanted subcutaneously in mice. *In-vitro* culture was performed for either three or five weeks in growth-factor-free medium consisting of DMEM supplemented with sodium pyruvate (Gibco), L-proline, supplemented Insulin Transferrine Selenium (B&D Bioscience, USA), dexamethasone, and L-ascorbic acid 2-phosphate. Medium was changed twice a week. After three and five weeks, constructs were processed for biochemical and gene-expression analysis.

For *in-vivo* studies, a total number of sixteen nine-week-old female NMRI nu/nu mice (Charles River Laboratories, the Netherlands) were used. Two separate incisions were made along the central line of the spine, after which four separate subcutaneous dorsal pockets were prepared by blunt dissection. After eight weeks, animals were terminated and samples were explanted for histological, biomechanical and biochemical analyses. Animal experiments were carried out with approval of the Animal Ethical Committee (EMC 2429).

Biochemical evaluation of the extracellular matrix

Alginate constructs were digested overnight at 56°C in papain (250 µg/mL in 0.2 M NaH₂PO₄, 0.01 M EDTA, containing 5 mM L-cystein; pH 6.0). After digestion, samples were subjected to biochemical analyses to determine the DNA, glycosaminoglycan (GAG), and hydroxyproline contents, as described previously. [40] In short, the amount of DNA was determined by Ethidium bromide (GibcoBR1), using calf thymus DNA as a standard. Sulfated GAGs (sGAGs) were quantified by the 1,9-Dimethylmethylene blue (DMMB) dye-binding assay (pH 1.75), using shark chondroitin sulphate C as a standard. For the hydroxyproline content, digests were hydrolysed, dried and redissolved in 150 µL water. Hydroxyproline contents were measured using chloramine-T and dimethylaminobenzaldehyde as reagents and hydroxyproline (Merck, Germany) as a standard.

Histological evaluation of the extracellular matrix

After eight weeks of subcutaneous implantation, constructs were harvested, set in 2% agarose, fixed in 4% formalin in PBS and embedded in paraffin. Paraffin-embedded sections (6 µm) were deparaffinised and rehydrated.

To allow the use of monoclonal mouse antibody collagen type II (II-II6B3 1:100; Developmental Studies Hybridoma Bank, USA) on constructs which had been implanted in mice, the primary antibody was pre-coupled overnight with goat anti-mouse biotin at 4°C (1:500; Jackson Laboratories, USA), followed by a two-hour incubation in 0.1% normal mouse serum (CLB, the Netherlands), to prevent unwanted binding of the anti-mouse antibodies to mouse immunoglobulins. [214]

Antigen retrieval was performed through incubation with 0.1% pronase for 30 minutes at 37°C, continued with a 30 minutes incubation with 1% hyaluronidase at 37°C. Non-specific binding sites were blocked with 10% goat serum and sections were stained with the pre-treated antibodies for 60 minutes. Sections were then incubated with enzyme-streptavidin conjugate (Label, 1:100, Biogenex, HK-321-UK, USA) in PBS/1% BSA, followed by incubation with Neu Fuchsin substrate (Chroma, Germany).

Biomechanical analysis

For mechanical characterization, constructs of 2.0 mm thick and 5 mm in diameter were created. The samples were placed in close-fitting Ø 5 mm stainless steel cylindrical wells. Mechanical testing was performed with a materials testing machine (Zwick Z005, Germany) equipped with a 10 N load cell, a built-in displacement control, and a cylindrical, plane-ended, stainless steel indenter (Ø 1.2 mm). Stress-strain testing was performed: the samples were compressed to a final height of 0.5 mm at a loading rate of 5 mm per minute. An in-house Matlab® script was used to locate the sample surface and measure the sample thickness. Force-displacement curves were then converted to stress-strain curves. Measurements of compressive modulus at 40% strain (E40%) were determined.

Gene-expression analyses

To further evaluate the contribution of each individual cell type (i.e. *hBMSCs*, *bECs* or *bNCs*) to cartilage matrix formation, species-specific gene-expression analyses was achieved. For total RNA isolation, alginate was dissolved in ice-cold 55 mM sodium citrate and 20 mM EDTA in 150 mM NaCl and centrifuged. Each cell-pellet was subsequently suspended in 1 mL RNA-Bee™ (TEL-TEST, USA). RNA was extracted with chloroform and purified from the supernatant using the RNeasy Micro Kit (Qiagen, Germany) according to the manufacturer's guidelines by on-column DNA-digestion. Total RNA of each sample was reverse transcribed into cDNA using RevertAid™ First Strand cDNA Synthesis Kit (MBI Fermentas, Germany).

For quantitative real-time Polymerase Chain Reaction (qRT-PCR) analysis, forward and reverse primers were designed using PrimerExpress 2.0 software (Applied Biosystems, USA) to meet TaqMan or SYBR Green requirements. Analysed genes are listed in table 2. RT-PCR was performed using TaqMan® Universal PCR Mastermix (Applied Biosystems) or qPCR Mastermix Plus for SYBR Green (Eurogentec, the Netherlands) according to the manufacturers' guidelines and using ABI PRISM® 7000 with SDS software version 1.7 (Applied Biosystems, the Netherlands). Relative gene expressions were calculated by means of the $2^{-\Delta\Delta CT}$ formula.

Statistical analysis

All data were analyzed with PSAW statistics 20.0 (SPSS Inc., USA). The mean and standard deviation were presented. *In-vitro* data represents at least three independent donors per condition performed in triplicate. For statistical evaluation of these experiments, a mixed linear model was used followed by Fisher's least significant post-hoc comparisons tests. 'Condition' and 'time point' were defined as fixed factors in the model. 'Donor' and 'sample number' were treated as random factors. For the *in-vivo* experiments six constructs per condition were used, with duplicate samples for three independent donors. For statistical evaluation of these experiments, one-way ANOVA was used followed by Fisher's least significant difference post-hoc comparisons tests. For all tests, values of $p < 0.05$ were considered statistically significant.

Primers and probes	
Human specific genes	
<i>hsGAPDH</i>	Fw: AGCTCACTGGCATGGCCTTC Rev: CGCCTGCTTCACCACCTTCT
<i>hsACAN</i>	Fw: CAGCCACCACCTACAAACGCAG Rev: CTGGGTGGGATGCACGTCAGC
Bovine specific genes	
<i>bsGAPDH</i>	Fw: GTCAACGGATTTGGTCGTATTGGG Rev: TGCCATGGGTGGAATCATATTGG
<i>bsACAN</i>	Fw: GGACACTCCTTGCAATTTGAGAA Rev: CAGGGCATTGATCTCGTATCG

Table 2. Sequences of primers and probes for qRT-PCR.

GAPDH = GlycerAldehyde 3-Phosphate DeHydrogenase ; *ACAN* = AggreCan ; *hs* = human-specific ; *bs* = bovine-specific.

RESULTS

Cartilage formation *in vitro*

After three weeks, DNA content significantly decreased over time in constructs containing *h*BMSCs ($p=0.019$), *b*ECs ($p=0.010$) or *h*BMSC/*b*ECs ($p<0.001$), though remained stable in *b*NCs or *h*BMSC/*b*NCs. (Figure 1) Similar results were obtained after 5 weeks. (Supplementary figure 1)

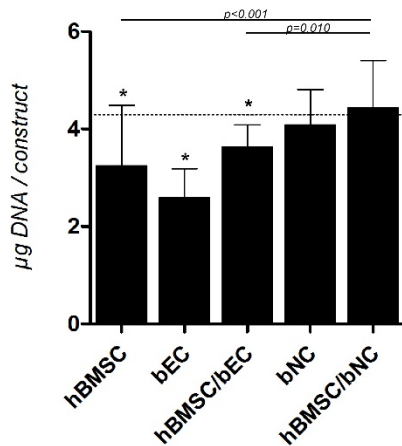


Figure 1. Cell content of constructs containing *h*BMSCs and/or chondrocytes, 3 weeks after *in-vitro* culture.

DNA content was determined at baseline before culture (dotted line), being on average 4.29 ± 0.96 µg DNA per construct, and after 3 weeks of culture. * indicates a p -value smaller than 0.05 compared to baseline. Data are shown as mean \pm SD. For statistical evaluation, a mixed model was used followed by a Fisher's least significant post-hoc comparisons test. *h*BMSC = human Bone-marrow-derived Mesenchymal Stem Cell ($n=3$ experiments with 3 different donors); *b*EC = bovine Ear Chondrocyte ($n=3$ experiments with 3 pools of donors); *b*NC = bovine Nasal Chondrocyte ($n=3$ experiments with 3 pools of donors). Per experiment, 3 samples were used for analyses.

Since constructs were cultured in the absence of chondrogenic factors, constructs containing solely *h*BMSCs produced very little sGAG (Figure 2A) and collagen (Figure 2B). To demonstrate the additional effect of *h*BMSCs in mixed-cell-type populations, a control condition - containing similar numbers of chondrocytes without the supplementation of *h*BMSCs - was evaluated (Figure 2 white lines). The additional effect of *h*BMSCs in mixed-cell-type populations was dependent on the chondrocyte-source used: the addition of *h*BMSCs to *b*NCs demonstrated a significant increase in the production of sGAG ($p=0.012$) and collagen ($p=0.007$) compared to their controls; no additional effects were observed in *h*BMSCs/*b*ECs. *h*BMSC/*b*NCs contained significantly more sGAG ($p=0.026$) and collagen ($p=0.040$) compared to *h*BMSC/*b*ECs. Normalization of the data to their initial number of seeded primary chondrocytes (PCs) revealed more distinct differences between mixed-cell-type and single-cell-type populations: *h*BMSCs/*b*ECs and *h*BMSC/*b*NCs produced more cartilage matrix per initial seeded chondrocyte than chondrocytes only. (Figure 2, right) Similar results were

obtained after 5 weeks. (Data not shown) These results demonstrate that *h*BMSCs have an additional effect on chondrocytes in mixed-cell-type populations *in vitro*, in particular in combination with *b*NCs.

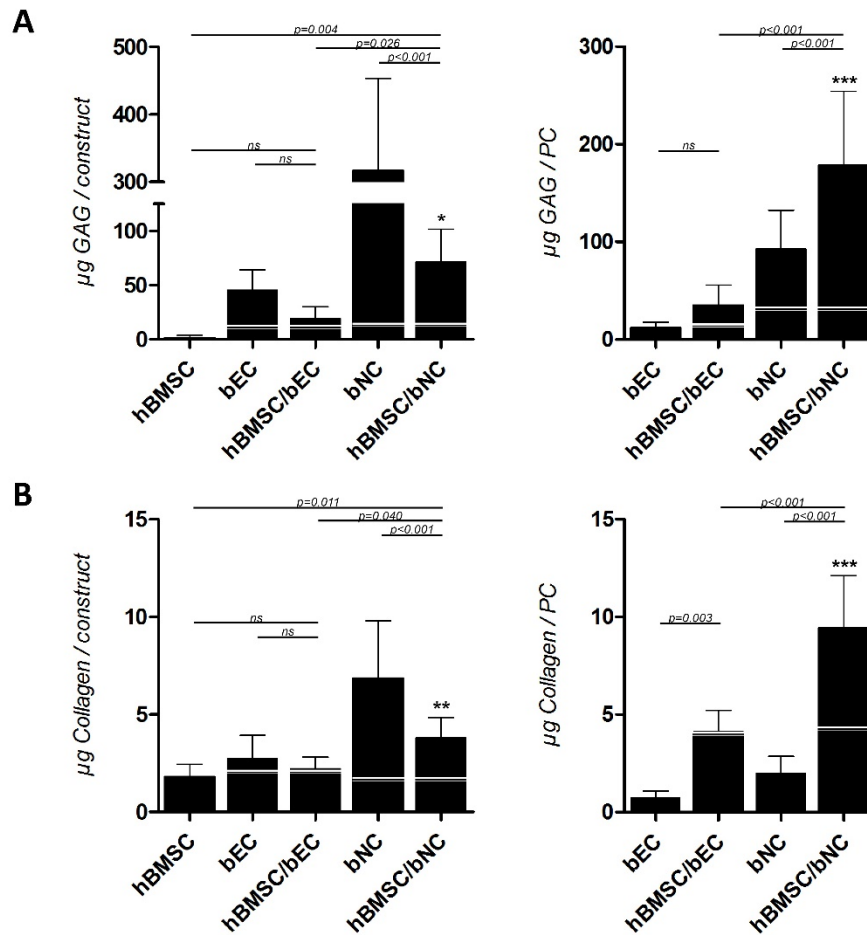


Figure 2. Cartilage matrix formation in constructs containing *h*BMSCs and/or chondrocytes, 3 weeks after *in-vitro* culture.

Biochemical evaluation of the sGAG (**A**) and collagen (**B**) content, 3 weeks after culture in alginate. The left graphs demonstrate the amount of matrix components per construct, whereas for the right graphs matrix production is normalized to the initial number of seeded PCs. A control condition - containing similar amounts of chondrocytes (0.8 million/ml) without supplementation of *h*BMSCs - was evaluated to determine the additional effect of *h*BMSCs (3.2 million/ml) on chondrocytes in co-cultures (white line). *, ** or *** indicates *p*-values smaller than 0.05, 0.01 or 0.001 respectively compared to the control condition. Data are shown as mean \pm SD. For statistical evaluation, a mixed model was used followed by a Fisher's least significant post-hoc comparisons test. PC = Primary Chondrocyte ; *h*BMSC = human Bone-marrow-derived Mesenchymal Stem Cell (*n*=3 experiments with 3 different donors) ; *b*EC = bovine Ear Chondrocyte (*n*=3 experiments with 3 pools of donors) ; *b*NC = bovine Nasal Chondrocyte (*n*=3 experiments with 3 pools of donors). Per experiment, 3 samples were used for analyses.

Cell behavior in co-cultures

Using a xenogeneic culture system enabled us to determine the contribution of each individual cell type (i.e. *hBMSCs*, *bECs* or *bNCs*) to cartilage matrix production using species-specific gene-expression analyses. First, *GAPDH*-gene expression was analysed after 5 weeks of *in-vitro* culture. *hBMSC/bECs* and *hBMSC/bNCs* contained cells from both bovine (EC or NC) and human (BMSC) origin. (Table 3) Then, chondrogenic gene expression was analysed by the *ACAN*-gene. In a growth-factor-free environment, *hBMSCs* hardly expressed *hsACAN*. Besides, *hsACAN* was hardly expressed in *hBMSC/bECs* or *hBMSC/bNCs* either. Conversely, *hBMSC/bECs* or *hBMSC/bNCs* - containing solely 20% bovine chondrocytes - expressed as much or even higher levels of *bsACAN* compared to their 100% controls: *hBMSC/bECs* vs *bECs* 3.96 ± 6.13 fold change; *hBMSC/bNCs* vs *bNCs* 4.56 ± 6.18 fold change. These data indicate that the formed cartilage matrix was from chondrocyte origin, which suggests a more trophic role for *hBMSCs* herein.

	<i>hsGAPDH</i>	<i>bsGAPDH</i>
<i>hBMSC</i>	24.1 ± 2.78	nd
<i>bEC</i>	nd	25.0 ± 2.4
<i>bNC</i>	nd	23.4 ± 1.7
<i>hBMSC/bEC</i>	24.0 ± 1.7	26.0 ± 2.7
<i>hBMSC/bNC</i>	24.8 ± 1.7	25.1 ± 2.4

Table 3. Gene-expression analyses, 5 weeks after *in vitro* culture.

Data are shown as mean CT-values ± SD of housekeeping genes. nd = not detected (ct-value > 35.00) ; *hsGAPDH* = human-specific *GAPDH* ; *bsGAPDH* = bovine-specific *GAPDH* ; *hBMSC* = human Bone-marrow-derived Mesenchymal Stem Cell (*n*=3 experiments with 3 different donors) ; *bEC* = bovine Ear Chondrocyte (*n*=3 experiments with 3 pools of donors) ; *bNC* = bovine Nasal Chondrocyte (*n*=3 experiments with 3 pools of donors). Per experiment, 3 samples were used for analyses.

Cartilage formation *in vivo*

After 8 weeks of implantation all constructs were identified and harvested. Constructs containing *bNCs* or *hBMSC/bNCs* resembled cartilage tissue in both color and texture, while constructs containing *hBMSCs*, *bECs* or *hBMSC/bECs* were still fragile and did not express a cartilaginous appearance. (Figure 3) After subcutaneous implantation, none of the constructs had mineralized or ossified. Collagen type II was abundantly present in constructs containing *bEC* or *bNCs* (both single-cell-type and mixed-cell-type populations), but was not visible in constructs containing *hBMSCs* only. (Figure 3).

In vivo, *hBMSC/bECs* and *hBMSC/bNCs* contained similar quantities of cartilage matrix as constructs containing chondrocytes only. Moreover *hBMSC/bNCs* produced significantly more sGAG (*p*=0.004) compared to *hBMSC/bECs*. (Figure 4A) Collagen production demonstrated a similar trend, albeit without statistical significant differences. (Figure 4B) Normalization of the data to their initial number of seeded PCs revealed more distinct

differences between mixed-cell-type and single-cell-type populations: *hBMSC/bNCs* produced significantly more sGAG and collagen per initial seeded PC compared to *bNCs* and *hBMSC/bECs* ($p<0.05$). (Figure 4, right)

After subcutaneous implantation, the elastic modulus was highest in constructs containing *bNCs*, although large variation between samples was observed. (Figure 5)

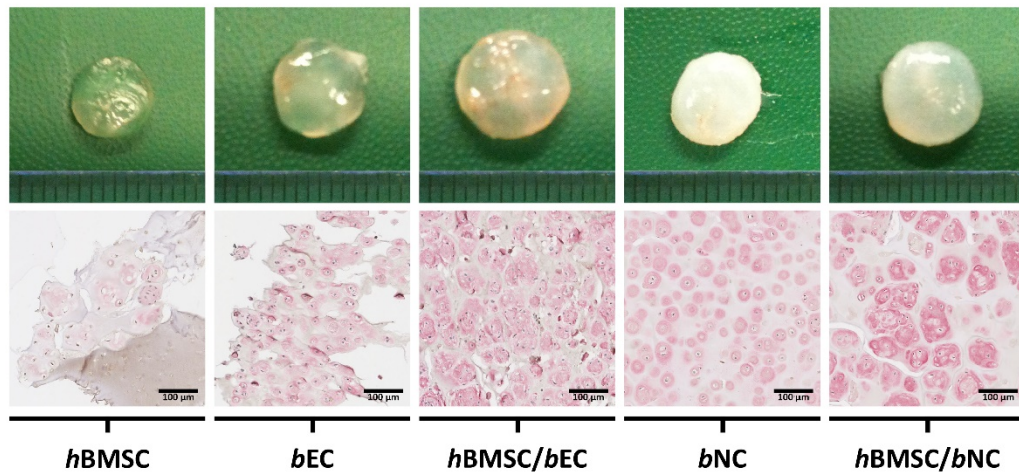


Figure 3. Cartilage matrix formation in constructs containing *hBMSCs* and/or chondrocytes, 8 weeks after subcutaneous implantation in mice.

Macroscopic appearance (*top row*) of cartilage constructs, as well as a collagen type II immunohistochemical staining (*bottom row*), 8 weeks after subcutaneous implantation. *hBMSC* = human Bone-marrow-derived Mesenchymal Stem Cell ($n=2$ experiments with 2 different donors) ; *bEC* = bovine Ear Chondrocyte ($n=2$ experiments with 3 pools of donors) ; *bNC* = bovine Nasal Chondrocyte ($n=2$ experiments with 3 pools of donors). Per experiment, 2 samples were used for analyses.

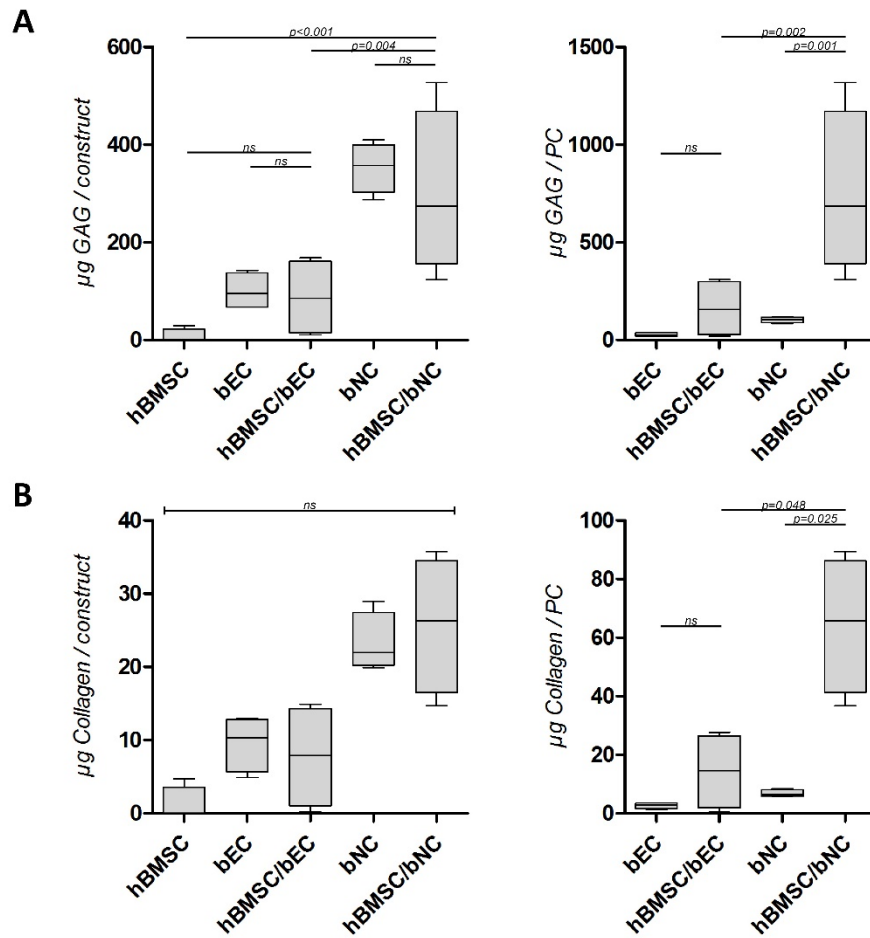


Figure 4. Cartilage matrix formation in constructs containing *hBMSCs* and/or chondrocytes, 8 weeks after subcutaneous implantation in mice.

Biochemical evaluation of the sGAG (**A**) and collagen (**B**) content, 8 weeks after subcutaneous implantation. The left graphs demonstrate the amount of matrix components per construct, whereas for the right graphs matrix production is normalized to the initial number of seeded PCs. Data are shown as box-whisker plots. For statistical evaluation, a one-way ANOVA was used followed by a Fisher's least significant difference post-hoc comparisons test. PC = Primary Chondrocyte ; *hBMSC* = human Bone-marrow-derived Mesenchymal Stem Cell ($n=2$ experiments with 2 different donors) ; *bEC* = bovine Ear Chondrocyte ($n=2$ experiments with 3 pools of donors) ; *bNC* = bovine Nasal Chondrocyte ($n=2$ experiments with 3 pools of donors). Per experiment, 2 samples were used for analyses.

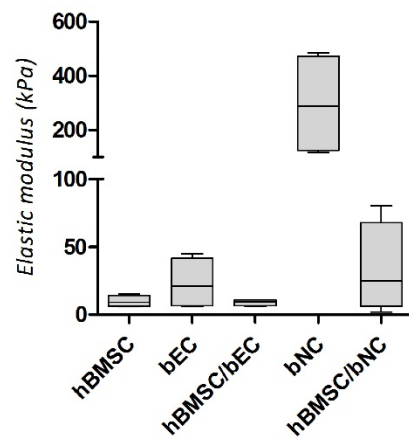


Figure 5. Biomechanical behavior in constructs containing *h*BMSCs and/or chondrocytes, 8 weeks after subcutaneous implantation in mice.

Biomechanical properties were determined 8 weeks after subcutaneous implantation. Data are shown as box-whisker plots. PC = Primary Chondrocyte ; *h*BMSC = human Bone-marrow-derived Mesenchymal Stem Cell ($n=2$ experiments with 2 different donors) ; *b*EC = bovine Ear Chondrocyte ($n=2$ experiments with 3 pools of donors) ; *b*NC = bovine Nasal Chondrocyte ($n=2$ experiments with 3 pools of donors). Per experiment, 2 samples were used for analyses.

DISCUSSION

The combination of chondrocytes and MSCs holds great promise for cell-based cartilage repair in the head and neck area as it reduces the required number of chondrocytes and extenuates most disadvantages of individually used cell types such as culture-expanded chondrocytes or MSCs. Mixed-cell cultures have been demonstrated to improve chondrogenesis [74] as well as to reduce hypertrophy and tissue mineralization [73, 75]. Unfortunately, most research on mixed-cell-based cartilage repair was performed with articular chondrocytes. So far, little research in this field has been performed on non-articular chondrocytes, such as ECs [77-79] or NCs [80]. This study evaluates the two most relevant cell sources for cell-based cartilage repair in the head and neck area - ECs and NCs - and replaced 80% of the chondrocytes with *h*BMSCs. In line with previous studies on mixed-cell-based cartilage repair, *h*BMSC/*b*ECs or *h*BMSC /*b*NCs produced similar quantities of cartilage matrix components as constructs containing chondrocytes only. Moreover, the cartilage tissue formed seemed stable and did not calcify *in vivo*. This suggests that 80% of the chondrocytes can be replaced by *h*BMSCs without influencing cartilage matrix production and stability. Therefore, mixed cultures of BMSCs and ECs or NCs could be very advantageous for cell-based cartilage repair in the head and neck area, as appropriate numbers of cells are more easily acquired from bone-marrow aspirates than from cartilage biopsies.

By using primary cells, we aimed to translate the procedure towards a single-stage clinical application. Currently, for articular cartilage repair, two clinical trials are already designed as single-stage procedures. [277, 278] Unfortunately, the little research performed on mixed-cell cultures using BMSCs and ECs [77-79] or NCs [80], impeded the translation of such basic research to a clinical application, since these studies made use of non-optimal culture conditions. First, instead of using primary chondrocytes, most research [77, 78, 80] was performed with culture-expanded chondrocytes, which requires a two-stages procedure: (1) a surgical procedure to harvest cartilage tissue for chondrocyte isolation and further culture-expansion ; (2) a surgical procedure to implant the cell-based cartilage graft. Second, others have cultured their constructs in growth-factor-enriched medium. [77, 80] Since growth factors stimulate the re-differentiation and differentiation of both culture-expanded chondrocytes and BMSCs, the use of growth factors might have interfered the underlying mechanisms of cell-cell interaction in their culture system. Moreover, clinical use of growth factors is limited by the problem of adequate delivery [279] and the requirement of special regulatory approval by the Food and Drug Administration or European Medicines Agency. Finally, so far only few studies have evaluated the cartilage-forming capacity of BMSC/ECs [77, 79] and BMSC/NCs (none) *in vivo*. Therefore, in an attempt to translate experimental research towards a single-stage clinical application in the future, we have studied the *in-vitro* and *in-vivo* capacity of *h*BMSCs mixed with primary *b*ECs or *b*NCs cultured in a growth-factor-free environment.

We made use of a xenogeneic culture system (i.e. bovine chondrocytes, human BMSCs). The species mismatch did not impede cartilage formation confirming previously published results of *h*BMSCs combined with xenogeneic chondrocytes. [74, 273-275] Moreover, by making use of a xenogeneic culture system we were able to determine the

contribution of each individual cell type to cartilage matrix production using species-specific gene-expression analyses. In this way, we proved that cartilage matrix formation originated from bovine chondrocytes and that *h*BMSCs fulfilled a trophic role herein. Although numerous cellular communication pathways have been hypothesized in order to explain beneficial effect of mixed cultures [73], this outcome was in accordance with previous studies, investigating the effect of MSCs on articular chondrocytes. [74, 263, 275, 280] We found no evidence that paracrine soluble factors released by chondrocytes enhanced the chondrogenic differentiation of *h*BMSCs, as stated by others. [255-259] Although the importance of juxtacrine or gap-junctional signalling is still unclear in literature [263], our mixed cells encapsulated in alginate hydrogels implicated that such signaling pathways are of less importance than paracrine signaling pathways, since the alginate hydrogel hinders direct cell-cell contact.

Besides the trophic effect of *h*BMSCs on chondrocytes we demonstrated that this effect was also depended on the chondrocyte source used. The differences between the chondrocyte sources was most obvious in the *in-vitro* experiments: *b*NCs were clearly stimulated by *h*BMSCs, while *b*ECs were not at all influenced by them. Although the *in-vivo* experiments showed a positive effect of *h*BMSCs on both *b*ECs and *b*NCs, it was obvious that the use of *b*NCs lead to constructs with a higher amount of sGAG and collagen and higher equilibrium modulus than *b*ECs. Clear subtype-specific differences in cartilage forming potential is in accordance with our previously published work, confirming that ECs and NCs have unique gene-expression profiles inducing dissimilar proliferation capacity, cartilage matrix formation and elastin fiber deposition. [40, 56]

Before this method can be successfully applied as a one-step clinical application, there are some limitations to overcome. First, the elastic modulus after 8 weeks of subcutaneous implantation was low and approximately 1% of that of native human ear or nasal cartilage. [281] Although the biomechanical properties of the constructs were rather low, alginate enabled a homogeneous cell distribution and prevented cells from floating out while permitting nutrient diffusion and oxygen transfer to the cells in order to create an environment to form new cartilage matrix with sufficient properties. [89] Therefore, injected into a mechanical stable scaffold, alginate could be an excellent cell-carrying gel for future cell-based cartilage repair. Secondary, the cell density used in this study might not be optimal to obtain engineered tissue that are clinical applicable. Our experimental set-up did not allow us to further increase cell density due to limitations in the number of cells available. Nevertheless it allowed us to study the interactions between the cell types. For clinical application, it would be ideal to only use low numbers of human primary chondrocytes supplemented with *h*BMSCs. We have combined *h*BMSCs and chondrocytes at a 4:1 ratio, as the effect of *h*BMSCs on articular chondrocytes was already studied by us at such ratio. Although others have used a 4:1 ratio for their research as well [74, 253], no consensus on optimal BMSCs-to-chondrocytes ratios have been established for ECs and NCs. Future research needs to clarify if we could further reduce the amount of primary chondrocytes without inhibiting cartilage matrix production. Finally, for future clinical application the use of allogeneic *h*BMSCs can be considered as MSCs have been demonstrated to be immune

privileged. [282] Alternatively, instead of using culture-expanded *h*BMSCs it might even be considered to use the mononuclear fraction of freshly isolated autologous bone marrow. [283]

In summary, this study demonstrates that constructs containing a combination of 80% *h*BMSCs and 20% *b*ECs or *b*NCs produced similar quantities of cartilage matrix components as constructs containing chondrocytes only. Therefore, 80% of the chondrocytes can easily be replaced by *h*BMSCs without influencing cartilage matrix production. Using this procedure, the chondrocytes need no culture-expansion *in vitro*, supporting the use of a one-stage cell-based cartilage repair procedure for cartilage defects in the head and neck area.

Acknowledgment

The authors would like to thank dr. Jeanine Hendriks (CellcoTec, Bilthoven, the Netherlands) for her valuable ideas during preparation of this manuscript. We further thank Nicole Kops (Department of Orthopaedics, Erasmus MC, University Medical Center, Rotterdam) for histological and immunohistochemical processing of the constructs. Last, we acknowledge the department of orthopaedic surgery for their assistance in obtaining bone marrow aspirates. The study was performed within the framework of EuroNanoMed (EAREG-406340-131009/1) and funded by SenterNovem.

Scaffolds

Chapter 7

Preparation and characterization of a decellularized cartilage scaffold for ear cartilage reconstruction

M.M. Pleumeekers, L. Utomo, L. Nimeskern, S. Nürnberger, K.S. Stok, F. Hildner, G.J.V.M. van Osch

Biomedical Materials, 2015. 10(1): p. 1-11.

ABSTRACT

Scaffolds are widely used to reconstruct cartilage. Yet, the fabrication of a scaffold with a highly organized microenvironment that closely resembles native cartilage remains a major challenge. Scaffolds derived from acellular extracellular matrices are able to provide such a microenvironment. Currently, no report specifically on decellularization of full thickness ear cartilage has been published. In this study, decellularized ear cartilage scaffolds were prepared and extensively characterized. Cartilage decellularization was optimized to remove cells and cell remnants from elastic cartilage. Following removal of nuclear material, the obtained scaffolds retained their native collagen and elastin contents as well as their architecture and shape. High magnification scanning electron microscopy showed no obvious difference in matrix density after decellularization. However, glycosaminoglycan content was significantly reduced, resulting in a loss of viscoelastic properties. Additionally, in contact with the scaffolds, human bone-marrow-derived mesenchymal stem cells remained viable and are able to differentiate towards the chondrogenic lineage when cultured *in vitro*. These results, including the ability to decellularize whole human ears, highlight the clinical potential of decellularization as an improved cartilage reconstruction strategy.

INTRODUCTION

Ear cartilage defects - either caused by congenital malformation, trauma or tumor destruction - are a commonly encountered problem in reconstructive surgery, since cartilage has a limited capacity for self-regeneration once damaged. Therefore, ear cartilage defects can ultimately lead to physical and aesthetic impairment. Despite the great demand for treating ear cartilage defects, current treatments using autologous cartilage are challenging. Not only because they require a high degree of surgical expertise, but also because they are associated with limited availability of autologous cartilage and can cause severe donor site morbidity.

For successful cartilage reconstruction, the properties of the three-dimensional (3D) matrix is of major importance, in: (1) providing temporary or permanent support while maintaining size and shape; and (2) providing specific structural, mechanical and biological cues to cells, which guide tissue remodeling. [82, 284] Ideally, the best scaffold for cartilage reconstruction should mimic the extracellular matrix (ECM) of the targeted tissue itself. As a result, several 3D scaffolds, including both natural and synthetic materials, have been developed and investigated for their use in cartilage reconstruction. [23, 83, 285] A frequently used alternative to autologous cartilage implants are synthetic materials such as porous polyethylene [286, 287]. Although this material is advantageous to work with it is prone to induce a foreign body reaction, the ensuing extrusion [124] in most cases resulting in removal of the entire implant. [288] Additionally, the biomechanical mismatch of the implants compared to normal ear cartilage can result in eventual collapse of the framework. [289]. So far, no ideal scaffold has emerged since the complex 3D composition and architecture of native ECM makes it extremely difficult to precisely mimic. Recently, natural acellular ECM scaffolds have become increasingly popular. These acellular ECM scaffolds are acquired by a process called decellularization: a method that requires chemical, physical and/or enzymatic treatments. [93] Decellularized ECM scaffolds provide a 3D ECM structure with immediate functional support without evoking an adaptive immune response upon implantation due to absence of donor cellular antigens. [94]

To date, various cartilaginous structures have already been decellularized including tracheal cartilage [94-99], articular cartilage [100-103], nasal cartilage [106, 110], intervertebral discs [104, 105] and meniscal cartilage [106-109]. Currently, no method to specifically decellularize full thickness ear cartilage that belongs to the elastic cartilage type, has been described in literature. In contrast to hyaline and fibrous cartilage, elastic cartilage contains additional thick elastic fibers, making it denser and therefore more challenging to decellularize. Furthermore, the ability to prepare scaffolds from whole cartilage tissue rather than scaffolds that are derived from ECM [290, 291], provides the opportunity to decellularize large tissues and structures that hold complex native shapes such as ears.

Therefore, the goal of this study was to prepare decellularized ear cartilage scaffolds and extensively characterize their biochemical and biomechanical properties, as well as investigate their cytocompatibility. Furthermore, by preparing human ear cartilage scaffolds with desirable size and shape, we show the potential of decellularized cartilage to improve human cartilage reconstruction.

MATERIALS AND METHODS

All chemicals were obtained from Sigma-Aldrich, St. Louis, USA unless stated otherwise.

Preparation of decellularized cartilage scaffolds

To obtain full thickness bovine ear cartilage (*bEC*), macroscopically intact cartilage was harvested from calves ($n=3$) less than 8 months old (T. Boer & Zn., Nieuwerkerk aan den IJssel, the Netherlands) and washed with phosphate buffered saline (PBS) after careful resection of the perichondrium. Bovine articular cartilage samples (*bAC*) were harvested from the metacarpophalangeal joints ($n=3$) and included as controls to compare decellularization outcomes. Samples were made using an 8 mm dermal biopsy punch (Spengler, Asnières sur Seine, France) and kept in PBS until decellularization. Human ear cartilage (*hEC*) was obtained from post mortem donors ($n=2$; M, 83 and 84 Y) who donated their bodies to medical science at Erasmus Medical Center (EMC; Rotterdam, the Netherlands). Dermal tissue was macroscopically removed, followed by careful removal of the perichondrium and samples were made using an 8 mm dermal biopsy punch. Untreated (i.e. native) cartilage samples were immediately stored dry at -80°C after harvest for biochemical analysis or in 4% formaldehyde for histological analysis and scanning electron microscopy (SEM).

All human and bovine cartilage samples were decellularized according to the protocol of Kheir, *et al.* [101], which was further optimized to specifically decellularize ear cartilage. Briefly, the samples were subjected to 2 overnight dry freeze-thaw cycles followed by 2 overnight freeze-thaw cycles at -20°C in hypotonic buffer (10 mM Tris-HCl in Mili-Q water, pH 8.0) following a 24 hour incubation in hypotonic buffer at 45°C . Next, samples were treated for 24 hours with an ionic detergent consistent of 0.1% sodium dodecyl sulfate (SDS), 0.1% ethylenediaminetetraacetic acid (EDTA) and 10 KIU/mL aprotinin in Mili-Q water. Then, samples were washed twice for 30 minutes in wash solution (PBS with 10 KIU/mL aprotinin) before a 24 hour wash at 45°C in wash solution. Since the protocol of Kheir *et al.* was not sufficient to reduce or remove cellular remnants, an elastase solution was incorporated into the protocol to improve the removal of cellular remnants. Therefore, the samples were treated next with a low concentration elastase solution (0.2 M Tris-HCl in Mili-Q water, 10 KIU/mL aprotinin and 0.03 U/mL elastase, pH 8.6) for 24 hours at 37°C , as a high concentration elastase would completely damage the matrix structure due to the complete depletion of elastin and glycosaminoglycans (GAGs). (Supplementary figure 1) Next, samples were washed twice and incubated for 3 hours at 37°C in nuclease solution (50 mM Tris-HCl in Mili-Q water, 10 mM MgCl, 50 $\mu\text{g}/\text{mL}$ bovine serum albumin (BSA), 50 U/mL DNase and 2.5 U/mL RNase, pH 7.5). Samples were washed again in wash solution and treated for 3 hours in decontamination solution (0.1% peracetic acid in PBS). All incubation and wash steps were performed with agitation. Finally, the samples were transferred to sterile tubes and washed twice for 30 minutes in sterile PBS before starting a 24 hour wash cycle in sterile PBS at 45°C . To assess the decrease in wet weight after decellularization, samples from one donor of both cartilage types were weighted directly after harvest and subjected to an individual decellularization treatment taking into account volume ratios of the used solutions. After the individual treatment, wet weight was determined again. Samples from the remaining donors

were decellularized in batches. Samples intended for histological analysis and SEM were stored in 4% formaldehyde and samples for biochemical analysis were stored dry at -80°C. Samples intended for biomechanical analysis were shipped to Eidgenössische Technische Hochschule (ETH; Zurich, Switzerland) in PBS containing protease inhibitors (Roche, Basel, Switzerland) at 4°C. Decellularized *b*EC scaffolds intended for seeding ($n=1$, in 6-fold) were pre-conditioned for at least 2 hours in Minimally Essential Medium Alpha (MEM- α ; Gibco, Carlsbad, USA) containing 10% fetal calf serum (FCS; Lonza, Verviers, Belgium), 50 $\mu\text{g}/\text{mL}$ gentamicin (Gibco) and 1.5 $\mu\text{g}/\text{mL}$ amphotericin B (Fungizone; Gibco) and stored at 4°C until seeding.

Biochemical analysis

Prior to biochemical analysis, wet weight was determined for all cartilage samples. For DNA, sGAG and collagen analysis, samples were digested overnight at 60°C in a papain solution (0.2 M $\text{Na}_2\text{H}_2\text{PO}_4$, 0.01 M $\text{EDTA}\cdot 2\text{H}_2\text{O}$, 250 $\mu\text{g}/\text{mL}$ papain, 5 mM L-cystein, pH 6.0). Bovine and human cartilage samples were digested in 400 and 500 μL papain solution, respectively. To assess the removal of nuclear components, the DNA content of the cartilage scaffolds was measured with the CyQUANT® (Invitrogen) proliferation assay. This assay is able to detect low amounts of DNA and has a detection limit of 10 ng per measurement. In short, 250 IU heparin (LEO Pharma, Ballerup, Denmark) and 125 μg RNase were added to the papain digests and incubated for 30 minutes at 37°C. Finally, 0.375 μL CyQUANT GR dye was added to each papain digested sample and fluorescence was immediately measured (excitation/emission: 480/520 nm) on a SpectraMax Gemini micro plate reader (Molecular Devices, Sunnyvale, USA), using calf thymus DNA as a standard.

A 1,9-Dimethylmethylen blue (DMMB; pH 3.0) assay [292] was performed to measure the sulphated GAG content of the cartilage scaffolds. The metachromatic reaction of DMMB was monitored using a VersaMax spectrophotometer at 530 and 590 nm. Shark chondroitin sulphate C was used as a standard.

A hydroxyproline assay [213] was performed to measure the total amount of collagen of the cartilage scaffolds. In short, the papain digests were hydrolyzed with equal volumes of 12 M HCl at 108°C for 20 hours, dried (Savant SPD 121P SpeedVac; Thermo Scientific, Massachusetts, USA) and re-dissolved in 1.5 mL Mili-Q water. Hydroxyproline contents were measured using a colorimetric method (extinction 570 nm), with chloramine-T and dimethylaminobenazldehyde as reagents. Hydroxyproline (Merck) was used as a standard to calculate the amount of collagen per sample.

Elastin content of the cartilage samples was measured using the Fastin™ Elastin Assay (Biocolor, Carrickfergus, UK) according to manufacturer's instructions. Briefly, cartilage samples were converted to water soluble α -elastin by 3 overnight heat extraction cycles at 100°C in 0.25M oxalic acid before adding the kit's dye. Absorption was measured at 513 nm on a VersaMax plate reader. α -elastin from bovine neck ligament (provided by manufacturer) was used as a standard.

Histological analysis

Untreated and decellularized samples were fixed in 4% formaldehyde and embedded in 3% agarose, dehydrated in an ascending series of alcohol, then embedded in paraffin and sectioned at 6 μm . Sections were stained with Gill's Haematoxylin and Eosin (H&E, Merck), Safranin-O and Resorcin Fuchsin (RF, Klinipath, Duiven, the Netherlands). Additionally, collagen type II and elastin were immunohistochemically visualized. Antigen retrieval for the collagen type II antibody (II-II 6B3; DSHB, Iowa, USA) was achieved by incubating in 0.1% pronase in PBS for 30 minutes at 37°C. Antigen retrieval of elastin (BA-4) was carried out by incubation in 0.25% trypsin in PBS for 20 minutes at 37°C. 10% goat serum in PBS was used to block non-specific binding sites. Next, sections were stained for 1 hour with primary antibodies against collagen type II (1:100) or elastin (1:1000). An enzyme-streptavidin conjugate (HK-321/325-UK; Biogenex, California, USA) in PBS/1% BSA at a dilution of 1:100 was used as label and visualized by Neu Fuchsin substrate (Chroma, Köngen, Germany).

Cell-seeded cartilage scaffolds were immediately embedded in Tissue-Tek OCT Compound (Sakura, Alphen aan den Rijn, the Netherlands) after harvest, sectioned at 6 μm , fixed in acetone and stained with H&E.

For SEM analysis, samples were dehydrated in a graded alcohol series, fractured by pulling at the distal end of the samples and dried with hexamethyldisilazane. Samples were then mounted on stubs, coated with palladium gold in a sputter coater (SC7620; Emitech/Quorum Technologies, Laughton, UK) and visually observed with a scanning electron microscope (JSM-6510; JEOL, Tokyo, Japan).

Biomechanical testing

Biomechanical properties of cartilage scaffolds were assessed using stress-relaxation-indentation as previously described [156]. In short, samples ($n=3$ with 6 samples per donor) were placed in close-fitting stainless steel cylindrical wells of 5 mm in diameter, while immersed in PBS supplemented with antibiotic/antimycotic solution. Mechanical testing was performed with a materials testing machine (Zwick Z005, Ulm, Germany) equipped with a 10 N load cell, a built-in displacement control, and a cylindrical, plane ended, stainless steel indenter ($\varnothing 0.35\text{mm}$). A preload of 3 mN was first applied on the sample to locate the sample surface and measure sample thickness, and held for 5 minutes. Five consecutive strain steps in 5% increments were applied up to a maximum strain of 25%. Samples were then left to relax for 20 minutes at each step. A custom MATLAB[®] script was used to convert the force-displacement data to stress-strain. Maximum stress (σ_{max}) equilibrium modulus (E_{eq}), relaxation time (τ) and relaxation half time ($t_{1/2}$) were determined from the stress-strain plots to determine intrinsic, flow-independent, and flow-dependent mechanical properties. [155]

Scaffold cytocompatibility

To assess toxicity and complete removal of the used chemicals during decellularization, the scaffolds were evaluated for their cytotoxicity with a methylthiazolyldiphenyltetrazolium bromide (MTT) assay. Bone-marrow derived mesenchymal stem cells (BMSCs) were isolated from bone marrow aspirates from patients undergoing total hip-replacement surgery (3 males, 67 ± 5 Y), with informed consent and approval of the Medical Ethics Committee (Albert

Schweitzer Hospital 2011/7). Cells were cultured at a density of 2300 cells/cm² at 37°C and 5% CO₂ in MEM- α , containing 10% FCS, 50 μ g/mL gentamicin, 1.5 μ g/mL Fungizone, 25 μ g/mL L-ascorbic acid 2-phosphate and 1 ng/mL basic Fibroblast Growth Factor 2 (bFGF2; R&D Systems, Minneapolis, USA), from now on referred to as 'MSC-expansion medium'. For toxicity tests, BMSCs were plated in a 24-well plate at a density of 40,000 cells/cm² and after 3 days of culture a decellularized cartilage scaffold was added to each well. Wells containing only medium or only BMSCs were included as controls. After 4 days, the cells and scaffolds were washed with PBS. Next, 5 mg/mL MTT-solution was added and incubated for 3 hours protected from light at 37°C and 5% CO₂. Finally, the scaffolds were removed from the wells and the MTT-solution was replaced with 100% ethanol (Boom, Meppel, the Netherlands), transferred to a 96-well plate and absorbance was measured at 670 and 570 nm on a VersaMax (Molecular Devices, Sunnyvale, USA). Toxicity experiments were conducted twice with independent BMSC and cartilage donors, with 3 decellularized bovine samples per cartilage type.

To further assess the interaction of cells with the decellularized cartilage scaffolds, BMSCs were seeded on the scaffolds by rotation in a tube rotator at 20 rpm (VWR, Radnor, Pennsylvania, USA) in 1.6 mL cell suspension containing $2 \cdot 10^6$ BMSCs/scaffold for 4 hours at 37°C. After seeding, the scaffolds were transferred to a 12-well plate (BD Biosciences) coated with 3% agarose (Eurogentec, Liège, Belgium) to prevent attachment of BMSCs to the culture well and cultured in 2 mL high glucose (4.5 g/L) Dulbecco's Modified Eagle Medium (DMEM-HG; Gibco) containing 50 μ g/mL gentamicin, 1.5 μ g/mL Fungizone, Insulin-Transferrin-Selenium (ITS+1, BD Biosciences, New Jersey, USA), 40 μ g/mL L-proline, 1mM sodium pyruvate (Gibco), 25 μ g/mL L-ascorbic acid 2-phosphate, 10 ng/mL Transforming Growth Factor beta 1 (TGF β 1; R&D Systems, Minneapolis, USA) and 10^{-7} M dexamethasone. To confirm the chondrogenic capacity of the seeded BMSCs, pellet cultures of 250,000 BMSCs/pellet were included as positive controls. Therefore, BMSCs were suspended at a density of $5 \cdot 10^5$ cells/mL. Aliquots of 0.5 mL cell-suspension were transferred into polypropylene tubes and pellets were formed by centrifuging at 200 G for 8 minutes. Negative controls included BMSCs cultured in monolayer in DMEM-HG containing 10% FCS, 50 μ g/mL gentamicin, 1.5 μ g/mL Fungizone and 25 μ g/mL L-ascorbic acid 2-phosphate in the absence of TGF β 1. Samples intended for gene-expression analysis and viability analysis were cultured for 21 days at 37°C and 5% CO₂ and medium was refreshed twice a week.

After culture, cell viability was evaluated with a LIVE/DEAD® assay (Invitrogen, Carlsbad, USA) according to manufacturer's instructions. Fluorescent imaging was performed on a Zeiss LSM 510 with the excitation laser set at 488 nm. A 505-530 nm band-pass filter was used to detect living cells and a 650 nm low-pass filter for detecting dead cells.

To assess the chondrogenic differentiation of the BMSCs cultured on the scaffolds, gene expression analysis was performed. RNA was isolated from the seeded scaffolds by snap freezing in liquid nitrogen followed by pulverization using a Mikro-Dismembrator (B. Braun Biotech International GmbH, Melsungen, Germany) at 2800 rpm. The tissue was homogenized with 18 μ L/mg sample RNA-Bee™ (Tel-Test Inc, Friendswood, USA) and 20% chloroform. RNA was isolated using the RNeasy Micro Kit (Qiagen, Hilden, Germany) according to manufacturer's instructions. Quantification of total extracted RNA was determined using a

NanoDrop ND-1000 spectrophotometer (Thermo Fisher Scientific Inc., Waltham, USA) at 260/280 nm. Next, complementary DNA (cDNA) was synthesized using the RevertAidTM First Strand cDNA Synthesis Kit (Fermentas GmbH, Leon-Rot, Germany) according to manufacturer's instructions. Finally, PCR analysis was accomplished with a Bio-Rad CFX96 Real-Time PCR Detection System using TaqMan[®] Universal PCR Master Mix (Applied Biosystems) or qPCRTM Mastermix Plus for SYBR[®] Green I (Eurogentec). Gene expression of collagen type II (*COL2A1*, Forward: GGCAATAGCAGGTTACGTACA; Reverse: CGATAACAGTCTTGCCCCACTT), SRY (sex determining region Y)-box 9 (*SOX9*, Forward: CAACGCCGAGCTCAGCA; Reverse: TCCACGAAGGGCCGC) and aggrecan (*ACAN*, Forward: TCGAGGACAGCGAGGCC, Reverse: TCGAGGGTGTAGCGTAGAGA) was evaluated. Glyceraldehyde-3-phosphate dehydrogenase (*GAPDH*, Forward: ATGGGGAAGGTGAAGGTCG; Reverse: TAAAGCAGCCCTGGTGACC), Beta-2-Microglobulin (*B2M*, Forward: TGCTCGCGCTACTCTCTCTT; Reverse: TCTGCTGGATGACGTGAGTAAAC) and hypoxanthine phosphoribosyltransferase 1 (*HPRT1*, Forward: TATGGACAGGACTGAACGTCTTG; Reverse: CACACAGAGGGCTACAATGTG), were used to determine a best-housekeeping-gene-index (BHKi) [211], which was used as reference for the expression of the genes of interest. The relative gene expression was calculated by the $2^{-\Delta CT}$ formula.

Statistics

The mean and standard deviation (SD) of the variables of interest were calculated using MS Excel 2013 and PASW Statistics 21.0 (SPSS Inc. Chicago, USA) for 3 independent bovine donors per cartilage type, with 6 samples per donor. For statistical evaluation, a mixed linear model was used followed by a Bonferroni's post-hoc comparisons test. Treatment and cartilage type were defined as fixed factors in the model, while donor was considered as a random factor. Linear regression analysis was performed to evaluate the relationship between amount of matrix components and biomechanical properties after decellularization. For analysis, the mechanical properties (i.e. σ_{max} , $t_{1/2}$ and E_{eq}) were defined as the dependent variables and matrix components (i.e. sGAG, collagen and elastin content) as independent variables. Differences in gene expression of the BMSCs seeded on decellularized cartilage scaffolds were determined by Mann-Whitney U-tests with the genes of interest (i.e. *SOX9*, *COL2A1* and *ACAN*) set as test variables. Differences between human decellularized and untreated cartilage samples for 1 donor in 6-fold, were determined by Mann-Whitney U-tests as well with the biochemical parameters (i.e. DNA, sGAG, collagen and elastin contents) as test variable. Differences were considered statistically significant for $p < 0.05$.

RESULTS

Decellularization of bovine ear cartilage

Bovine cartilage samples were decellularized according to the protocol of Kheir, *et al.*, [101] that was further optimized to specifically decellularize *bEC* by the addition of a treatment with a low concentration elastase solution. Bovine articular cartilage (*bAC*) samples were taken as controls, since AC decellularization has been performed by Kheir, *et al.* (Supplementary figure 2) After decellularization, *bEC* scaffolds and *bAC* control scaffolds retained their cartilage-like appearance, although samples seemed more translucent after the decellularization process. After decellularization, wet weight reduced by $26.1 \pm 4.9\%$ in *bEC* and an $8.4 \pm 2.6\%$ wet weight reduction was measured in *bAC*. The thickness of decellularized *bEC* scaffolds was significantly reduced ($p < 0.001$) by 23.5% (1.37 ± 0.32 mm) when compared to untreated *bEC* scaffolds (1.72 ± 0.40 mm), while no obvious reduction in sample diameter was observed. (Figure 1A).

To assess decellularization efficiency, cell content was analyzed histologically (H&E stain) and biochemically. DNA content was significantly reduced ($p < 0.001$) and undetectable (< 10 ng/sample) after decellularization, compared to untreated *bEC*. Similar results were obtained in the decellularized *bAC* control scaffolds; DNA was significantly reduced ($p < 0.001$) and undetectable after decellularization compared to untreated *bAC*. Histological analysis showed that the cell remnants were diminished after decellularization and those that were still present were clearly reduced in size and weakly stained for H&E. The ECM itself was weakly stained compared to the untreated scaffolds, although the overall structure of the ECM was virtually intact. (Figure 1B)

SEM analysis showed no obvious changes in the extracellular matrix after decellularization compared to untreated cartilage. The decellularized *bAC* and *bEC* scaffolds retained their dense matrix consistent of fine, intact collagen fibers similar to that of untreated cartilage. In untreated *bEC*, the thick elastic fibers were deeply embedded and intertwined within a homogeneous collagen network and this 3D organization was retained after decellularization. (Figure 1C)

Scaffold characterization

To characterize the matrix properties of the decellularized *bEC* scaffolds, the sGAG, total collagen and elastin contents were measured biochemically in addition to histological evaluation. The sGAG content of decellularized *bEC* scaffolds significantly reduced to 3% ($p < 0.001$) compared to untreated *bEC*, which was confirmed by histological analysis when stained for Safranin-O. The total collagen content of untreated *bEC* did not reduce after decellularization, but significantly increased ($p = 0.011$). This phenomenon appears to be due to the normalization of the collagen content to the sample wet weight, since wet weight was reduced after decellularization while the collagen content most likely did not. As sGAG content was strongly reduced by the decellularization procedure, the relative contribution of collagens to the overall wet weight increased, resulting in the observed increase in collagen content. Furthermore, immunohistochemical analysis confirmed the retention of collagen type II after decellularization. As for the retention of elastin, no statistical difference was

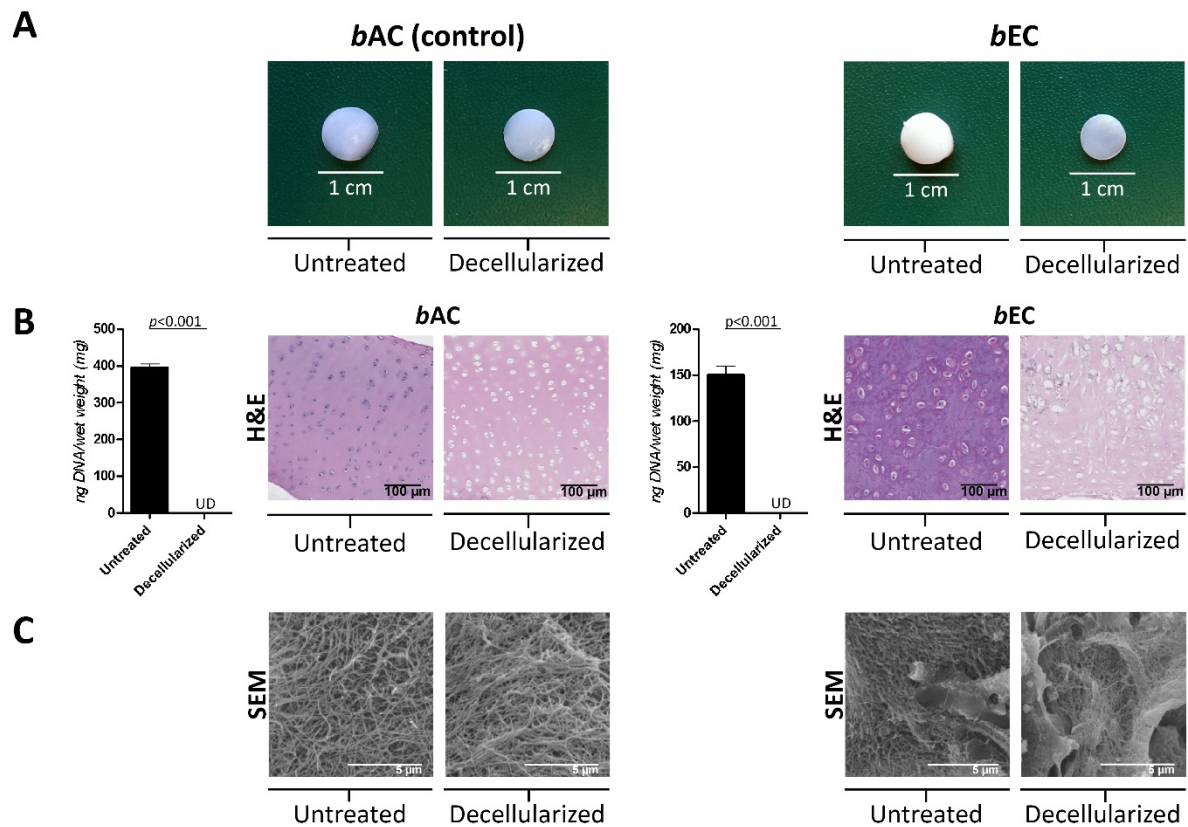


Figure 1. Morphological and cellular content of decellularized bovine cartilage.

(A) Photograph of cartilage samples (\varnothing 8 mm) before and after decellularization. **(B)** DNA content and histological H&E stain after decellularization show removal of nuclear materials and reduction in cell remnants. Data shown as mean \pm SD for 3 donors, 6 samples per donor. Histological images are representative for all donors. *bAC* = bovine articular ; *bEC* = bovine ear cartilage ; UD = Undetectable. **(C)** Scanning electron microscopy (SEM) shows a highly organized collagen network that remains intact after decellularization ($n=1$).

seen between the elastin content of decellularized *bEC* scaffolds compared to untreated *bEC* ($p=0.535$). Histological analysis revealed that after decellularization, elastin was mainly retained directly around lacunae when stained for RF. (Figure 2A)

The biomechanical properties of decellularized cartilage scaffolds were assessed using stress-relaxation-indentation. A statistically significant reduction of all compressive parameters was seen in decellularized *bEC* scaffolds compared to the untreated *bEC* samples ($p < 0.001$); Equilibrium modulus (E_{eq}) of the decellularized *bEC* scaffolds was 8.7% of the untreated *bEC* scaffolds. Similarly, maximum stress (σ_{max}) and relaxation half time ($t_{1/2}$) were reduced to 9.2% and 32% of the untreated values, respectively. Specifically, σ_{max} in the decellularized *bEC* scaffolds was 0.54 ± 0.36 MPa and 5.83 ± 2.18 MPa in untreated *bEC*. $t_{1/2}$ in the decellularized *bEC* samples was 0.74 ± 0.45 s. compared to untreated 2.31 ± 1.5 s. (Figure 2B) Similar changes in matrix integrity and viscoelasticity were seen in the control group consisting of decellularized *bAC* scaffolds. (Supplementary figure 2)

Linear regression analysis was used to correlate ECM components and biomechanical properties. R^2 -values showed that the sGAG, collagen and elastin content of the scaffolds were responsible for more than 50% of the biomechanical properties of decellularized cartilage

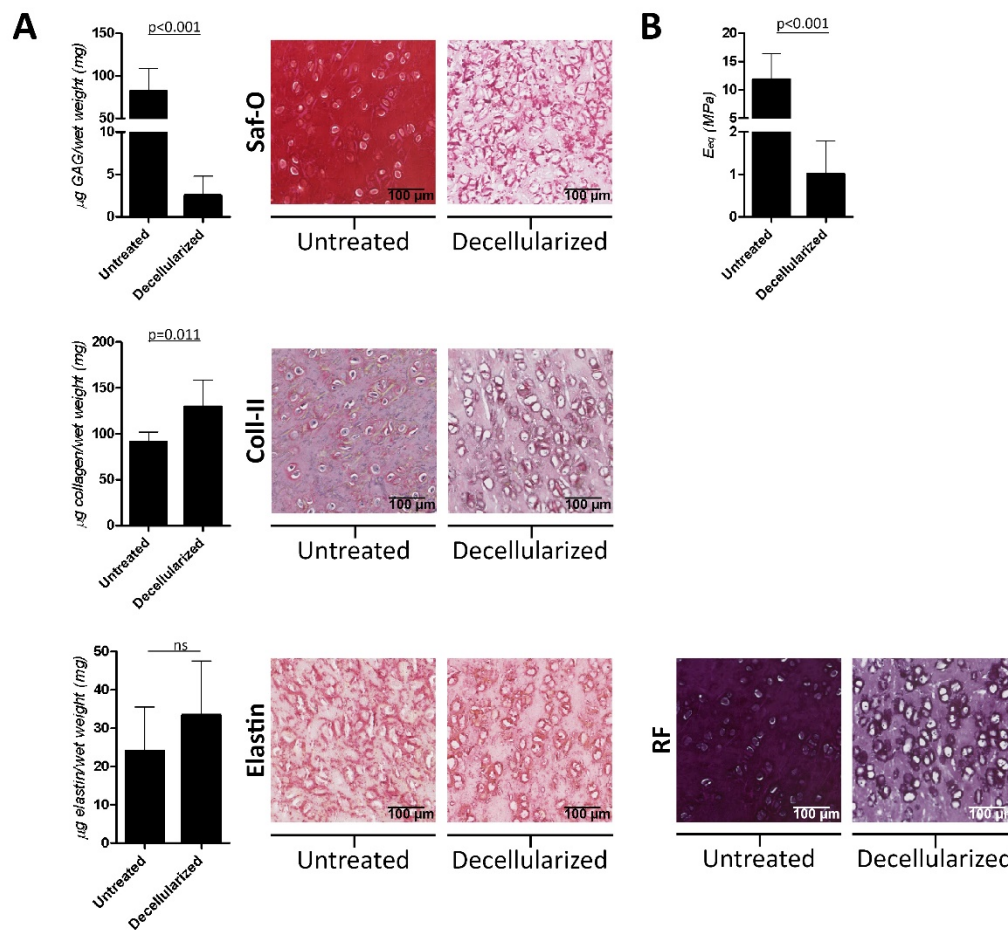


Figure 2. Matrix integrity and mechanical properties of decellularized bovine ear cartilage scaffolds.

(A) sGAG, collagen and elastin contents of untreated and decellularized bovine ear cartilage scaffolds. Less intense Safranin-O (Saf-O) staining confirmed sGAG reduction, while immunohistochemistry of collagen type II (Coll-II, counterstained with haematoxylin), elastin and resorcin fuchsin (RF) stain confirmed retention of these matrix components. Histological images are representative for all donors. **(B)** Equilibrium modulus after decellularization. Data shown as mean \pm SD for 3 donors, 6 samples per donor for sGAG and collagen analysis. Elastin data is shown as mean \pm SD for 2 donors, 6 samples per donor and missing values are excluded.

scaffolds: E_{eq} ($R^2 = 0.64$), $t_{1/2}$ ($R^2 = 0.51$) and σ_{max} ($R^2 = 0.618$). sGAG content was statistically significantly correlated to E_{eq} ($p = 0.002$), σ_{max} ($p = 0.005$) and $t_{1/2}$ ($p = 0.001$) of the decellularized *bEC* and *bAC* scaffolds.

Decellularized ear cartilage scaffolds are not cytotoxic and allow chondrogenic differentiation of human BMSCs

To assess the cytocompatibility of the *bEC* scaffolds, the metabolic activity of plated human BMSCs in the presence of decellularized *bEC* scaffolds was measured after 4 days of culture. No statistically significant effect on the metabolic activity of the BMSCs due to the decellularized scaffolds was found ($p = 0.559$). Relative to the control wells, $90.76 \pm 8.22\%$ of the cells were viable in the presence of a decellularized *bEC* scaffold, compared to the

conditions in the absence of a scaffold. This indicates that decellularized *bEC* scaffolds are non-cytotoxic and suitable for cell seeding.

To evaluate survival of human BMSCs in contact with decellularized *bEC* scaffolds, a LIVE/DEAD® assay was performed after 21 days of culture. Living BMSCs emitted a bright green fluorescence and showed a stretched morphology. Evaluation of z-stacks indicated that the seeded BMSCs were present on the surface of the scaffold. Unseeded, decellularized *bEC* scaffolds served as a control and no sign of living cells was observed in these controls. Histological sections showed that after 21 days, BMSCs were attached to the decellularized scaffolds, yet no migration into the scaffolds was observed. (Figure 3A)

Gene-expression analysis of *GAPDH*, *B2M* and *HPRT1*, confirmed the presence of BMSCs on decellularized *bEC* scaffolds after cell-seeding. In decellularized, non-seeded control scaffolds, the expression of either housekeeping gene was non-detectable (CT-values >40). The chondrogenic potential of BMSCs in pellet culture was confirmed by the expression of the chondrogenic-specific genes *SOX9*, *COL2A1* and *ACAN*, while low expression presented after culturing in monolayer (negative control). Gene expression levels after seeding and culturing on decellularized *bEC* scaffolds, were similar to pellet culture. This shows that decellularized *bEC* scaffolds support the retention of the chondrogenic capacity of human BMSCs *in vitro*. (Figure 3B)

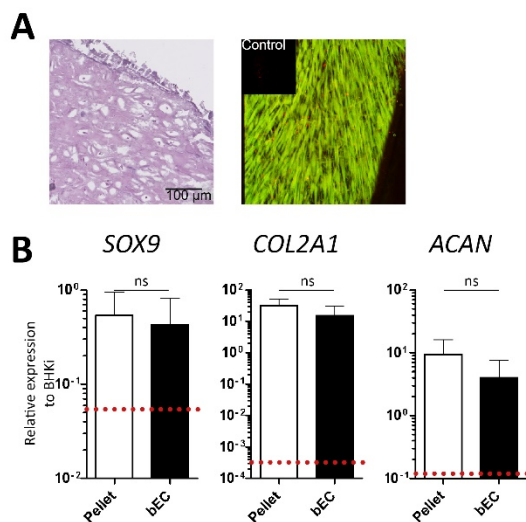


Figure 3. Decellularized cartilage supports chondrogenesis.

(A) H&E stain of decellularized ear cartilage scaffolds seeded with BMSCs shows attachment but limited migration (left). Fluorescent imaging (right) confirms viability after 21 days of culture. Images are representative for all samples. Control image consists of an unseeded, decellularized *bEC* scaffold. (B) Relative expression of the chondrogenic markers SRY (sex determining region Y)-box 9 (*SOX9*), Collagen type II (*COL2A1*) and aggrecan (*ACAN*) are similar to that of BMSCs in pellet culture (positive control). Dotted line represents the relative expression after culturing in monolayer (negative control). Data shown as mean ± SD for 1 donor in 6-fold, relative to the best housekeeper index (BHKi) determined by the expression of Glyceraldehyde-3-phosphate dehydrogenase (*GAPDH*), Beta-2-Microglobulin (*B2M*) and hypoxanthine phosphoribosyltransferase 1 (*HPRT1*).

Decellularization of human ear cartilage

To investigate the potential clinical implementation of a decellularized scaffold with desirable size and shape, human ear cartilage (*hEC*) was decellularized and characterized. On gross examination, the size and shape of the whole human ear was preserved after decellularization. (Figure 4A) The DNA content significantly reduced by 99.93% ($p=0.002$) after decellularization compared to untreated *hEC*. Staining for H&E revealed the removal of most nuclear material, with minimal disruption of the ECM structure. (Figure 4B) sGAG and elastin contents were significantly reduced in the decellularized *hEC* scaffolds by 75.3% ($p=0.002$) and 48.8% ($p=0.010$), respectively. No statistically significant reduction was seen in the total collagen content ($p=0.180$) after decellularization and histological staining of the decellularized *hEC* scaffolds confirmed the biochemical analysis. (Figure 4C) The Eeq of the *hEC* scaffolds was 2.51 ± 1.26 MPa after decellularization and high magnification SEM of the decellularized *hEC* scaffolds showed a dense collagen matrix intertwined with thick elastic fibers. (Figure 4D)

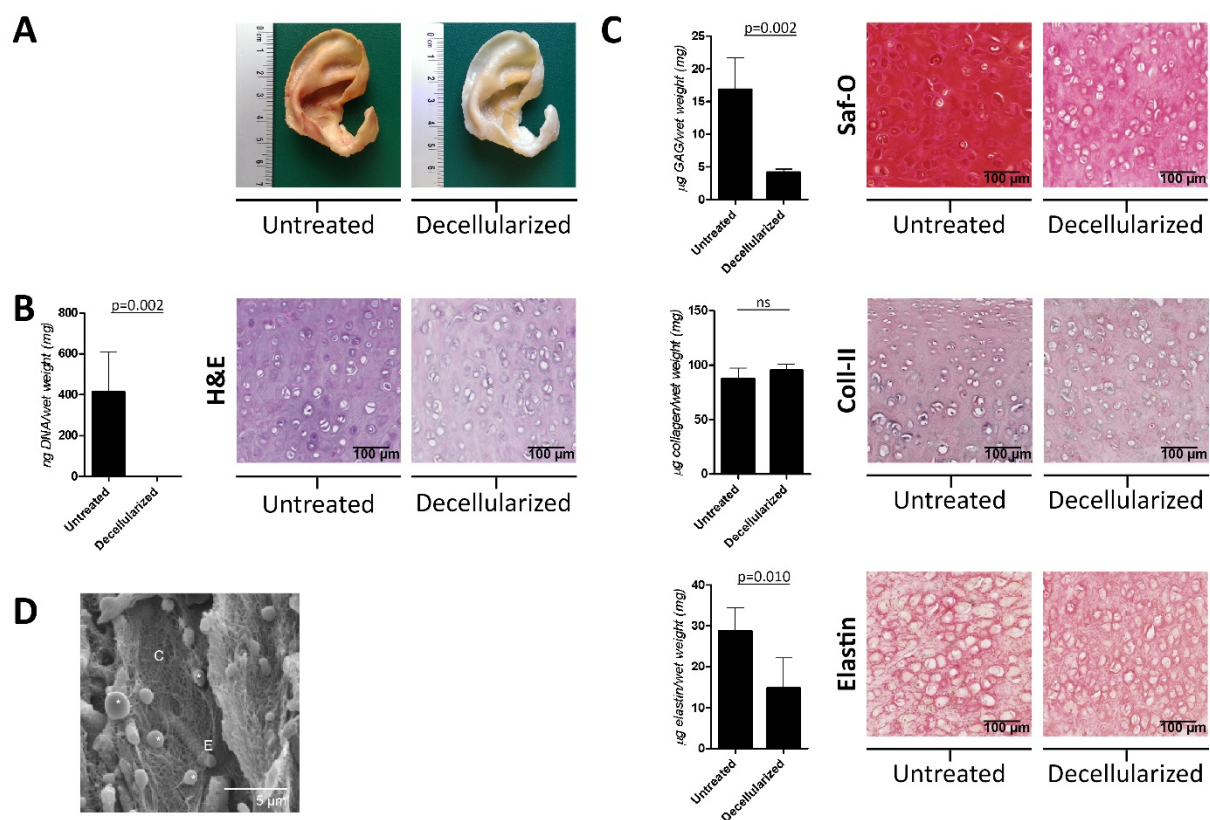


Figure 4. Human ear cartilage decellularization.

(A) The size and shape of a whole human ear is preserved after decellularization. (B) DNA was statistically significantly reduced after decellularization and a reduction in cell remnants is seen on histology (H&E stain). (C) sGAG, collagen and elastin contents of untreated and decellularized human ear cartilage. Histological stains confirm the findings. Data shown as mean \pm SD for 1 donor in 6-fold. (D) High magnification scanning electron microscopy (SEM) of decellularized ear cartilage shows thick elastic fibers deeply embedded in a complex collagen network ($n=1$). C = Collagen ; E = Elastin ; * = cross-section of transected elastic fibers.

DISCUSSION

For successful cartilage regeneration 3D-scaffolds are crucial. We were able to obtain decellularized bovine and human scaffolds from whole full-thickness ear cartilage (EC) tissue. These scaffolds preserved their native collagen and elastin contents, as well as their major architecture and shape. Furthermore, these decellularized EC scaffolds were non-cytotoxic and have the capacity to allow chondrogenic differentiation of human BMSCs *in vitro*.

To date, decellularized scaffolds are extensively used for the reconstruction of various tissues and organs. [293] In addition, several cartilaginous structures have been decellularized. These studies, however, mainly focus on hyaline (i.e. articular cartilage, nasal cartilage, tracheal cartilage) or fibrous (i.e. meniscal cartilage, annulus fibrosis) cartilaginous tissues. Other cartilage decellularization techniques described in literature are the fabrication of decellularized ECM-derived scaffolds, by either pulverizing cartilage tissue [290, 291] or stacking thin cartilage slices. [294] Although these seem effective methods to decellularize the tissue, its major drawback is that it completely disrupts the native tissue architecture and/or shape. In fact, no method to specifically decellularize full thickness EC has been described in literature yet. This study is the first to evaluate structural and functional properties of decellularized full-thickness EC scaffolds of both bovine (*bEC*) and human (*hEC*) origin.

Various decellularization protocols are proposed for cartilaginous tissues, each aiming to maximize the decellularization effect, while reducing any adverse effect of the process on the structural composition and functionality of the remaining ECM. Therefore, decellularization outcome was evaluated based on: (1) the removal of cellular material and (2) matrix integrity which was characterized by its components, architecture and biomechanical properties. First, removal of native cellular material is highly imperative, as it reduces the possibility of an immune reaction in case of *in vivo* implantation. For this reason, one of the criteria for successful decellularization is to reduce the DNA content to less than 50 ng/mg tissue. [295] Unfortunately, most recently developed decellularization protocols for cartilage do not meet this requirement at all [100, 105]. Decellularized cartilage scaffolds still show distinct cell remnants on histological examination [94-96, 99-101, 104, 105, 296-299] or need multiple decellularization cycles to remove nuclear material, [101, 299] leading to further degradation of the ECM. To specifically decellularize EC, the samples were decellularized according to the protocol of Kheir *et al.* [101] which was further optimized to ensure the decellularization outcome was satisfactory for EC and cell remnants reduced. The incorporation of an additional 24 hour incubation with a low concentration of elastase (0.03 U/mL), enabled the removal of nuclear material and a reduction of cell remnants in decellularized *bEC* scaffolds and near-complete removal in decellularized full size human ear cartilage scaffolds. It should be noted though, that the 10 ng detection limit of the DNA assay, concerns a fraction of papain digest used in the DNA assay (50 μ L). Because the DNA content was undetectable in that fraction of the decellularized *bEC* scaffolds, it is reasonable to assume that DNA was removed from the entire scaffolds after decellularization.

Second, the balance between the removal of nuclear material and preserving the matrix integrity should be considered carefully. We showed that the decellularized EC scaffolds preserved their native collagen and elastin contents, as well as their major architecture and shape, while sGAG content significantly decreased during the process.

Collagen, the most abundant protein present within the ECM, is of major importance, providing mechanical strength and guiding chondrogenic differentiation. [300] Additionally, the number of collagen cross-links contributes to the mechanical properties of newly formed cartilage. [301] Naturally, we expect these cross-links to be greater in scaffolds derived from native cartilage, than in synthetic scaffolds or ECM-derived scaffolds. Therefore, the retention of collagen during decellularization is crucial. Although collagen type I-elastin-GAG scaffolds were produced before [302], the dense elastic network that is interspersed with the collagen fibrils is not as highly organized as that of native ear cartilage [164, 303], while high magnification SEM showed that the decellularized EC retained the complex interaction between the elastic fibers and fine collagen network. Following decellularization, sGAG content decreased significantly which corresponds with previously reported findings by others [100, 101] and was most likely caused by the SDS-treatment during decellularization. Consequently with the sGAG reduction, the viscoelastic material properties of the decellularized EC scaffolds also reduced, which is in agreement with findings previously reported by others. [304] Depletion of sGAGs might be required to allow cells and cell residuals to leave the matrix. [305] Depending on the eventual application of the scaffold, sGAG depletion might also improve ingrowth of cells with chondrogenic capacity into the scaffold and thereby allowing matrix remodeling and revitalization of the graft.

To completely assess functionality of the decellularized scaffold, mechanical properties were evaluated, since it should provide sufficient mechanical strength to compensate for that of the damaged tissue. After decellularization, biomechanical properties reduced significantly. Nevertheless, the decellularized *bEC* scaffolds presented superior mechanical properties compared to that of other commonly used natural or synthetic biomaterials for cartilage TE. For instance, low equilibrium moduli were found by unconfined compression in various hydrogels; maximum E_{eq} of 0.03 MPa in 2% alginate constructs [210], 0.3 MPa in 20% polyethylene glycol and 0.5 MPa in 15% agarose [306], showing that these hydrogels only reach a maximum of 50% of the E_{eq} of our decellularized EC scaffolds. Additionally, the E_{eq} of synthetic co-polymer scaffolds was 0.05-0.25 MPa [307], which was only 5.5-25% found in our decellularized *bEC* scaffolds.

To assure long lasting properties and fully functional cartilage, eventual revitalization of the scaffold is a requirement. It is therefore important that we can prepare scaffolds that are non-cytotoxic after decellularization so cells can attach and survive. We showed that our decellularized scaffolds were non-cytotoxic and the seeded BMSCs were still viable after 21 days of culture. Furthermore, the scaffold allowed chondrogenic differentiation of BMSCs. We have used BMSCs in this work to evaluate the cell supportive capacity of our scaffold, the final choice of cell sources would mainly depend on the application and could be any cell with chondrogenic potential such as chondrocytes, perichondrium cells or adipose derived mesenchymal stem cells. [40, 54] Moreover, it would not be unlikely that seeding prior to implanting a decellularized scaffold is required, as it is the scaffold that could provide support for cells present at the implantation site to grow in. To revitalize and remodel the matrix, migration of cells throughout the matrices needs to be further optimized. In this respect, the reduction of sGAGs in the decellularized scaffolds will be advantageous [305], since it has been reported that chondrocyte adhesion is prevented by sGAGs. [308] Given that cell adhesion is

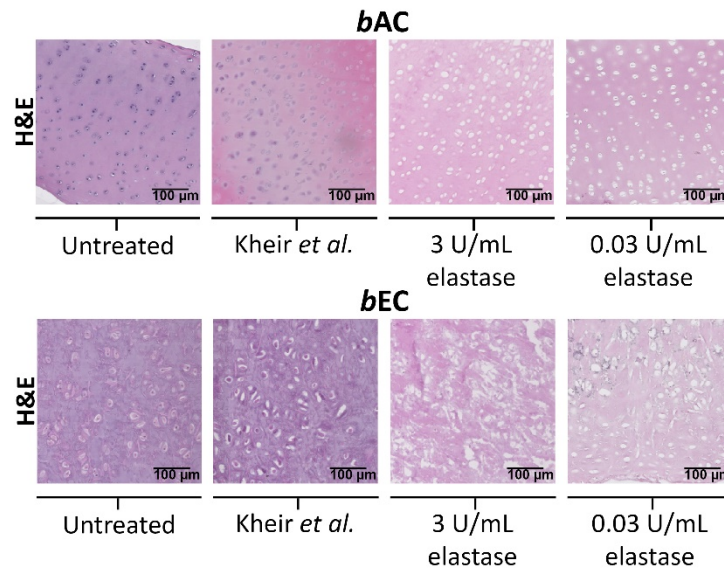
essential for cell migration, partial or even complete depletion of sGAGs could be beneficial to realize cartilage revitalization, as it has been shown that chondrogenic progenitor cells possess the capacity to migrate through degraded cartilage and repair ECM. [309] This indicates that optimization of cell migration could lead to matrix synthesis and restored biomechanical properties of the revitalized cartilage. Recovery of biomechanical properties due to matrix deposited by cells was previously seen by Reiffel *et al.* [160], who reported *de novo* cartilage deposition and a 30-fold increase in Eeq 3 months after *in vivo* implantation of a collagen type I hydrogel. This showed that the biomechanical properties returned to the native situation.

Finally, the decellularized *hEC* scaffolds and whole human ear preserved their size and shape after decellularization. Also, approximately 25% more sGAGs were retained than in the decellularized *bEC*. The maturity of the *hEC* matrix might cause better retention of sGAG. In human ears, the ECM components and especially elastic fibers structurally change over the years. [164] When stained for elastin, the elastic fibers in our *bEC* are mainly directly located as a band around the lacunae whereas in *hEC*, this network extends more into the ECM, confirming what is shown previously by Ito *et al.* [164] This difference in elastic fibers in adult cartilage, could have protected the ECM from degradation during decellularization. Importantly, this retention was also reflected in the Eeq of the *hEC* scaffolds, which was not reduced compared to that of native *hEC* (3.3 ± 1.3 MPa for Eeq) measured in our previous work. [155] This shows that the decellularization process can also be translated to human tissue and provides the possibility to use decellularized ear cartilage as an improved reconstruction strategy.

In conclusion, decellularization can provide scaffolds made of natural materials, even allogeneic or xenogeneic, for reconstruction of defects in cartilaginous structures. We have prepared decellularized ear cartilage scaffolds with an architecture and matrix composition that closely resembles native cartilage and that have the capacity to support chondrogenic differentiation of BMSCs. Furthermore, the translation of the decellularization method to whole human ear cartilage shows the possibility to use decellularization as an improved reconstruction strategy for large cartilage defects that hold complex shapes. In order to implement the method as a clinical treatment, long term *in vivo* studies should be conducted to assess the scaffold functionality and characteristics after implantation.

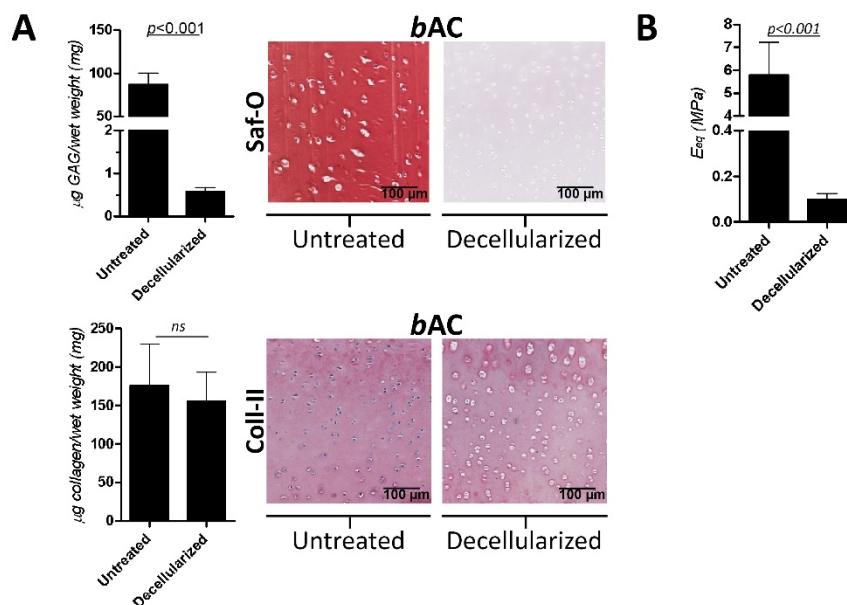
Acknowledgements

The authors would like to thank Prof. dr. Gert-Jan Kleinrensink (dept. of Neurosciences and Erasmus MC SkillsLab) and Cornelia Schneider (LBI/Red Cross Blood Transfusion Service of Upper Austria) for providing human cartilage. Thanks to Marcel Vermeij (dept. of Pathology, Erasmus MC) for his help with the RF stain, dr. Gert-Jan Kremers (Optical Imaging Centre, Erasmus MC) for his help with fluorescent imaging, Prof. dr. Heinz Redl (LBI for Experimental and Clinical Traumatology) for his comments on the manuscript. And finally, the authors would like to thank Mairéad Cleary (dept. of Orthopaedics, Erasmus MC/University College Dublin) for thoroughly reading the manuscript and providing constructive comments. This study was partially supported by the FFG-Bridge grant CartiScaff (842455).



Supplementary figure 1. Optimization of the decellularization protocol for ear cartilage.

The protocol of Kheir *et al.* [101] was optimized by the incorporation of a low dose elastase to specifically decellularize full thickness ear cartilage, since decellularization outcome was not satisfactory as cell remnants remained clearly visible on histological examination (haematoxylin and eosin stain). A high concentration of elastase (3 U/mL) resulted in complete disruption of the matrix and complete removal of cell remnants. A low concentration elastase (0.03 U/mL) preserved the matrix to a greater extent, while allowing for a clear reduction in cell remnants.



Supplementary figure 2. Matrix integrity and mechanical properties of bovine articular cartilage scaffolds.

Bovine articular cartilage samples were decellularized and included as controls to compare decellularization outcome. **(A)** sGAG content reduced while collagen content was retained. Histological images are representative for all donors. Saf-O = Safranin-O ; Coll-II = collagen type II (counterstained with haematoxylin). **(B)** Equilibrium modulus after decellularization. Data shown as mean \pm SD for 3 donors, 6 samples per donor.

Chapter 8

Novel bilayer bacterial nanocellulose scaffold supports neocartilage formation *in vitro* and *in vivo*

H. Martínez Ávila, E. Feldmann, M.M. Pleumeekers, L. Nimeskern, W. Kuo, W.C. de Jong, S. Schwarz, R. Müller, J. Hendriks, N. Rotter, G.J.V.M. van Osch, K.S. Stok, P. Gatenholm

Biomaterials, 2015. 44: p. 122-33.

ABSTRACT

Tissue engineering provides a promising alternative therapy to the complex surgical reconstruction of auricular cartilage by using ear-shaped autologous costal cartilage. Bacterial nanocellulose is proposed as a promising scaffold material for auricular cartilage reconstruction, as it exhibits excellent biocompatibility and secures tissue integration. Thus, this study evaluates a novel bilayer bacterial nanocellulose scaffold for auricular cartilage tissue engineering. Bilayer bacterial nanocellulose scaffolds, composed of a dense nanocellulose layer joined with a macroporous composite layer of nanocellulose and alginate, were seeded with human nasoseptal chondrocytes and cultured *in vitro* for up to 6 weeks. To scale up for clinical translation, bilayer bacterial nanocellulose scaffolds were seeded with a low number of freshly isolated (uncultured) human nasoseptal chondrocytes combined with freshly isolated human mononuclear cells from bone marrow in alginate and subcutaneously implanted in nude mice for 8 weeks. 3D morphometric analysis showed that bilayer bacterial nanocellulose scaffolds have a porosity of 75% and mean pore size of 50 ± 25 μm . Furthermore, endotoxin analysis and *in vitro* cytotoxicity testing revealed that the produced bilayer bacterial nanocellulose scaffolds were non-pyrogenic (0.15 ± 0.09 EU/ml) and non-cytotoxic (cell viability: $97.8 \pm 4.7\%$). This study demonstrates that bilayer bacterial nanocellulose scaffolds offer a good mechanical stability and maintain a structural integrity while providing a porous architecture that supports cell ingrowth. Moreover, bilayer bacterial nanocellulose scaffolds provide a suitable environment for culture-expanded NCs as well as a combination of freshly isolated nasoseptal chondrocytes and mononuclear cells to form cartilage *in vitro* and *in vivo* as demonstrated by immunohistochemistry, biochemical and biomechanical analyses.

INTRODUCTION

Serious auricular defects such as anotia and microtia, along with auricle damage caused by cancer and trauma, demand an effective treatment for auricular cartilage reconstruction. For such cases, the field of tissue engineering (TE) provides a promising potential alternative therapy to the conventional and complex surgical reconstruction of auricular cartilage by using ear-shaped autologous costal and nasoseptal cartilage [124, 310, 311]. Bacterial nanocellulose (BNC), a novel biomaterial with excellent biocompatibility and remarkable tissue integration capability [312-316], has been evaluated for several TE strategies and has shown to support adhesion, proliferation and differentiation of different cell types [317-323]. BNC is a natural biopolymer synthesized by various bacteria species, particularly *Gluconacetobacter xylinus* [90, 324]. Its three-dimensional (3D) and interconnected network is composed of highly hydrated nanofibrils ranging from 70 to 140 nm in width, similar to collagen fibrils found in extracellular matrix (ECM) of several tissues, with high tensile strength [319, 325]. BNC is considered a hydrogel since it is mostly composed of water in its native state (99%). All together, these outstanding properties make BNC an exceptional biomaterial for many biomedical applications [326-328], including auricular cartilage reconstruction [316, 322, 329].

Although several groups have attempted to engineer auricular cartilage [124], few successful outcomes have been reported [330-332]. Development of artificial auricular grafts with adequate mechanical properties has been identified as a key factor for successful auricular cartilage TE [333]. Most studies that have used biodegradable scaffold materials have resulted in poor structural integrity (i.e. shape and size stability) of the auricular scaffold after implantation; caused by the short-lived chemical and mechanical stability [136, 334-337]. On the other hand, recent studies that have investigated the use of non-degradable biomaterials for auricular cartilage reconstruction have reported a better structural integrity of the implant [330, 332, 338] - likely caused by the chemical stability of the support biomaterial, which translates into long-lasting mechanical properties even after implantation. As opposed to the many biodegradable scaffolds previously evaluated for auricular cartilage TE, the long-term structural integrity of BNC scaffolds should not be compromised after implantation since humans do not produce enzymes capable of breaking down cellulose [339]. Besides being a chemically stable material, BNC with increased cellulose content of 17% (densified hydrogel) is a competitive scaffold material for repair, reconstruction or regeneration of auricular cartilage since it matches the elastic mechanical properties (e.g. equilibrium modulus) of human auricular cartilage [329], can be fabricated in patient-specific auricular shapes [340] and exhibits excellent biocompatibility *in vivo* - causing a minimal foreign body response [316].

When densified, BNC hydrogel is a mechanically and biologically appropriate biomaterial for use in auricular cartilage reconstruction [316, 329]. However, its dense nanocellulose network prevents cells from penetrating the material. To circumvent this problem, several techniques have been developed to support cell ingrowth in BNC scaffolds by tuning pore size and pore interconnectivity during biosynthesis of BNC [341], via laser ablation [318] and freeze-dry processing [342, 343]. Such macroporous BNC scaffolds have been shown to provide an adequate environment that supports ingrowth and differentiation

of chondrocytes. For example, human primary articular, auricular and nasoseptal chondrocytes cultured in macroporous BNC scaffolds *in vitro* have been shown to adhere, migrate, proliferate and maintain their chondrogenic phenotype - as confirmed by the synthesis of cartilage-specific ECM [322, 343, 344].

Engineering stable and functional auricular cartilage tissue also depends on the cell source used. Pleumeekers *et al.* showed that human auricular and nasoseptal chondrocytes possess a high chondrogenic capacity *in vivo*, making them attractive cell sources for auricular cartilage repair [345]. The use of cells in cartilage repair is an attractive strategy as it may result in regeneration of the lost tissue. However, the clinical application of a cell-aided treatment does feature challenges – a limited supply of autologous chondrocytes with the proper phenotype being the most stringent one. To cancel out cell culture, including the concomitant laboratory logistics and the double surgery, autologous cells should be isolated within the operating room and applied directly. In addition, the combination of chondrocytes with a less limited source of autologous cells, such as bone marrow mononuclear cells (MNCs), can overcome the challenge of having too few cells and may even increase the treatment's performance [346, 347]. By resuspending the cells in alginate, also the factor of cell loss after scaffold seeding can be diminished whilst simultaneously providing the cells with a 3D environment to suppress dedifferentiation [348].

Several studies that have evaluated BNC as a scaffold material for auricular cartilage TE [316, 322, 329, 343] have contributed to the design and development of BNC scaffolds with a two-layer (bilayer) architecture. This study investigates the *in vitro* and *in vivo* performance of bilayer BNC scaffolds, composed of a dense nanocellulose layer joined with a macroporous composite layer of nanocellulose and alginate, designed to be mechanically stable and maintain a long-term structural integrity while providing a porous architecture that supports cell ingrowth and neocartilage formation. Moreover, this study explores the application of a clinically relevant strategy by seeding a low number of freshly isolated (uncultured) human chondrocytes combined with freshly isolated human MNCs, in order to test the translation of this auricular cartilage TE technology to the clinic.

MATERIALS AND METHODS

Chemicals were obtained from Sigma-Aldrich, USA unless stated otherwise.

Fabrication and purification of bilayer BNC scaffolds

Production of dense and porous scaffold layers

BNC hydrogel disks with increased cellulose content (i.e. dense layer) were produced and purified as described elsewhere [316]. Briefly, a suspension of *Gluconacetobacter xylinus* (ATCC[®] 700178, LGC Standards, Sweden) was inoculated in 250 ml conical flasks containing sterile culture medium (described by Matsuoka *et al.* [349]) and cultured at 30°C for 18 days, until large BNC cylinders (Ø 48 mm × 20 mm) were biosynthesized. The BNC cylinders were purified in a built-in-house perfusion system and compressed to 1 mm in height to increase the cellulose content. The compressed BNC pellicles were frozen to -80°C overnight and lyophilized (Heto PowerDry PL3000, Thermo Fisher Scientific, MA, USA) for 3 days. Dense BNC disks (Ø 8 mm × 1 mm) were then cut with a sterile biopsy punch (Miltex GmbH, Germany). The criterion for selecting the thickness of the dense BNC layer is based on morphometric analysis from MRI scans of human auricular cartilage, where Nimeskern *et al.* reported a cartilage thickness of 1.15 ± 0.10 mm [350].

BNC/alginate composite scaffolds (i.e. porous layer) were fabricated by a freeze-drying process. First, purified BNC pellicles were homogenized with a blender, until a pulp consistency was obtained, and then with a dispersing element (S25N-18G, IKA, Germany) at 25,000 rpm for 20 minutes. Afterwards, the homogenized BNC suspension was steam sterilized (100 kPa, 121°C for 20 minutes) and the cellulose content was determined using a halogen moisture analyzer (HB43, Mettler-Toledo, OH, USA). The following steps were carried out in sterile conditions. The BNC suspension was mixed with 1.1% w/w clinical grade alginate dissolved in 0.9% NaCl (CellMed AG, Germany) to get a final composition of 90% dry weight BNC and 10% dry weight alginate compared to the total dry weight. The weight of alginate solution (W_{Alg}) added to a known weight of BNC suspension (W_{BNC}) was calculated by using the formula: $W_{Alg} = W_{BNC} \times (\%DW_{Alg} \div \%DW_{BNC}) \times (\%CC_i \div \%AC_i)$. Where $\%DW_{Alg}$ and $\%DW_{BNC}$ are the targeted percent dry weight of alginate (10%) and BNC (90%) compared to the total dry weight; and $\%CC_i$ and $\%AC_i$ are the initial cellulose and alginate concentrations. The BNC/alginate mixture was then dispersed at 25,000 rpm for 15 minutes, transferred to sterile containers (TP52, Gosselin, France) and degased in a vacuum desiccator. The containers were then placed inside Nalgene[®] cryo freezing containers (Thermo Fisher Scientific) and frozen to -80°C overnight at a rate of 1°C/min. The frozen BNC/alginate mixtures were lyophilized for 5 days to sublimate the ice crystals, creating a macroporous architecture. The dry BNC/alginate sponges were then sliced to 2 mm-thick slices and porous BNC/alginate composite scaffolds (Ø 8 mm × 2 mm) were cut with a sterile biopsy punch (Miltex GmbH).

Fabrication of bilayer BNC scaffolds

A novel cellulose solvent system (i.e. ionic liquid EMIMAc) was used to attach the dense and porous layers and achieve a strong interfacial molecular bonding between the layers. The following steps were carried out in sterile conditions. First, dry homogenized BNC was

dissolved in ionic liquid 1-ethyl-3-methylimidazolium acetate (EMIMAc) at a concentration of 10 mg/ml. The cellulose solvent solution was preheated to 80°C and then smeared on the dense BNC layers. Subsequently, the porous layers were aligned on top of the dense layers and the bilayer BNC scaffolds were placed on a heating plate at 80°C for 2 minutes to accelerate the dissolution of nanocellulose at the interface. The bilayer BNC scaffolds were then stabilized in 100 mM CaCl₂ in ethanol to precipitate the dissolved cellulose between the layers (i.e. attach the layers), while simultaneously crosslinking the alginate to bind the BNC in the porous layer. The scaffolds were then rehydrated and washed in non-pyrogenic conical tubes (TPP, Switzerland) with endotoxin-free water (HyClone™ cell culture-grade water, Thermo Fisher Scientific) supplemented with 20 mM CaCl₂ to remove residuals of the ionic liquid EMIMAc and endotoxins. The scaffolds were purified under orbital motion (320 rpm) at 37°C for 14 days, during which the endotoxin-free water and conical tubes were changed every second or third day. Subsequently, the bilayer BNC scaffolds (Ø 8 mm × 3 mm) were steam sterilized (as described above) in endotoxin-free water and stored until use at 4°C.

Characterization of bilayer BNC scaffolds

The morphology of bilayer BNC scaffolds was characterized by scanning electron microscopy (SEM) and micro-computed tomography (microCT). Moreover, the purity of the bilayer BNC scaffolds was analyzed throughout the purification process by bacterial endotoxin testing, infrared spectroscopy analysis and *in vitro* cytotoxicity testing.

Scanning electron microscopy

Samples were lyophilized (as described previously), thereafter sputter coated with a gold film and analyzed using a Leo Ultra 55 field emission gun SEM (Carl Zeiss, Germany).

Micro-computed tomography

Bilayer BNC scaffolds ($n=3$) were incubated in 0.1 M CaCl₂ solution at room temperature overnight and subsequently quenched in liquid nitrogen and lyophilized for 24 hours. The dry scaffolds were scanned with microCT (µCT50, Scanco Medical AG, Switzerland) at 45 kVp and 1 µm nominal resolution. The internal microstructure of the porous layer was then segmented automatically using a constrained Gaussian filter to suppress noise and a global threshold (25% of maximal grayscale value). 3D morphometric parameters such as scaffold porosity (Sc.Po), volume-weighted mean pore size (Pore.Th), scaffold wall thickness (Wall.Th), and scaffold wall number (Wall.N) were calculated using the manufacturer's morphometry software (IPL, Scanco Medical AG) according to the guidelines established for the assessment of bone microstructure. [351]

Bacterial endotoxin testing

Endotoxin extraction from the bilayer BNC scaffolds was done in accordance to the international standard ISO 10993-12:2009 (Sample preparation and reference materials). After 14 days of purification, bilayer BNC scaffolds ($n=3$) were weighed and placed in depyrogenated sample containers (Lonza, Belgium). Endotoxin-free water was added to the containers using the ratio of 0.1 grams of BNC/ml of extraction medium. The extraction was

done at $37 \pm 1^\circ\text{C}$ for 72 ± 2 hours under orbital motion at 160 rpm. Endotoxin analysis was performed with the PyroGeneTM Recombinant Factor C assay by Lonza. This assay has a minimum detection limit of 0.005 Endotoxin Units (EU) per milliliter. According to the USA Food and Drug Administration [352], endotoxin levels in medical devices are not to exceed 0.5 EU/ml or 20 EU/device [352].

Attenuated Total Reflectance Fourier Transform Infrared spectroscopy

Removal of EMIMAc residues from the bilayer BNC scaffolds was analyzed with Attenuated Total Reflectance Fourier Transform Infrared (ATR-FTIR) spectroscopy. Samples ($n=2$ per group) were freeze-dried after day 1, 7 and 14 of purification. The porous layer was removed from the bilayer BNC scaffolds to expose the interface. This interface, visible on the dense BNC layer, was analyzed with a single reflection ATR accessory fitted with a monolithic diamond crystal (GladiATRTM, Pike Technologies, WI, USA). The sample was placed on the small crystal area and a force was applied on the sample to push it onto the diamond surface. ATR-FTIR spectroscopy measurements were made with a System 2000 FT-IR spectrometer (PerkinElmer, MA, USA) in the mid-infrared region, 4000 to 400 cm^{-1} . 20 scans were taken with a resolution of 4 cm^{-1} . Pure EMIMAc solution and pure dried BNC films were used as controls.

In-vitro cytotoxicity testing

Removal of EMIMAc residues from the bilayer BNC scaffolds was also evaluated by *in vitro* cytotoxicity testing, according to the international standard ISO 10993-5:2009. Bilayer BNC scaffolds ($n=4$ per time point) were incubated in growth medium (RPMI 1640 medium supplemented with 1% fetal bovine serum (FBS), and antibiotics (100 U/ml penicillin and 100 $\mu\text{g/ml}$ streptomycin); Biochrom, Germany) for 24 hours to extract potential cytotoxic residues. All incubations were done in standard culture conditions (37°C , 5% CO_2 and 95% relative humidity). Meanwhile, sensitized L929 cells (ACC 2, DSMZ, Germany) were seeded in 96-well cell culture plates (1.0×10^4 cells per well) and incubated for 24 hours to allow cell adhesion. The medium was removed and 100 μl of extract or control solutions was added to each well and incubated for 24 hours. Cell culture inserts (ThinCertTM, Greiner BioOne, Germany) incubated in growth medium served as negative control ($n=8$), while 10% dimethylsulfoxide in growth medium served as positive control ($n=8$). After 24 hours of incubation in extract or control solutions, the medium was removed, 100 μl medium were mixed with 20 μl of CellTiter 96[®] AQueous one solution reagent (Promega, WI, USA) MTS and added to each well, followed by incubation for 2 hours at 37°C . Growth medium with reagent solution (without cells) served as blank ($n=8$). After incubation with the reagent, absorbance was measured photometrically (Infinite M200 Pro, Tecan AG, Switzerland) at a wavelength of 490 nm and a reference wavelength of 680 nm. The average absorbance value of the negative control was used to compute the cell viability, where the negative control was regarded as 100% viability. The cytotoxic potential of the test samples was classified as highly cytotoxic when cell viability was below 50%, slightly cytotoxic when it was between 51% and 70% and non-cytotoxic when cell viability was above 71%.

Cell study I: performance of bilayer BNC scaffolds *in vitro*

Isolation and expansion of human nasoseptal chondrocytes

Nasoseptal cartilage was obtained from 1 female patient (19 years) undergoing routine reconstructive septorhinoplasty at the Department of Otorhinolaryngology of Ulm University Medical Center (Ulm, Germany), as waste material after surgery, with approval of the local medical ethics committee (no. 152/08). The isolation of nasoseptal chondrocytes (NC) from the cartilage was done by enzymatic digestion of the tissue with 0.3% type II collagenase (Worthington Biochemical, NJ, USA) in growth medium (DMEM/Ham's F-12 supplemented with 10% FBS and 0.5% gentamycin; Biochrom) for 16 hours at 37°C under agitation. Cells were separated by filtration through a 100-µm cell strainer and resuspended in growth medium. Subsequently, cell viability was determined using trypan blue staining and NCs were seeded in culture flasks at a density of 5,000 cells/cm² for expansion in monolayer culture. Once a cell confluence of about 85% was reached, the cells were trypsinized and cryopreserved.

Cell culture of human chondrocytes in bilayer BNC scaffolds

NCs were thawed and expanded one time in growth medium as described above. Once sub-confluent, cells were detached and resuspended in differentiation medium (NH ChondroDiff Medium; Miltenyi Biotec, Germany) supplemented with 0.5% gentamycin. Prior to cell seeding, bilayer BNC scaffolds ($n=30$) were incubated in differentiation medium for 24 hours. The medium was discarded and 50 µl of cell suspension containing 1.0×10^6 cells was seeded into the porous scaffold layer (10,000 cells/mm³). Cells were allowed to attach to the scaffolds for 4 hours in standard culture conditions (37°C, 5% CO₂ and 95% relative humidity), before transferring the seeded scaffolds to differentiation medium. Cell-seeded bilayer BNC scaffolds were cultured for up to 6 weeks and the medium was changed twice a week.

Histological and immunohistochemical analyses

During the *in-vitro* culture, constructs were harvested weekly for qualitative evaluation of neocartilage synthesized by the chondrocytes. The constructs were fixed in 10% neutral buffered formalin solution supplemented with 20 mM CaCl₂ at room temperature overnight, embedded in paraffin and sectioned (5 µm). For assessment of sulfated glycosaminoglycans (sGAG) and cell distribution within the bilayer BNC scaffolds, longitudinal sections were stained with Alcian blue and counterstained with Mayer's hematoxylin. Furthermore, seeded scaffolds were processed for immunohistochemical staining to detect cartilage specific proteins such as aggrecan (AB1031; Millipore, MA, USA), type II collagen (II-II6B3; DSHB, IA, USA) and the dedifferentiation marker type I collagen (ab34710; Abcam, UK). An enzymatic antigen retrieval step was performed before incubation with primary antibodies. For aggrecan staining, slides were incubated in 0.5 U/ml chondroitinase ABC in PBS for 20 min at 32°C, followed by incubation with primary antibody for 1 hour at a 1/100 dilution. For type II collagen staining, slides were incubated in 1% hyaluronidase in PBS and 0.2% pronase (Calbiochem, Germany) in PBS, each for 15 min at 37°C, followed by incubation with primary antibody for 1 hour at a 1/4000 dilution. For type I collagen staining, slides were incubated in proteinase K (Dako, Germany) for 5 minutes at room temperature, followed by incubation with primary antibody for 1 hour at a 1/400 dilution. For visualization of these markers, the

LSAB+System-HRP kit (Dako), which is based on the labeled streptavidin biotin method, was used according to the manufacturer's protocol. Sections were counterstained with hematoxylin.

Gene expression analysis

Samples were harvested after 2, 4 and 6 weeks of *in vitro* culture, snap-frozen and stored at -80°C until analyzed. For total RNA isolation, frozen constructs were placed in 2 ml microcentrifuge tubes in quadruples and 100 µl of lysis buffer (10 µl β-Mercaptoethanol per 1 ml Buffer RLT; Qiagen, Germany) was added to each tube. The samples were disrupted and homogenized for 2 minutes using a TissueLyser LT (Qiagen). Subsequently, 500 µl of lysis buffer was added to each tube and the cell lysate was used for total RNA isolation using RNeasy Mini Kit (Qiagen), according to manufacturer's protocol. Total RNA was quantified using a multimode microplate reader (Infinite M200 Pro, Tecan AG) at 260/280 nm. cDNA was synthesized from the extracted RNA using QuantiTect Reverse Transcription Kit (Qiagen), according to manufacturer's protocol, in a PeqSTAR thermocycler (96 Universal Gradient, PeqLab, Germany). For real-time two-step RT-PCR analysis, the sense and antisense primers used are listed in Table 1. The following genes were analyzed: aggrecan (*ACAN*), collagen type IIA1 (*COL2A1*), versican (*VCAN*) and collagen type IA1 (*COL1A1*). Glyceraldehyde 3-phosphate dehydrogenase (*GAPDH*) was used as housekeeping gene. Real-time two-step RT-PCR was performed using the Real Time ready RNA Virus Master assay and LightCycler® 2.0 instrument (Roche, Germany). Relative gene expression levels were calculated by means of the $2^{-\Delta CT}$ formula.

	UPL probe#	Sense primer	Antisense primer
Target genes			
<i>ACAN</i>	79	5'-TGCAGCTGTCACTGTAGAACTT-3'	5'-ATAGCAGGGGATGGTGAGG-3'
<i>COL1A1</i>	15	5'-ATGTTTCAGCTTTGTGGACCTC-3'	5'-CTGTACGCAGGTGATTGGTG-3'
<i>COL2A1</i>	19	5'-CCCTGGTCTTGGTGGAAC-3'	5'-TCCTTGCATTACTCCCAACTG-3'
<i>VCAN</i>	54	5'-GCACCTGTGTGCCAGGATA-3'	5'-CAGGGATTAGAGTGACATTCATCA-3'
Housekeeping gene			
<i>GAPDH</i>	60	5'-GCTCTCTGCTCCTCCTGTTC-3'	5'-ACGACCAAATCCGTTGACTC-3'

Table 1. Sequences of target genes and reference gene for real-time two-step PCR.

Cell study II: performance of bilayer BNC scaffolds *in vivo*

Rapid isolation of human nasoseptal chondrocytes and bone marrow mononuclear cells

Nasoseptal cartilage was obtained from male and female patients ($n=47$; mean age 31 years; age range 18-69 years) undergoing routine reconstructive septorhinoplasty at the Department of Otorhinolaryngology of Ulm University Medical Center (Ulm, Germany) as waste material

after surgery, with approval of the local medical ethics committee (no. 152/08). The collected nasoseptal cartilage was washed with PBS containing penicillin-streptomycin and stored in standard culture medium at 37°C, 5% CO₂, until further use. The 47 nasoseptal cartilage biopsies were divided in three pools for the chondrocyte isolations. Bone marrow aspirate was collected from three donors (mean age 70 years, 2 males, 1 female) during total hip replacement surgery, after acquiring written patient consent. The isolations of NCs from the cartilage and MNCs from the bone marrow were performed by CellCoTec (Bilthoven, the Netherlands). Patented clinically applied protocols were used to isolate the cells within the hour [347]. In brief, cartilage pieces were digested enzymatically under mechanical stimulation. Upon rapid digestion, any remaining debris was filtered out with a 100-µm cell strainer. For the collection of MNCs, the bone marrow aspirate was relieved of its erythrocyte content using lysis buffer. Standard cell buffer was used for washing steps. Cell numbers and viability were measured using the Bürker-Türk method with trypan-blue exclusion.

Seeding of bilayer BNC scaffolds with MNCs and NCs

First, bilayer BNC scaffolds were freeze-dried in order to improve cell uptake during the cell seeding. To further improve the retention of cells in the scaffolds, cells were seeded in 1.1 % w/w alginate solution (CellMed AG). Cells encapsulated in alginate were then seeded in bilayer BNC scaffolds as a combination of 80% freshly isolated human MNCs and 20% freshly isolated human NCs at a total cell concentration of 20×10^6 cells/ml alginate (MNC/NC, $n=4$). 200 µl of the cell-alginate suspension was seeded into the porous layer of each scaffold. A cell-free alginate solution acted as a negative control (Cell-free, $n=4$). Subsequently, the alginate was instantaneously crosslinked with sterile 100 mM CaCl₂ for 10 minutes and washed with 0.9% NaCl, followed by high glucose DMEM (Dulbecco's Modified Eagle's Medium).

Subcutaneous implantation of constructs in mice

To evaluate the stability of the bilayer BNC scaffolds and neocartilage formation *in vivo*, MNC/NC-seeded and cell-free bilayer BNC scaffolds were implanted subcutaneously on the dorsal side of 9-week-old nude female mice ($n=2$; NMRI nu/nu, Charles River Laboratories, the Netherlands). Mice were placed under general anesthesia using 2.5% isoflurane. Two separate subcutaneous incisions of approximately 1 cm were made along the central line of the spine (1 at the shoulders and 1 at the hips), after which 4 separate subcutaneous pockets were prepared by blunt dissection of the subcutaneous tissue. The overall behavior and wound healing at the implant sites were assessed macroscopically over the implantation period. Eight weeks after subcutaneous implantation, animals were terminated and samples were explanted. Each sample was cut in half and one part was used for histology and the other part for biomechanical and biochemical analyses. Animal experiments were carried out with approval of the local Animal Experiments Committee of the Erasmus MC, Rotterdam, the Netherlands (EMC 2429).

Histological and immunohistochemical analyses

After 8 weeks of subcutaneous implantation, constructs were harvested, set in 2% agarose, fixed in 10% neutral buffered formalin solution, embedded in paraffin and sectioned (6 µm).

To examine proteoglycans present in the newly synthesized ECM, deparaffinized sections were stained with Safranin O and fast green. To allow the use of the monoclonal mouse antibody collagen type II (II-II6B3, 1:100; DSHB) on constructs which had been implanted in nude mice, we coupled the first and second antibody before applying them on the sections to prevent unwanted binding of the anti-mouse antibodies to mouse immunoglobulins, as described previously [214]. In short, the primary antibody was pre-coupled overnight with goat anti-mouse biotin at 4°C (1:500; Jackson Laboratories, ME, USA), followed by a 2 hour incubation in 0.1% normal mouse serum (CLB, the Netherlands) in order to capture the unbound second antibody. Antigen retrieval was performed through incubation with 0.1% pronase in PBS for 30 minutes at 37°C, followed by a 30 minute incubation with 1% hyaluronidase in PBS at 37°C. Non-specific binding sites were blocked with 10% goat serum in PBS and sections were stained with the pre-treated antibodies for 60 minutes. Sections were then incubated with enzyme-streptavidin conjugate (1:100; Biogenex, California, USA) in PBS/1% BSA, followed by incubation with Neu Fuchsin substrate (Chroma, Germany). Positive staining for type II collagen was confirmed with the use of native ear cartilage. A monoclonal mouse IgG1 antibody (X0931; Dako) was used as a negative control.

Biochemical analysis

Sulfated glycosaminoglycans (sGAG) were quantified using the 1,9-Dimethylmethylene blue (DMMB) dye-binding assay. First, alginate was dissolved in 55 mM sodium citrate and digested overnight at 56°C in papain (250 µg/ml in 0.2 M NaH₂PO₄, 0.01 M EDTA, containing 5 mM L-cysteine; pH 6.0). To be suitable for cell cultures containing alginate, the DMMB-pH-level was decreased to pH 1.75, as described previously [353]. The metachromatic reaction of DMMB was monitored using a spectrophotometer. Absorption ratios of 540 and 595 nm were used to determine the sGAG content with chondroitin sulfate C derived from shark as a standard. The amount of sGAG was expressed per tissue wet weight ($n=4$).

Biomechanical analysis

Mechanical properties of the retrieved constructs ($n=8$, MNC/NC-seeded and cell-free scaffolds) and non-implanted bilayer BNC scaffolds containing cell-free alginate solution ($n=5$, non-implanted group) were assessed with uniaxial materials testing machine (Z005, Zwick GmbH, Germany) equipped with a 10 N load cell, a cylindrical plane-ended stainless steel indenter (Ø 0.35 mm) and a built-in displacement control. Bilayer BNC scaffolds were placed in close-fitting stainless steel cylindrical wells containing PBS supplemented with 1% antibiotic/antimycotic solution. Stress relaxation testing was performed as described previously [354]. Briefly, a preload of 3 mN was first applied on the sample to locate the sample surface and measure sample thickness, and held for 5 minutes. Five successive strain steps were then applied in 5% increments of the original sample thickness, and specimens were left to relax for 20 minutes at each step. The hold time was defined as the time necessary to reach equilibrium. Two locations were tested on each sample (center of the sample, and 1.2 mm off-center). Measurements of maximum stress (σ_{\max}), instantaneous modulus (E_{in}) and equilibrium modulus (E_{eq}) were computed from the stress-strain curves, which are normalized for sample thickness. Additionally, a relaxation half-life time ($t_{1/2}$), defined as the

time needed for the stress to decrease to half of its maximum value, was computed to estimate the viscoelastic relaxation after the first strain application, as described previously [329].

Statistical analysis

Statistical analyses were performed with Statgraphics Centurion Version 17 (Statpoint Technologies, VA, USA). For cytotoxicity analysis, comparison of means was assessed by one-way ANOVA, followed by Tukey's HSD test for post hoc comparisons. For biochemical analysis, a two-sample Kolmogorov-Smirnov test was performed for comparing two groups. For biomechanical analysis, comparison of means was assessed by one-way ANOVA and Tukey's HSD test. When the data did not meet the requirements for a parametric test, a Kruskal-Wallis test was performed, followed by the Mann-Whitney test for post hoc comparisons. Values of $p < 0.05$ were considered statistically significant. The mean and standard deviation (SD) are presented.

RESULTS

Production and morphological characterization of bilayer BNC scaffolds

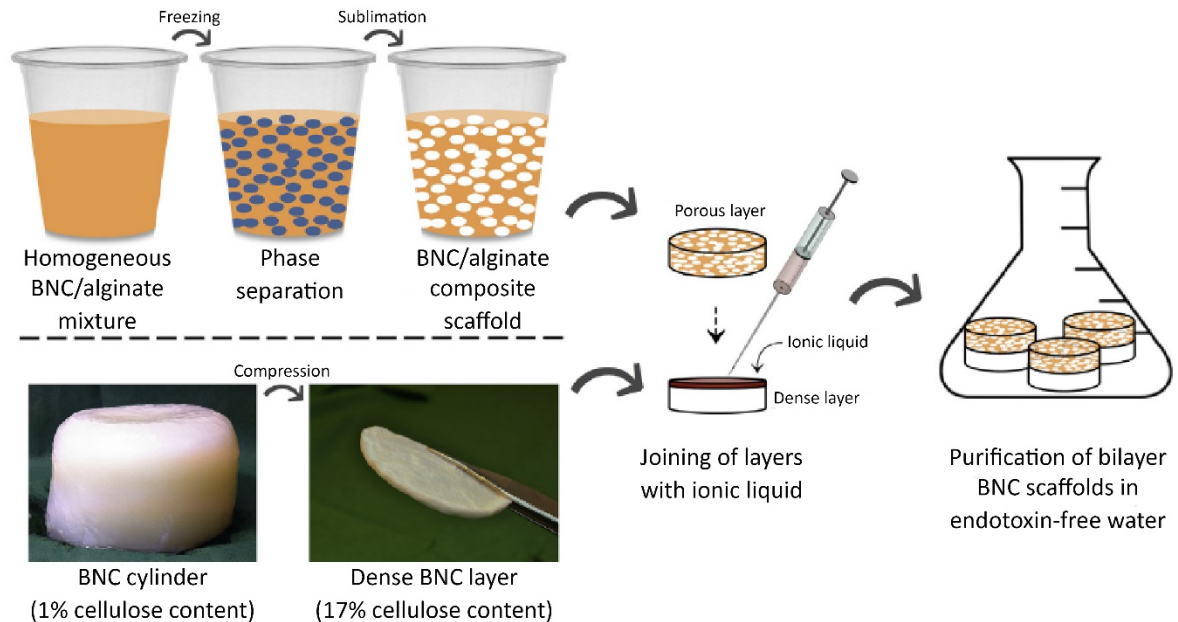


Figure 1. Fabrication and purification process of bilayer BNC scaffolds composed of a dense nanocellulose layer joined with a macroporous composite layer.

BNC hydrogel disks with cellulose content of 17% (i.e. dense layer) were produced by compression, whereas BNC/alginate composite scaffolds (i.e. porous layer) were fabricated by a freeze-drying process. A novel cellulose solvent system (i.e. ionic liquid EMIMAc) was used to achieve a strong interfacial molecular bonding between the dense and porous layers. The bilayer BNC scaffolds were then washed with endotoxin-free water for 14 days to yield non-pyrogenic and non-cytotoxic scaffolds.

Bilayer BNC scaffolds, composed of a dense nanocellulose layer joined with a macroporous composite layer of nanocellulose and alginate, were successfully fabricated. (Figures 1 and 2) The dense and porous layers were stable and firmly attached, which facilitated the handling of the scaffolds during the purification process and throughout the study. SEM images revealed a compact BNC network structure in the dense layer and a macroporous structure in the porous layer. However, information about the pore size distribution was not possible to extract from these images (Figure 2B, C). Scanning and reconstruction with microCT of the micro- and macro-structures of the porous layer allowed computation of the 3D morphometric parameters by distance transformation. The Sc.Po, Pore.Th, Wall.Th and Wall.N of a typical porous layer of a BNC bilayer scaffold was 75%, $50 \pm 25 \mu\text{m}$, $18 \pm 10 \mu\text{m}$ and 21 mm^{-1} , respectively. (Figure 2F, G)

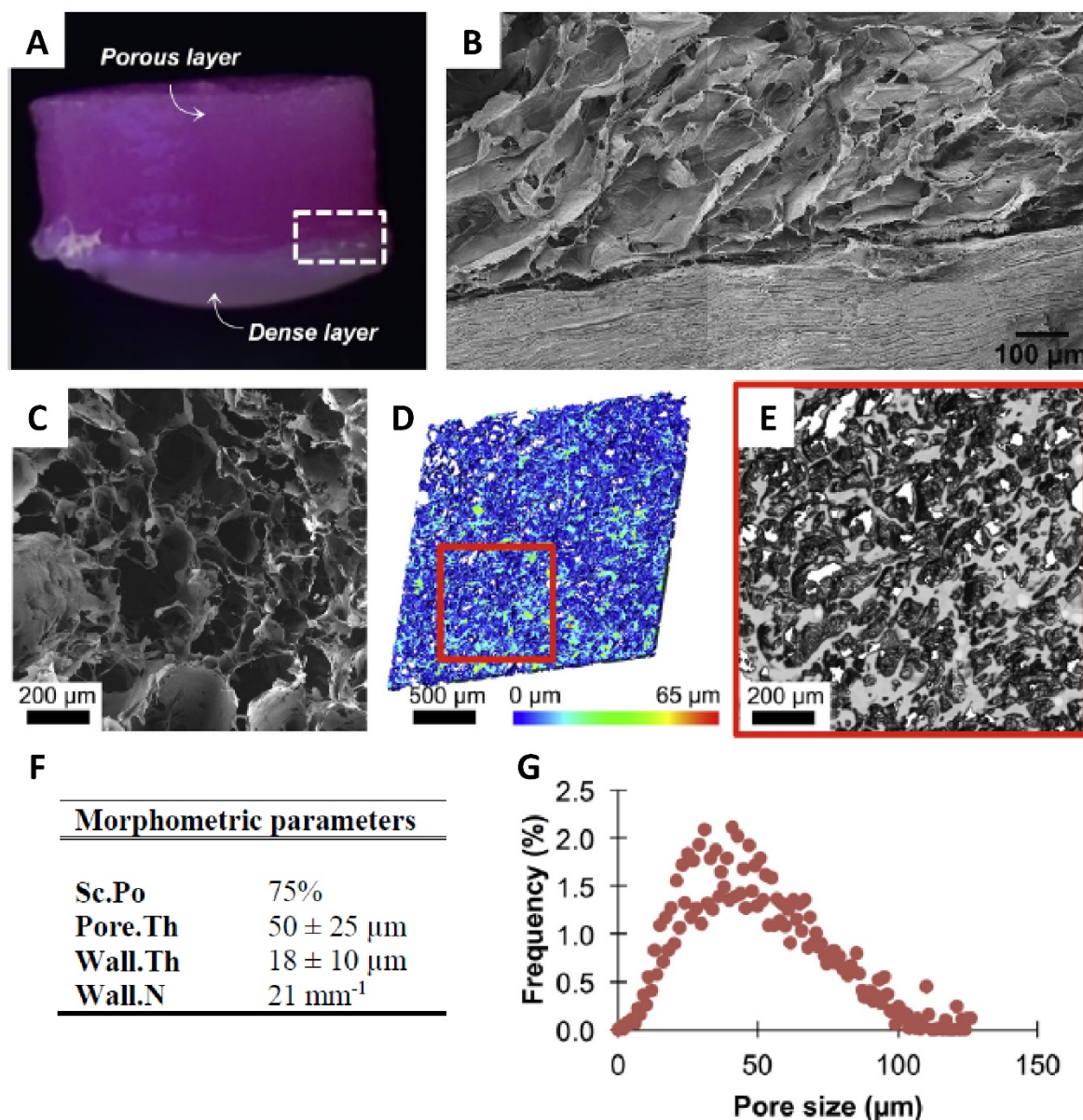


Figure 2. Scanning electron microscopy and microtomography of bilayer BNC scaffold.

(A) Photograph of bilayer BNC scaffold (side view). Comparison between **(B,C)** scanning electron microscopy images of bilayer BNC scaffolds and **(D)** 3D reconstructed model of the porous layer using microtomography. Similar honeycomb arrangement of sheet-like structures is visible in both images. **(E)** Higher magnification of the area marked red in **(D)**. Morphometric analysis of segmented porous layer: **(F)** Morphometric parameters (Sc.Po = Scaffold Porosity ; Pore.Th = Volume-weighted mean pore size ; Wall.Th = Scaffold Wall Thickness ; and Wall.N = Scaffold Wall Number) and **(G)** histogram of pore size distribution.

Purification of bilayer BNC scaffolds

The bilayer BNC scaffolds were successfully purified from endotoxins, as shown by the low endotoxin level ($0.15 \pm 0.09 \text{ EU/ml}$) found after 14 days of washing with endotoxin-free water. (Table 2) This value is three times lower than the endotoxin limit (0.5 EU/ml) set by the FDA for medical devices [352]. The result from endotoxin analysis verified the effectiveness of the purification process to remove endotoxins from the bilayer BNC scaffolds.

Sample#	Dilution	Results (EU/ml)	Spike recovery (%)	Status	Mean \pm SD (EU/ml)
1	1/10	0.26	59	Valid	0.15 \pm 0.09
2	1/10	0.10	90	Valid	
3	1/10	0.10	55	Valid	

Table 2.

Results from bacterial endotoxin testing. Assay sensitivity 0.005 Endotoxin Units per ml (EU/ml). Valid test parameter: each sample is tested with a positive product control (PPC) of 0.1 EU/ml. If the spike recovery is between 50 and 200 % of the PPC, the result is valid. According to the FDA, endotoxin levels in medical devices are not to exceed 0.5 EU/ml or 20 EU/device. [352]

The removal of EMIMAc residues from the bilayer BNC scaffolds was analyzed with ATR-FTIR spectroscopy. The strong peak at wavenumber 1566 cm^{-1} , observed in the ATR spectrum of EMIMAc solution, was used to detect EMIMAc residues in the ATR spectra of bilayer BNC scaffolds. This peak is composed of two overlapped peaks that correspond to the carboxyl group of the acetate and an underlying ring mode of the cation, as shown by previous studies. [355, 356] A small peak at 1566 cm^{-1} was also found in the ATR spectra of bilayer BNC scaffolds after 1 and 7 days of purification. However, the absence of the peak at 1566 cm^{-1} in the ATR spectra of samples that were washed for 14 days confirmed the removal of EMIMAc residues from the bilayer BNC scaffolds. (Figure 3A) *In-vitro* cytotoxicity testing supported this observation. An one-way ANOVA was conducted to compare the effect of cytotoxic residues extracted from BNC bilayer scaffolds (i.e. at 7 and 14 days of purification) and control conditions on cell viability. There was a significant effect of extracted cytotoxic residues on levels of cell viability for the four conditions, $F(3, 20) = 120.42$, $p < 0.0001$, $\omega = 0.97$. Post hoc comparisons using the Tukey HSD test indicated that the mean cell viability for the 14-day condition ($97.8 \pm 4.7\%$) was significantly higher than the 7-day ($18.4 \pm 3.6\%$) and positive control conditions ($25.6 \pm 5.5\%$) at the $p < 0.05$ level. Furthermore, there was no significant difference between the negative control and 14-day conditions. Thus, the cytotoxic potential of bilayer BNC scaffolds, after 14 days of washing with endotoxin-free water, was classified as non-cytotoxic (cell viability $> 71\%$). (Figure 3B)

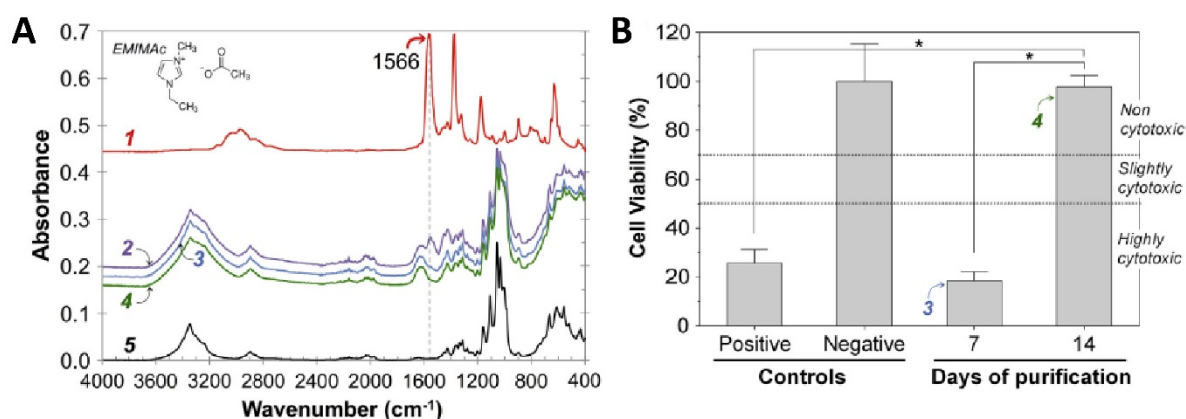


Figure 3. Purification and cytotoxicity testing of bilayer BNC scaffold.

(A) ATR spectra of (1) 1-Ethyl-3-methylimidazolium acetate (EMIMAc) ; bilayer BNC scaffolds after (2) 1 day, (3) 7 days and (4) 14 days of purification in endotoxin-free water ; and (5) pure BNC. **(B)** *In vitro* cytotoxicity testing of bilayer BNC scaffolds after 7 and 14 days of purification in endotoxin-free water ($n=4$ per time point). Post hoc comparisons using the Tukey HSD test indicated that the mean cell viability for the 14-day condition ($97.8 \pm 4.7\%$) was significantly higher than the 7-day ($18.4 \pm 3.6\%$) and positive control conditions ($25.6 \pm 5.5\%$) at the $*p < 0.05$ level. Furthermore, there was no significant difference between the negative control and 14-day conditions. Thus, the cytotoxic potential of bilayer BNC scaffolds after 14 days of purification was classified as non-cytotoxic (cell viability $>71\%$). Error bars represent the standard deviation of the mean.

Performance of bilayer BNC scaffolds and neocartilage formation *in vitro*

Gross examination of the cell-seeded constructs throughout the 6 weeks of cell culture revealed that the adhesion between the dense support layer and porous layer remained good. Moreover, the size and shape of the bilayer BNC scaffolds remained stable during the cell culture. Deposition of ECM by the NCs seeded in bilayer BNC scaffolds was assessed qualitatively by immunohistological staining. During 3D culture, NCs produced and accumulated cartilage-specific ECM components in the bilayer BNC scaffolds. A positive staining for sGAGs was found around clusters of chondrocytes in the porous layer after 2 weeks of culture, as shown by the Alcian blue staining. (Figure 4A) Moreover, synthesis and accumulation of sGAGs, aggrecan as well as type II collagen increased visibly during 3D culture. (Figure 4A-C) After 6 weeks of 3D culture, a homogeneous production of chondrogenic ECM was observed throughout the porous layer, even at the center. However, fibrocartilage ECM was also synthesized by the NCs in the bilayer BNC scaffolds, as demonstrated by the positive immunostaining of type I collagen. (Figure 4D)

The capacity of NCs to synthesize cartilage-specific ECM components when seeded in the BNC scaffold was also investigated on the basis of the expression of the chondrogenic marker genes *ACAN* and *COL2A1*. To assess whether the NCs were able to redifferentiate and maintain their chondrogenic phenotype, the expression not only of the chondrogenic markers but also of the dedifferentiation markers, *VCAN* and *COL1A1*, was determined. Gene expression analyses confirmed the positive immunostains of aggrecan, type II and type I collagen. NCs cultured in bilayer BNC scaffolds were able to express *ACAN* and *COL2A1*. The expression of both chondrogenic markers increased clearly during 3D culture for up to 6

weeks. *ACAN* and *COL2A1* expression after 6 weeks was 3.4- and 4.9-fold higher, respectively, compared to gene expression levels at week 2. Expression of *COL1A1* was also upregulated during 3D culture, where after 6 weeks was 1.7-fold higher compared to gene expression levels at week 2. On the other hand, expression of *VCAN* remained relatively close to zero during the 6 weeks of 3D culture. (Figure 4E, F) The upregulation of the chondrogenic markers *ACAN* and *COL2A1* was clearly enhanced compared to the expression of dedifferentiation markers, revealing the chondrogenic potential of the NCs in the bilayer BNC scaffolds.

Cell ingrowth and cell distribution in the bilayer BNC scaffolds were also assessed by histological analysis. As demonstrated in figure 4A, the porous layer supported the ingrowth of NCs and facilitated a homogeneous cell distribution. However, it took 4 weeks of *in-vitro* culture to get a dense and homogenous cell distribution since there was a substantial loss of cells after seeding in medium. As a means to increase the number of cells retained in the scaffolds, cells were seeded in alginate solution. This significantly improved cell retention in the scaffolds, even after 1 day of seeding. (Data not shown)

Performance of bilayer BNC scaffolds and neocartilage formation *in vivo*

The stability and neocartilage formation in MNC/NC-seeded and cell-free bilayer BNC scaffolds were evaluated after 8 weeks of subcutaneous implantation in nude mice. The mice survived until the end of the study period, during which no extrusion of constructs was observed. At 8 weeks post-implantation, a thin fibrous capsule surrounded all MNC/NC-seeded and cell-free bilayer BNC scaffolds - considered a normal non-pathological foreign body reaction. Macroscopic examination of the explants revealed that the shape and size of the bilayer BNC scaffolds remained stable and no delamination of the dense and porous layers was observed in any of the constructs. Furthermore, bilayer BNC scaffolds seeded with MNCs and NCs encapsulated in alginate had a macroscopically cartilage-like appearance. These MNC/NC-seeded constructs were stiffer and more stable upon handling, compared to bilayer BNC scaffolds seeded with cell-free alginate solution. The cells encapsulated in alginate were homogeneously distributed in the porous layer of the scaffolds at 8 weeks post-implantation, as observed by the histology images. (Figure 5B)

Proteoglycan synthesis was examined using a Safranin-O staining. As expected, no positive stain for Safranin-O was found in the cell-free bilayer BNC scaffolds. Depositions of proteoglycans were observed in the MNC/NC-seeded bilayer BNC scaffolds after 8 weeks of subcutaneous implantation, as shown by the strong Safranin-O stain surrounding the cells. (Figure 5B) The results pointing towards chondrogenic ECM produced by the cells in the bilayer BNC scaffolds were confirmed by the positive immunostaining of type II collagen, which was intensely stained in areas of the construct. (Figure 5B) Moreover, a Kolmogorov-Smirnov test indicated a significant difference ($p < 0.05$) between mean sGAG content for MNC/NC-seeded ($0.87 \pm 0.65 \mu\text{g sGAG/mg wet weight}$) and cell-free bilayer BNC scaffolds ($0.07 \pm 0.11 \mu\text{g sGAG/mg wet weight}$). sGAG-production in the MNC/NC group was almost 12-fold higher compared to the control condition. (Figure 5C)

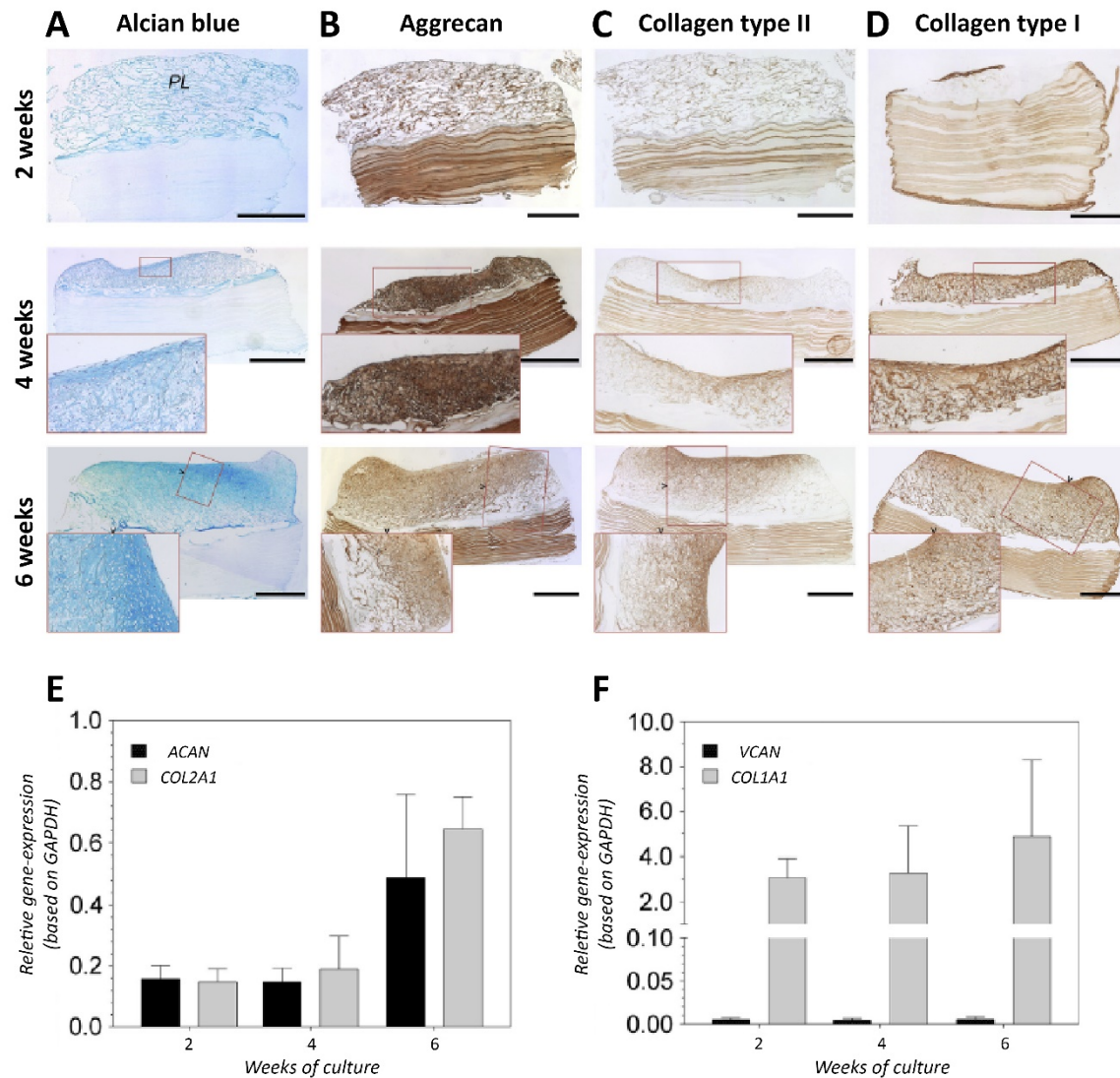


Figure 4. Performance of bilayer BNC scaffolds and neocartilage formation *in vitro*.

Histological and immunohistochemical analysis of human NCs after 2, 4 and 6 weeks of culture *in vitro* on bilayer BNC scaffolds. Samples were stained with (A) Alcian blue to detect deposition of sGAG (PL = porous layer). Immunohistochemical staining was used to detect cartilage-specific proteins such as (B) aggrecan, (C) collagen type II and (D) the dedifferentiation marker collagen type I. (E and F) Gene-expression analysis of human NCs seeded in bilayer BNC scaffolds and cultured *in vitro* for 2, 4 and 6 weeks ($n=4$ per time point). Gene-expression levels of ACAN, COL2A1, COL1A1 and VCAN relative to the housekeeping gene glyceraldehyde 3-phosphate dehydrogenase (GAPDH). Error bars represent the standard deviation of the mean. The scale bar indicates 1 mm.

Biomechanical analysis

A typical stress relaxation behavior was observed in all bilayer BNC scaffolds (MNC/NC-seeded and cell-free controls), and the following measurements were determined for the MNC/NC-seeded constructs at 8 weeks post-implantation; 0.76 ± 0.19 MPa for E_{in} , 0.19 ± 0.08 MPa for E_{eq} , 0.16 ± 0.07 MPa for σ_{max} and 7.1 ± 3.4 seconds for $t_{1/2}$. A one-way ANOVA was conducted to compare the effect of implantation and seeding of MNC/NCs on initial matrix stiffness (i.e. E_{in}) of the constructs at 8 weeks post-implantation. There was a significant effect of

implantation and seeding of MNC/NCs on instantaneous modulus for the three conditions, $F(2, 23) = 16.10$, $p < 0.0001$, $\omega = 0.73$. Post hoc comparisons using the Tukey HSD test indicated that the mean E_{in} for the MNC/NC condition (0.76 ± 0.19 MPa) was significantly higher than the non-implanted (0.42 ± 0.15 MPa) and cell-free conditions (0.32 ± 0.10 MPa) at the $p < 0.05$ level. The cell-free implanted condition did not significantly differ from the non-implanted condition. (Figure 5D)

Moreover, a Kruskal–Wallis test was conducted to compare the effect of implantation and seeding of MNC/NCs on relaxation kinetics (i.e. $t_{1/2}$) and intrinsic properties (i.e. E_{eq} and σ_{max}) of the constructs at 8 weeks post-implantation. The median $t_{1/2}$ values of the constructs were significantly affected by the implantation and seeding of MNC/NCs, $H(2) = 17.46$, $p < 0.001$. However, E_{eq} and σ_{max} were not significantly affected by the tested conditions, $H(2) = 4.19$, $p = 0.12$ and $H(2) = 1.12$, $p = 0.57$, respectively. Post hoc comparisons using the Mann–Whitney tests indicated that the median $t_{1/2}$ for the MNC/NC condition was significantly higher than the non-implanted ($U = 3$, $p < 0.001$, $r = -0.74$) and cell-free conditions ($U = 48$, $p < 0.01$, $r = -0.66$). No significant differences in $t_{1/2}$ were detected between the cell-free and non-implanted conditions. A 2.4- and 3.4-fold higher E_{in} and $t_{1/2}$, respectively, were observed in the MNC/NC-seeded constructs compared to the cell-free group. Likewise, a 1.8- and 3.6-fold higher E_{in} and $t_{1/2}$, respectively, was observed in the MNC/NC-seeded constructs compared to the non-implanted group. (Figure 5D)

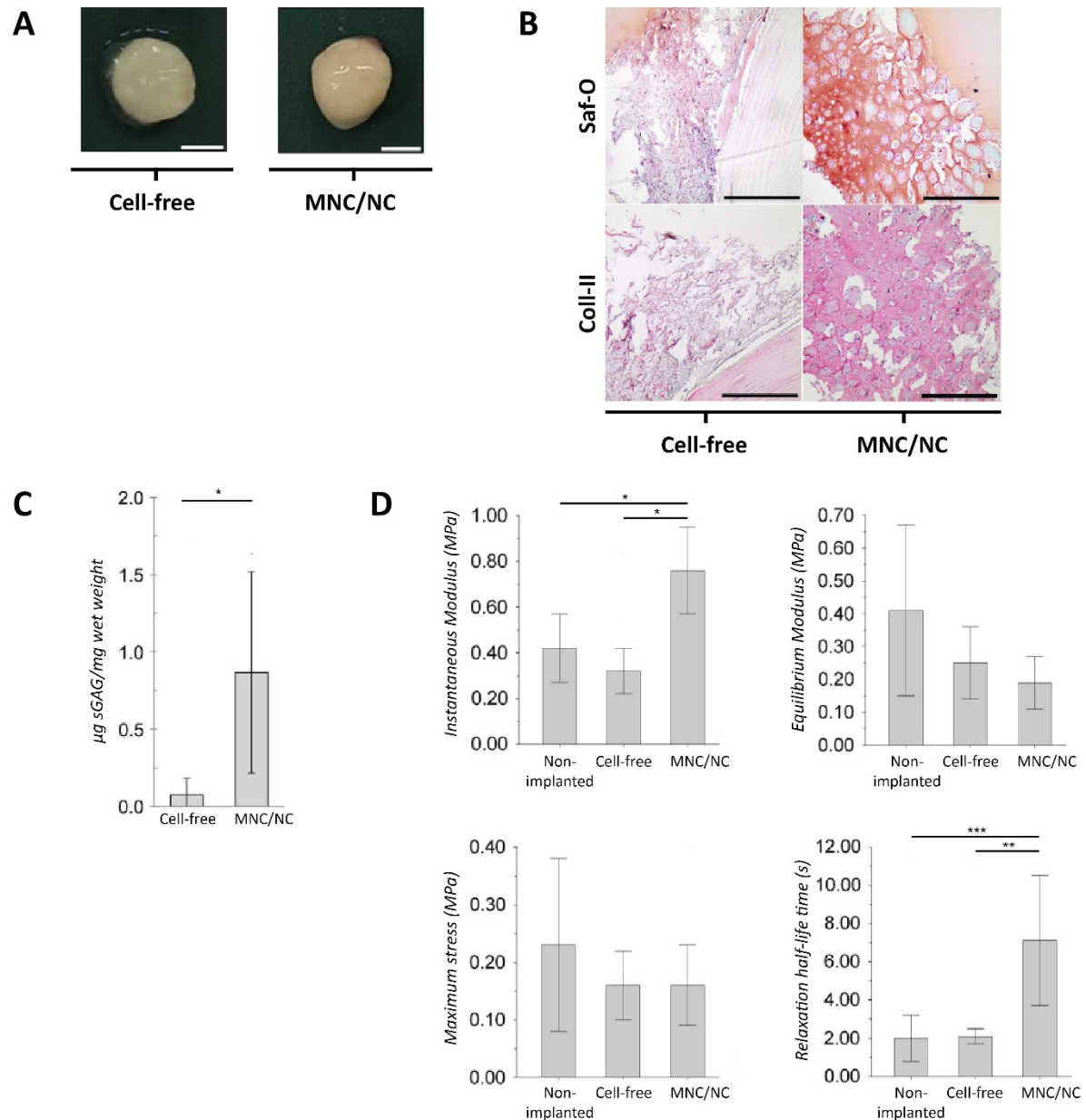


Figure 5. Performance of bilayer BNC scaffolds and neocartilage formation *in vivo*.

(A) Photographs of cell-free and MNC/NC-seeded bilayer BNC scaffolds after 8 weeks of subcutaneous implantation. **(B)** Histological evaluation of ECM in bilayer BNC scaffolds seeded with a combination of freshly isolated NCs and MNCs in alginate after 8 weeks of subcutaneous implantation. Safranin-O stain was used to examine proteoglycans present in the newly synthesized ECM, whereas immunohistochemical analysis was used to detect type II collagen. **(C)** Cell-free and MNC/NC-seeded bilayer BNC scaffolds were analysed for sGAG content after 8 weeks of subcutaneous implantation ($n=4$ per group). A two-sample Kolmogorov-Smirnov test indicated a significant difference between mean sGAG content for MNC/NC-seeded and cell-free bilayer BNC scaffolds. **(D)** Biomechanical evaluation of cell-free and MNC/NC-seeded constructs after 8 weeks of subcutaneous implantation ($n=4$ per group), and non-implanted bilayer BNC scaffolds with cell-free alginate solution ($n=5$). Post hoc comparisons using the Tukey HSD test indicated that the mean E_{in} for the MNC/NC condition was significantly higher than the non-implanted and cell-free conditions. Moreover, post hoc comparisons using the Mann Whitney tests indicated that the median $t_{1/2}$ for the MNC/NC condition was significantly higher than the non-implanted and cell-free conditions. Error bars represent the standard deviation of the mean. *, ** or *** indicates p-values less than 0.05, 0.01 or 0.001, respectively. The scale bars indicate 4 mm **(A)** and 1 mm **(B)**.

DISCUSSION

A novel bilayer BNC scaffold was successfully evaluated for auricular cartilage TE. This study demonstrates that non-pyrogenic and non-cytotoxic bilayer BNC scaffolds offer a good mechanical stability and maintain a structural integrity while providing a porous architecture that supports cell ingrowth. Moreover, bilayer BNC scaffolds, together with alginate, provide a suitable environment for human nasoseptal chondrocytes to form cartilage.

As shown by the endotoxin analysis, the purification process reduced the endotoxins in the bilayer BNC scaffolds to a level well below the endotoxin limit set by the FDA for medical devices [352]. This low endotoxin content (0.15 ± 0.09 EU/ml) found in the bilayer BNC scaffolds is in good agreement with our previous results (0.10 EU/ml, [316]), where densified BNC hydrogel disks (i.e. dense layer) of similar dimensions were considered non-pyrogenic after purification with endotoxin-free water for 14 days.

The ionic liquid EMIMAc offers a novel cellulose solvent system to achieve a strong interfacial molecular bonding between the cellulosic dense and porous layers. We are not aware of any other methods that can achieve such result. On the other hand, using EMIMAc increases the risk of having cytotoxic compounds in the bilayer BNC scaffolds, if these residues are not properly removed during the purification process. Since the toxicity of ionic liquids is not well understood, the use of EMIMAc to fabricate the bilayer BNC scaffolds was investigated with precaution. The cytotoxicity of imidazole ionic liquids has been studied in a human lung carcinoma epithelial cell line model, and it was found that the alkyl-chain length of the ionic liquid has an influence on cytotoxicity [357]. However, the cytotoxicity of EMIMAc, in particular, has not been studied in eukaryotes. Consequently, we analyzed the removal of EMIMAc from the bilayer BNC scaffolds with ATR-FTIR spectroscopy, followed by *in-vitro* cytotoxicity testing with sensitized L929 cells. The strong peak at wavenumber 1566 cm^{-1} was used to detect EMIMAc residues in the ATR spectra of bilayer BNC scaffolds, as it has been shown that this peak is composed of two overlapped peaks that correspond to the carboxyl group of the acetate and an underlying ring mode of the cation [355, 356]. Since the peak at 1566 cm^{-1} was found in the ATR spectra of bilayer BNC scaffolds that had been washed for 1 and 7 days, it was considered necessary to continue washing the scaffolds in endotoxin-free water. The washing process proved to be successful in removing the EMIMAc residues, as first observed in the ATR spectra of samples that were washed for 14 days. The absence of this peak confirmed the removal of EMIMAc from the BNC bilayer scaffolds.

In-vitro cytotoxicity testing supported our findings from ATR-FTIR. Bilayer BNC scaffolds washed for 7 days still had residues of EMIMAc that were highly cytotoxic to L929 cells (cell viability: $18.4 \pm 3.6\%$). However, these residues were further reduced after the purification process with endotoxin-free water; yielding non-cytotoxic bilayer BNC scaffolds. These results are in good agreement with our previous study which evaluated the cytotoxic potential of pure densified BNC hydrogel disks (i.e. dense layer) and found the material to be non-cytotoxic [316]. Altogether, the results from ATR-FTIR and *in vitro* cytotoxicity testing demonstrated that EMIMAc residues were successfully removed from the bilayer BNC scaffolds after the purification process with endotoxin-free water; whereat no peak at 1566 cm^{-1} and no cytotoxic effects were observed.

Macroscopic examination of the bilayer BNC scaffolds after the *in vitro* and *in vivo* studies revealed that the adhesion between the dense and porous layers remained stable, as there were no signs of adhesive failure. We postulate that the interfacial bonding between the layers is like a molecular welding process. As the BNC-EMIMAc solution partly dissolves both surfaces at the interface, this makes it possible for the long chains of BNC to diffuse into both layers. Once the dissolved BNC is precipitated in ethanol, the interface structure is locked, which results in a stable interfacial bonding. We have observed that when pulling the dense and porous layers apart, the scaffold breaks at the porous layer, similar to a structural failure. In contrast, a weak adhesion would have had resulted in an adhesive or cohesive failure at the interface. Based on this observation we speculate that the interfacial bonding between the layers is stronger than the structure of the porous layer, although in this study the interfacial strength of the bilayer BNC scaffolds was not measured.

The compact BNC network structure of the dense layer provided a good mechanical stability, while the interconnected high porosity layer (75% porosity with mean pore size of $50 \pm 25 \mu\text{m}$) supported the ingrowth and homogeneous distribution of NCs throughout this layer. In agreement with our previous study, which evaluated BNC/alginate composite scaffolds *in vitro* [343], bilayer BNC scaffolds also supported the redifferentiation of NCs to a more chondrogenic phenotype, which led to the formation of neocartilage; as demonstrated by the increase in gene expression of chondrogenic marker genes *ACAN* and *COL2A1* and homogeneous distribution of cartilage-specific ECM after 6 weeks of *in vitro* culture. Although, the expression of dedifferentiation marker *VCAN* remained constantly low, a strong expression of *COL1A1* was observed during the *in vitro* culture. The presence of *COL2A1* and *COL1A1* indicates a subpopulation of NCs that did not switch to a chondrogenic phenotype during 3D culture in bilayer BNC scaffolds under chondrogenic medium conditions.

After 6 weeks of *in-vitro* culture, a rich and homogenous distribution of cells and neocartilage was observed throughout the porous layer of the scaffold, even in the center, which is known to be a critical region in static 3D culture due to the limited supply of nutrients and oxygen. This outcome could have been accelerated by increasing the percentage of cells retained in the scaffolds after cell seeding, as there was a substantial loss of cells when these were seeded in medium. Embedding the cells in alginate significantly improved cell retention in the scaffolds after seeding. Alginate was chosen, since it has been successfully used to seed chondrocytes in a scaffold for *in vivo* implantation [358, 359] and this hydrogel is well known to maintain a chondrogenic phenotype of human chondrocytes and stimulate neocartilage formation [348].

In the *in-vivo* study we explored the application of a clinically relevant strategy, by seeding bilayer BNC scaffolds with a low number of freshly isolated human chondrocytes combined with freshly isolated human mononuclear cells, in order to test the translation of this auricular cartilage TE technology to the clinic. At 8 weeks post-implantation, deposition of cartilage matrix components such as proteoglycan and type II collagen were observed predominantly in MNC/NC-seeded constructs. The strong Safranin-O stain surrounding the cells showed the presence of proteoglycans in the newly synthesized ECM, while the presence of type II collagen was confirmed by immunohistochemistry. These results, showing the formation of neocartilage in the porous layer, were further confirmed by biochemical analysis;

where sGAG-production in the MNC/NC-seeded bilayer BNC scaffolds was significantly higher than the control condition (12-fold).

The presence of cartilage matrix in the bilayer BNC scaffolds was also supported by biomechanical analysis. At 8 weeks post-implantation, a significantly higher initial matrix stiffness and improved relaxation kinetics (i.e. higher E_{in} and $t_{1/2}$ values) were observed in the MNC/NC-seeded scaffolds compared to the non-implanted and cell-free conditions. In fact, the effect size (i.e. ω and $r > 0.5$) obtained from the E_{in} and $t_{1/2}$ data represents a large effect by the MNC/NC condition. However, there was no significant difference in E_{eq} and σ_{max} for the three conditions. Considering the improved relaxation kinetics in the MNC/NC-seeded constructs, we conclude that the ability of the MNC/NC-seeded scaffolds to attract and trap water was enhanced through the production and accumulation of proteoglycans and glycosaminoglycans in the bilayer BNC scaffolds. Nevertheless, since the intrinsic scaffold properties did not improve in the MNC/NC-seeded constructs compared to the no cell control (no difference in E_{eq}), it implies that collagen matrix was not effectively produced in the porous layer. To put the results from the biomechanical analysis in a clinical context, the values for instantaneous and equilibrium moduli measured from the MNC/NC-seeded constructs after 8 weeks of implantation were 8.4- and 17.4-fold lower, respectively, compared to human auricular cartilage (e.g. 6.4 ± 3.2 MPa for E_{in} and 3.3 ± 1.3 MPa for E_{eq} [329]). Therefore, the engineered cartilage as such would not be suitable for immediate ear cartilage replacement; rather modifications in cell concentration and perhaps a longer implantation period needs to be considered.

The present study has certain limitations. Firstly, cell density plays a critical role when engineering functional and stable cartilage. Others have demonstrated that cell densities greater than 20×10^6 cells/ml are desirable, while low cell densities resulted in decreased cartilage formation [360]. During embryology of cartilage, densely packed and proliferative mesenchymal cells are responsible for depositing the vast amount of cartilage ECM. In cartilage TE, early phase of cartilage development needs to be simulated to generate functional and stable cartilage. Therefore, in order to enhance the outcome of tissue-engineered auricular cartilage, a higher cell density is needed to benefit from increased cell-cell contacts signaling chondrogenic ECM deposition and preventing the dedifferentiation process. Despite the limitations already stated, our findings support that bilayer BNC scaffolds in combination with alginate provide a suitable environment for MNCs and NCs to support the synthesis of neocartilage. Of equal importance, the use of freshly isolated human chondrocytes and mononuclear cells in the *in vivo* study gave us an indication of the potential of this strategy to advance the translation of cell-aided treatments to the clinic.

Most auricular cartilage TE strategies have revolved around biodegradable scaffolds, where the hypothetical optimum has been the scaffold's degradation orchestrated by the neo-tissue formation. It would be ideal if the scaffold could be degraded by the time the neocartilage has reached full mechanical strength. However, fine-tuning this intricate play has proven to be a challenge in TE. If the material degrades too rapidly, the neocartilage will collapse. Whereas if it degrades too late, it could induce a continuous inflammation that would affect the cartilage formation and when the material is finally degraded it would leave holes in the tissue, making it more prone to crack or collapse. Thus, we aim for a hybrid implant –

BNC well integrated with the host and neo-tissue. The non-degradable BNC will provide long-term structural integrity after implantation, and has previously shown remarkable integration with the host tissue in different animal models [313, 314, 316, 361]. A novel BNC scaffold designed with a bilayer architecture that integrates mechanical stability and high porosity was successfully fabricated and evaluated for auricular cartilage TE, *in vitro* and *in vivo*. In conclusion, this study demonstrates that non-pyrogenic and non-cytotoxic bilayer BNC scaffolds can be successfully produced. Furthermore, such scaffolds, together with alginate, provide a suitable environment for culture-expanded human nasoseptal chondrocytes and freshly isolated human nasoseptal chondrocytes combined with freshly isolated human mononuclear cells to form cartilage *in vitro* and *in vivo*. Most studies that have used biodegradable materials to engineer auricular cartilage have resulted in poor structural integrity of the scaffold after implantation due to the short-lived chemical stability of the scaffold material. This study found that bilayer BNC scaffolds offer a good mechanical stability and maintain a structural integrity while providing a porous architecture that supports cell ingrowth and neocartilage formation, as demonstrated by immunohistochemistry, biochemical and biomechanical analyses. Ongoing work focuses on developing bilayer BNC scaffolds in the shape of a human auricle, aiming to provide an effective treatment to serious auricular defects.

Acknowledgements

This study was performed within the framework of EuroNanoMed (EAREG-406340-131009/1) and was supported by the Swedish Research Council (2009-7838), Federal Ministry of Education and Research (13N11076), SenterNovem (ENM09001) and the Swiss National Science Foundation (NRP63). The authors acknowledge dr. Annette Jork and CellMed AG (Alzenau, Germany) for providing medical grade alginate; Athanasios Mantas and Anders Mårtensson at Chalmers University of Technology (Gothenburg, Sweden) for assistance with scaffold production and FTIR analysis, respectively; and Priscila Martínez Ávila at The University of Texas at Arlington for helping with statistical analysis. The antibody used for immunohistochemical type II collagen detection (II-II6B3) was obtained from the Developmental Studies Hybridoma Bank, created by the NICHD of the NIH and maintained at the University of Iowa, Department of Biology, Iowa City, IA 52242, USA.

Discussion and summary

Chapter 9

Discussion and future perspectives for clinical application

Cartilage plays an important role in the form and function of the face as it provides flexibility and mechanical support to soft tissues. Once damaged, cartilage defects or deficits can lead to functional problems and major aesthetic impairment. Unfortunately, cartilage has a very limited capacity for self-regeneration. Currently, these defects are reconstructed with autologous cartilage grafts or artificial implants. Although autologous cartilage grafting has been used successfully, the procedure requires a high degree of surgical expertise, is associated with limited availability of autologous cartilage and can cause severe donor site morbidity. Besides, the alternative use of artificial implants is questioned in the head and neck area, since implants in this area are prone to induce a foreign body reaction and frequently lead to extrusion. [276] Cartilage tissue engineering offers a promising solution for restoring missing or destructed cartilage and has the potential to overcome limitations of current treatments, re-establishing unique biological and functional properties of the tissue. The successful translation of tissue-engineering strategies to clinical application is however limited and mainly focusses on articular and tracheal cartilage tissue engineering. This thesis focusses on the generation of a tissue-engineered cartilaginous framework for the reconstruction of cartilage defects in the face and evaluates the suitability of *cells* or combination of cells on natural *scaffolds*. Therefore, the following research questions have been answered:

- Q1** What are the biomechanical and biochemical characteristics of native facial cartilages (i.e. ear and nasal cartilages)?
- Q2** Which cells or combination of cells are most suitable for cell-based cartilage repair in the head and neck area?
- Q3** Which natural scaffolds (i.e. alginate, bacterial nanocellulose, decellularized extracellular matrix (ECM)) are a suitable candidate for future cell-based cartilage repair in the head and neck area?

Cartilage characteristics

- Q1** *What are the biomechanical and biochemical characteristics of native facial cartilages (i.e. ear and nasal cartilages)?*

Replacing damaged or missing cartilage requires an accurately sculpted cartilaginous framework that provides sufficient strength and stiffness to substitute for the biomechanical properties of the damaged cartilage in order to resist tissue deformation. Moreover, a cartilage framework that is too stiff may give an unnatural contour and may cause shearing forces of the overlying tissue, resulting in graft failure. Currently, costal cartilage is widely used as graft material for the replacement of facial cartilages. However, its biomechanical properties are evidently different from that of ear and nasal cartilages. [362] Ideally, tissue-engineered cartilage should overcome this biomechanical mismatch and possess similar biomechanical properties to native tissue. To date, most research on biomechanical characterization of native cartilages has been performed on articular cartilage (reviewed by Little *et al.* [158]) and only few studies have characterized the biomechanical properties of human facial cartilages, such as ear [23, 24, 363] and nasal cartilages [25-30]. However, these

studies were relatively small and frequently used tensile behaviour to reflect biomaterial properties, which requires large sample dimensions and complicates the translation towards biomechanical properties of tissue-engineered cartilage constructs. **Chapters two and three** present the equilibrium behaviour (Eeq) of stress-relaxation indentation to study biomechanical behaviour of native facial cartilages (i.e. ear, nasoseptal and alar cartilages) to obtain a benchmark against which to evaluate tissue-engineering strategies. In general, indentation Eeq of human adult facial cartilages ranged from approximately 1-15 MPa. (Table 1)

Cartilage subtype	Biomechanical property	Value
Ear cartilage	Equilibrium modulus	4.5 ± 1.7 MPa
Anti-tragus	Equilibrium modulus	7.2 ± 4.7 MPa
Tragus	Equilibrium modulus	5.4 ± 2.4 MPa
Concha	Equilibrium modulus	4.5 ± 2.2 MPa
Anti-helix	Equilibrium modulus	3.6 ± 2.1 MPa
Scapha	Equilibrium modulus	3.1 ± 1.0 MPa
Helix	Equilibrium modulus	2.2 ± 1.2 MPa
Nasal cartilage	Equilibrium modulus	
Septum	Equilibrium modulus	15.7 ± 7.4 MPa
Ala nasi	Equilibrium modulus	1.3 ± 0.5 MPa
Costal cartilage	Equilibrium modulus	20.0 ± 14.7 MPa [364]
Articular cartilage	Equilibrium modulus	3.5 ± 1.1 MPa [156]

Table 1. Native human cartilages.

The indentation equilibrium modulus, Eeq, used in our studies compares well with that of costal and articular cartilage using the same test setup.

Ear and alar cartilage had significantly lower equilibrium moduli compared to septal cartilage, and regional variations were observed. (Table 1) Griffin *et al.* have recently measured regional biomechanical behaviour of facial cartilages using compressive Young's modulus on human ear and nasal cartilages [28, 363], indicating similar results. Although cartilage biomechanical behaviour is difficult to directly compare in various experimental setups, they similarly state that ear and alar cartilage have lower moduli compared to septal cartilage, with helical cartilage being the softest region of the ear. [28, 363] To be able to understand biomechanical behaviour of facial cartilages, one should realise that cartilage biomechanics are determined by ECM composition and architecture. In hyaline cartilage (i.e. nasoseptal cartilage), biomechanical behaviour is mainly the consequence of the swelling of negatively charged aggregated proteoglycans trapped into a collagen fiber network. [202] The biomechanical properties of ear and alar cartilage are also influenced by the presence of an elastin fiber

network in the ECM. In fact, compressive biomechanical integrity appears mainly assigned by elastin, whereas in hyaline cartilage this is principally provided by a complex relationship between the collagen network entrapping glycosaminoglycans. [202] Biomechanically, elastin is responsible for the physical properties of elasticity, reversible extensibility and elastic recoil. [144] Moreover, elastin is localized in close proximity to proteoglycans, altering the proteoglycan-ECM binding paradigm we know from hyaline cartilage, and thereby influencing biomechanical behaviour. [202] Therefore, elastic cartilage displays a distinctly different response to load compared to hyaline nasal cartilage which exhibits high resistance to instantaneous loads. [202]

In **chapter three** it appeared that cell density was significantly higher in alar cartilage than in cartilage obtained from the ear or septal cartilage. Besides, alar chondrocytes were larger, occupying a considerable part of the ECM. Although high cell density does not directly influence cartilage biomechanical behavior [162], lower volume of ECM fraction (due to higher cell fraction) is likely to affect biomechanics. [176]

Knowledge of the biochemical and biomechanical properties of the cartilage ECM in the head neck area will benefit future tissue engineering therapies. However, biomechanical properties of the ECM are not only determined by the amount of ECM components, but is also considerably influenced by ECM fiber orientation as well as binding between components. [301] Better insight into the three-dimensional (3D) interconnected ECM network will provide valuable information for future cell-based therapies. Especially when selecting and preparing a 3D scaffold (see below). Altogether, we have set a benchmark against which to evaluate cartilage tissue-engineering strategies in the head and neck area.

Cell sources

Q2 *Which cells or combination of cells are most suitable for cell-based cartilage repair in the head and neck area?*

Monoculture

Defining an appropriate cell source for successful cell-based cartilage repair in the head and neck area, is crucial. The goal of creating clinically relevant tissue-engineered cartilages places specific requirements on the cell source. The ideal cell source should meet specific requirements, including the availability of large quantities of cells with minimal invasive accessibility and the ability to produce cartilage ECM that resembles cartilage both in form and function.

The most obvious cell source for cartilage repair are chondrocytes themselves. However, to generate a cartilage construct of reasonable size, large numbers of chondrocytes are required, necessitating the use of culture-expansion. In **chapter four**, the cartilage-forming capacity of human culture-expanded chondrocytes from several anatomical locations (i.e. articular joint, ear, and nose) were studied. Independent on their origin, culture-expanded chondrocytes dedifferentiate; they change phenotypically to a fibroblast-like morphology and lose their chondrogenic potential. [61] As a result, chondrogenic gene-expression is reduced as well as their ability to produce cartilage ECM components. Redifferentiation and thereby restoration

of chondrogenic potential can however be facilitated in the presence of induction factors, like biological or biophysical stimuli. [365] However, induction factors can enhance but never emulate the complex process of cartilage regeneration and may have unpredictable effects on future clinical outcome.

Multipotent mesenchymal stem cells (MSCs) achieved considerable attention as alternative cells. They can undergo multiple population doublings without losing their chondrogenic potential and have the capacity to differentiate into cartilage tissue under appropriate culture conditions. [64-68] Furthermore, MSCs are easily available from several tissues, including bone marrow and adipose tissue, which makes culture-expansion unnecessary. However, their role in cell-based cartilage repair is currently debated, since MSCs terminally differentiate through the process of endochondral ossification. They produce cartilage ECM that is unstable (**chapter four**) and predisposed to mineralization and ossification *in vivo*. [69-71, 240, 241] However, significant research is required to understand and predict MSC behavior during chondrogenic differentiation and to prevent terminal differentiation. Therefore, the single use of either chondrocytes or MSCs is being questioned as appropriated cell sources for cell-based cartilage repair in the head and neck area.

Co-culture

Currently, combining both cell sources holds great promise for cell-based cartilage repair as it reduces the required number of chondrocytes and diminishes many disadvantages of both individual cell types. By decreasing the amount of chondrocytes required ($\leq 20\%$ of the total cell mixture), culture-expansion is no longer necessary, which allows the use of freshly isolated primary chondrocytes leading to improved cartilage formation. [76] The attribution of chondrocytes and stem cells are both essential in co-culture and are further discussed below.

(1) Chondrocytes

As the foundation of plastic reconstructive surgery focuses on replacing 'like tissue with like tissue', it seems only logical that for the reconstruction of cartilage defects in the head and neck area, location and type-specific chondrocytes are used. In **chapter four** we emphasize that only chondrocytes derived from elastic cartilage are able to produce an elastin-rich cartilage matrix and that chondrocytes derived from hyaline cartilage are not. Moreover, the properties of the ECM of location-specific hyaline chondrocytes (i.e. nasal or articular chondrocytes) are mutually different and remarkably related to their origin. Thereby, we further completed former research [56, 366] and conclude that location and type-specific chondrocytes ultimately result in cartilage regeneration of similar molecular nature. This means that for the reconstruction of cartilage defects in the head and neck area, ear and nasal chondrocytes are favorably used to repair ear or nasal cartilage defects respectively. Unfortunately, most co-culture research on cartilage repair has been performed on chondrocytes derived from articular cartilage and only few studies studied the combination of MSCs and non-articular chondrocytes such as ear [77-79, 367, 368] or nasal chondrocytes [80]. In **chapter six** we demonstrate that cartilage constructs containing a combination of 80 percent MSCs and 20 percent of primary ear or nasal chondrocytes produce similar quantities of cartilage matrix components as constructs containing chondrocytes only. Therefore, 80

percent of the chondrocytes can easily be replaced by MSCs without influencing cartilage matrix production. Co-culture supports the use of primary chondrocytes without the interference of culture-expansion and the process of redifferentiation, and only requires a small tissue biopsy of undamaged cartilage. Moreover, the use of cartilage remnants can be considered, such as chondrocytes derived from microtic cartilage. [79, 369, 370]

(2) Stem cells

Pluripotent stem cells, like human embryonic stem cells (ESCs) [371] or induced pluripotent stem cells (iPSCs) [372], are highly potential cell sources for tissue engineering purposes. These cells have unlimited capacity for self-renewal and the ability to differentiate into any mature cell type. In combination with chondrocytes, pluripotent stem cells improve cartilage formation *in vitro* and *in vivo*. [373-376] However, the use of human ESCs and iPSCs is currently impeded by the risk of teratoma formation and oncogenicity. [377, 378] Moreover, the application of human ESCs raise ethical concerns regarding their isolation from human embryos. To date, pluripotent stem cells seems mainly valuable for research purposes and not yet for clinical application.

Stem cells that have been most extensively studied for their application in chondrogenic co-cultures are MSCs. Unlike pluripotent stem cells, MSCs are multipotent possessing committed lineage differentiation potential and lacking unlimited self-renewal capacity. They are however (1) easily available from several tissues, including bone marrow, adipose tissue, synovium, peripheral blood, dental pulp, placenta, umbilical cord, and skeletal muscle [63], (2) have the ability to reconstitute cartilage tissue by the ability to chondrogenically differentiate [80, 253-262], and (3) possess chondro-inductive capacity that enables chondrocytes to facilitate cartilage repair and regeneration [379]. To date, MSCs from adipose tissue (AMSCs) and bone marrow (BMSCs) are best characterized. Our results from **chapter five and six** support a general trophic or immunomodulatory role for human AMSCs and BMSCs on chondrocytes in co-culture, in accordance to Wu [246] and Maumus *et al.* [247]. Although both cell sources share comparable immunomodulatory modalities and their immunophenotypes and gene-expression profiles are greater than 90% identical [380], they do not necessarily behave the same. Differences on molecular level have been recognized by others, reviewed by Strioga *et al.* [380] For instance, gene-expression profiles of BMSCs were only involved in WNT-signaling and differentiation pathways, whereas genes expressed uniquely by AMSCs were responsible for cellular communication and transcription control. [232] In addition, 18% of the generated proteins were found to be differentially produced between AMSCs and BSMCs [232]: compared to BMSCs, AMSCs secrete significantly more VEGF-D [269], IGF-1 [269, 270], IL-8 [269] and IL-6 [269, 271], and significantly less SDF-1 [272] and TFG β 1 [272]. Finally, dissimilarities were also observed between AMSCs and BMSCs in monoculture in **chapter four**. These location-specific MSCs possessed distinctive proliferation capacities and a dissimilar potential to chondrogenically differentiate. However, whether the differences between AMSCs and BMSCs are fully explained by the uniqueness of the stem cell population, or are just inherent to their heterogeneity and related to isolation and culture protocols, remains unclear. Most importantly, despite the minor differences between these

MSC-populations, AMSCs and BMSC seem both appropriate candidates for co-culture therapy in the head and neck area.

However, only few studies have directly compared their behavior in co-cultures. [80, 246, 247] Unfortunately, these studies demonstrate conflicting outcomes and have never translated to animal or preclinical research. Acharya *et al.* demonstrated enhanced chondrocyte proliferation capacity and improved sGAG formation in pellets containing BMSC/chondrocytes compared to AMSC/chondrocytes. [80] Besides, 3 independent co-culture studies using AMSCs showed limited or decreased effects of AMSCs on chondrogenesis. [243-245] Such effect was hardly seen in co-culture studies using BMSCs, which may propose that, compared to BMSCs, AMSCs seem less efficient in co-culture. Although we could not find a general beneficial effect of human BMSCs in co-cultures compared to human AMSCs in **chapter five**, we did show that *in vitro*, BMSC/chondrocytes outperformed AMSC/chondrocytes and hypertrophic gene expression was lower in BMSC/chondrocytes. True dissimilarities between human AMSCs and BMSCs in co-culture are unfortunately hard to expose, as human MSC-cultures are highly heterogeneous and distinct population subsets probably interfere with the reciprocal communication pathways in co-culture. Therefore, the purification of distinct subsets of human MSCs might enhance the particular capability of AMSCs and BMSCs in co-culture by eliminating interfering cells with limited potential, or even cells with inhibitory activity.

Unfortunately, in depth understanding of the cellular interaction pathways between MSCs and chondrocytes is under debate in literature. Numerous cellular communication pathways have been hypothesized in order to explain the beneficial effect in co-cultures [73]: (1) Chondrocyte-driven MSC-differentiation or (2) MSC-driven chondro-induction are considered the most plausible of them. [81] In recent years, the trophic and paracrine functions of MSCs appeared most critical in this process, rather than simple chondrogenic differentiation of MSCs alone as stated previously. [80, 253-262] In accordance to former research [74, 246, 263-268], we demonstrate (**chapter five and six**) that both AMSCs and BMSCs improve chondrocyte proliferation as well as ECM formation, which suggests a predominantly trophic role for MSCs in co-culture. We emphasize the importance of paracrine signaling pathways in co-culture comparatively to juxtacrine or gap-junctional signaling. The importance of direct cell-cell contact is still unclear in literature. [263] Nevertheless, in **chapter five and six**, such signaling pathways remained less important, as co-culture constructs were made of alginate hydrogel, impeding direct cell-cell contact. Moreover, in pellet culture no beneficial effect of direct cell-cell contact was observed. On the contrary, MSC-driven chondro-induction was less pronounced in Transwell® system and this effect was even further reduced by MSC-conditioned medium. Although direct cell-cell contact seems less significant than paracrine signaling, it seems correspondingly important to secure a certain cell-cell distance for optimal cell communication.

The fact that MSCs full fill a trophic role in co-culture and have been demonstrated to be immune privileged, it seems no longer necessary to use autologous MSCs only. The use of allogeneic MSCs have already been used for the treatment of steroid-resistant graft-versus-host disease, acute respiratory distress syndrome and Crohn's disease. [381] Even a few clinical trials have been commenced using allogeneic MSCs for cell-based cartilage repair in

the joint. (Reviewed by Vonk *et al.* [381]) The use of allogeneic MSCs gives the opportunity to generate “prefabricated” cell populations. Distinct isolation and co-culture protocols, as well as the effect of allogeneic MSCs on several scaffold materials, needs to be further elucidated for their possible future clinical use in cell-based cartilage repair in the head and neck area.

In conclusion, the combination of chondrocytes and MSCs holds great promise for cell-based cartilage repair in the head and neck area. Location and type-specific chondrocytes in combination with generally available MSCs are specifically recommended in this thesis.

Scaffolds

Currently, several 3D scaffolds have been developed and investigated for their use in cell-based cartilage repair. [83] They can be roughly classified into synthetic and natural scaffolds, and numerous of them have been introduced in the field of cartilage tissue engineering. [83] In this thesis, we have focussed on natural scaffolds only. In particular, the quality and suitability of alginate, bacterial nanocellulose and decellularized ECM were studied for tissue engineering purposes in the head and neck area.

Q3 *Which natural scaffolds (i.e. alginate, bacterial nanocellulose, decellularized ECM) are a suitable candidate for future cell-based cartilage repair in the head and neck area?*

Matrix-derived scaffolds

Scaffold selection have been an important pillar of the tissue engineering process. The contemporary concept of scaffold engineering is to mimic the natural micro-architecture of the 3D ECM of the targeted tissue itself. Scaffold design should thereby substitute for the cell natural environment providing instantaneous cell support and guiding tissue development and remodelling. Intuitively, native ECM has the potential to be the most ideal scaffold for tissue engineering and regenerative therapies. Preservation of native ECM is best retained through the process of decellularization. [93]

Decellularized ECM-derived scaffolds demonstrate immediate functional support [382] without evoking an adaptive immune response upon implantation due to absence of donor cellular and nuclear antigens [94]. Moreover, ECM-derived scaffolds provide specific structural, mechanical and biological cues to cells guiding tissue regeneration and remodeling. [82] The preparation as well as the biocompatibility of a decellularized cartilaginous ECM was extensively studied in **chapter seven**. In fact, we were the first to evaluate structural and functional properties of decellularized full-thickness ear cartilage scaffolds. Ear cartilage was decellularized utilizing the protocol of Kheir *et al.* [101] and modified by the incorporation of a 24 hour course of elastase (0.03 U/mL). The mechanism by which elastase contributed decellularization is unfortunately unknown. Elastin is however, one of the main ingredients of the pericellular matrix surrounding chondrocytes in elastic cartilage. [383] Degradation of this matrix protein would logically disintegrate the pericellular matrix facilitating the outflow of cellular material. Moreover, elastase does not only hydrolyse elastin proteins, but is also involved in the cleavage of other matrix components such as proteoglycans, collagens and fibronectin. [384-386] Breaking down these matrix components will further weaken the tightly interconnected ECM and will likely enhance decellularization. The decellularization protocol

described in **chapter seven** preserved native collagen and elastin contents of ear cartilage tissue, as well as cartilage major architecture and shape.

Despite recent progress in cartilage decellularization, there are some barriers that limit potential clinical application. First, the ability to revitalise ECM-derived cartilage scaffolds is critical for future clinical implementation. Recellularized ECM-derived scaffolds were non-cytotoxic and had the capability to allow chondrogenic differentiation of human MSCs (**chapter seven**). However, cell migration throughout the scaffold was non-existing and needs to be further improved to actually revitalize and thereby remodel tissue. Secondary, the complexity of cartilage structures in the head and neck area sets high standards to scaffold design. The shortage of (allogeneic) donors and the inability to accurately match cartilage shape of (allogeneic or xenogeneic) donor facial cartilages, impede its translation to clinical therapy. [295] Altogether, we have introduced a method to decellularized cartilage tissue while preserving its native 3D architecture and shape, providing an interesting scaffold for cartilage therapy in the head and neck area.

Matrix-inspired scaffolds

Another way to - at least partially - mimic structural and functional characteristics of native tissue microenvironment is the generation of ECM-inspired scaffolds. Basic requirements for biomimetic scaffold engineering demand (1) a scaffold with sufficient mechanical strength to retain size and shape ; (2) a 3D structure that allows tissue regeneration and homeostasis ; and (3) a biomaterial that is biocompatible without introducing an inflammatory response. In this thesis we used alginate and bacterial nanocellulose scaffolds for cell-based cartilage repair. Their properties based on these requirements are further discussed below.

(1) Biomechanical strength

For successful tissue-engineered cartilage, the 3D scaffold must provide sufficient mechanical strength in order to maintain size and shape when subjected to the forces of the implanted environment. Alginate biomechanical properties did not match mechanical stiffness of facial cartilages (1-15 MPa) and ranged from approximately 1 to 1000 kPa. [88] Due to its relatively poor biomechanical strength, alginate itself is not suspected to maintain size and shape after direct subcutaneous implantation. Bacterial nanocellulose, on the other hand, has biomechanical properties that reaches values analogous to facial cartilages. [155]

(2) Tissue regeneration and homeostasis

Biomimetic scaffold design must provide a natural 3D micro-environment that allows tissue regeneration and homeostasis. Cell-scaffold interactions are critical herein and fundamental for initial cell attachment, subsequent migration, proliferation, differentiation, and later tissue remodelling. Alginate permits the encapsulation of cells rather than actual cell attachment. Alginate encapsulation enables homogeneous 3D cell distribution and prevents cells from floating out. [387] Meanwhile, bacterial nanocellulose provides excellent cell attachment and migration, although cell migration is limited to the surface of the scaffold (i.e. impermeability). In **chapter eight** a bilayer bacterial nanocellulose scaffold, composed of a dense and a macroporous nanocellulose layer, was designed that enabled 3D cell migration. Both alginate

[388] and bacterial nanocellulose scaffolds [389] support tissue regeneration and homeostasis of several tissues including cartilage. Besides, in order to secure a viable tissue, scaffolds should facilitate diffusion of oxygen and nutrients, and removal of waste products. Both alginate [89, 388] and bacterial nanocellulose [92, 390] have high swollen 3D architecture, that enables sufficient nutrient diffusion and oxygen transfer to the residing cells.

(3) Biocompatibility

Scaffold biocompatibility is crucial for the overall success rate of a tissue engineering therapy. Biocompatibility is generally defined as “the ability of a biomaterial to perform with an appropriate host response in a specific situation”. [391] Moreover, scaffold biocompatibility not only depends on the ability to ensure cell viability (i.e. cytotoxicity). It is also the biological response of host tissue to the implanted scaffold material that can induce inflammation along with fibrous encapsulation of the material (i.e. foreign body reaction). The biocompatibility of highly purified alginate (Cellmed, Germany) has already been studied by others and is highly biocompatible both *in vitro* and *in vivo*. [251] In fact, alginate is already used for applications such as pharmaceutical applications, microencapsulation technology and wound dressings. [388, 392] The biocompatibility of bacterial nanocellulose was evaluated in **chapter eight** and more intensively studied by Martínez Ávila *et al.* according to the standards of ISO 10993. [393] Bacterial nanocellulose scaffold are non-cytotoxic and non-pyogenic. [393] Moreover, after subcutaneous implantation, these scaffolds induce minimal host response. [393] Both alginate and bacterial nanocellulose supported neocartilage formation *in vitro* and *in vivo* (this thesis) making them attractive biocompatible scaffolds for the reconstruction of cartilage defect in the head and neck area.

Another component of biocompatibility is biomaterial degradation, since the products of degradation can possibly influence biocompatibility in time. Neither alginate nor bacterial nanocellulose degrade, as mammals lack the enzyme alginase or cellulase respectively. They rather slowly dissolve in time. [388, 394] Both alginate [388] and bacterial nanocellulose [389] have shown mild inflammatory response after subcutaneous implantation that decreased in time. Moreover, derivatives of these biomaterials have already been used safely as biomedical devices in a clinical application. [395, 396]

In conclusion, both alginate and bacterial nanocellulose have characteristics that - at least partially - match the properties of the chondrogenic ECM itself. Alginate has poor biomechanical properties and is typically used as a cell-laden hydrogel, created to encapsulate cells. Infused into a biomechanical stable bacterial nanocellulose scaffold could be an excellent scaffold for future cell-based cartilage repair in the head and neck area. In **chapter eight** this concept was first introduced, showing that alginate-infused bacterial nanocellulose scaffolds are biocompatible and support neocartilage formation both *in vitro* and *in vivo*. Therefore, the combination of alginate and bacterial nanocellulose could provide a potential therapy for the reconstruction of cartilage defect in the head and neck area. Especially, when we could further emerge it to a bioprinting technology as written below.

Bioprinting

Recent developments in 3D bioprinting have brought immense excitement to the field of tissue engineering. In 3D bioprinting, scaffold biomaterials and living cells are accurately deposited in a layer-by-layer fashion. [397] Thereby, 3D bioprinting has the ability to control spatial placement of living cells relative to their neighboring cells or scaffold environment. Which in turn provides the ability to recreate the complexity of living tissues that mimic natural micro-architecture of the targeted tissue itself. The primary printing technology used for tissue engineering purposes is inkjet “drop-on-demand” bioprinting. [398] Essentially, inkjet bioprinting technology is based on digitally controlled ejection of drops of “bioink” from a print head onto a substrate. These bioinks are the building blocks of the regenerated tissue and contain living cells and/or scaffold biomaterials. [399] Both alginate [400, 401] and bacterial nanocellulose [402, 403] have been demonstrated to be excellent bioinks for 3D bioprinting purposes. They have shown good printability [400, 404] and high biocompatibility [400, 405]. So far, the clinical application of inkjet bioprinting has only sparsely been applied in the field of cartilage regeneration. [402, 404, 406] 3D bioprinting gives the opportunity to tissue engineer complex 3D tissues with high reproducibility, making it a very promising technique for the reconstruction of cartilage defects in the head and neck area.

Future perspectives

Over the past decades, there has been significant progress in the treatment of cartilage defects using tissue engineering strategies. Recently, the field is slowly changing from bench to bedside with a number of clinical and preclinical studies ongoing worldwide. (reviewed by Huang *et al.* [118]) However, these studies basically involve cell-based articular cartilage repair instead of the regeneration of cartilage defects in the head and neck area. Such translational research necessitates governmental oversight that guards efficacy and safety of innovative cell-based therapies in order to protect and guarantee public health. Ultimately, an one-step surgical therapy is preferred for the reconstruction of cartilage defects in the head and neck area.

Regulatory aspects of clinical application

The European Medicines Agency (EMA) and the Food and Drug Administration (FDA) are responsible for the surveillance and evaluation of medicinal products and devices in the European Union and United States respectively. However, the lack of a regulatory framework for tissue-engineered products (TEPs) has significantly impeded the translation of tissue engineering therapies to clinical application. [407] The introduction of Advanced Therapy Medicinal Products (ATMPs) in the European Union [408] and Human Cells and Tissues and Cellular- and Tissue-Based Products (HCT/Ps) in the United States [409], have substantially contributed to global biotechnology market growth [410] and provide a legitimate tool for overseeing TEPs. At present, only few cell-based therapies are awarded marketing authorization by the EMA or FDA. [410, 411] Of these TEPs, CarticelTM, ChondroCelect[®] and MACI[®] are the only licensed therapies for the reconstruction of cartilage defects. These advanced technologies are however entirely focused on the reconstruction of articular

cartilage defects. So far, no TEPs have been authorized for the treatment of cartilage defects in the head and neck area.

The manufacturing of TEPs that comply EMA or FDA guidelines require good manufacturing practices (GMP) [412] along with good laboratory practices and good clinical practices. As defined, GMP-protocols cover practically all aspects of product manufacturing and “ensure that products are consistently produced and controlled to the quality standards appropriate to their intended use”. [412, 413] Process performance and product quality are all comprised in GMP-protocols, including the training of qualified personnel, the validation and control of materials and procedures, the identity and sterility of the equipment, facility requirements, product traceability and reproducibility. Considering this, the translation of fundamental cell-based therapy into clinical product following GMP-guidelines is very challenging. Therefore, understanding and recognition of the regulatory environment early in the development of a cell-based therapy is critical for the overall success of TEPs.

Translation towards a cell-based therapy

Tissue engineering strategies could technically simplify and thereby improve the surgical treatment of cartilage defect in the head and neck area. Although our research could not directly translate towards a clinical cell-based therapy, it has identified potential for future translational research. First, the combination of chondrocytes and MSCs has held great promise for cell-based cartilage repair in the head and neck area. For implementation of such therapy, an optimal cell density and ratio of MSCs to chondrocytes is imperative. Puelacher *et al.* already recommended cell densities greater than 20×10^6 cells per milliliter. [239] That means that for the reconstruction of - for example - the ear, one should require 140×10^6 cells in total, assuming that the volume of adult ear cartilage comprises approximately 7 milliliter (data not shown). Using only 20% primary chondrocytes (at a MSC-chondrocyte ratio of 4:1) as described previously, [74, 246] a feasible amount of 28×10^6 chondrocytes and 112×10^6 MSCs are necessary. However, no consensus on optimal co-culture ratios is yet available. Future research needs to clarify if we could increase cell density while further reduce the number of primary chondrocytes without inhibiting cartilage matrix production and stability.

In the translation towards a cell-based therapy, the selection of a scaffold is crucial as stated before. Recent advances in the field of cartilage tissue engineering have been driven from “cell-based” towards “cell-free” regenerative therapies. [414] Acellular biomaterials mimic native ECM and thereby attract native progenitor cells to migrate into the biomaterial and trigger chondrogenic differentiation. To date, acellular biomaterials have shown promising regenerative effects on various tissues (Acellular biomaterials: an evolving alternative to cell-based therapies. Burdick. 2013) including articular cartilage [415]. However, it is less likely that these acellular biomaterials have similar effect on cartilage defects in the head and neck area, as native progenitor cells are generally missing (i.e. congenital, trauma, cancer) or genetically diseased (i.e. congenital remnants). Therefore, for future cell-based cartilage repair in the head and neck area a cellular 3D scaffold that - at least partially - mimics structural and functional characteristics of native tissue microenvironment is imperative.

In conclusion, this thesis has focussed on the generation of a tissue-engineered cartilaginous framework for the reconstruction of cartilage defects in the head and neck area

and has identified potential for future translational research. For cell source selection, we recommend to use location and type-specific chondrocytes. Interestingly, 80 percent of chondrocytes can be replaced by MSCs without influencing cartilage matrix production nor stability. Thereby, the use of primary cells is warranted, as MSCs can be obtained relatively easy in larger numbers. In this co-culture procedure, a general trophic or immunomodulatory role is provided by MSCs. For scaffold selection, we recommend to use a 3D scaffolds that mimic natural micro-architecture of the 3D ECM of the targeted tissue itself. Although decellularized scaffolds are intuitively the most ideal scaffold for tissue engineering therapies, their application seems currently mainly valuable for research purposes and not yet for clinical application in the head and neck area. Therefore, we have focussed on natural matrix-inspired scaffolds (i.e. alginate and bacterial nanocellulose). Both alginate and bacterial nanocellulose have characteristics that - at least partially - match the properties of the chondrogenic ECM itself. The combination of alginate and bacterial nanocellulose could provide a potential therapy for the reconstruction of cartilage defect in the head and neck area.

Chapter 10

Summary

Cartilage tissue engineering can offer promising solutions for restoring cartilage defects in the head and neck area and has the potential to overcome limitations of current treatments, reestablishing unique biological and functional properties of the tissue. This thesis focuses on the requirements that are necessary for future cell-based cartilage repair in the head and neck area. Specifically, the suitability of *cells* or combination of cells on natural *scaffolds* were evaluated.

Cartilage is a highly complex avascular tissue comprising chondrocytes surrounded by a dense extracellular matrix that contains various macromolecules such as proteoglycans, collagens and elastin. Due to its avascular nature, cartilage has a very limited capacity for self-repair once damaged. Tissue engineering is a promising potential treatment modality for the reconstruction of such defects. Cartilage morphology and molecular composition as well as the fundamentals of tissue engineering are introduced in **chapter one**.

Chapter two and three established a precise biomechanical and biochemical characterization of native human ear and nasal cartilages (i.e. nasoseptal and alar cartilages) in order to set a benchmark against which to evaluate cartilage tissue engineering attempts. In general, indentation E_{eq} of human adult facial cartilages ranged from approximately 1-15 MPa. Ear cartilage had significantly lower stiffness compared to nasal cartilage, although regional variations were observed. Ear cartilage biomechanical properties are most likely related to the presence of elastin in the extracellular matrix.

Defining an appropriate cell source for successful cell-based cartilage repair in the head and neck area is crucial. Currently, cell-based cartilage repair is predominantly based on two distinct cell types: chondrocytes and mesenchymal stem cells. However, their individual use is associated with specific disadvantages. First, chondrocyte-based cartilage repair is limited by the ability to obtain sufficient numbers of chondrocytes, necessitating the use of culture-expansion. During culture expansion, chondrocytes change phenotypically to a fibroblast morphology and lose their chondrogenic potential; they dedifferentiate. Second, mesenchymal-stem-cell-based cartilage repair is hampered by the phenomenon of chondrocyte hypertrophy. During chondrogenic differentiation, they undergo terminal differentiation through the process of endochondral ossification and produce cartilage that is unstable and predisposed to mineralization and ossification *in vivo*. In **chapter four**, the cartilage-forming capacity of cells from several anatomical locations were studied. Independent on their origin (i.e. articular joint, ear, and nose), culture-expanded chondrocytes dedifferentiated. After chondrogenic stimulation, ear and nasal chondrocytes were most potent for cartilage regeneration *in vivo*. Moreover, location and type-specific chondrocytes resulted in cartilage regeneration of their original molecular nature.

Currently, the combination of chondrocytes and mesenchymal stem cells holds great promise for cell-based cartilage repair as it reduces the required number of chondrocytes and diminishes many disadvantages of the individual cell types. Co-cultures of primary chondrocytes (i.e. articular, ear, and nasal chondrocytes) and mesenchymal stem cells (i.e. adipose-tissue-derived and bone-marrow-derived mesenchymal stem cells) were further elucidated in **chapter five and six**. Eighty percent of the chondrocytes could be replaced by mesenchymal stem cells without influencing cartilage matrix production nor stability. Clear location and type-specific differences were observed in co-cultures containing articular, ear

or nasal chondrocytes. Meanwhile, large differences between adipose-tissue-derived and bone-marrow-derived mesenchymal stem cells in co-culture were hard to expose. In co-culture, we found no evidence that cartilage formation was the consequence of chondrogenic lineage differentiation of mesenchymal stem cells. In contrast, the cartilage matrix that was formed, clearly originated from chondrocytes, which suggested a predominantly trophic role for mesenchymal stem cells. The trophic and paracrine function of mesenchymal stem cells herein appeared essential rather than mesenchymal stem cells actively undergoing chondrogenic differentiation. We showed that stem cell trophic function is a general feature that applies to both adipose-tissue-derived and bone-marrow-derived mesenchymal stem cells. Co-culture supports the application of a one-stage cell-based cartilage repair procedure for cartilage defects in the head and neck area. Ear and nasal chondrocytes in combination with generally available mesenchymal stem cells are specifically recommend for the reconstruction of ear and nasal cartilage defects respectively.

For successful cartilage regeneration, the properties of the three dimensional scaffold are of equivalent importance. The contemporary concept of scaffold engineering is to - at least partially - mimic the natural micro-architecture of the three dimensional extracellular matrix of the targeted tissue itself. Intuitively, native extracellular matrix has the potential to be the most ideal scaffold for tissue engineering and regenerative therapies. Preservation of native extracellular matrix is best retained through the process of decellularization. The decellularization protocol described in **chapter seven** preserved native collagen and elastin contents of full-thickness ear cartilage tissue, as well as cartilage major architecture and shape. Moreover, decellularized scaffolds were non-cytotoxic and supported chondrogenic differentiation of mesenchymal stem cells *in vitro*. Thereby, we have introduced a decellularized matrix-derived scaffold with potential therapeutic benefits.

However, at this stage, the shortage of donors and the inability to accurately match cartilage shape of donor facial cartilages, impedes its translation towards a clinical therapy for cartilage defect in the head and neck area. Therefore, natural scaffolds, in particular alginate and bacterial nanocellulose have been further characterized for their use in cartilage tissue engineering. Both alginate and bacterial nanocellulose scaffolds support cartilage tissue regeneration and homeostasis. Besides, bacterial nanocellulose has biomechanical properties that reaches values analogous to facial cartilages. Alginate, on the other hand, has poor biomechanical properties and is typically used as a cell-laden hydrogel, created to encapsulate cells. In **chapter eight** bacterial nanocellulose scaffolds were infused with cells encapsulated in alginate. These hybrid scaffolds were biocompatible and supported neocartilage formation both *in vitro* and *in vivo*. Therefore, the combination of alginate and bacterial nanocellulose could provide a potential therapy for the reconstruction of cartilage defect in the head and neck area.

Our research has identified potential for future translational research in the head and neck area. Tissue engineering strategies could technically simplify and thereby improve the surgical treatment of cartilage defect in the head and neck area.

Chapter 11

Nederlandse samenvatting

Kraakbeendefecten in het hoofd-/halsgebied zijn een uitdagend probleem voor de reconstructief chirurg. Kraakbeen tissue engineering lijkt een veelbelovende alternatieve therapie. Dit proefschrift richt zich op de verschillende aspecten van kraakbeen tissue engineering in het hoofd-/halsgebied. Specifiek worden het gebruik van *cellen* (of combinatie van cellen) op natuurlijke *scaffolds of dragermaterialen* besproken.

Kraakbeen is een zeer unieke vorm van bindweefsel en zorgt in het hoofd-/hals gebied voor de vorm en functie van onder andere oren en neus. Het bestaat voor een fractie uit chondrocyten omgeven door een grote hoeveelheid extracellulaire matrix. De opbouw en structuur van deze matrix bepaalt de eigenschappen van het kraakbeen, waarbij grofweg drie typen onderscheiden kunnen worden: hyalien, elastisch en fibrotisch kraakbeen. Wanneer kraakbeen in het hoofd-/halsgebied beschadigd is geraakt of congenitaal onvoldoende gevormd, herstelt het zich niet of nauwelijks. Tissue engineering, oftewel de regeneratie van weefsel uit levende cellen, is mogelijk een veelbelovende alternatieve therapie voor de behandeling van deze defecten. In **hoofdstuk één** worden de eigenschappen en moleculaire samenstelling van de verschillende kraakbeentypen beschreven. Daarnaast wordt het concept van tissue engineering geïntroduceerd en welke rol deze zou kunnen hebben bij de reconstructie van kraakbeendefecten in het hoofd-/halsgebied.

Voor kraakbeen tissue engineering is het allereerst van belang de intrinsieke kenmerken van het oorspronkelijke weefsel te kennen, zodat een benchmark verkregen kan worden waarmee getissue-engineerd kraakbeen vergeleken kan worden. In **hoofdstuk twee en drie** worden de biomechanische en biochemische eigenschappen van humaan oor- en neuskraakbeen (septum en ala nasi) uitvoerig geanalyseerd. In het algemeen kon gesteld worden dat de biomechanische eigenschappen (uitgedrukt in indentatie E_{eq}) van humaan volwassen kraakbeen van het aangezicht varieerden van 1-15 MPa. Oorkraakbeen had aanzienlijk lagere biomechanische eigenschappen in vergelijking met neuskraakbeen, hoewel er regionale variaties werden waargenomen binnen de verschillende kraakbeentypen. De biomechanische eigenschappen van oorkraakbeen konden voornamelijk worden toegeschreven aan de aanwezigheid van elastine in de extracellulaire matrix van oorkraakbeen.

Het selecteren van cellen of een combinatie van cellen is van cruciaal belang in de regeneratieve geneeskunde. Momenteel is kraakbeen tissue engineering voornamelijk gebaseerd op twee verschillende soorten cellen, namelijk: chondrocyten en mesenchymale stamcellen. Wanneer deze cellen echter onafhankelijk van elkaar worden gebruikt, brengt dat tot op heden specifieke nadelen met zich mee. Allereerst, kraakbeen tissue engineering gebaseerd op alléén chondrocyten wordt aanzienlijk beperkt door de hoeveelheid kraakbeen dat kan worden gebiopteerd. Doordat de opbrengst van chondrocyten hierdoor beperkt is, is expanderen (vermenigvuldigen) van chondrocyten in een laboratorium noodzakelijk. Echter, tijdens het expanderen veranderen chondrocyten van vorm en functie en verliezen zij hun kraakbeeneigenschappen: zij dedifferentiëren. Ten tweede, kraakbeen tissue engineering gebaseerd op alléén mesenchymale stamcellen wordt belemmerd door het feit dat stamcellen tijdens het differentiatieproces van stamcel naar chondrocyt niet in staat zijn kraakbenig te blijven en uiteindelijk terminaal differentiëren via het proces van enchondrale ossificatie. Terminaal gedifferentieerd (of hypertrofisch) kraakbeen is instabiel en heeft een grote kans

te mineraliseren en ossificeren *in vivo*. In **hoofdstuk vier** wordt de kraakbeenvormende capaciteit van verschillende cellen van verschillende anatomische locaties vergeleken. Geëxpandeerde chondrocyten dedifferentieerden onafhankelijk van hun origine (gewricht, oor, neus). Na chondrogene stimulatie bleken chondrocyten van oor- en neuskraakbeen het meest potent voor kraakbeen tissue engineering *in vivo*. Tevens waren locatie- en kraakbeentype specifieke chondrocyten in staat kraakbeen te produceren met specifieke kraakbeeneigenschappen en moleculaire samenstelling, gerelateerd aan de eigenschappen van het originele donorkraakbeen. Dit betekent dat chondrocyten van oor- en neuskraakbeen het meest geschikt lijken voor de reconstructie van oor- en neuskraakbeendefecten respectievelijk.

Recente inzichten tonen dat de combinatie van chondrocyten en mesenchymale stamcellen ("co-kweken") een positief effect heeft op de kraakbeenvorming en daardoor een veelbelovend concept lijkt voor de behandeling van kraakbeendefecten in het hoofd-/halsgebied. "Co-kweken" heeft een aantal voordelen ten opzicht van het onafhankelijk gebruik van cellen zoals eerder beschreven. Door het combineren van cellen, kan een groot aantal chondrocyten vervangen worden door mesenchymale stamcellen. Hierdoor kan gebruik worden gemaakt van primaire cellen; cellen die direct ingezet kunnen worden voor reconstructiedoeleinden zonder een daarvoorafgaande *in vitro* expansie fase. In **hoofdstuk vijf en zes** wordt het "co-kweken" van primaire chondrocyten (gewricht, oor, neus) in combinatie met mesenchymale stamcellen (vet, beenmerg) verder bestudeerd. Kraakbeenproductie en stabiliteit werden niet negatief beïnvloed door het vervangen van tachtig procent van de chondrocyten door mesenchymale stamcellen. Kraakbeen regeneratie bleek in "co-kweek" niet het resultaat van chondrogene differentiatie van mesenchymale stamcellen, maar eerder het gevolg van toenemende kraakbeenproductie door chondrocyten onder invloed van stamcellen. Voor de mesenchymale stamcellen bleek uiteindelijk dan ook meer een trofische rol weggelegd in "co-kweek". Deze trofische functie werd in gelijke mate gezien bij zowel stamcellen uit vet als uit beenmerg en is meest waarschijnlijk een algemene functie van de stamcel onafhankelijk van zijn origine. Dit in tegenstelling tot de origine van de verschillende typen chondrocyten (gewricht, oor, neus). Ook in "co-kweek" waren deze locatie- en kraakbeentype specifieke chondrocyten in staat kraakbeen te produceren met specifieke eigenschappen gerelateerd aan het originele donorkraakbeen. De combinatie van primaire chondrocyten en mesenchymale stamcellen, voorkomt een periode van expansie, en ondersteunt de mogelijkheid om in de toekomst een één-stap-techniek te kunnen verwezenlijken voor de behandeling van kraakbeendefect in het hoofd-/halsgebied. Chondrocyten van oor- en neuskraakbeen in combinatie met mesenchymale stamcellen worden hierin specifiek aangeraden voor de reconstructie van oor- en neuskraakbeendefecten respectievelijk.

Naast het selecteren van geschikte cellen, is ook de selectie van een scaffold essentieel voor kraakbeen tissue engineering. Een ideale scaffold heeft een driedimensionale structuur, welke de micro-architectuur van het oorspronkelijke weefsel of specifiek - de extracellulaire matrix van het oorspronkelijke weefsel - zo veel mogelijk nabootst. Het lijkt dan ook niet meer dan vanzelfsprekend, dat een scaffold ontstaan vanuit de oorspronkelijke extracellulaire matrix het meest geschikt is voor regeneratieve doeleinden. Decellularisatie is een manier om

deze oorspronkelijke matrix te vergaren. In **hoofdstuk zeven** wordt het decellularisatieprotocol van bovien en humaan oorkraakbeen beschreven. Na decellularisatie, werd een matrix gerealiseerd waarin geen cellen of celresten meer konden worden aangetoond. Daarnaast, kon de hoeveelheid collageen en elastine tijdens het decellularisatieproces behouden blijven, evenals de vorm en architectuur van het kraakbeen. Gedecellulariseerd kraakbeen bleek niet cytotoxisch waardoor mesenchymale stamcellen in staat waren chondrogeen te differentiëren na contact met deze scaffolds. Gedecellulariseerde kraakbeenscaffolds bieden daardoor mogelijk een veelbelovende therapie voor de behandeling van kraakbeendefecten in de toekomst.

Echter, de translatie van deze potentiële therapie naar een definitieve behandeling van kraakbeendefecten in het hoofd-/halsgebied, lijkt heden belemmerd door een tekort aan donoren en het onvermogen om de kraakbeenvorm van de donor nauwkeurig te laten overeenkomen met de specifieke eisen van het te regenereren kraakbeen in het aangezicht. Naast gedecellulariseerde scaffolds - scaffolds die zijn geëxtraheerd vanuit de oorspronkelijk extracellulaire matrix - zijn er ook scaffolds in ontwikkeling die de driedimensionale architectuur van oorspronkelijke matrix zoveel mogelijk proberen na te bootsen. Deze scaffolds kunnen grofweg onderverdeeld worden in natuurlijke en synthetische scaffolds. In dit proefschrift wordt specifiek gebruik gemaakt van twee natuurlijk scaffolds, te weten alginaat en bacterieel nanocellulose. Beide scaffolds ondersteunen kraakbeenregeneratie en –hemostase. Daarnaast zijn de biomechanische eigenschappen van bacterieel nanocellulose scaffold vergelijkbaar met de eigenschappen van aangezichtskraakbeen, zoals oor- en neuskraakbeen. Deze biomechanische eigenschappen heeft alginaat niet. Alginaat gel wordt voornamelijk gebruikt voor het inkapselen van levende cellen, waarbij het alginaat voor een homogene distributie van cellen zorgt en tevens voorkomt dat cellen uit de gel kunnen vallen. In **hoofdstuk acht** worden scaffolds van bacterieel nanocellulose geïnfundeerd met een cel-alginaat gel. Deze hybride scaffold bleek biocompatibel en was in staat kraakbeen regeneratie te ondersteunen *in vitro* en *in vivo*. De combinatie van beide materialen lijkt dan ook een potentiële therapie voor de reconstructie van kraakbeendefecten in het hoofd-/halsgebied.

De resultaten van dit proefschrift zijn een belangrijke stap voor de toekomstige behandeling van kraakbeendefecten in het hoofd-/halsgebied. Door gebruik te maken van tissue-engineering technieken kunnen huidige chirurgisch technieken worden vereenvoudigd wat naar verwachting een positieve invloed zal hebben op de behandeling van kraakbeendefecten van het aangezicht.

References

1. McDowell, F., *The classic reprint. Ancient ear-lobe and rhinoplastic operations in India*. Plast Reconstr Surg, 1969. **43**(5): p. 515-22.
2. Micali, G., *The Italian contribution to plastic surgery*. Ann Plast Surg, 1993. **31**(6): p. 566-71.
3. Tagliacozzi, G., *De curtorum chirurgia per insitionem libri duo*. 1597, Venice.
4. Seidenberg, B., et al., *Immediate reconstruction of the cervical esophagus by a revascularized isolated jejunal segment*. Ann Surg, 1959. **149**(2): p. 162-71.
5. Gillies, H., *Reconstruction of the external ear with special reference to the use of maternal ear cartilages as the supporting structure*. Revue de Chirurgie Structrice, 1937. **7**.
6. Gillies, H., *A new free graft applied to reconstruction of the nostril*. British Journal of Surgery, 1943. **30**: p. 305.
7. Tanzer, R.C., *Total reconstruction of the external ear*. Plast Reconstr Surg Transplant Bull, 1959. **23**(1): p. 1-15.
8. Brent, B., *Microtia repair with rib cartilage grafts: a review of personal experience with 1000 cases*. Clin Plast Surg, 2002. **29**(2): p. 257-71, vii.
9. Nagata, S., *A new method of total reconstruction of the auricle for microtia*. Plast Reconstr Surg, 1993. **92**(2): p. 187-201.
10. Burget, G.C. and F.J. Menick, *Nasal support and lining: the marriage of beauty and blood supply*. Plast Reconstr Surg, 1989. **84**(2): p. 189-202.
11. Menick, F.J., *Nasal reconstruction: art and practice*. . 2008: Saunders-Elsevier.
12. Menick, F.J., *Nasal reconstruction*. Plast Reconstr Surg, 2010. **125**(4): p. 138e-150e.
13. Neligan, P.C., *Plastic surgery*. 3 ed. Craniofacial, head and neck surgery, ed. E.D. Rodriguez. Vol. 3. 2013: Elsevier Inc.
14. Peer, A.L., *Diced cartilage grafts*. . Archives of Otolaryngology, 1943. **38**(156).
15. Young, F., *Autogenous cartilage grafts: An experimental study*. . Surgery 1941. **10**(7).
16. Peer, L.A., *Reconstruction of the auricle with diced cartilage grafts in a Vitallium ear mold*. Plastic and reconstructive surgery 1948. **3**: p. 653-666.
17. Wintsch, K., *Reconstruction of the collapsed nose*. . Surgical Rehabilitation in Leprosy., 1974.
18. Tovey, F.I., *Reconstruction of the nose in leprosy patients*. Lepr Rev, 1965. **36**(4): p. 215-20.
19. Ousterhout, D.K. and E.J. Stelnicki, *Plastic surgery's plastics*. Clin Plast Surg, 1996. **23**(1): p. 183-90.
20. Rubin, J. and M. Yaremchuk, *Complications and toxicities of implantable biomaterials used in facial reconstructive and aesthetic surgery: a comprehensive review of the literature*. Plast Reconstr Surg, 1997. **100**(5): p. 1336-1353.
21. Peled, Z.M., et al., *The use of alloplastic materials in rhinoplasty surgery: a meta-analysis*. Plast Reconstr Surg, 2008. **121**(3): p. 85e-92e.
22. Langer, R. and J.P. Vacanti, *Tissue engineering*. Science, 1993. **260**(5110): p. 920-6.
23. Nayyer, L., et al., *Design and development of nanocomposite scaffolds for auricular reconstruction*. Nanomedicine, 2014. **10**(1): p. 235-46.
24. Zopf, D.A., et al., *Biomechanical evaluation of human and porcine auricular cartilage*. Laryngoscope, 2015. **125**(8): p. E262-8.
25. Rotter, N., et al., *Age-related changes in the composition and mechanical properties of human nasal cartilage*. Arch Biochem Biophys, 2002. **403**(1): p. 132-40.
26. Richmon, J.D., et al., *Tensile biomechanical properties of human nasal septal cartilage*. Am J Rhinol, 2005. **19**(6): p. 617-22.
27. Richmon, J.D., et al., *Compressive biomechanical properties of human nasal septal cartilage*. Am J Rhinol, 2006. **20**(5): p. 496-501.
28. Griffin, M.F., et al., *Biomechanical characterisation of the human nasal cartilages; implications for tissue engineering*. J Mater Sci Mater Med, 2016. **27**(1): p. 11.
29. Westreich, R.W., et al., *Defining nasal cartilage elasticity: biomechanical testing of the tripod theory based on a cantilevered model*. Arch Facial Plast Surg, 2007. **9**(4): p. 264-70.
30. Alkan, Z., et al., *Tensile characteristics of costal and septal cartilages used as graft materials*. Arch Facial Plast Surg, 2011. **13**(5): p. 322-6.
31. Muiznieks, L.D. and F.W. Keeley, *Molecular assembly and mechanical properties of the extracellular matrix: A fibrous protein perspective*. Biochim Biophys Acta, 2013. **1832**(7): p. 866-75.
32. Hardingham, T., B.C. Heng, and P. Gribbon, *New approaches to the investigation of hyaluronan networks*. Biochem Soc Trans, 1999. **27**(2): p. 124-7.
33. Eyre, D.R. and H. Muir, *The distribution of different molecular species of collagen in fibrous, elastic and hyaline cartilages of the pig*. Biochem J, 1975. **151**(3): p. 595-602.

34. Muir, H., *The chondrocyte, architect of cartilage. Biomechanics, structure, function and molecular biology of cartilage matrix macromolecules*. Bioessays, 1995. **17**(12): p. 1039-48.
35. Sophia Fox, A.J., A. Bedi, and S.A. Rodeo, *The basic science of articular cartilage: structure, composition, and function*. Sports Health, 2009. **1**(6): p. 461-8.
36. Grunhagen, T., et al., *Nutrient supply and intervertebral disc metabolism*. J Bone Joint Surg Am, 2006. **88 Suppl 2**: p. 30-5.
37. Fox, A.J., A. Bedi, and S.A. Rodeo, *The basic science of human knee menisci: structure, composition, and function*. Sports Health, 2012. **4**(4): p. 340-51.
38. Becker, I., S.J. Woodley, and M.D. Stringer, *The adult human pubic symphysis: a systematic review*. J Anat, 2010. **217**(5): p. 475-87.
39. Naumann, A., et al., *Tissue engineering of autologous cartilage grafts in three-dimensional in vitro macroaggregate culture system*. Tissue Eng, 2004. **10**(11-12): p. 1695-706.
40. Pleumeekers, M.M., et al., *The in vitro and in vivo capacity of culture-expanded human cells from several sources encapsulated in alginate to form cartilage*. Eur Cell Mater, 2014. **27**: p. 264-80; discussion 278-80.
41. El Sayed, K., et al., *Heterotopic autologous chondrocyte transplantation--a realistic approach to support articular cartilage repair?* Tissue Eng Part B Rev, 2010. **16**(6): p. 603-16.
42. Lohan, A., et al., *In vitro and in vivo neo-cartilage formation by heterotopic chondrocytes seeded on PGA scaffolds*. Histochem Cell Biol, 2011. **136**(1): p. 57-69.
43. Zhang, L. and M. Spector, *Comparison of three types of chondrocytes in collagen scaffolds for cartilage tissue engineering*. Biomed Mater, 2009. **4**(4): p. 045012.
44. Isogai, N., et al., *Comparison of different chondrocytes for use in tissue engineering of cartilage model structures*. Tissue Eng, 2006. **12**(4): p. 691-703.
45. Lee, J., et al., *Comparison of articular cartilage with costal cartilage in initial cell yield, degree of dedifferentiation during expansion and redifferentiation capacity*. Biotechnol Appl Biochem, 2007. **48**(Pt 3): p. 149-58.
46. Asawa, Y., et al., *Aptitude of auricular and nasoseptal chondrocytes cultured under a monolayer or three-dimensional condition for cartilage tissue engineering*. Tissue Eng Part A, 2009. **15**(5): p. 1109-18.
47. Malicev, E., et al., *Comparison of articular and auricular cartilage as a cell source for the autologous chondrocyte implantation*. J Orthop Res, 2009. **27**(7): p. 943-8.
48. Kafienah, W., et al., *Three-dimensional tissue engineering of hyaline cartilage: comparison of adult nasal and articular chondrocytes*. Tissue Eng, 2002. **8**(5): p. 817-26.
49. Johnson, T.S., et al., *Integrative repair of cartilage with articular and nonarticular chondrocytes*. Tissue Eng, 2004. **10**(9-10): p. 1308-15.
50. Chung, C., et al., *Differential behavior of auricular and articular chondrocytes in hyaluronic acid hydrogels*. Tissue Eng Part A, 2008. **14**(7): p. 1121-31.
51. Panossian, A., et al., *Effects of cell concentration and growth period on articular and ear chondrocyte transplants for tissue engineering*. Plast Reconstr Surg, 2001. **108**(2): p. 392-402.
52. Tay, A.G., et al., *Cell yield, proliferation, and postexpansion differentiation capacity of human ear, nasal, and rib chondrocytes*. Tissue Eng, 2004. **10**(5-6): p. 762-70.
53. Xu, J.W., et al., *Injectable tissue-engineered cartilage with different chondrocyte sources*. Plast Reconstr Surg, 2004. **113**(5): p. 1361-71.
54. Van Osch, G.J., et al., *Considerations on the use of ear chondrocytes as donor chondrocytes for cartilage tissue engineering*. Biorheology, 2004. **41**(3-4): p. 411-21.
55. Afizah, H., et al., *A comparison between the chondrogenic potential of human bone marrow stem cells (BMSCs) and adipose-derived stem cells (ADSCs) taken from the same donors*. Tissue Eng, 2007. **13**(4): p. 659-66.
56. Hellingman, C.A., et al., *Differences in cartilage-forming capacity of expanded human chondrocytes from ear and nose and their gene expression profiles*. Cell Transplant, 2011. **20**(6): p. 925-40.
57. Henderson, J.H., et al., *Cartilage tissue engineering for laryngotracheal reconstruction: comparison of chondrocytes from three anatomic locations in the rabbit*. Tissue Eng, 2007. **13**(4): p. 843-53.
58. Kusuvara, H., et al., *Tissue engineering a model for the human ear: assessment of size, shape, morphology, and gene expression following seeding of different chondrocytes*. Wound Repair Regen, 2009. **17**(1): p. 136-46.
59. Karlsson, C., et al., *Differentiation of human mesenchymal stem cells and articular chondrocytes: analysis of chondrogenic potential and expression pattern of differentiation-related transcription factors*. J Orthop Res, 2007. **25**(2): p. 152-63.

60. van Osch, G.J.V.M., et al., *Considerations on the use of ear chondrocytes as donor chondrocytes for cartilage tissue engineering*. Biorheology, 2004. **41**(3-4): p. 411-421.
61. Von Der Mark, K., et al., *Relationship between cell shape and type of collagen synthesised as chondrocytes lose their cartilage phenotype in culture*. Nature, 1977. **267**(5611): p. 531-532.
62. Caplan, A.I., *Mesenchymal stem cells*. J Orthop Res, 1991. **9**(5): p. 641-50.
63. Nazempour, A. and B.J. Van Wie, *Chondrocytes, Mesenchymal Stem Cells, and Their Combination in Articular Cartilage Regenerative Medicine*. Ann Biomed Eng, 2016. **44**(5): p. 1325-54.
64. Johnstone, B., et al., *In vitro chondrogenesis of bone marrow-derived mesenchymal progenitor cells*. Exp Cell Res, 1998. **238**(1): p. 265-72.
65. Caplan, A.I., *Review: mesenchymal stem cells: cell-based reconstructive therapy in orthopedics*. Tissue Eng, 2005. **11**(7-8): p. 1198-211.
66. Pittenger, M.F., et al., *Multilineage potential of adult human mesenchymal stem cells*. Science, 1999. **284**(5411): p. 143-7.
67. Zuk, P.A., et al., *Human adipose tissue is a source of multipotent stem cells*. Mol Biol Cell, 2002. **13**(12): p. 4279-95.
68. Zuk, P.A., et al., *Multilineage cells from human adipose tissue: implications for cell-based therapies*. Tissue Eng, 2001. **7**(2): p. 211-28.
69. Pelttari, K., et al., *Premature induction of hypertrophy during in vitro chondrogenesis of human mesenchymal stem cells correlates with calcification and vascular invasion after ectopic transplantation in SCID mice*. Arthritis Rheum, 2006. **54**(10): p. 3254-66.
70. Farrell, E., et al., *In-vivo generation of bone via endochondral ossification by in-vitro chondrogenic priming of adult human and rat mesenchymal stem cells*. BMC Musculoskelet Disord, 2011. **12**: p. 31.
71. Farrell, E., et al., *Chondrogenic priming of human bone marrow stromal cells: a better route to bone repair?* Tissue Eng Part C Methods, 2009. **15**(2): p. 285-95.
72. Scotti, C., et al., *Recapitulation of endochondral bone formation using human adult mesenchymal stem cells as a paradigm for developmental engineering*. Proc Natl Acad Sci U S A, 2010. **107**(16): p. 7251-6.
73. Hendriks, J., J. Riesle, and C.A. van Blitterswijk, *Co-culture in cartilage tissue engineering*. J Tissue Eng Regen Med, 2007. **1**(3): p. 170-8.
74. Wu, L., et al., *Trophic effects of mesenchymal stem cells increase chondrocyte proliferation and matrix formation*. Tissue Eng Part A, 2011. **17**(9-10): p. 1425-36.
75. Leijten, J.C., et al., *Cell sources for articular cartilage repair strategies: shifting from monocultures to cocultures*. Tissue Eng Part B Rev, 2013. **19**(1): p. 31-40.
76. Meretoja, V.V., et al., *Articular chondrocyte redifferentiation in 3D co-cultures with mesenchymal stem cells*. Tissue Eng Part C Methods, 2014. **20**(6): p. 514-23.
77. Kang, N., et al., *Effects of co-culturing BMSCs and auricular chondrocytes on the elastic modulus and hypertrophy of tissue engineered cartilage*. Biomaterials, 2012. **33**(18): p. 4535-44.
78. Lv, X., et al., *Chondrogenesis by co-culture of adipose-derived stromal cells and chondrocytes in vitro*. Connect Tissue Res, 2012. **53**(6): p. 492-7.
79. Zhang, L., et al., *Regeneration of human-ear-shaped cartilage by co-culturing human microtia chondrocytes with BMSCs*. Biomaterials, 2014. **35**(18): p. 4878-87.
80. Acharya, C., et al., *Enhanced chondrocyte proliferation and mesenchymal stromal cells chondrogenesis in coculture pellets mediate improved cartilage formation*. J Cell Physiol, 2012. **227**(1): p. 88-97.
81. de Windt, T.S., et al., *Concise review: unraveling stem cell cocultures in regenerative medicine: which cell interactions steer cartilage regeneration and how?* Stem Cells Transl Med, 2014. **3**(6): p. 723-33.
82. Lutolf, M.P., P.M. Gilbert, and H.M. Blau, *Designing materials to direct stem-cell fate*. Nature, 2009. **462**(7272): p. 433-41.
83. Huttmacher, D.W., *Scaffolds in tissue engineering bone and cartilage*. Biomaterials, 2000. **21**(24): p. 2529-43.
84. Lu, L., et al., *Biodegradable polymer scaffolds for cartilage tissue engineering*. Clin Orthop Relat Res, 2001(391 Suppl): p. S251-70.
85. Mano, J.F., et al., *Natural origin biodegradable systems in tissue engineering and regenerative medicine: present status and some moving trends*. J R Soc Interface, 2007. **4**(17): p. 999-1030.
86. Lee, K.Y. and D.J. Mooney, *Hydrogels for tissue engineering*. Chem Rev, 2001. **101**(7): p. 1869-79.
87. Wang, L., et al., *Evaluation of sodium alginate for bone marrow cell tissue engineering*. Biomaterials, 2003. **24**(20): p. 3475-81.
88. Drury, J.L., R.G. Dennis, and D.J. Mooney, *The tensile properties of alginate hydrogels*. Biomaterials, 2004. **25**(16): p. 3187-99.

89. Hauselmann, H.J., et al., *Synthesis and turnover of proteoglycans by human and bovine adult articular chondrocytes cultured in alginate beads*. Matrix, 1992. **12**(2): p. 116-29.
90. Brown, R.M., Jr., J.H. Willison, and C.L. Richardson, *Cellulose biosynthesis in Acetobacter xylinum: visualization of the site of synthesis and direct measurement of the in vivo process*. P Natl Acad Sci USA, 1976. **73**(12): p. 4565-9.
91. Backdahl, H., et al., *Mechanical properties of bacterial cellulose and interactions with smooth muscle cells*. Biomaterials, 2006. **27**(9): p. 2141-9.
92. Jozala, A.F., et al., *Bacterial nanocellulose production and application: a 10-year overview*. Appl Microbiol Biotechnol, 2016. **100**(5): p. 2063-72.
93. Badylak, S.F., D. Taylor, and K. Uygun, *Whole-organ tissue engineering: decellularization and recellularization of three-dimensional matrix scaffolds*. Annu Rev Biomed Eng, 2011. **13**: p. 27-53.
94. Ma, R., et al., *Structural integrity, ECM components and immunogenicity of decellularized laryngeal scaffold with preserved cartilage*. Biomaterials, 2013. **34**(7): p. 1790-8.
95. Baiguera, S., et al., *Tissue engineered human tracheas for in vivo implantation*. Biomaterials, 2010. **31**(34): p. 8931-8.
96. Macchiarini, P., et al., *Clinical transplantation of a tissue-engineered airway*. Lancet, 2008. **372**(9655): p. 2023-30.
97. Macchiarini, P., et al., *First human transplantation of a bioengineered airway tissue*. J Thorac Cardiovasc Surg, 2004. **128**(4): p. 638-41.
98. Laurance, J., *British boy receives trachea transplant built with his own stem cells*. BMJ, 2010. **340**: p. c1633.
99. Elliott, M.J., et al., *Stem-cell-based, tissue engineered tracheal replacement in a child: a 2-year follow-up study*. Lancet, 2012. **380**(9846): p. 994-1000.
100. Elder, B.D., D.H. Kim, and K.A. Athanasiou, *Developing an articular cartilage decellularization process toward facet joint cartilage replacement*. Neurosurgery, 2010. **66**(4): p. 722-7; discussion 727.
101. Kheir, E., et al., *Development and characterization of an acellular porcine cartilage bone matrix for use in tissue engineering*. J Biomed Mater Res A, 2011. **99**(2): p. 283-94.
102. Lumpkins, S.B., N. Pierre, and P.S. McFetridge, *A mechanical evaluation of three decellularization methods in the design of a xenogeneic scaffold for tissue engineering the temporomandibular joint disc*. Acta Biomaterialia, 2008. **4**(4): p. 808-816.
103. von Rechenberg, B., et al., *Changes in subchondral bone in cartilage resurfacing--an experimental study in sheep using different types of osteochondral grafts*. Osteoarthritis Cartilage, 2003. **11**(4): p. 265-77.
104. Chan, L.K., et al., *Decellularized bovine intervertebral disc as a natural scaffold for xenogenic cell studies*. Acta Biomater, 2013. **9**(2): p. 5262-72.
105. Mercuri, J.J., S.S. Gill, and D.T. Simionescu, *Novel tissue-derived biomimetic scaffold for regenerating the human nucleus pulposus*. J Biomed Mater Res A, 2011. **96**(2): p. 422-35.
106. Schwarz, S., et al., *Decellularized Cartilage Matrix as a Novel Biomatrix for Cartilage Tissue-Engineering Applications*. Tissue Engineering Part A, 2012. **18**(21-22): p. 2195-2209.
107. Stapleton, T.W., et al., *Development and characterization of an acellular porcine medial meniscus for use in tissue engineering*. Tissue Engineering Part A, 2008. **14**(4): p. 505-518.
108. Sandmann, G.H., et al., *Generation and characterization of a human acellular meniscus scaffold for tissue engineering*. J Biomed Mater Res A, 2009. **91**(2): p. 567-74.
109. Stabile, K.J., et al., *An acellular, allograft-derived meniscus scaffold in an ovine model*. Arthroscopy, 2010. **26**(7): p. 936-48.
110. Elsaesser, A.F., et al., *In Vitro Cytotoxicity and In Vivo Effects of a Decellularized Xenogeneic Collagen Scaffold in Nasal Cartilage Repair*. Tissue Eng Part A, 2014.
111. Wescoe, K.E., et al., *The role of the biochemical and biophysical environment in chondrogenic stem cell differentiation assays and cartilage tissue engineering*. Cell Biochem Biophys, 2008. **52**(2): p. 85-102.
112. Williams, G.M., S.M. Klisch, and R.L. Sah, *Bioengineering cartilage growth, maturation, and form*. Pediatr Res, 2008. **63**(5): p. 527-34.
113. Fortier, L.A., et al., *The role of growth factors in cartilage repair*. Clin Orthop Relat Res, 2011. **469**(10): p. 2706-15.
114. Jakob, M., et al., *Specific growth factors during the expansion and redifferentiation of adult human articular chondrocytes enhance chondrogenesis and cartilaginous tissue formation in vitro*. J Cell Biochem, 2001. **81**(2): p. 368-77.
115. van der Kraan, P.M., et al., *Interaction of chondrocytes, extracellular matrix and growth factors: relevance for articular cartilage tissue engineering*. Osteoarthritis Cartilage, 2002. **10**(8): p. 631-7.

116. Xu, L., et al., *Mesenchymal Stem Cells Reshape and Provoke Proliferation of Articular Chondrocytes by Paracrine Secretion*. Sci Rep, 2016. **6**: p. 32705.
117. Crowley, C., M. Birchall, and A.M. Seifalian, *Trachea transplantation: from laboratory to patient*. J Tissue Eng Regen Med, 2015. **9**(4): p. 357-67.
118. Huang, B.J., J.C. Hu, and K.A. Athanasiou, *Cell-based tissue engineering strategies used in the clinical repair of articular cartilage*. Biomaterials, 2016. **98**: p. 1-22.
119. Fulco, I., et al., *Engineered autologous cartilage tissue for nasal reconstruction after tumour resection: an observational first-in-human trial*. Lancet, 2014. **384**(9940): p. 337-46.
120. Rotter, N., *Reconstruction of auricular cartilage using tissue-engineering techniques*. Operative techniques in otolaryngology, 2008. **19**(4): p. 278-284.
121. Brent, B., *Auricular repair with autogenous rib cartilage grafts: two decades of experience with 600 cases*. Plast Reconstr Surg, 1992. **90**(3): p. 355-74; discussion 375-6.
122. Walton, R.L. and E.K. Beahm, *Auricular reconstruction for microtia: Part II. Surgical techniques*. Plast Reconstr Surg, 2002. **110**(1): p. 234-49; quiz 250-1, 387.
123. Arevalo-Silva, C.A., et al., *Internal support of tissue-engineered cartilage*. Arch Otolaryngol Head Neck Surg, 2000. **126**(12): p. 1448-52.
124. Bichara, D.A., et al., *The tissue-engineered auricle: past, present, and future*. Tissue engineering. Part B, Reviews, 2012. **18**(1): p. 51-61.
125. Cao, Y., et al., *Comparative study of the use of poly(glycolic acid), calcium alginate and pluronics in the engineering of autologous porcine cartilage*. J Biomater Sci Polym Ed, 1998. **9**(5): p. 475-87.
126. Cao, Y., et al., *Transplantation of chondrocytes utilizing a polymer-cell construct to produce tissue-engineered cartilage in the shape of a human ear*. Plast Reconstr Surg, 1997. **100**(2): p. 297-302; discussion 303-4.
127. Haisch, A., et al., *A tissue-engineering model for the manufacture of auricular-shaped cartilage implants*. Eur Arch Otorhinolaryngol, 2002. **259**(6): p. 316-21.
128. Isogai, N., et al., *Tissue engineering of an auricular cartilage model utilizing cultured chondrocyte-poly(L-lactide-epsilon-caprolactone) scaffolds*. Tissue Eng, 2004. **10**(5-6): p. 673-87.
129. Isogai, N., et al., *Cytokine-rich autologous serum system for cartilaginous tissue engineering*. Ann Plast Surg, 2008. **60**(6): p. 703-9.
130. Kamil, S.H., et al., *Normal features of tissue-engineered auricular cartilage by flow cytometry and histology: patient safety*. Otolaryngol Head Neck Surg, 2003. **129**(4): p. 390-6.
131. Kamil, S.H., et al., *Tissue engineering of a human sized and shaped auricle using a mold*. Laryngoscope, 2004. **114**(5): p. 867-70.
132. Liu, Y., et al., *In vitro engineering of human ear-shaped cartilage assisted with CAD/CAM technology*. Biomaterials, 2010. **31**(8): p. 2176-83.
133. Neumeister, M.W., T. Wu, and C. Chambers, *Vascularized tissue-engineered ears*. Plast Reconstr Surg, 2006. **117**(1): p. 116-22.
134. Ruszymah, B.H., et al., *Formation of tissue engineered composite construct of cartilage and skin using high density polyethylene as inner scaffold in the shape of human helix*. Int J Pediatr Otorhinolaryngol, 2011. **75**(6): p. 805-10.
135. Saim, A.B., et al., *Engineering autogenous cartilage in the shape of a helix using an injectable hydrogel scaffold*. Laryngoscope, 2000. **110**(10 Pt 1): p. 1694-7.
136. Shieh, S.J., S. Terada, and J.P. Vacanti, *Tissue engineering auricular reconstruction: in vitro and in vivo studies*. Biomaterials, 2004. **25**(9): p. 1545-57.
137. Xu, J.W., et al., *Tissue-engineered flexible ear-shaped cartilage*. Plast Reconstr Surg, 2005. **115**(6): p. 1633-41.
138. Nimeskern, L., et al., *Quantitative evaluation of mechanical properties in tissue-engineered auricular cartilage*. Tissue Eng Part B Rev, 2014. **20**(1): p. 17-27.
139. Joshi, M.D., et al., *Interspecies variation of compressive biomechanical properties of the meniscus*. J Biomed Mater Res, 1995. **29**(7): p. 823-8.
140. Mow, V.C. and X.E. Guo, *Mechano-electrochemical properties of articular cartilage: their inhomogeneities and anisotropies*. Annu Rev Biomed Eng, 2002. **4**: p. 175-209.
141. Rotter, N., et al., *Age dependence of biochemical and biomechanical properties of tissue-engineered human septal cartilage*. Biomaterials, 2002. **23**(15): p. 3087-94.
142. Humzah, M.D. and R.W. Soames, *Human intervertebral disc: structure and function*. Anat Rec, 1988. **220**(4): p. 337-56.

143. Naumann, A., et al., *Immunochemical and mechanical characterization of cartilage subtypes in rabbit*. J Histochem Cytochem, 2002. **50**(8): p. 1049-58.
144. DeBelle, L. and A.M. Tamburro, *Elastin: molecular description and function*. Int J Biochem Cell Biol, 1999. **31**(2): p. 261-72.
145. Gosline, J., et al., *Elastic proteins: biological roles and mechanical properties*. Philos Trans R Soc Lond B Biol Sci, 2002. **357**(1418): p. 121-32.
146. Bichara, D.A., et al., *Porous poly(vinyl alcohol)-alginate gel hybrid construct for neocartilage formation using human nasoseptal cells*. J Surg Res, 2010. **163**(2): p. 331-6.
147. Britt, J.C. and S.S. Park, *Autogenous tissue-engineered cartilage: evaluation as an implant material*. Arch Otolaryngol Head Neck Surg, 1998. **124**(6): p. 671-7.
148. Chang, S.C., et al., *Tissue engineering of autologous cartilage for craniofacial reconstruction by injection molding*. Plast Reconstr Surg, 2003. **112**(3): p. 793-9; discussion 800-1.
149. Isogai, N., et al., *Combined chondrocyte-copolymer implantation with slow release of basic fibroblast growth factor for tissue engineering an auricular cartilage construct*. J Biomed Mater Res A, 2005. **74**(3): p. 408-18.
150. Ting, V., et al., *In vitro prefabrication of human cartilage shapes using fibrin glue and human chondrocytes*. Ann Plast Surg, 1998. **40**(4): p. 413-20; discussion 420-1.
151. Duda, G.N., et al., *Mechanical quality of tissue engineered cartilage: results after 6 and 12 weeks in vivo*. J Biomed Mater Res, 2000. **53**(6): p. 673-7.
152. Buikstra, J.E.a.U., D.H., *Standards for data collection from human skeletal remains: Proceedings of a seminar at the field museum of natural history*. 1994.
153. Tillmann, B.N., *Atlas der anatomie des menschen*. 2010: Springer Berlin Heidelberg.
154. Gray, H., *Anatomy of the human body*. 20th Edition ed. 1918: Lea & Febiger.
155. Nimeskern, L., et al., *Mechanical evaluation of bacterial nanocellulose as an implant material for ear cartilage replacement*. J Mech Behav Biomed Mater, 2013. **22**: p. 12-21.
156. Stok, K.S., et al., *Mechano-functional assessment of human mesenchymal stem cells grown in three-dimensional hyaluronan-based scaffolds for cartilage tissue engineering*. J Biomed Mater Res A, 2010. **93**(1): p. 37-45.
157. Prockop, D.J. and S. Udenfriend, *A specific method for the analysis of hydroxyproline in tissues and urine*. Anal Biochem, 1960. **1**: p. 228-39.
158. Little, C.J., N.K. Bawolin, and X. Chen, *Mechanical properties of natural cartilage and tissue-engineered constructs*. Tissue Eng Part B Rev, 2011. **17**(4): p. 213-27.
159. Mow, V.C., et al., *Biphasic creep and stress relaxation of articular cartilage in compression? Theory and experiments*. J Biomech Eng, 1980. **102**(1): p. 73-84.
160. Reiffel, A.J., et al., *High-fidelity tissue engineering of patient-specific auricles for reconstruction of pediatric microtia and other auricular deformities*. PLoS One, 2013. **8**(2): p. e56506.
161. O'Sullivan, N.A., et al., *Adhesion and integration of tissue engineered cartilage to porous polyethylene for composite ear reconstruction*. J Biomed Mater Res B Appl Biomater, 2015. **103**(5): p. 983-91.
162. Mow, V.C., *Biphasic and quasilinear viscoelastic theories for hydrated soft tissues*, in *Biomechanics of diarthrodial joints*, A. Ratcliffe, Editor. 1990, Springer New York. p. 215-260.
163. Meijerman, L., C. van der Lugt, and G.J. Maat, *Cross-sectional anthropometric study of the external ear*. J Forensic Sci, 2007. **52**(2): p. 286-93.
164. Ito, I., et al., *A morphological study of age changes in adult human auricular cartilage with special emphasis on elastic fibers*. Laryngoscope, 2001. **111**(5): p. 881-6.
165. Sforza, C., et al., *Age- and sex-related changes in the normal human ear*. Forensic Sci Int, 2009. **187**(1-3): p. 110 e1-7.
166. Bank, R.A., et al., *The increased swelling and instantaneous deformation of osteoarthritic cartilage is highly correlated with collagen degradation*. Arthritis Rheum, 2000. **43**(10): p. 2202-10.
167. Suki, B. and J.H. Bates, *Lung tissue mechanics as an emergent phenomenon*. J Appl Physiol (1985), 2011. **110**(4): p. 1111-8.
168. Wagenseil, J.E. and R.P. Mecham, *Elastin in large artery stiffness and hypertension*. J Cardiovasc Transl Res, 2012. **5**(3): p. 264-73.
169. Buschmann, M.D. and A.J. Grodzinsky, *A molecular model of proteoglycan-associated electrostatic forces in cartilage mechanics*. J Biomech Eng, 1995. **117**(2): p. 179-92.
170. Frank, E.H. and A.J. Grodzinsky, *Cartilage electromechanics--I. Electrokinetic transduction and the effects of electrolyte pH and ionic strength*. J Biomech, 1987. **20**(6): p. 615-27.

171. Lai, W.M., J.S. Hou, and V.C. Mow, *A triphasic theory for the swelling and deformation behaviors of articular cartilage*. J Biomech Eng, 1991. **113**(3): p. 245-58.
172. Li, L.P., M.D. Buschmann, and A. Shirazi-Adl, *A fibril reinforced nonhomogeneous poroelastic model for articular cartilage: inhomogeneous response in unconfined compression*. J Biomech, 2000. **33**(12): p. 1533-41.
173. McCutchen, C.W., *Cartilages is poroelastic, not viscoelastic (including an exact theorem about strain energy and viscous loss, and an order of magnitude relation for equilibration time)*. J Biomech, 1982. **15**(4): p. 325-7.
174. Mow, V.C. and J.M. Mansour, *The nonlinear interaction between cartilage deformation and interstitial fluid flow*. J Biomech, 1977. **10**(1): p. 31-9.
175. Spilker, R.L., J.K. Suh, and V.C. Mow, *A finite element analysis of the indentation stress-relaxation response of linear biphasic articular cartilage*. J Biomech Eng, 1992. **114**(2): p. 191-201.
176. Guilak, F., et al., *The deformation behavior and mechanical properties of chondrocytes in articular cartilage*. Osteoarthritis Cartilage, 1999. **7**(1): p. 59-70.
177. Suh, J.K. and R.L. Spilker, *Indentation analysis of biphasic articular cartilage: nonlinear phenomena under finite deformation*. J Biomech Eng, 1994. **116**(1): p. 1-9.
178. June, R.K. and D.P. Fyhrie, *Temperature effects in articular cartilage biomechanics*. J Exp Biol, 2010. **213**(Pt 22): p. 3934-40.
179. Mow, V.C., et al., *Biphasic indentation of articular cartilage--II. A numerical algorithm and an experimental study*. J Biomech, 1989. **22**(8-9): p. 853-61.
180. Edwards, C.A. and W.D. O'Brien, Jr., *Modified assay for determination of hydroxyproline in a tissue hydrolyzate*. Clin Chim Acta, 1980. **104**(2): p. 161-7.
181. Driscoll, B.P. and S.R. Baker, *Reconstruction of nasal alar defects*. Arch Facial Plast Surg, 2001. **3**(2): p. 91-9.
182. Ray, E., et al., *Review of options for burned ear reconstruction*. J Craniofac Surg, 2010. **21**(4): p. 1165-9.
183. Kridel, R.W., et al., *Long-term use and follow-up of irradiated homologous costal cartilage grafts in the nose*. Arch Facial Plast Surg, 2009. **11**(6): p. 378-94.
184. Bhandari, P.S., *Total ear reconstruction in post burn deformity*. Burns, 1998. **24**(7): p. 661-70.
185. Yanaga, H., et al., *Generating ears from cultured autologous auricular chondrocytes by using two-stage implantation in treatment of microtia*. Plast Reconstr Surg, 2009. **124**(3): p. 817-25.
186. Qing-Hua, Y., et al., *The significance of the biomechanical properties of costal cartilage in the timing of ear reconstruction surgery*. J Plast Reconstr Aesthet Surg, 2011. **64**(6): p. 742-6.
187. Anthwal, N. and H. Thompson, *The development of the mammalian outer and middle ear*. J Anat, 2016. **228**(2): p. 217-32.
188. Som, P.M. and T.P. Naidich, *Illustrated review of the embryology and development of the facial region, part 1: Early face and lateral nasal cavities*. AJNR Am J Neuroradiol, 2013. **34**(12): p. 2233-40.
189. Popko, M., et al., *Histological structure of the nasal cartilages and their perichondrial envelope. I. The septal and lobular cartilage*. Rhinology, 2007. **45**(2): p. 148-52.
190. Mansfield, J.C., et al., *Collagen fiber arrangement in normal and diseased cartilage studied by polarization sensitive nonlinear microscopy*. J Biomed Opt, 2008. **13**(4): p. 044020.
191. Zhu, X., et al., *Monitoring wound healing of elastic cartilage using multiphoton microscopy*. Osteoarthritis Cartilage, 2013. **21**(11): p. 1799-806.
192. McKee, C.T., et al., *Indentation versus tensile measurements of Young's modulus for soft biological tissues*. Tissue Eng Part B Rev, 2011. **17**(3): p. 155-64.
193. Hsieh, C.H., et al., *Surface ultrastructure and mechanical property of human chondrocyte revealed by atomic force microscopy*. Osteoarthritis Cartilage, 2008. **16**(4): p. 480-8.
194. Sanchez-Adams, J., R.E. Wilusz, and F. Guilak, *Atomic force microscopy reveals regional variations in the micromechanical properties of the pericellular and extracellular matrices of the meniscus*. J Orthop Res, 2013. **31**(8): p. 1218-25.
195. Marrese, M., V. Guarino, and L. Ambrosio, *Atomic Force Microscopy: A Powerful Tool to Address Scaffold Design in Tissue Engineering*. J Funct Biomater, 2017. **8**(1).
196. Guilak, F., et al., *Control of stem cell fate by physical interactions with the extracellular matrix*. Cell Stem Cell, 2009. **5**(1): p. 17-26.
197. Chavan, D., et al., *Ferrule-top nanoindenter: an optomechanical fiber sensor for nanoindentation*. Rev Sci Instrum, 2012. **83**(11): p. 115110.
198. Oliver, W.C., *An improved technique for determining hardness and elastic modulus using load and displacement sensing indentation experiments*. Journal of materials research, 1992. **7**(6): p. 1564-1583.

199. Kobayashi, S., et al., *Reconstruction of human elastic cartilage by a CD44+ CD90+ stem cell in the ear perichondrium*. Proc Natl Acad Sci U S A, 2011. **108**(35): p. 14479-84.
200. Yanaga, H., et al., *Clinical application of cultured autologous human auricular chondrocytes with autologous serum for craniofacial or nasal augmentation and repair*. Plast Reconstr Surg, 2006. **117**(6): p. 2019-30; discussion 2031-2.
201. Nimeskern, L., et al., *Mechanical and biochemical mapping of human auricular cartilage for reliable assessment of tissue-engineered constructs*. J Biomech, 2015. **48**(10): p. 1721-9.
202. Nimeskern, L., et al., *Tissue composition regulates distinct viscoelastic responses in auricular and articular cartilage*. J Biomech, 2016. **49**(3): p. 344-52.
203. Verhaegen, P.D., et al., *Adaptation of the dermal collagen structure of human skin and scar tissue in response to stretch: an experimental study*. Wound Repair Regen, 2012. **20**(5): p. 658-66.
204. Roy, R., et al., *Analysis of bending behavior of native and engineered auricular and costal cartilage*. J Biomed Mater Res A, 2004. **68**(4): p. 597-602.
205. Stoddart, M.J., et al., *Cells and biomaterials in cartilage tissue engineering*. Regen Med, 2009. **4**(1): p. 81-98.
206. Seda Tigli, R., et al., *Comparative chondrogenesis of human cell sources in 3D scaffolds*. J Tissue Eng Regen Med, 2009. **3**(5): p. 348-60.
207. Sakaguchi, Y., et al., *Comparison of human stem cells derived from various mesenchymal tissues: superiority of synovium as a cell source*. Arthritis Rheum, 2005. **52**(8): p. 2521-9.
208. Yoshimura, H., et al., *Comparison of rat mesenchymal stem cells derived from bone marrow, synovium, periosteum, adipose tissue, and muscle*. Cell Tissue Res, 2007. **327**(3): p. 449-62.
209. Vinardell, T., et al., *A comparison of the functionality and in vivo phenotypic stability of cartilaginous tissues engineered from different stem cell sources*. Tissue Eng Part A, 2012. **18**(11-12): p. 1161-70.
210. Wong, M., et al., *Development of mechanically stable alginate/chondrocyte constructs: effects of guluronic acid content and matrix synthesis*. J Orthop Res, 2001. **19**(3): p. 493-9.
211. Pfaffl, M.W., et al., *Determination of stable housekeeping genes, differentially regulated target genes and sample integrity: BestKeeper--Excel-based tool using pair-wise correlations*. Biotechnol Lett, 2004. **26**(6): p. 509-15.
212. Enobakhare, B.O., D.L. Bader, and D.A. Lee, *Quantification of sulfated glycosaminoglycans in chondrocyte/alginate cultures, by use of 1,9-dimethylmethylene blue*. Anal Biochem, 1996. **243**(1): p. 189-91.
213. Creemers, L.B., et al., *Microassay for the assessment of low levels of hydroxyproline*. Biotechniques, 1997. **22**(4): p. 656-8.
214. Hierck, B.P., et al., *Modified indirect immunodetection allows study of murine tissue with mouse monoclonal antibodies*. J Histochem Cytochem, 1994. **42**(11): p. 1499-502.
215. Grogan, S.P., et al., *Visual histological grading system for the evaluation of in vitro-generated neocartilage*. Tissue Eng, 2006. **12**(8): p. 2141-9.
216. Yaeger, P.C., et al., *Synergistic action of transforming growth factor-beta and insulin-like growth factor-I induces expression of type II collagen and aggrecan genes in adult human articular chondrocytes*. Exp Cell Res, 1997. **237**(2): p. 318-25.
217. Lee, C.S., et al., *Regulating in vivo calcification of alginate microbeads*. Biomaterials, 2010. **31**(18): p. 4926-34.
218. Hellingman, C.A., W. Koevoet, and G.J. van Osch, *Can one generate stable hyaline cartilage from adult mesenchymal stem cells? A developmental approach*. J Tissue Eng Regen Med, 2012. **6**(10): p. e1-e11.
219. Kanczler, J.M. and R.O. Oreffo, *Osteogenesis and angiogenesis: the potential for engineering bone*. Eur Cell Mater, 2008. **15**: p. 100-14.
220. Alsberg, E., et al., *Cell-interactive alginate hydrogels for bone tissue engineering*. J Dent Res, 2001. **80**(11): p. 2025-9.
221. Tomiya, M., et al., *Skeletal unloading induces a full-thickness patellar cartilage defect with increase of urinary collagen II CTx degradation marker in growing rats*. Bone, 2009. **44**(2): p. 295-305.
222. Barry, F., et al., *Chondrogenic differentiation of mesenchymal stem cells from bone marrow: differentiation-dependent gene expression of matrix components*. Exp Cell Res, 2001. **268**(2): p. 189-200.
223. Kern, S., et al., *Comparative analysis of mesenchymal stem cells from bone marrow, umbilical cord blood, or adipose tissue*. Stem Cells, 2006. **24**(5): p. 1294-301.
224. De Ugarte, D.A., et al., *Comparison of multi-lineage cells from human adipose tissue and bone marrow*. Cells Tissues Organs, 2003. **174**(3): p. 101-9.

225. Izadpanah, R., et al., *Biologic properties of mesenchymal stem cells derived from bone marrow and adipose tissue*. J Cell Biochem, 2006. **99**(5): p. 1285-97.
226. Lee, R.H., et al., *Characterization and expression analysis of mesenchymal stem cells from human bone marrow and adipose tissue*. Cell Physiol Biochem, 2004. **14**(4-6): p. 311-24.
227. Im, G.I., Y.W. Shin, and K.B. Lee, *Do adipose tissue-derived mesenchymal stem cells have the same osteogenic and chondrogenic potential as bone marrow-derived cells?* Osteoarthritis Cartilage, 2005. **13**(10): p. 845-53.
228. Rider, D.A., et al., *Autocrine fibroblast growth factor 2 increases the multipotentiality of human adipose-derived mesenchymal stem cells*. Stem Cells, 2008. **26**(6): p. 1598-608.
229. Huang, J.I., et al., *Chondrogenic potential of progenitor cells derived from human bone marrow and adipose tissue: a patient-matched comparison*. J Orthop Res, 2005. **23**(6): p. 1383-9.
230. Liu, T.M., et al., *Identification of common pathways mediating differentiation of bone marrow- and adipose tissue-derived human mesenchymal stem cells into three mesenchymal lineages*. Stem Cells, 2007. **25**(3): p. 750-60.
231. Mehlhorn, A.T., et al., *Differential expression pattern of extracellular matrix molecules during chondrogenesis of mesenchymal stem cells from bone marrow and adipose tissue*. Tissue Eng, 2006. **12**(10): p. 2853-62.
232. Noel, D., et al., *Cell specific differences between human adipose-derived and mesenchymal-stromal cells despite similar differentiation potentials*. Exp Cell Res, 2008. **314**(7): p. 1575-84.
233. Rebelatto, C.K., et al., *Dissimilar differentiation of mesenchymal stem cells from bone marrow, umbilical cord blood, and adipose tissue*. Exp Biol Med (Maywood), 2008. **233**(7): p. 901-13.
234. Segawa, Y., et al., *Mesenchymal stem cells derived from synovium, meniscus, anterior cruciate ligament, and articular chondrocytes share similar gene expression profiles*. J Orthop Res, 2009. **27**(4): p. 435-41.
235. Winter, A., et al., *Cartilage-like gene expression in differentiated human stem cell spheroids: a comparison of bone marrow-derived and adipose tissue-derived stromal cells*. Arthritis Rheum, 2003. **48**(2): p. 418-29.
236. Estes, B.T., et al., *Isolation of adipose-derived stem cells and their induction to a chondrogenic phenotype*. Nat Protoc, 2010. **5**(7): p. 1294-311.
237. Han, E.H., et al., *Contribution of proteoglycan osmotic swelling pressure to the compressive properties of articular cartilage*. Biophys J, 2011. **101**(4): p. 916-24.
238. Bastiaansen-Jenniskens, Y.M., et al., *TGFbeta affects collagen cross-linking independent of chondrocyte phenotype but strongly depending on physical environment*. Tissue Eng Part A, 2008. **14**(6): p. 1059-66.
239. Puelacher, W.C., et al., *Tissue-engineered growth of cartilage: the effect of varying the concentration of chondrocytes seeded onto synthetic polymer matrices*. Int J Oral Maxillofac Surg, 1994. **23**(1): p. 49-53.
240. Farrell, M.J., et al., *Functional properties of bone marrow-derived MSC-based engineered cartilage are unstable with very long-term in vitro culture*. J Biomech, 2014. **47**(9): p. 2173-82.
241. Scotti, C., et al., *Engineering of a functional bone organ through endochondral ossification*. Proc Natl Acad Sci U S A, 2013. **110**(10): p. 3997-4002.
242. Hubka, K.M., et al., *Enhancing chondrogenic phenotype for cartilage tissue engineering: monoculture and coculture of articular chondrocytes and mesenchymal stem cells*. Tissue Eng Part B Rev, 2014. **20**(6): p. 641-54.
243. Hildner, F., et al., *Human adipose-derived stem cells contribute to chondrogenesis in coculture with human articular chondrocytes*. Tissue Eng Part A, 2009. **15**(12): p. 3961-9.
244. Lee, *Adipose stem cells can secrete angiogenic factors that inhibit hyaline cartilage regeneration*. Stem Cell Research & Therapy, 2012. **3**(35).
245. Lopa, S., et al., *Influence on chondrogenesis of human osteoarthritic chondrocytes in co-culture with donor-matched mesenchymal stem cells from infrapatellar fat pad and subcutaneous adipose tissue*. Int J Immunopathol Pharmacol, 2013. **26**(1 Suppl): p. 23-31.
246. Wu, L., et al., *Trophic effects of mesenchymal stem cells in chondrocyte co-cultures are independent of culture conditions and cell sources*. Tissue Eng Part A, 2012. **18**(15-16): p. 1542-51.
247. Maumus, M., et al., *Adipose mesenchymal stem cells protect chondrocytes from degeneration associated with osteoarthritis*. Stem Cell Res, 2013. **11**(2): p. 834-44.
248. Gharibi, B. and F.J. Hughes, *Effects of medium supplements on proliferation, differentiation potential, and in vitro expansion of mesenchymal stem cells*. Stem Cells Transl Med, 2012. **1**(11): p. 771-82.
249. Martin, I., et al., *Fibroblast growth factor-2 supports ex vivo expansion and maintenance of osteogenic precursors from human bone marrow*. Endocrinology, 1997. **138**(10): p. 4456-62.

250. Choi, K.M., et al., *Effect of ascorbic acid on bone marrow-derived mesenchymal stem cell proliferation and differentiation*. J Biosci Bioeng, 2008. **105**(6): p. 586-94.
251. Jork, A., et al., *Biocompatible alginate from freshly collected Laminaria pallida for implantation*. Appl Microbiol Biotechnol, 2000. **53**(2): p. 224-9.
252. Pleumeekers, M.M., et al., *Cartilage Regeneration in the Head and Neck Area: Combination of Ear or Nasal Chondrocytes and Mesenchymal Stem Cells Improves Cartilage Production*. Plast Reconstr Surg, 2015. **136**(6): p. 762e-74e.
253. Bian, L., et al., *Coculture of human mesenchymal stem cells and articular chondrocytes reduces hypertrophy and enhances functional properties of engineered cartilage*. Tissue Eng Part A, 2011. **17**(7-8): p. 1137-45.
254. Fischer, J., et al., *Human articular chondrocytes secrete parathyroid hormone-related protein and inhibit hypertrophy of mesenchymal stem cells in coculture during chondrogenesis*. Arthritis Rheum, 2010. **62**(9): p. 2696-706.
255. Aung, A., et al., *Osteoarthritic chondrocyte-secreted morphogens induce chondrogenic differentiation of human mesenchymal stem cells*. Arthritis Rheum, 2011. **63**(1): p. 148-58.
256. Yang, H.N., et al., *The use of green fluorescence gene (GFP)-modified rabbit mesenchymal stem cells (rMSCs) co-cultured with chondrocytes in hydrogel constructs to reveal the chondrogenesis of MSCs*. Biomaterials, 2009. **30**(31): p. 6374-85.
257. Ahmed, N., et al., *Soluble signalling factors derived from differentiated cartilage tissue affect chondrogenic differentiation of rat adult marrow stromal cells*. Cell Physiol Biochem, 2007. **20**(5): p. 665-78.
258. Hwang, N.S., et al., *Morphogenetic signals from chondrocytes promote chondrogenic and osteogenic differentiation of mesenchymal stem cells*. J Cell Physiol, 2007. **212**(2): p. 281-4.
259. Cooke, M.E., et al., *Structured three-dimensional co-culture of mesenchymal stem cells with chondrocytes promotes chondrogenic differentiation without hypertrophy*. Osteoarthritis Cartilage, 2011. **19**(10): p. 1210-8.
260. Lee, J.S. and G.I. Im, *Influence of chondrocytes on the chondrogenic differentiation of adipose stem cells*. Tissue Eng Part A, 2010. **16**(12): p. 3569-77.
261. Carlesimo, M., et al., *Diffuse plane xanthoma and monoclonal gammopathies*. Eur J Dermatol, 2009. **19**(6): p. 640-1.
262. Liu, X., et al., *In vivo ectopic chondrogenesis of BMSCs directed by mature chondrocytes*. Biomaterials, 2010. **31**(36): p. 9406-14.
263. Zuo, Q., et al., *Co-cultivated mesenchymal stem cells support chondrocytic differentiation of articular chondrocytes*. Int Orthop, 2013. **37**(4): p. 747-52.
264. Meretoja, V.V., et al., *Enhanced chondrogenesis in co-cultures with articular chondrocytes and mesenchymal stem cells*. Biomaterials, 2012. **33**(27): p. 6362-9.
265. Tsuchiya, K., *The effect of coculture of chondrocytes with mesenchymal stem cells on their cartilaginous phenotype in vitro*. Materials Science and Engineering C, 2004. **24**: p. 391-396.
266. Levorson, E.J., et al., *Direct and indirect co-culture of chondrocytes and mesenchymal stem cells for the generation of polymer/extracellular matrix hybrid constructs*. Acta Biomater, 2014. **10**(5): p. 1824-35.
267. Platas, J., et al., *Conditioned media from adipose-tissue-derived mesenchymal stem cells downregulate degradative mediators induced by interleukin-1beta in osteoarthritic chondrocytes*. Mediators Inflamm, 2013. **2013**: p. 357014.
268. Wang, M., et al., *Trophic stimulation of articular chondrocytes by late-passage mesenchymal stem cells in coculture*. J Orthop Res, 2013. **31**(12): p. 1936-42.
269. Hsiao, S.T., et al., *Comparative analysis of paracrine factor expression in human adult mesenchymal stem cells derived from bone marrow, adipose, and dermal tissue*. Stem Cells Dev, 2012. **21**(12): p. 2189-203.
270. Li, T.S., et al., *Direct comparison of different stem cell types and subpopulations reveals superior paracrine potency and myocardial repair efficacy with cardiosphere-derived cells*. J Am Coll Cardiol, 2012. **59**(10): p. 942-53.
271. Yoo, K.H., et al., *Comparison of immunomodulatory properties of mesenchymal stem cells derived from adult human tissues*. Cell Immunol, 2009. **259**(2): p. 150-6.
272. Dmitrieva, R.I., et al., *Bone marrow- and subcutaneous adipose tissue-derived mesenchymal stem cells: differences and similarities*. Cell Cycle, 2012. **11**(2): p. 377-83.
273. Mo, X.T., et al., *Variations in the ratios of co-cultured mesenchymal stem cells and chondrocytes regulate the expression of cartilaginous and osseous phenotype in alginate constructs*. Bone, 2009. **45**(1): p. 42-51.

274. Hendriks, J., et al., *Primary chondrocytes enhance cartilage tissue formation upon co-culture with a range of cell types*. Soft Matter, 2010. **6**(20): p. 5080-5088.
275. Tsuchiya, K., et al., *The effect of coculture of chondrocytes with mesenchymal stem cells on their cartilaginous phenotype in vitro*. Materials Science and Engineering: C, 2004. **24**(3): p. 391-396.
276. Rettinger, G., *Risks and complications in rhinoplasty*. GMS Curr Top Otorhinolaryngol Head Neck Surg, 2007. **6**: p. Doc08.
277. van Buul, G.M., et al., *Mesenchymal stem cells reduce pain but not degenerative changes in a mono-iodoacetate rat model of osteoarthritis*. J Orthop Res, 2014. **32**(9): p. 1167-74.
278. Saris, D.B.F., *IMPACT: Safety and Feasibility of a Single-stage Procedure for Focal Cartilage Lesions of the Knee*. <http://clinicaltrials.gov>, Ongoing. **NCT02037204**.
279. Lieberman, J.R., S.C. Ghivizzani, and C.H. Evans, *Gene transfer approaches to the healing of bone and cartilage*. Mol Ther, 2002. **6**(2): p. 141-7.
280. Polacek, M., et al., *The secretory profiles of cultured human articular chondrocytes and mesenchymal stem cells: implications for autologous cell transplantation strategies*. Cell Transplant, 2011. **20**(9): p. 1381-93.
281. Nimeskern, L., Pleumeekers, M. M., Martinez, H., Sundberg, J., Gatenholm, P., van Osch, G. J. V. M., Muller, R., Stok, K. S., *Mechanical and biochemical map of ear cartilage for tunable biomaterials in tissue engineering*. Journal of Biomechanics, 2012. **45**(1): p. S651.
282. Pigott, J.H., et al., *Investigation of the immune response to autologous, allogeneic, and xenogeneic mesenchymal stem cells after intra-articular injection in horses*. Vet Immunol Immunopathol, 2013. **156**(1-2): p. 99-106.
283. Bekkers, J.E., et al., *One-stage focal cartilage defect treatment with bone marrow mononuclear cells and chondrocytes leads to better macroscopic cartilage regeneration compared to microfracture in goats*. Osteoarthritis Cartilage, 2013. **21**(7): p. 950-6.
284. Prendergast, P.J., R. Huiskes, and K. Soballe, *ESB Research Award 1996. Biophysical stimuli on cells during tissue differentiation at implant interfaces*. J Biomech, 1997. **30**(6): p. 539-48.
285. Walser, J., M.D. Caversaccio, and S.J. Ferguson, *Electrospinning Auricular Shaped Scaffolds for Tissue Engineering*. Biomed Tech (Berl), 2013.
286. Romo, T., 3rd, P.M. Presti, and H.R. Yalamanchili, *Medpor alternative for microtia repair*. Facial Plast Surg Clin North Am, 2006. **14**(2): p. 129-36, vi.
287. Sivayoham, E. and T.J. Woolford, *Current opinion on auricular reconstruction*. Curr Opin Otolaryngol Head Neck Surg, 2012. **20**(4): p. 287-90.
288. Cenzi, R., et al., *Clinical outcome of 285 Medpor grafts used for craniofacial reconstruction*. J Craniofac Surg, 2005. **16**(4): p. 526-30.
289. Nayyer, L., et al., *Tissue engineering: revolution and challenge in auricular cartilage reconstruction*. Plastic and reconstructive surgery, 2012. **129**(5): p. 1123-37.
290. Kang, H., et al., *In vivo cartilage repair using adipose-derived stem cell-loaded decellularized cartilage ECM scaffolds*. J Tissue Eng Regen Med, 2014. **8**(6): p. 442-53.
291. Yang, Q., et al., *A cartilage ECM-derived 3-D porous acellular matrix scaffold for in vivo cartilage tissue engineering with PKH26-labeled chondrogenic bone marrow-derived mesenchymal stem cells*. Biomaterials, 2008. **29**(15): p. 2378-87.
292. Farndale, R.W., D.J. Buttle, and A.J. Barrett, *Improved quantitation and discrimination of sulphated glycosaminoglycans by use of dimethylmethylene blue*. Biochimica et biophysica acta, 1986. **883**(2): p. 173-7.
293. Badylak, S.F., et al., *Engineered whole organs and complex tissues*. Lancet, 2012. **379**(9819): p. 943-52.
294. Gong, Y.Y., et al., *A sandwich model for engineering cartilage with acellular cartilage sheets and chondrocytes*. Biomaterials, 2011. **32**(9): p. 2265-73.
295. Crapo, P.M., T.W. Gilbert, and S.F. Badylak, *An overview of tissue and whole organ decellularization processes*. Biomaterials, 2011. **32**(12): p. 3233-43.
296. Conconi, M.T., et al., *Tracheal matrices, obtained by a detergent-enzymatic method, support in vitro the adhesion of chondrocytes and tracheal epithelial cells*. Transpl Int, 2005. **18**(6): p. 727-34.
297. Partington, L., et al., *Biochemical changes caused by decellularization may compromise mechanical integrity of tracheal scaffolds*. Acta Biomater, 2013. **9**(2): p. 5251-61.
298. Remlinger, N.T., et al., *Hydrated xenogeneic decellularized tracheal matrix as a scaffold for tracheal reconstruction*. Biomaterials, 2010. **31**(13): p. 3520-6.
299. Zang, M., et al., *Decellularized tracheal matrix scaffold for tissue engineering*. Plastic and reconstructive surgery, 2012. **130**(3): p. 532-40.

300. Chen, C.W., et al., *Type I and II collagen regulation of chondrogenic differentiation by mesenchymal progenitor cells*. J Orthop Res, 2005. **23**(2): p. 446-53.
301. Bastiaansen-Jenniskens, Y.M., et al., *Contribution of collagen network features to functional properties of engineered cartilage*. Osteoarthritis Cartilage, 2008. **16**(3): p. 359-66.
302. Daamen, W.F., et al., *Preparation and evaluation of molecularly-defined collagen-elastin-glycosaminoglycan scaffolds for tissue engineering*. Biomaterials, 2003. **24**(22): p. 4001-9.
303. Kostovic-Knezevic, L., Z. Bradamante, and A. Svajger, *Ultrastructure of elastic cartilage in the rat external ear*. Cell Tissue Res, 1981. **218**(1): p. 149-60.
304. Mow, V.C., A. Ratcliffe, and A.R. Poole, *Cartilage and diarthrodial joints as paradigms for hierarchical materials and structures*. Biomaterials, 1992. **13**(2): p. 67-97.
305. Schwarz, S., et al., *Decellularized cartilage matrix as a novel biomatrix for cartilage tissue-engineering applications*. Tissue engineering. Part A, 2012. **18**(21-22): p. 2195-209.
306. Roberts, J.J., et al., *Comparative study of the viscoelastic mechanical behavior of agarose and poly(ethylene glycol) hydrogels*. J Biomed Mater Res B Appl Biomater, 2011. **99**(1): p. 158-69.
307. Woodfield, T.B., et al., *Design of porous scaffolds for cartilage tissue engineering using a three-dimensional fiber-deposition technique*. Biomaterials, 2004. **25**(18): p. 4149-61.
308. Hunziker, E.B. and E. Kapfinger, *Removal of proteoglycans from the surface of defects in articular cartilage transiently enhances coverage by repair cells*. J Bone Joint Surg Br, 1998. **80**(1): p. 144-50.
309. Koelling, S., et al., *Migratory chondrogenic progenitor cells from repair tissue during the later stages of human osteoarthritis*. Cell Stem Cell, 2009. **4**(4): p. 324-35.
310. Tanzer, R.C., *Total reconstruction of the auricle. The evolution of a plan of treatment*. Plastic and reconstructive surgery, 1971. **47**(6): p. 523-33.
311. Persichetti, P., et al., *Septal cartilage graft for posttraumatic ear reconstruction*. Plastic and reconstructive surgery, 2011. **128**(6): p. 773e-5e.
312. Mello, L.R., et al., *Duraplasty with biosynthetic cellulose: An experimental study*. J Neurosurg, 1997. **86**(1): p. 143-150.
313. Helenius, G., et al., *In vivo biocompatibility of bacterial cellulose*. J Biomed Mater Res A, 2006. **76**(2): p. 431-8.
314. Andrade, F.K., et al., *Studies on the biocompatibility of bacterial cellulose*. Journal of Bioactive and Compatible Polymers, 2013. **28**(1): p. 97-112.
315. Pertile, R.A., et al., *Bacterial Cellulose: Long-Term Biocompatibility Studies*. Journal of biomaterials science. Polymer edition, 2011.
316. Martínez Ávila, H., et al., *Biocompatibility evaluation of densified bacterial nanocellulose hydrogel as an implant material for auricular cartilage regeneration*. Applied microbiology and biotechnology, 2014. **98**(17): p. 7423-7435.
317. Svensson, A., et al., *Bacterial cellulose as a potential scaffold for tissue engineering of cartilage*. Biomaterials, 2005. **26**(4): p. 419-431.
318. Ahrem, H., et al., *Laser-structured bacterial nanocellulose hydrogels support ingrowth and differentiation of chondrocytes and show potential as cartilage implants*. Acta Biomater, 2014. **10**(3): p. 1341-53.
319. Bäckdahl, H., et al., *Mechanical properties of bacterial cellulose and interactions with smooth muscle cells*. Biomaterials, 2006. **27**(9): p. 2141-2149.
320. Zaborowska, M., et al., *Microporous bacterial cellulose as a potential scaffold for bone regeneration*. Acta Biomaterialia, 2010. **6**(7): p. 2540-2547.
321. Martínez Ávila, H., et al., *Mechanical stimulation of fibroblasts in micro-channeled bacterial cellulose scaffolds enhances production of oriented collagen fibers*. J Biomed Mater Res A, 2012. **100**(4): p. 948-57.
322. Feldmann, E.M., et al., *Description of a novel approach to engineer cartilage with porous bacterial nanocellulose for reconstruction of a human auricle*. J Biomater Appl, 2013.
323. Bodin, A., et al., *Tissue-engineered conduit using urine-derived stem cells seeded bacterial cellulose polymer in urinary reconstruction and diversion*. Biomaterials, 2010. **31**(34): p. 8889-8901.
324. Deinema, M. and L.P.T.M. Zevenhuizen, *Formation of cellulose fibrils by gram-negative bacteria and their role in bacterial flocculation*. Arch Mikrobiol, 1971. **78**(1): p. 42-57.
325. Fink, H.P., et al., *Investigation of the supramolecular structure of never dried bacterial cellulose*. Macromol Symp, 1997. **120**: p. 207-217.
326. Czaja, W.K., et al., *The future prospects of microbial cellulose in biomedical applications*. Biomacromolecules, 2007. **8**(1): p. 1-12.

327. Gatenholm, P. and D. Klemm, *Bacterial Nanocellulose as a Renewable Material for Biomedical Applications*. MRS Bulletin, 2010. **35**(03): p. 208-213.
328. Petersen, N. and P. Gatenholm, *Bacterial cellulose-based materials and medical devices: current state and perspectives*. Appl Microbiol Biot, 2011. **91**(5): p. 1277-86.
329. Nimeskern, L., et al., *Mechanical evaluation of bacterial nanocellulose as an implant material for ear cartilage replacement*. J Mech Behav Biomed, 2013. **22**(0): p. 12-21.
330. Lee, S.J., et al., *Engineered cartilage covered ear implants for auricular cartilage reconstruction*. Biomacromolecules, 2011. **12**(2): p. 306-13.
331. Yanaga, H., et al., *Generating Ears from Cultured Autologous Auricular Chondrocytes by Using Two-Stage Implantation in Treatment of Microtia*. Plastic and reconstructive surgery, 2009. **124**(3): p. 817-825 10.1097/PRS.0b013e3181b17c0e.
332. Zhou, L., et al., *Engineering ear constructs with a composite scaffold to maintain dimensions*. Tissue engineering. Part A, 2011. **17**(11-12): p. 1573-81.
333. Nimeskern, L., et al., *Quantitative evaluation of mechanical properties in tissue-engineered auricular cartilage*. Tissue engineering. Part B, Reviews, 2014. **20**(1): p. 17-27.
334. Cao, Y., et al., *Transplantation of chondrocytes utilizing a polymer-cell construct to produce tissue-engineered cartilage in the shape of a human ear*. Plastic and reconstructive surgery, 1997. **100**(2): p. 297-302; discussion 303-4.
335. Haisch, A., et al., *A tissue-engineering model for the manufacture of auricular-shaped cartilage implants*. European archives of oto-rhino-laryngology : official journal of the European Federation of Oto-Rhino-Laryngological Societies, 2002. **259**(6): p. 316-21.
336. Isogai, N., et al., *Tissue engineering of an auricular cartilage model utilizing cultured chondrocyte-poly(L-lactide-epsilon-caprolactone) scaffolds*. Tissue engineering, 2004. **10**(5-6): p. 673-87.
337. Kusuhara, H., et al., *Tissue engineering a model for the human ear: assessment of size, shape, morphology, and gene expression following seeding of different chondrocytes*. Wound repair and regeneration : official publication of the Wound Healing Society [and] the European Tissue Repair Society, 2009. **17**(1): p. 136-46.
338. Ruszymah, B.H.I., et al., *Formation of tissue engineered composite construct of cartilage and skin using high density polyethylene as inner scaffold in the shape of human helix*. International journal of pediatric otorhinolaryngology, 2011. **75**(6): p. 805-810.
339. Béguin, P. and J.-P. Aubert, *The biological degradation of cellulose*. FEMS Microbiology Reviews, 1994. **13**(1): p. 25-58.
340. Martínez Ávila, H., et al., *Bioprinting of 3D patient-specific auricular scaffolds*. Journal of tissue engineering and regenerative medicine, 2012. **6**: p. 153.
341. Bäckdahl, H., et al., *Engineering microporosity in bacterial cellulose scaffolds*. J Tissue Eng Regen Med, 2008. **2**(6): p. 320-330.
342. Chiaoprakobkij, N., et al., *Characterization and biocompatibility of bacterial cellulose/alginate composite sponges with human keratinocytes and gingival fibroblasts*. Carbohydrate Polymers, 2011. **85**(3): p. 548-553.
343. Sundberg, J., et al., *Evaluation of macroporous bacterial nanocellulose scaffolds for ear cartilage tissue engineering*. In: *Tissue Engineering and Regenerative Medicine International Society World Congress, Vienna, Austria, September 5-8, 2012*. J Tissue Eng Regen Med, 2012. **6** (Suppl. 1): p. 1-429.
344. Andersson, J., et al., *Behavior of human chondrocytes in engineered porous bacterial cellulose scaffolds*. J Biomed Mater Res A, 2010. **94**(4): p. 1124-32.
345. Pleumeekers, M.M., et al., *The in vitro and in vivo capacity of culture-expanded human cells from several sources encapsulated in alginate to form cartilage*. European cells & materials, 2014. **27**: p. 264-80; discussion 278-80.
346. de Windt, T.S., et al., *Concise review: unraveling stem cell cocultures in regenerative medicine: which cell interactions steer cartilage regeneration and how?* Stem cells translational medicine, 2014. **3**(6): p. 723-33.
347. Hendriks, J.A.A., et al., *Cartilage cell processing system*, in *USPTO.gov*, U.S.P.a.T. Office, Editor. 2014, Cellcotec B.V.: US.
348. Häuselmann, H.J., et al., *Phenotypic stability of bovine articular chondrocytes after long-term culture in alginate beads*. Journal of cell science, 1994. **107** (Pt 1): p. 17-27.
349. Matsuoka M, T.T., Matsushita K, Adachi O, Yoshinaga F, *A synthetic medium for bacterial cellulose production by Acetobacter xylinum subsp. sucrofermentation*. Biosci Biotechnol Biochem, 1996. **60**: p. 575-9.

350. Nimeskern, L., et al., *Magnetic Resonance Imaging of the Ear for Patient-Specific Reconstructive Surgery*. PloS one, 2014. **9**(8): p. e104975.
351. Bouxsein, M.L., et al., *Guidelines for assessment of bone microstructure in rodents using micro-computed tomography*. Journal of bone and mineral research : the official journal of the American Society for Bone and Mineral Research, 2010. **25**(7): p. 1468-86.
352. FDA, U.S., *Guidance for Industry - Pyrogen and Endotoxins Testing: Questions and Answers*, U.S.D.o.H.H. Services, Editor. June 2012, U.S. Food and Drug Administration: Silver Spring. p. 8.
353. Enobakhare, B.O., D.L. Bader, and D.A. Lee, *Quantification of sulfated glycosaminoglycans in chondrocyte/alginate cultures, by use of 1,9-dimethylmethylene blue*. Analytical biochemistry, 1996. **243**(1): p. 189-91.
354. Stok, K.S., et al., *Mechano-functional assessment of human mesenchymal stem cells grown in three-dimensional hyaluronan-based scaffolds for cartilage tissue engineering*. Journal of biomedical materials research. Part A, 2010. **93**(1): p. 37-45.
355. Dhumal, N.R., H.J. Kim, and J. Kiefer, *Molecular interactions in 1-ethyl-3-methylimidazolium acetate ion pair: a density functional study*. The journal of physical chemistry. A, 2009. **113**(38): p. 10397-404.
356. Viell, J. and W. Marquardt, *Concentration measurements in ionic liquid-water mixtures by mid-infrared spectroscopy and indirect hard modeling*. Applied Spectroscopy, 2012. **66**(2): p. 208-17.
357. Chen, H.-L., et al., *Cytotoxicity of Imidazole Ionic Liquids in Human Lung Carcinoma A549 Cell Line*. J Chin Chem Soc-Taip, 2014. **61**(7): p. 763-769.
358. Marijnissen, W.J., et al., *Alginate as a chondrocyte-delivery substance in combination with a non-woven scaffold for cartilage tissue engineering*. Biomaterials, 2002. **23**(6): p. 1511-7.
359. Marijnissen, W.J., et al., *Tissue-engineered cartilage using serially passaged articular chondrocytes. Chondrocytes in alginate, combined in vivo with a synthetic (E210) or biologic biodegradable carrier (DBM)*. Biomaterials, 2000. **21**(6): p. 571-80.
360. Puelacher, W.C., et al., *Tissue-engineered growth of cartilage: the effect of varying the concentration of chondrocytes seeded onto synthetic polymer matrices*. International journal of oral and maxillofacial surgery, 1994. **23**(1): p. 49-53.
361. Malm, C.J., et al., *Small calibre biosynthetic bacterial cellulose blood vessels: 13-months patency in a sheep model*. Scandinavian Cardiovascular Journal, 2012. **46**(1): p. 57-62.
362. Lau, A., et al., *Indentation stiffness of aging human costal cartilage*. Acta Biomater, 2008. **4**(1): p. 97-103.
363. Griffin, M.F., et al., *Biomechanical Characterisation of the Human Auricular Cartilages; Implications for Tissue Engineering*. Ann Biomed Eng, 2016.
364. Nimeskern, L., *Spatial and temporal mapping of native auricular elastic cartilage*. Abstracts Annual Meeting, Swiss Society for Biomedical Engineering, 2011.
365. Chen, S., et al., *Strategies to minimize hypertrophy in cartilage engineering and regeneration*. Genes Dis, 2015. **2**(1): p. 76-95.
366. Jansen, I.D., et al., *Type II and VI collagen in nasal and articular cartilage and the effect of IL-1alpha on the distribution of these collagens*. J Mol Histol, 2010. **41**(1): p. 9-17.
367. Morrison, K.A., et al., *Optimizing cell sourcing for clinical translation of tissue engineered ears*. Biofabrication, 2016. **9**(1): p. 015004.
368. Zhao, X., et al., *Chondrogenesis by bone marrow-derived mesenchymal stem cells grown in chondrocyte-conditioned medium for auricular reconstruction*. J Tissue Eng Regen Med, 2016.
369. Zhang, L., et al., *Co-culture of microtic chondrocyte with BMSC to generate tissue engineered cartilage*. Tissue Eng Part A, 2011.
370. Melgarejo-Ramirez, Y., et al., *Characterization of pediatric microtia cartilage: a reservoir of chondrocytes for auricular reconstruction using tissue engineering strategies*. Cell Tissue Bank, 2016. **17**(3): p. 481-9.
371. Thomson, J.A., et al., *Embryonic stem cell lines derived from human blastocysts*. Science, 1998. **282**(5391): p. 1145-7.
372. Takahashi, K., et al., *Induction of pluripotent stem cells from adult human fibroblasts by defined factors*. Cell, 2007. **131**(5): p. 861-72.
373. Bigdeli, N., et al., *Coculture of human embryonic stem cells and human articular chondrocytes results in significantly altered phenotype and improved chondrogenic differentiation*. Stem Cells, 2009. **27**(8): p. 1812-21.
374. Qu, C., et al., *Chondrogenic differentiation of human pluripotent stem cells in chondrocyte co-culture*. Int J Biochem Cell Biol, 2013. **45**(8): p. 1802-12.

375. Vats, A., et al., *Chondrogenic differentiation of human embryonic stem cells: the effect of the micro-environment*. Tissue Eng, 2006. **12**(6): p. 1687-97.
376. Hwang, N.S., S. Varghese, and J. Elisseeff, *Derivation of chondrogenically-committed cells from human embryonic cells for cartilage tissue regeneration*. PLoS One, 2008. **3**(6): p. e2498.
377. Okita, K., T. Ichisaka, and S. Yamanaka, *Generation of germline-competent induced pluripotent stem cells*. Nature, 2007. **448**(7151): p. 313-7.
378. Shih, C.C., et al., *Human embryonic stem cells are prone to generate primitive, undifferentiated tumors in engrafted human fetal tissues in severe combined immunodeficient mice*. Stem Cells Dev, 2007. **16**(6): p. 893-902.
379. Caplan, A.I. and J.E. Dennis, *Mesenchymal stem cells as trophic mediators*. J Cell Biochem, 2006. **98**(5): p. 1076-84.
380. Strioga, M., *Same or not the same? Comparison of adipose tissue-derived versus bone marrow-derived mesenchymal stem and stromal cells*. Stem Cells Dev, 2012. **0**(0): p. 1-29.
381. Vonk, L.A., et al., *Autologous, allogeneic, induced pluripotent stem cell or a combination stem cell therapy? Where are we headed in cartilage repair and why: a concise review*. Stem Cell Res Ther, 2015. **6**: p. 94.
382. Brown, B.N. and S.F. Badylak, *Extracellular matrix as an inductive scaffold for functional tissue reconstruction*. Transl Res, 2014. **163**(4): p. 268-85.
383. Mansfield, J., et al., *The elastin network: its relationship with collagen and cells in articular cartilage as visualized by multiphoton microscopy*. J Anat, 2009. **215**(6): p. 682-91.
384. Loeser, R.F., *Chondrocyte integrin expression and function*. Biorheology, 2000. **37**(1-2): p. 109-16.
385. Mao, Y. and J.E. Schwarzbauer, *Fibronectin fibrillogenesis, a cell-mediated matrix assembly process*. Matrix Biol, 2005. **24**(6): p. 389-99.
386. Shotton, D.M. and H.C. Watson, *Three-dimensional structure of tosyl-elastase*. Nature, 1970. **225**(5235): p. 811-6.
387. Rowley, J.A., G. Madlambayan, and D.J. Mooney, *Alginate hydrogels as synthetic extracellular matrix materials*. Biomaterials, 1999. **20**(1): p. 45-53.
388. Lee, K.Y. and D.J. Mooney, *Alginate: properties and biomedical applications*. Prog Polym Sci, 2012. **37**(1): p. 106-126.
389. Petersen, N. and P. Gatenholm, *Bacterial cellulose-based materials and medical devices: current state and perspectives*. Appl Microbiol Biotechnol, 2011. **91**(5): p. 1277-86.
390. Karim, Z., *Nanocellulose as novel supportive functional material for growth and development of cells*. Cell Developmental Biology, 2015. **4**(2).
391. Williams, D.F., *The Williams dictionary of biomaterials*. 1999, Liverpool University Press.
392. Paredes Juarez, G.A., et al., *Immunological and technical considerations in application of alginate-based microencapsulation systems*. Front Bioeng Biotechnol, 2014. **2**: p. 26.
393. Martinez Avila, H., et al., *Biocompatibility evaluation of densified bacterial nanocellulose hydrogel as an implant material for auricular cartilage regeneration*. Appl Microbiol Biotechnol, 2014. **98**(17): p. 7423-35.
394. Lin, N., *Nanocellulose in biomedicine: Current status and future prospect*. European Polymer Journal, 2014. **59**: p. 302-325.
395. Pertile, R.A., et al., *Bacterial cellulose: long-term biocompatibility studies*. J Biomater Sci Polym Ed, 2012. **23**(10): p. 1339-54.
396. Orive, G., et al., *Biocompatibility evaluation of different alginates and alginate-based microcapsules*. Biomacromolecules, 2005. **6**(2): p. 927-31.
397. Murphy, S.V. and A. Atala, *3D bioprinting of tissues and organs*. Nat Biotechnol, 2014. **32**(8): p. 773-85.
398. Di Bella, C., et al., *3D Bioprinting of Cartilage for Orthopedic Surgeons: Reading between the Lines*. Front Surg, 2015. **2**: p. 39.
399. Gu, B.K., et al., *3-dimensional bioprinting for tissue engineering applications*. Biomater Res, 2016. **20**: p. 12.
400. Axpe, E. and M.L. Oyen, *Applications of Alginate-Based Bioinks in 3D Bioprinting*. Int J Mol Sci, 2016. **17**(12).
401. Daly, A.C., et al., *A comparison of different bioinks for 3D bioprinting of fibrocartilage and hyaline cartilage*. Biofabrication, 2016. **8**(4): p. 045002.
402. Markstedt, K., et al., *3D Bioprinting Human Chondrocytes with Nanocellulose-Alginate Bioink for Cartilage Tissue Engineering Applications*. Biomacromolecules, 2015. **16**(5): p. 1489-96.

403. Nguyen, D., et al., *Cartilage Tissue Engineering by the 3D Bioprinting of iPS Cells in a Nanocellulose/Alginate Bioink*. Sci Rep, 2017. **7**(1): p. 658.
404. Muller, M., et al., *Alginate Sulfate-Nanocellulose Bioinks for Cartilage Bioprinting Applications*. Ann Biomed Eng, 2017. **45**(1): p. 210-223.
405. Torres, F.G., S. Commeaux, and O.P. Troncoso, *Biocompatibility of bacterial cellulose based biomaterials*. J Funct Biomater, 2012. **3**(4): p. 864-78.
406. Cui, X., et al., *Direct human cartilage repair using three-dimensional bioprinting technology*. Tissue Eng Part A, 2012. **18**(11-12): p. 1304-12.
407. Lee, M.H., et al., *Considerations for tissue-engineered and regenerative medicine product development prior to clinical trials in the United States*. Tissue Eng Part B Rev, 2010. **16**(1): p. 41-54.
408. Commission., E., *Regulation 1394/2007 for Advanced Therapy Medicinal Products*. 2007.
409. FDA, U.S., *Title 21 of the Code of Federal Regulations (CFR) Part 1271 Human Cells, Tissues and Cell and Tissue Based Products*. 2001.
410. Abou-El-Enein, M., A. Elsanhoury, and P. Reinke, *Overcoming Challenges Facing Advanced Therapies in the EU Market*. Cell Stem Cell, 2016. **19**(3): p. 293-7.
411. Yano, K., *Regulatory approval for autologous human cells and tissue products in the United States, the European Union, and Japan*. Regenerative Therapy, 2015. **1**: p. 45-56.
412. Liikanen, E., *Commission directive 2003/94/European Commission*. Official Journal of the European Union, 2003: p. 22-26.
413. Eaker, S., et al., *Concise review: guidance in developing commercializable autologous/patient-specific cell therapy manufacturing*. Stem Cells Transl Med, 2013. **2**(11): p. 871-83.
414. Brittberg, M., *Cellular and Acellular Approaches for Cartilage Repair: A Philosophical Analysis*. Cartilage, 2015. **6**(2 Suppl): p. 4S-12S.
415. Lebourg, M., et al., *Cell-free cartilage engineering approach using hyaluronic acid-polycaprolactone scaffolds: a study in vivo*. J Biomater Appl, 2014. **28**(9): p. 1304-15.

Appendices

PHD PORTFOLIO

Name PhD-student: Mieke Marianne Pleumeekers
Erasmus MC department: Otorhinolaryngology
Research school: MolMed
PhD period: July 2010 - June 2018
Promotor: Prof. dr. G.J.V.M. van Osch
Co-promotor: Dr. ir. K.S. Stok

1. PhD training

	Workload (ECTS)
General courses	
- '11 Biomedical English Writing and Communication	4.0
In-depth courses	
- '13 Optical imaging course: <i>Practical introduction to laser scanning microscopy</i>	0.3
- '16 International course on microsurgery Skillslab Erasmus MC	1.4
Seminars and workshops	10.0
- '10-'13 Wetenschapsdag KNO	
- '11 Regenerative medicine - module 2: <i>Molecular and cellular basis of regenerative medicine</i>	
- 15 th -17 th MolMed day	
- '10-'17 Wetenschapsdag NVPC	
- '17 Jonge vrouwen in de academie	
Oral presentations	
• Based on <i>The in vitro and in vivo capacity of culture-expanded human cells from several sources encapsulated in alginate to form cartilage.</i>	
- 4 th International Conference on Tissue Engineering, Crete, Greece	1.0
- '12 Tissue engineering and Regenerative Medicine Society TERMIS World Congress, Vienna, Austria	1.0
- '12 Annual meeting of the Dutch Society of Matrix Biology (NVMB), Lunteren, the Netherlands	1.0
• Based on <i>Trophic effects of adipose-tissue-derived and bone-marrow-derived mesenchymal stem cells enhance cartilage generation by chondrocytes in co-culture.</i>	
- '13 Tissue engineering and Regenerative Medicine Society TERMIS European Congress, Istanbul, Turkey	1.0
• Based on <i>Cartilage regeneration in the head and neck area: Combination of ear or nasal chondrocytes and mesenchymal stem cells improves cartilage production.</i>	
- '13 Annual meeting of the Dutch Society for Plastic Surgery (NVPC), Nijmegen, the Netherlands	1.0

1. PhD training (continue)

	Workload (ECTS)
Poster presentations	
<ul style="list-style-type: none">• Based on <i>The in vitro and in vivo capacity of culture-expanded human cells from several sources encapsulated in alginate to form cartilage.</i>	
- 4 th International Conference on Tissue Engineering, Crete, Greece	1.0
- '11 Dutch Symposium Experimental Research Surgical Specialties (SEOHS), Rotterdam, the Netherlands	1.0
- '12 Tissue engineering and Regenerative Medicine Society TERMIS World Congress, Vienna, Austria	1.0
- '12 Molecular Medicine postgraduate school (MolMed), Rotterdam, the Netherlands	1.0
- '13 Tissue engineering and Regenerative Medicine Society TERMIS European Congress, Istanbul, Turkey	1.0
<ul style="list-style-type: none">• Based on <i>Cartilage regeneration in the head and neck area: Combination of ear or nasal chondrocytes and mesenchymal stem cells improves cartilage production.</i>	
- '13 Molecular Medicine postgraduate school (MolMed), Rotterdam, the Netherlands	1.0

2. Teaching and other activities

	Workload (ECTS)
Supervision thesis	
- '12-'13 Supervising Master's thesis, Lizette Utomo, Technical medicine student, Utwente <i>Preparation and characterization of a decellularized cartilage scaffolds for ear cartilage reconstruction.</i>	10.0
- '11-'12 Supervising Minor's thesis, Linde Zhou, Technical medicine student, Utwente <i>Tissue engineering cartilage: Biochemical and biomechanical evaluation of human cartilage subtypes.</i>	4.0
- '12 Supervising Junior Med students <i>Decellularization</i>	2.0
Other	
- Presentation award at the 4 th International Conference on Tissue Engineering, Crete, Greece	
- '17 Fundamental research award: <i>Labrat</i> , the Dutch Society for Plastic Surgery (NVPC)	
- Organizing the 16 th Esser Course: <i>Around the wrist</i> , Rotterdam, the Netherlands	5.0
- Organizing the 15 th Wondcongres: <i>Geschiedenis van de wondbehandeling en vergeten technieken & Innovaties en management van de wondzorg</i> , Rotterdam, the Netherlands	5.0
- '12 Travel grant ReMedic	

PUBLICATIONS

M.M. Pleumeekers, L. Nimeskern, J.L.M. Koevoet, N. Kops, R.M.L. Poublon, K.S. Stok, G.J.V.M. van Osch. *The in vitro and in vivo capacity of culture-expanded human cells from several sources encapsulated in alginate to form cartilage*. European Cells & Materials, 2014. 27: p. 264-80.

M.M. Pleumeekers, L. Nimeskern, J.L.M. Koevoet, M. Karperien, K.S. Stok, G.J.V.M. van Osch. *Cartilage regeneration in the head and neck area: Combination of ear or nasal chondrocytes and mesenchymal stem cells improves cartilage production*. Plastic and Reconstructive Surgery, 2015. 136(6): p. 762e-74e.

M.M. Pleumeekers, L. Utomo, L. Nimeskern, S. Nürnberger, K.S. Stok, F. Hildner, G.J.V.M. van Osch. *Preparation and characterization of a decellularized cartilage scaffold for ear cartilage reconstruction*. Biomedical Materials, 2015. 10(1): p. 015010.

L. Nimeskern, **M.M. Pleumeekers**, D.J. Pawson, J.L.M. Koevoet, I. Lehtoviita, M.B. Soyka, C. Rösli, D. Holzmann, G.J.V.M. van Osch, R. Müller, K.S. Stok. *Mechanical and biochemical mapping of human auricular cartilage for reliable assessment of tissue-engineered constructs*. Journal of Biomechanics, 2015. 48(10): p. 1721-9.

H. Martínez Ávila, E. Feldmann, **M.M. Pleumeekers**, L. Nimeskern, W. Kuo, W.C. de Jong, S. Schwarz, R. Müller, J. Hendriks, N. Rotter, G.J.V.M. van Osch, K.S. Stok, P. Gatenholm. *Novel bilayer bacterial nanocellulose scaffold supports neocartilage formation in vitro and in vivo*. Biomaterials, 2015. 44: p. 122-33.

M.M. Pleumeekers, L. Nimeskern, J.L.M. Koevoet, M. Karperien, K.S. Stok, G.J.V.M. van Osch. *Trophic effects of adipose-tissue-derived and bone-marrow-derived mesenchymal stem cells enhance cartilage generation by chondrocytes in co-culture*. PLoS One, 2017. 13(2): p. 1-23.

E.J. Bos, **M.M. Pleumeekers**, M. Helder, N. Kuzmin, K. van der Laan, M.L. Groot, G.J.V.M. van Osch, P.P.M. van Zuijlen. *Structural and mechanical comparison of human ear, alar and septal cartilage*. Plastic and Reconstructive Surgery Global Open, 2018. 6(1): p. 1-9.

DANKWOORD

Prof. dr. G.J.V.M. van Osch

Allerbeste Gerjo. 'Brave meisjes schrijven zelden geschiedenis' is het eerste wat er in me opkomt als ik jou zou moeten beschrijven. Je bent een ware inspirator, totally on top of your game. Internationaal gezien schrikt men soms van jouw directheid, maar ik waardeer in jou het allermeeft dat jij zegt wat je denkt en doet wat je zegt en daarnaast keihard werkt om jouw beoogde doelen te bereiken. Je zou een Rotterdammer kunnen zijn! Ik mis onze EAREG-tripjes en voortgangsbesprekingen, waarbij we samen konden brainstormen over het interpreteren van heden behaalde resultaten en filosoferen over nieuwe experimenten. Bedankt dat je me de kans hebt gegeven me wetenschappelijk en persoonlijk te kunnen ontwikkelen.

Dr. ir. K.S. Stok

Dear Kathryn, dear co-promotor. Thank you very much for taking place in the graduation committee today all the way from Australia. Please, be gentle. You have been a great supervisor during my PhD-training. You have helped me to understand, and inspired me to enjoy the principles of cartilage biomechanical engineering. Your knowledge in this field has no boundaries. For me, you are just a professor in-the-make!

Commissie

Beste prof. dr. Mathijssen, prof. dr. Van Zuijlen en prof. dr. ir. Malda, leden van de kleine commissie. Hartelijk dank voor het kritisch lezen en beoordelen van dit proefschrift. Beste Irene, ik voel mij vereerd dat ook jij hebt plaatsgenomen in mijn kleine commissie. Ik hoop dat door dit proefschrift de liefde voor fundamenteel onderzoek ook binnen de plastische chirurgie een beetje meer is aangewakkerd. Prof. dr. Kleinrensink, dr. Daatema en dr. Hendriks, dank voor uw bereidheid om plaats te nemen in de grote commissie.

EAREG-team

Team EAREG - team Göteborg (Paul Gatenholm, Héctor Martínez Ávila, Johan Sundberg), Zurich (Ralph Müller, Kathryn Stok, Luc Nimeskern), Ulm (Nicole Rotter, Silke Schwarz, Eva-Maria Feldmann), Bilthoven (Jeanine Hendriks, Jens Riesle, Wilco de Jong) and Alzenau (Annette Jork) - our multidisciplinary scientific collaboration has opened my eyes to new ideas and methods. The EAREG-meetings were far most the highlights of my PhD-training.

Et al.

Dear co-authors, without you, this thesis would not have been possible. Especially I would like to thank Luc, Héctor, Ernst-Jan and Lizette. Dear Luc, we slaved ourselves through a million samples of half a million donors of 6 different experiments. We made it! Dear Héctor. You were able to put all our multidisciplinary work and ideas into one outstanding paper. Good luck with your new company. Hopefully our paths will cross again in the future. Beste Ernst-Jan, onze samenwerking begon bij dat ene moment: 'Cut the crap'. Lieve Lizette, het ontzettend harde werken als masterstudent heeft uiteindelijk geleid tot een prachtig artikel

maar nog belangrijker de start van jouw eigen PhD-training. Die fles bubbels gaan we ooit drinken!

Bastiaan Tuk

Daar waar het allemaal begon. Beste Bas, ik denk niet dat je doorhebt dat jij diegene bent die mij verliefd heeft laten worden op het fundamentele onderzoek. Wanneer gaan we samen brainstormen?

Het fundament van de 16^{de}

Lieve Wendy, Nicole en Sandra. Zonder jullie ben ik nergens. Wendy, Godmother van de celkweek, wij hebben uren doorgebracht in het lab en jij hebt mij alle kneepjes van het vak geleerd. Behalve hoofdrekenen, want dat kan ik nog steeds niet... Nicole, het is mij nog steeds een raadsel waarom iemand die zo secuur haar labjournaal bijhoudt, toch zo chaotisch kan zijn! Door jou hebben mijn muisjes - mogen hun zielen rusten in vrede - een ontspannen en liefdevol leven gekend (behalve dan het muisje dat tussen deksel en bak terecht kwam). Sandra, je bent toch wel een beetje m'n moeder van de afdeling. Zonder jou geen structuur, zonder jou geen gezelligheid!

Paranimfen/vakidioten

Lieve Caroline en Lizette. Zo blij dat jullie mijn paranimfen zijn! Caroline, nu jouw lieve Hanna geboren is en mijn PhD-kindje eindelijk op eigen voeten kan staan, kunnen we misschien eindelijk weer eens de tijd vinden om ergens een goud muurtje op te zoeken?! Lizette, eindelijk iemand die net zo slecht kan drinken als ik. Wetenschappelijk gezien ga je wel door het geluid en ben je me nog net niet voorbijgevlogen! Ik ga er dan ook vanuit dat jij vandaag de moeilijke vragen voor je rekening neemt?!

Doctoren, dokters en ander gespuis

Lieve lotgenoten van de 16^{de}. Dank voor de gezelligheid tijdens CTCR-meetings, labdag, cake-van-de-week, congressen en kweeksessies. Lieve Marloes en Nienke, onze frustraties, overwinningen, relatieperikelen, irritaties en behaalde publicaties zijn allemaal de revue gepasseerd, maar hebben uiteindelijk geleid tot drie topboekjes! Chirurgen (in opleiding) van het Franciscus Gasthuis, onder jullie vleugels eindelijk dokter geworden. Lieve plastische collega's, ik ben er trots op in het mooiste Rotterdam opgeleid te mogen worden. Plastic fantastic!

Vrienden

Lieve vrienden: lieve oud-huisgenootjes, 'Mooie hockeymeisjes', hockeyteam, 'Oude taartjes', tennisvrienden en 'Derde-kerstdag-genoten'. Eindelijk meer tijd voor jullie!

Familie

Wilhelmina Lange - van Heuvelen, lieve oma Mien, mater familias. Ik voel mij vereerd dat ik u dan eindelijk mijn promotieboekje kan overhandigen, wetende dat u waarschijnlijk de enige bent die het zal lezen. Lieve Lily en Peter, betere schoonouders kan ik mij niet wensen. De

extra oppasdagen hebben mij de mogelijkheid gegeven nog even de laatste puntjes op de 'i' te zetten (eigenlijk het hele alfabet nog even onder de loep te nemen...). Zusters, allerliefste Olga en Laura. Jullie zijn er gewoon altijd. Lieve papa en mama, lieve Bèr en Marjan. Alle ingrediënten die nodig zijn voor de totstandkoming van dit proefschrift heb ik van jullie gekregen: doorzettingsvermogen en hoge pijngrens, ratio en een kritische blik, maar vooral het denken in oplossingen. Jullie steun, liefde en onvoorwaardelijk vertrouwen werkt motiverend! Dankjewel voor alles.

Mijn allerliefsten

Allerliefste Piet en Olli, mijn allerliefste en allerleukste huisgenootjes. Als ik ook maar een fractie van jullie energie had gehad, dan was dit promotieboekje een lustrum eerder af geweest. Lieve Piet, alles is leuker met jou.

CURRICULUM VITAE



Mieke Marianne Pleumeekers was born on the 29th of December 1983 in Rotterdam, the Netherlands. After graduating from Johannes Calvijn in Rotterdam in 2002, she started medical school at the Erasmus University of Rotterdam. During an elective internship at the surgery department in Mzuzu, Malawi, she got in touch with facial plastic surgery. From that moment on, Mieke was fascinated by its technical and artistic challenges and was offered the chance to work her final months of medical school at the plastic and reconstructive surgery at Erasmus MC in Rotterdam (prof. dr. S.E.R. Hovius). She received her medical degree in 2009 and worked another 6 months as a senior

house officer in plastic and reconstructive surgery at Erasmus MC in Rotterdam (prof. dr. S.E.R. Hovius). During this period of time, she was introduced to the Connective Tissue Cells and Repair group (CTCR-group; department of Orthopaedics and Otorhinolaryngology) of prof. dr. G.V.J.M. van Osch and her PhD-training was initiated July 2010. The research was performed within the framework of a European research consortium: EuroNanoMed (EAREG-406340-131009/1). During her PhD-training, Mieke was accepted as a trainee at the department of plastic and reconstructive surgery Erasmus MC in Rotterdam (prof. dr. I.M.J. Mathijssen). Her residency started the 1st of December 2014 at the general surgery department at the Franciscus Gasthuis en Vlietland in Rotterdam (dr. T.M.A.L. Klem).